The SnapLocX Connection:
A Novel Approach to Interlocking Steel W-Shape Column Splices

Megan G. Hinaus

A thesis submitted in partial fulfillment of the requirements for the degree of

Master of Science in Civil Engineering

University of Washington

2024

Committee:

Jeffrey W. Berman

Dawn E. Lehman

Travis E. Thonstad

Program Authorized to Offer Degree:

Civil and Environmental Engineering

University of Washington

Abstract

The SnapLocX Connection:
A Novel Approach to Interlocking Steel W-Shape Column Splices

Megan G. Hinaus

Chair of the Supervisory Committee:
Jeffrey W. Berman
Department of Civil and Environmental Engineering

Column splices are critical components in steel structures above three stories that ensure the stability and integrity of the building framework. Splices are required when standard column lengths are insufficient for the design height of the structure. Standard erection practice for W-shape column splices begins with lowering an upper column onto a lower column guided by ironworkers, and while one column may arrive pre-welded or bolted with the connecting plates, the connecting column must be bolted and welded onsite. These labor-intensive on-site processes contribute to schedule delays, creating risky conditions that include fall, pinching, and welding hazards.

Funded by the American Institute of Steel Construction (AISC), this thesis presents the first part of a multi-phase project to develop and manufacture an industry-ready solution for improving column erection. The SnapLocX Connection utilizes shop-bolted plates connected to the lower column that act as snapping plates, while shop-welded plates are secured to the column above the splice. The designed splice connection allows crane operators and ironworkers to drop the upper column down into the lower column, where the prefabricated SnapLocX Connection would secure the two columns to each other. This process would eliminate additional scheduled time

for further assembly compared to traditional assembly, as the temporary erection stage and site welding and bolting are bypassed completely.

This thesis developed a design methodology for the SnapLocX Connection. To accomplish this, the necessary loading requirements from building codes are reviewed, and the limit states controlling the connection component design strengths are organized into a coherent design process. A design tool was developed in MatLab to ensure that the components can achieve the snapping assembly behavior with an elastic response. An example SnapLocX Connection was designed and evaluated under the identified limit states. Finally, sets of standardized designs were developed for a wide range of column pairs that could be spliced in practice. The result is a set of tables that act as design aids for practitioners to easily select the necessary connection components for most possible column splice pairings.

Table of Contents

List of Figures

List of Tables

List of Variables

A_b : Unthreaded area of bolt

A_e : Effective net area of cross-section

A_g : Gross cross-sectional area

A_{gv} : Gross area of cross-section subject to shear

A_n : Nominal cross-sectional area

A_{nt}: : Net area of the cross-section subject to tension

A_{nv} : Net area of the cross-section subject to shear

A_{pb} : Projected area in bearing

A_{we} : Effective area of the weld

b_{EDGE} : Edge of a plate to the center of a bolt-hole

$b_{EDGE_{min}}$: Minimum edge requirements for bolts as defined by *the Steel Specification*

b_{END} : The distance from the lower end of a plate to the center of the lower, fixed bolts

$b_{f_{LC}}$: Flange width of the Lower Column

$b_{f_{UC}}$: Flange width of the Upper Column

b_{IP} : Width of the IP

b_{LLP} : Width of the LLP

b_{OP} : Width of the OP

b_{offset} : Dimension from the center of the upper bolt row to the upper end of the Lower Column

b_{SP} : Width of the SP

b_{ULP} : Width of the ULP

$\boldsymbol{b_{weld}}$: Fillet weld along a plate-width

$\boldsymbol{C}$: Eccentrically loaded bolt group coefficient

$\boldsymbol{C_3}$: Required clearance for column fillet as provided in Table 7-15: "Entering and Tightening Clearance, in." from *the Manual*

$\boldsymbol{c}$: Maximum bending stress through plate cross-section

$\boldsymbol{D_1}$: Displacement curve for Beam 1

$\boldsymbol{D_2}$: Initial displacement curve for Beam 2

$\boldsymbol{D_{2_{next}}}$: Next iterative displacement curve for Beam 2

$\boldsymbol{D_{12_0}}$: Displacement curve for Beams 1 and 2 superimposed from the first curve calculation of Beam 2

$\boldsymbol{D_{12_{next}}}$: Next iterative displacement curve superimposed from D_1 and $D_{2_{next}}$

$\boldsymbol{D_{total}}$: Total displacement curve of the OP combining $D_{12_{next}}$ and D_{uplift}

$\boldsymbol{D_{uplift}}$: Displacement curve when calculating instantaneous uplift at L_1

$\boldsymbol{d_b}$: Diameter of the bolts

$\boldsymbol{d_h}$: Diameter of the drilled bolt holes

$\boldsymbol{d_{LC}}$: Depth of the Lower Column

$\boldsymbol{d_{KEY}}$: Design diameter of the SK

$\boldsymbol{d_{KEY_r}}$: Required diameter of the SK

$\boldsymbol{d_m}$: Moment arm

$\boldsymbol{d_{SK}}$: Diameter of the Shear Key slot

$\boldsymbol{d_{UC}}$: Depth of the Upper Column

$\boldsymbol{E}$: Young's Modulus of material

$\boldsymbol{e_x}$: Centroid of a bolt group to the plane of force

$\boldsymbol{F_1}$: Force required to displace OP $\delta_{1_{end}}$

$F_{1_{rxn}}$: Reaction force at fixed end for Beam 1

F_{EXX} : Fillet metal classification strength

F_n : Nominal tensile or shear strength of bolt classification

F_{nv} : Nominal shear stress of bolt classification

F_{nw} : Nominal stress of weld metal

F_u : Ultimate stress of material

F_{up} : Uplift force for instantaneous uplift at disc springs

F_y : Nominal yield stress

$F_{y_{IP}}$: Nominal yield stress of the IP

$F_{y_{KEY}}$: Nominal yield stress of the SK

$F_{y_{LLP}}$: Nominal yield stress of the LLP

$F_{y_{OP}}$: Nominal yield stress of the OP

$F_{y_{UC}}$: Nominal column yield strength of the Upper Column

$F_{y_{weld}}$: Nominal yield stress of the fillet weld

H : Assumed minimum building story height

h : Conical height of the disc spring

$h_{initial}$: Initial estimation for h

h_{new} : Next estimation for h

I_{OP} : Moment of inertia for the OP

I_{weld} : Moment of inertia for a weld

ID : Inner diameter of the disc spring

IP : Inner Plate of the SnapLocX Connection

$\boldsymbol{k}$: Factor of column axial load

$\boldsymbol{k_{1_{LC}}}$: Distance from the center web to the flange toe of the Lower Column

$\boldsymbol{k_{1_{max}}}$: Maximum allowable distance from the center web to the flange toe of W-shapes

$\boldsymbol{k_{OP}}$: Stiffness of the OP

$\boldsymbol{L_1}$: Length from the center of the lower, fixed bolts to the center of the upper disc spring bolts

$\boldsymbol{L_2}$: Length from the center of the upper, disc spring bolts to the lower edge of the ULP

$\boldsymbol{L_{col}}$: Length of the column

$\boldsymbol{L_{IP}}$: Length of the IP

$\boldsymbol{L_{LLP}}$: Length of the LLP

$\boldsymbol{L_{OP}}$: Length of the OP

$\boldsymbol{L_{SK}}$: Length from the lower edge of the OP to the center of the SK

$\boldsymbol{L_{SP}}$: Length of the SP

$\boldsymbol{L_{tot}}$: Total length observed OP length

$\boldsymbol{L_{ULP}}$: Length of the ULP

$\boldsymbol{L_{weld}}$: Length of fillet weld

$\boldsymbol{LLP}$: Lower Lock Plate of the SnapLocX Connection

$\boldsymbol{l_c}$: Clear distance in direction of force

$\boldsymbol{l_{c_{low}}}$: Clear distance from the lower bolt row to lower end of plate

$\boldsymbol{l_{c_{up}}}$: Clear distance from lower bolt row to upper bolt

$\boldsymbol{M}$: Ratio factor of α for the disc spring

$\boldsymbol{M_1}$: Moment curve for Beam 1

$\boldsymbol{M_{12_0}}$: Initial superimosed moment curve from M_1 and M_2

$\boldsymbol{M_{12_{next}}}$: Next iterative moment curve superimposed from M_1 and $M_{2_{next}}$

$\boldsymbol{M_2}$: Initial moment curve for Beam 2

$\boldsymbol{M_{2_{f_0}}}$: Initial moment reaction at the fixed end of Beam 2

$\boldsymbol{M_{2_{f_{next}}}}$: Iterated moment reaction at the fixed end of Beam 2

$\boldsymbol{M_{2_{next}}}$: Next iterative moment curve for Beam 2

$\boldsymbol{M_{demand}}$: Maximum bending moment on the OP

$\boldsymbol{M_n}$: Nominal moment capacity

$\boldsymbol{M_{p_x}}$: Moment demand on the splice from the Upper Column in the strong axis

$\boldsymbol{M_{p_y}}$: Moment demand on the splice from the Upper Column in the weak axis

$\boldsymbol{M_{total}}$: Total moment curve of the OP combining $M_{12_{next}}$ and M_{uplift}

$\boldsymbol{M_{uplift}}$: Moment curve of OP during instantaneous uplift

$\boldsymbol{M_{weld}}$: Moment demand of weld

$\boldsymbol{M_{allow}}$: Moment capacity of the OP due to bending

$\boldsymbol{n_b}$: Number of bolts

$\boldsymbol{n_{bg}}$: Number of bolt groups

$\boldsymbol{n_{col}}$: Number of bolt columns

$\boldsymbol{n_{KEY}}$: Number of SKs

$\boldsymbol{n_s}$: Total number of disc springs on each bolt, including parallel and series

$\boldsymbol{n_{s_b}}$: Number of bolts with disc springs

$\boldsymbol{n_{s_p}}$: Number of springs in parallel on a bolt

$\boldsymbol{n_{s_s}}$: Number of springs in series on a bolt

n_{weld} : Number of welds resisting force

OD : Outer diameter of the disc spring

OD_{MAX} : Maximum allowable disc spring outer diameter

OH : Overall height of the disc spring

$OH_{initial}$: Initial estimation for OH

OH_{new} : Next estimation for OH

OP : Outer Plate of the SnapLocX Connection

P_n : Nominal strength

P_{pt} : Total pretension in the upper bolts

P_s : Spring force for a given deformation in the disc springs

P_{s_2} : Force exerted on bolts from springs due to δ_{s_2}

$P_{s_{2_{next}}}$: Next estimated spring force from Beam 2 iterations

$P_{s_{total}}$: Total force expressed by the spring

P_u : Axial load

P_{weld} : Shear demand on IP welds

P_{δ_s} : Nonlinear force curve for spring deformation

R : Radius of the disc spring from the centerline to the bearing edge

$R_{2_{f_0}}$: Initial reaction force at the simply supported end of Beam 2

$R_{2_{f_{next}}}$: Iterated reaction force at the simply supported end of Beam 2

$R_{2_{s_0}}$: Initial reaction force at the fixed end of Beam 2

$R_{2_{s_{next}}}$: Iterated reaction force at the fixed end of Beam 2

$R_{constant}$: Constant used in the calculation for R

$\boldsymbol{R_{constant_{initial}}}$: Initial estimation for $R_{constant}$

$\boldsymbol{R_{constant_{new}}}$: Next estimation for $R_{constant}$

$\boldsymbol{R_{initial}}$: Initial estimation for R

$\boldsymbol{R_n}$: Nominal strength

$\boldsymbol{R_{new}}$: Next estimation for R

$\boldsymbol{R_u}$: Required design strength from LRFD

$\boldsymbol{r_n}$: Available bolt shear

$\boldsymbol{s}$: Bolt spacing horizontally

$\boldsymbol{SK}$: Shear Key of the SnapLocX Connection

$\boldsymbol{SP}$: Shim Plate of the SnapLocX Connection

$\boldsymbol{T}$: Minimum design strength in tension

$\boldsymbol{t}$: Thickness

$\boldsymbol{t_{f_b}}$: Bearing thickness of bolts on column flange

$\boldsymbol{t_{f_{LC}}}$: Flange thickness of the Lower Column

$\boldsymbol{t_{f_{UC}}}$: Flange thickness of the Upper Column

$\boldsymbol{t_{IP}}$: Design thickness of the IP

$\boldsymbol{t_{IP_r}}$: Required thickness of the IP

$\boldsymbol{t_{IP_{weld}}}$: Design thickness of the Inner Plate weld to the Lower Column

$\boldsymbol{t_{IP_{weld_r}}}$: Required thickness of the IP weld for given shear demand

$\boldsymbol{t_{LLP}}$: Thickness of the LLP

$\boldsymbol{t_{LLP_r}}$: Required thickness of the LLP

$\boldsymbol{t_{OP}}$: Thickness of the OP

t_{SK} : Thickness of the SK cylinder

$t_{SK_{weld}}$: Design thickness of SK weld

$t_{SK_{weld_r}}$: Required design thickness of the SK weld

t_{SP} : Thickness of the SP

t_{ULP} : Thickness of the ULO

t_{weld} : Weld thickness

U : Shear lag factor

U_{bs} : Block shear reduction factor

ULP : Upper Lock Plate of the SnapLocX Connection

V_1 : Shear curve from Beam 1

V_{12_0} : Initial shear curve superimposed from V_1 and V_2

$V_{12_{next}}$: Next, iterative shear curve superimposed from V_1 and $V_{2_{next}}$

V_2 : Initial shear curve from Beam 2

$V_{2_{next}}$: Next iterative shear curve for Beam 2

V_{total} : Total shear curve of the OP combining $V_{12_{next}}$ and V_{uplift}

V_{uplift} : Shear curve during instantaneous uplift

V_x : Strong axis shear demand

$V_{x_{max}}$: Maximum allowable strong axis shear demand from the Upper Column

V_y : Weak axis shear demand

$V_{y_{max}}$: Maximum allowable weak axis shear demand from the Upper Column

W : Total weight of the column

w_{col} : Nominal weight per unit length of the column

$\boldsymbol{X}$: Edge displacement of uncompressed disc spring, $t\sin(\beta)$

$\boldsymbol{X_{initial}}$: Initial estimation of edge displacement of an uncompressed disc spring, $t\sin(\beta)$

$\boldsymbol{X_{new}}$: Next estimation for X

$\boldsymbol{Y}$: Change in the Y-axis of the disc spring thickness of an uncompressed disc, $t\cos(\beta)$

$\boldsymbol{Y_{initial}}$: Initial estimation for change in the Y-axis of the disc spring thickness of an uncompressed disc, $t\cos(\beta)$

$\boldsymbol{Y_{new}}$: Next estimation for Y

$\boldsymbol{\bar{y}}$: Centroid of object

$\boldsymbol{Z_{x_{max}}}$: maximum X-axis plastic section

$\boldsymbol{Z_{x_{UC}}}$: Plastic section of the Upper Column about the X-axis (strong axis)

$\boldsymbol{Z_{y_{max}}}$: Maximum Y-axis plastic section

$\boldsymbol{Z_{y_{UC}}}$: Plastic section of the Upper Column about the Y-axis (weak axis)

$\boldsymbol{\alpha}$: Ratio of ID/OD of the disc spring

$\boldsymbol{\beta}$: Angle of conical disc height in the disc spring

$\boldsymbol{\beta_{initial}}$: Initial estimation for the β

$\boldsymbol{\beta_{solved}}$: Next estimation for β

$\boldsymbol{\delta}$: Range of spring deformation

$\boldsymbol{\delta_{1_{end}}}$: Required end displacement for modeled cantilever beam excluding δ_{up}

$\boldsymbol{\delta_{beam}}$: Displacement along the beam

$\boldsymbol{\delta_{Force}}$: Spring deformation curve from force

$\boldsymbol{\delta_{max}}$: Maximum, required OP displacement, equal to t_{ULP}

$\boldsymbol{\delta_{next}}$: Next spring deformation estimate from Beam 1 and 2 superposition

$\boldsymbol{\delta_{s_0}}$: Initial deformation of the disc springs to create pretensioning in the upper bolts

$\boldsymbol{\delta_{s_1}}$: Displacement of the OP at L_1 using D_1

$\boldsymbol{\delta_{s_2}}$: Initial spring deformation set equal to δ_{s_1}

$\boldsymbol{\delta_{s_{2_{next}}}}$: Estimation of final spring deformation calculated from $D_{12_0}(L_1)$ or $D_{12_{next}}(L_1)$

$\boldsymbol{\delta_{s_{total}}}$: Spring deformation from pretensioning and OP displacement

$\boldsymbol{\delta_{s_{total_{next}}}}$: Next calculation for total spring deformation

$\boldsymbol{\delta_{up}}$: OP free end displacement due to F_{up}

$\boldsymbol{\mu}$: Friction coefficient

$\boldsymbol{\sigma_{bending}}$: Stress demand at the IP welds from bending

$\boldsymbol{\sigma_{cap}}$: Stress capacity

$\boldsymbol{\sigma_{total}}$: Total demanded stress on the IP welds

$\boldsymbol{\sigma_{weld}}$: Stress demand on weld from V_x

$\boldsymbol{\phi}$: Resistance factor

Chapter 1: Introduction

1.1 Steel Column Splices

Column splices are critical components in steel structures greater than three stories, ensuring the stability and integrity of the building framework. Splices are required when standard column lengths are insufficient for the design height of the structure due to transportation considerations or necessary variations in cross-section shapes.

Current industry standards use bolted and/or welded plates to connect column components. Common splice variations connect two sections with end plates, also known as cover plates, at the end column face (shown left in Figure 1.1) or with cover plates welded or bolted to the columns' web and flanges (shown right in Figure 1.1). Load is transferred from the upper column to the lower column through direct compressive bearing of the flanges or directly through the plates and connecting bolts when experiencing tension. For columns in steel gravity framing where the factored loads produce only axial load in the columns, there are no requirements for splice flexural strength in any American Institute of Steel Construction (AISC) specifications or other building code reference standards. The required shear strength of column splices in steel gravity framing depends on the seismic criteria used to design the lateral force-resisting system, as described later in this document. [1]

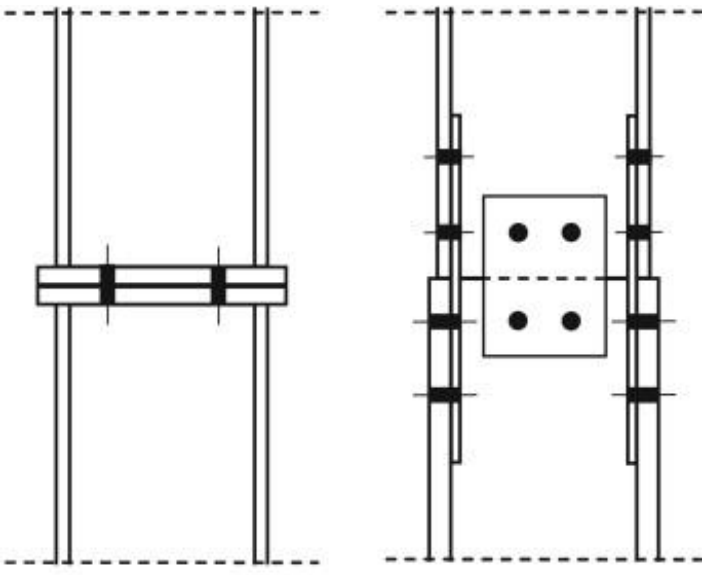

Figure 1.1: Typical W-shape steel column splices illustrating end plate splice (left) and internal flange cover plate splice (right) [2].

Recommendations for designing spliced connections, as reported at the NASCC Steel Conference in 2016, emphasize ensuring proper erection and worker safety [3]. The suggested guidelines include designing for welds and bolts based on the required forces and avoiding the overuse of completed joint penetration welds, especially for field welded splices where the columns have a design tension demand. For gravity column design, W14 shapes are recommended for clean column lines. Complex geometry splices should undergo trial fits in the shop before being transported and assembled on-site. Safety considerations for ironworkers should be included in calculating column strength, accounting for a 200-pound ironworker and a 70-pound tool belt. Welded splices should be left in their as-welded condition for aesthetics. Special considerations must be given to field-welded systems, considering splice alignment, temporary support, in and out-of-position welding access, and post-welding inspection. Although field welding can be more dangerous, it can reduce splice weight evaluated in loading requirements or provide aesthetics. [3]

1.2 On-site Construction of Column Splices

Standard erection practice for W-shape column splices begins with lowering an upper column onto a lower column guided by ironworkers. While one column may arrive with plates pre-bolted or pre-welded, the connecting column must be bolted and/or welded onsite. In some designs temporary bolts, meeting the Occupational Safety and Health Administration (OSHA) requirements, hold the two columns in place while plates are welded to the columns. Final bolting and/or welding is generally completed some time later, requiring a return visit from ironworkers.

These on-site processes are labor-intensive and contribute to schedule delays. Risky conditions during splicing include fall risks for workers and equipment, the risk of column pinching during assembly, and weld hazards such as metal fumes, eye damage, and burns. Data collected by the U.S. Department of Labor found that steel erection is among the top 10 hazardous occupations [4].

Ironworker labor conditions can be improved, and steel gravity frame erection time can be reduced by implementing a new column splice design. A prefabricated design would eliminate on-site welding and bolting, thereby reducing fall risks and welding hazards and increasing

erection efficiency. Additionally, an improved column placement guide would reduce pinching during the placement of columns. [5]

1.3 SnapLocX Connection Solution for Speeding Steel Construction

This report, funded by the American Institute of Steel Construction (AISC), presents the first part of a multi-phase project to develop and manufacture an industry-ready solution for improving column erection. AISC presented a SpeedConnection challenge, inviting engineers across America to propose fast and easy steel connection designs, including concepts for column splices. A winning column splice design was submitted by co-PI and Industry Advisor for this project, Reid Zimmerman of KPFF Engineers.

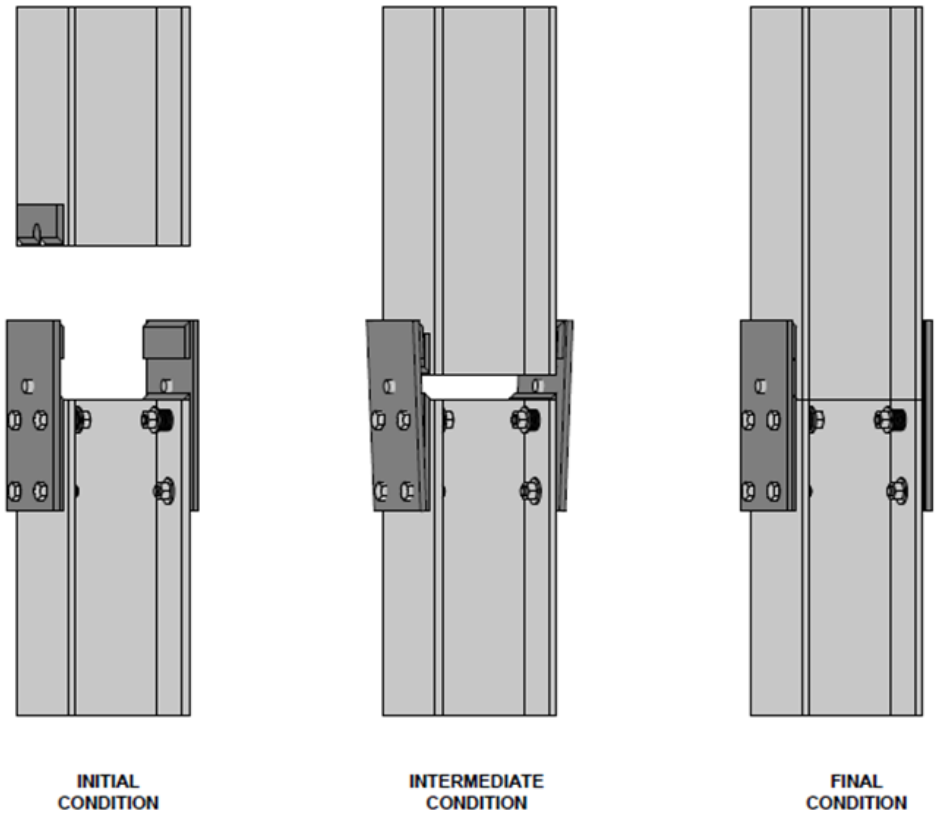

Figure 1.2: Proposed assembly of the SnapLocX Connection design.

The SnapLocX Connection prepared by Zimmerman is intended to remove all field welding and bolting from gravity column connections to simplify the erection of steel gravity framing. The simplification of on-site work is intended to improve ironworker safety through the "snap-and-lock" action of the plates on prefabricated columns. Figure 1.2 displays the SnapLocX

Connection concept during the columns' initial, intermediate, and final conditions, demonstrating how the plates will deform during installation.

The SnapLocX Connection utilizes shop-bolted plates affixed to the lower column that act as snapping plates and shop-welded plates on the column above the splice. This connection design limits the number of required bolts to eight, all located on the lower column. The snapping plate bolted to the lower column can deform without yielding via its own flexibility and with the use of disc springs (Belleville washers) on the upper row of bolts.

The SnapLocX Connection is also designed to accelerate the construction of subsequent floor framing. In standard building construction, a crane and ironworker are required to place the upper column and install OSHA-required temporary erection bolts. After additional columns are placed, workers must return to the previous columns to finalize the configuration by performing field welding or adding additional bolts. The SnapLocX Connection would be fabricated entirely in the shop and shipped to the construction site preassembled.

Due to its snapping configuration, the SnapLocX Connection allows crane operators and ironworkers to drop the upper column down into the lower column, where the prefabricated SnapLocX Connection would secure the two columns to each other. This process would eliminate additional scheduled time for further assembly compared to traditional methods, as the temporary erection stage and site welding and bolting are bypassed completely. Once locked into place, the connection can immediately resist all load effects across the splice. By utilizing standard methods and materials to produce a novel product, the SnapLocX Connection can easily be implemented into current column splicing.

1.4 Research Objectives

The research objectives outlined for this thesis have been constructed to facilitate the conceptual development of the SnapLocX Connection and demonstrate the feasibility of the connection from a design standpoint. The objectives are to:

- Design a SnapLocX Connection column splice for reasonable column shape pairings.
- Evaluate an example design connection for weak and strong axis shear, flexural yielding, and organizing the various design limit states.

- Standardize the example design considerations across W10, W12, and W14 column pairings.
- Create a splice catalogue for structural engineers and fabricators.

Future work may involve conducting large-scale experiments of the designed SnapLocX Connection.

1.5 Overview of Report

This report summarizes the literature review and analytical research of the current fabrication and construction of W-shape steel column splices. The research, design, and analysis processes focus on snapping mechanisms for column shapes W14, W12, and W10, using disc spring washers under the design provisions provided by AISC. Catalogues of standardized connections are developed based on analytical research.

Chapter 2 reviews prior research and literature relevant to the design of the SnapLocX Connection. A report from OSHA emphasizes column erection and splice hazards that should be considered during a design. Research in stiffness and strength of column splices was reviewed to identify gaps in research and design for rapid interlocking assembly for wide flange steel column connections. Additionally, literature on disc springs was also examined to provide a background on their behavior and design considerations for use in a column splice connection.

Chapter 3 introduces the conceptualization of the SnapLocX Connection design, which, through the snapping and locking splice components, aims to reduce the need for on-site welding and bolting.

Chapter 4 reviews the critical design considerations required for a wide flange column connection, as given in various building code reference standards. Strength considerations include shear requirements in the strong and weak axis directions, snapping plate flexural yielding during assembly, bolt spacing considerations, and the OSHA requirements for splice flexural strength.

Chapter 5 standardizes computations from the example design considerations for splices of W10, W12, and W14 of the same shape class. Plate sizes and families are introduced and a catalogue assigns connection plate elements, bolts, and disc springs to a given column splice pairing.

Chapter 6 concludes the report with a summary of the research performed, research conclusions, and recommendations for future research on the SnapLocX Connection.

Chapter 2: Literature Review

The following chapter reviews analytical and experimental literature as it is related to the evolution of the SnapLocX Connection for steel column connections. It draws on research surrounding topics on column splices and analyses of disc springs. These studies contribute to the design and improvement of the SnapLocX Connection system.

2.1 OSHA: Safety Standards for Steel Erection [5]

The Occupational Safety and Health Administration sets requirements for safety during steel erection in a document titled *Safety Standards for Steel Erection* and denote the *OSHA Requirements* herein. This standard identifies hazards and outlines safety standards for ironworkers during steel construction, including those related to welding and column splices. OSHA emphasizes that building components should require the same attention to safety standards as are necessary for the building's occupants. The document calls for the use of preventative, controllable, or preferable methods to eliminate or reduce nearly all hazards.

The *OSHA Requirements* highlights specific hazards associated with the placement and securement of columns. Column splices that require multiple numbers of parts, tools, bolts, nuts, washers, etc., increase the risk of falling and dropping objects, creating overhead hazards. Reducing the parts required for assembly would also reduce the amount of hands-on work required of the employees to place and secure the column, decreasing the possibility of pinching, crushing, or cutting fingers or limbs. Reducing the number of parts involved in column erection can improve worker safety, but it must not impact the column splice strength.

While many professionals consider welding connections faster than bolting, they present significant safety concerns. Hazards associated with welding can arise from environmental factors, creating more slip and fall risks and creating falling object hazards for other workers. Welding can also lead to bodily injuries, including back injuries from equipment and injuries associated with vision impairment from the welding hood. Additional concerns with field welding include extended construction time due to tack and final welds and post-weld inspection, potential structural integrity concerns if not performed correctly, and the increased construction cost of hiring welders.

The *OSHA Requirements* also states that worker hazards can be reduced by minimizing the number of interactions a worker has with a splice. There is an increased risk of falling or slipping when working on a splice in a wet environment or with steel members encased in a protective coating. Consequently, it is recommended that it is safest and most accessible for workers only to visit a connection once.

The Steel Erection Negotiated Rule Making Advisory Committee (SENRAC) and assisting engineers determined that each column splice must resist a minimum eccentric gravity load of 300 lbs, similar to the requirement for column anchorage, applied 18 in. in all directions from the outer face. This eccentric gravity load requirement eliminates collapse hazards from column instability during erection.

2.1.1 SnapLocX Design Considerations from OSHA Safety Standards

According to the *OSHA Requirements*, the conceptualization and design of the SnapLocX Connection must address current column erection hazards to enhance worker safety and reduce construction time. Annually, approximately 35 fatalities and 2,300 injuries occur due to steel construction-related activities, as detailed in Table 2-1 [5]. Even minor modifications in steel construction processes and designs can significantly improve health and safety outcomes.

Table 2-1: Estimated yearly worker injuries, deaths, and preventable statistics following health and safety requirements. [5]

	Number of fatalities and lost-workday injuries currently occurring among iron workers (a)	**Number of fatalities and lost-workday injuries preventable by compliance with the existing standard**	**Additional number of fatalities and lost-workday injuries preventable by compliance with the final standard**	**Total number of fatalities and lost-workday injuries preventable by compliance with the existing and final standards**	**Number of fatalities and lost-workday injuries judged not to be preventable by either standard based on analysis of accident and fatality data**
Fatalities	35	8	22	30	5
Lost-Workday Injuries	2,279	303	838	1,142	1,137

To mitigate worker hazards and lower construction costs, the design of the SnapLocX Connection should aim to eliminate or reduce the need for on-site bolting and welding. This can be achieved by delivering columns with prefabricated splice components that lock into place

during installation. Additionally, the SnapLocX Connection must be designed to withstand a 300-pound eccentric gravity load to ensure column stability during construction, as all column splices must be per the *OSHA Requirements*.

2.2 Column Splices

The current body of research on column splices reveals a notable gap in W-shape interlocking column splices adapted for rapid assembly. Existing studies predominantly concentrate on stability design criteria and connection stiffness and strength of a column splice [1], [2], [6], [7].

Column splice connections for reinforced concrete occupies the majority of research into column building materials where rebar is placed at splice locations [8], [9], [10]. Studies concerning steel column splices primarily revolve around Square Hollow Section (SHS) shapes [11]. Although research has been successfully implemented for W-shape beam splices, their applicability to gravity frame columns remains heavily unknown [12].

This literature review addresses the research gap in gravity frames while also noting previous research beneficial to the splice design criteria.

2.2.1 Column Splices as Treated in the AISC Manual of Steel Construction [13]

The "Column Splices" Section in Part 14: "Design of Beam Bearing Plates, Column Base Plates, Anchor Rods, and Column Splices" of the AISC Manual of Steel Construction, 16th Edition, denoted *the Manual* herein, provides a comprehensive overview of the AISC requirements governing the current design and analysis of column splices [13].

The Manual recommends that column splices should be consistently located at the same height throughout a structure. The design approach for column splices idealizes full bearing across the spliced faces, with bolt tensioning and welding fabrication typically occurring on-site. The design capacity is engineered to be significantly greater than the anticipated loads the fabricated column would be subject to.

Safety is vital during the erection of columns and columns with column splices, requiring a thorough inspection of the structure, equipment, and personnel involved. An inspection of all welds on lifting and stability devices is mandatory. Groove welds of a splice are frequently examined with ultrasonic methods, while fillet welds undergo inspection with magnetic particle

(MT) or liquid dye penetrant (PT) methods. Weld inspections are conducted in the shop before the columns arrive on site and during field erection to guarantee no damage has occurred during shipping.

The axial force transfer within column splices is provided through bearing at the column ends with additional connecting plates provided when needed. The determination of bearing from one column face to another requires sufficient bearing area, i.e., overlap between the upper and lower column cross sections. Notably, as the nominal weight per foot of a W-shape increases for each nominal depth, both the flange and web thickness increase accordingly and bearing area is different for splices of different sections even within one nominal section depth (i.e., with the W14 shapes).

The available bearing strength ($\phi\ R_n$)of a finished surface is derived from *the Steel Specification*., where F_y represents the minimum yield stress of the connecting columns and A_{pb} represents the projected bearing area between the upper and lower flanges. The nominal bearing strength (R_n), provided in Equation 2-1, is combined with the resistance factor for bearing (ϕ), as referenced in Equation 2-2, to determine the design bearing strength.

$$R_n = 1.8\ F_y\ A_{pb}$$

Equation 2-1

$$\phi = 0.75$$

Equation 2-2

The design strength for bearing is considered highly conservative compared to axial strength and is rarely the critical design strength limit. In addition to axial and bearing strength considerations, column splices are required to withstand tension resulting from dead and lateral load combinations.

Shear forces generated by lateral loads are distributed through the column and are countered by friction on contact-bearing surfaces, flange plates, web plates, or butt plates. If the required shear force exceeds the capacity of a standard column splice, as stated in Table 14-3 from *the Manual* and provided below in Table 2-2 for reference, a sufficient column connection must be engineered.

The column splices listed in Table 2-2 satisfy OSHA's force requirement of 300 lbs at 18 in. from the column faces, ensuring compliance with safety standards.

For flange-plated column splices, *the Manual* offers detailed descriptions of typical column splices that adhere to AISC/ANSI 360-22, the Specifications for Structural Steel Buildings, denoted *the Steel Specification* herein [14].These details outline typical designed features but are not requirements. It is assumed that designed splices feature a heavier lower column; however, heavier lower columns don't necessarily have a deeper section than their upper column pairing. The full bearing of a splice occurs when columns from the same nominal group are centered over each other. In cases where additional bearing strength is needed, finished fillers may bear on the larger column, while unfinished fillers may be used otherwise.

Table 14-3 in *the Manual* presents W-shape column splices with all-bolted and flange-plated columns, provided in Cases I and II. These cases typically utilize the same size high-strength bolts across the splice, with bolt spacing and edge distances meeting requirements set in *the Steel Specification*.

Cases IV and V are designated for W-shape, all-welded flange-plated column connections. Welds are typically created using standard E70XX electrodes with a required 1/16 in. clearance. Weld lengths allow for 2 in. of unwelded distance above and below the splice location, providing flexibility in the splice arrangement.

Cases VI and VII in *the Manual* detail splices that use a combination of bolts and welds, where it is likely that the strength of the welds surpasses the strength of the bolts. In these cases, weld lengths may be reduced considering the weld design strength exceeds the demanded strength, including assembly loading.

Further information is provided for directly welded W-shaped flange column splices, butt-plated W-shaped column splices, and Hollow Structural Section (HSS) cap plate splices.

Table 2-2: Sample of referenced Table 14-3 from the Manual for column splice connection Case I – Case III. Additional cases can be located in Part 14 of the Manual. [13]

Table 14-3
Typical Column Splices
Case I:
All-bolted flange-plated column splices between columns with depth d_u and d_l nominally the same.

Column Size	Gage g_u or g_l in.	Flange Plates: Type	Width in.	Thk. in.	Length
W14×455 to 730	13½	1	16	¾	1′ 6½
257 to 426	11½	1	14	⅝	1′ 6½
145 to 233	11½	1	14	½	1′ 6½
90 to 132	11½	2	14	⅜	1′ 0½
43 to 82	5½	2	8	⅜	1′ 0½
W12×120 to 336	5½	2	8	⅝	1′ 0½
40 to 106	5½	2	8	⅜	1′ 0½
W10×33 to 112	5½	2	8	⅜	1′ 0½
W8×31 to 67	5½	2	8	⅜	1′ 0½
24 & 28	4	2	6	⅜	1′ 0½
Gages shown may be modified if necessary to accommodate fittings elsewhere on the column.					

Case I-A: $d_l = (d_u + \frac{1}{4}$ in.) to $(d_u + \frac{5}{8}$ in.)	Flange plates: Select g_u for upper column; select g_l and flange plate dimensions for lower columns (see table above). Fillers: None. Shims: Furnish sufficient strip shims $2\frac{1}{2}\times\frac{1}{8}$ to provide 0 to $\frac{1}{16}$-in. clearance each side.
Case I-B: $d_l = (d_u - \frac{1}{4}$ in.) to $(d_u + \frac{1}{8}$ in.)	Flange plates: Same as Case I-A. Fillers (shop bolted under flange plates): Select thickness as $\frac{1}{8}$-in. for $d_l = d_u$ and $d_l = (d_u + \frac{1}{8}$ in.) or as $\frac{1}{4}$-in. for $d_l = (d_u - \frac{1}{8}$ in.) and $d_l = (d_u - \frac{1}{4}$ in.) Select width to match flange plate and length as 0′ 9 for Type 1 or 0′ 6 for Type 2. Shims: Same as Case I-A.
Case I-C: $d_l = (d_u + \frac{3}{4}$ in.) and over.	Flange plates: Same as Case I-A. Fillers (shop bolted to upper column): Select thickness as $(d_l - d_u) / 2$ minus $\frac{1}{8}$ in. or $\frac{3}{16}$ in., whichever results in $\frac{1}{8}$-in. multiples of filler thickness. Select width to match flange plate, but not greater than upper column flange width. Select length as 1′ 0 for Type 1 or 0′ 9 for Type 2. Shims: Same as Case I-A.
For lifting devices, see Figure 14-10.	

Table 14-3 (continued)
Typical Column Splices
Case I:
All-bolted flange-plated column splices between columns with depth d_u and d_l nominally the same.

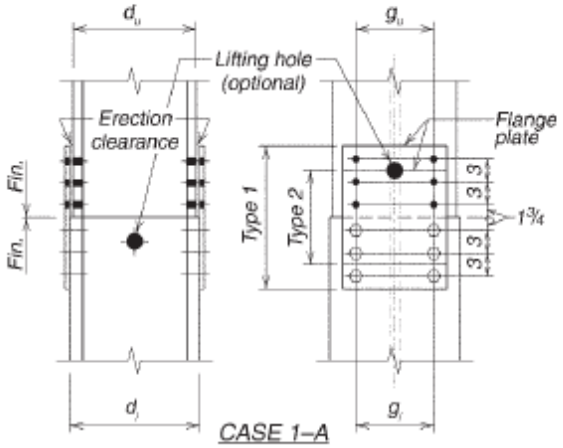

CASE 1–A

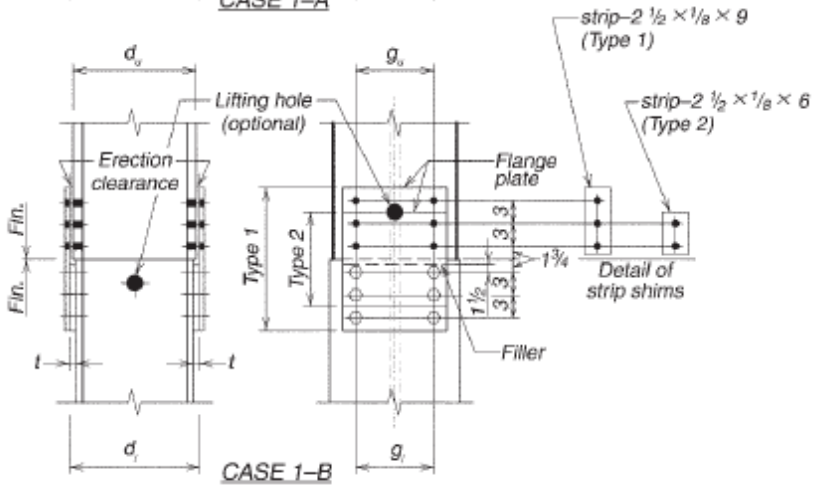

CASE 1–B

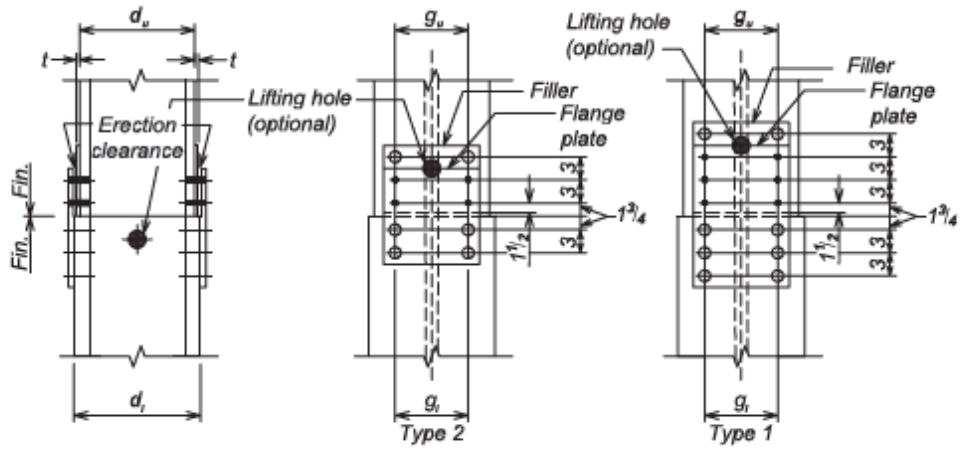

CASE 1-C

Table 14-3 (continued)
Typical Column Splices
Case II:
All-bolted flange-plated column splices between columns with depth d_u nominally 2 in. less than depth d_l.

Fillers on upper column developed for bearing on lower column.	Flange plates: Same as Case I-A. Fillers (shop bolted to upper column): Select thickness as $(d_l - d_u) / 2$ minus $\frac{1}{8}$-in. or $\frac{3}{16}$-in., whichever results in $\frac{1}{8}$-in. multiples of filler thickness. Select bolts through fillers (including bolts through flange plates) on each side to develop bearing strength of the filler. Select width to match flange plate, but not greater than upper column flange width unless required for bearing strength. Select length as required to accommodate required number of bolts. Shims: Same as Case I-A.

Table 14-3 (continued)
Typical Column Splices
Case III:
All-bolted flange-plated and butt-plated column splices between columns with depth d_u nominally 2 in. less than depth d_l.

Fillers on upper column developed for bearing on lower column.

Column Size	Gage g_u or g_l	Flange Plates			
		Type	Width	Thk.	Length
W14×455 to 730	13½	1	16	¾	1′ 8½
257 to 426	11½	1	14	⅝	1′ 8½
145 to 233	11½	1	14	½	1′ 8½
90 to 132	11½	2	14	⅜	1′ 2½
43 to 82	5½	2	8	⅜	1′ 2½
W12×120 to 336	5½	2	8	⅝	1′ 2½
40 to 106	5½	2	8	⅜	1′ 2½
W10×33 to 112	5½	2	8	⅜	1′ 2½
W8×31 to 67	5½	2	8	⅜	1′ 2
24 & 28	3½	2	8	⅜	1′ 2

Gages shown may be modified if necessary to accommodate fittings elsewhere on the column.

Flange plates: Select g_u for upper column, select g_l and flange plate dimensions for lower column (see table above).
Fillers (shop bolted to upper column): Same as Case I-C.
Shims: Same as Case I-A.
Butt plate: Select thickness as 1½-in. for W8 upper column or two inches for others. Select width the same as upper column and length as $d_l - \frac{1}{4}$ in.

For lifting devices, see Figure 14-10.

Table 14-3 (continued)
Typical Column Splices
Case II and III:
All-bolted flange-plated column splices between columns with depth d_u nominally 2 in. less than depth d_l.

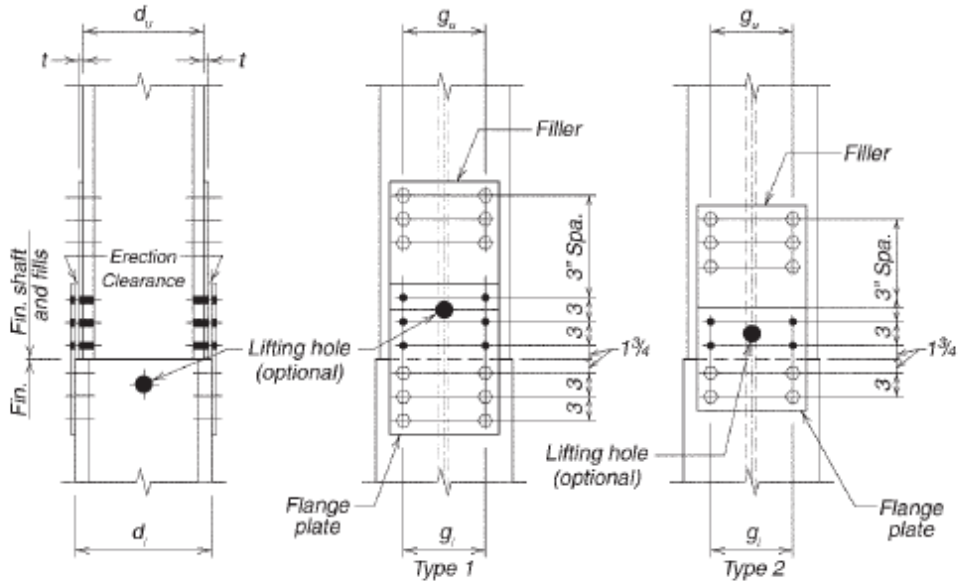

CASE II

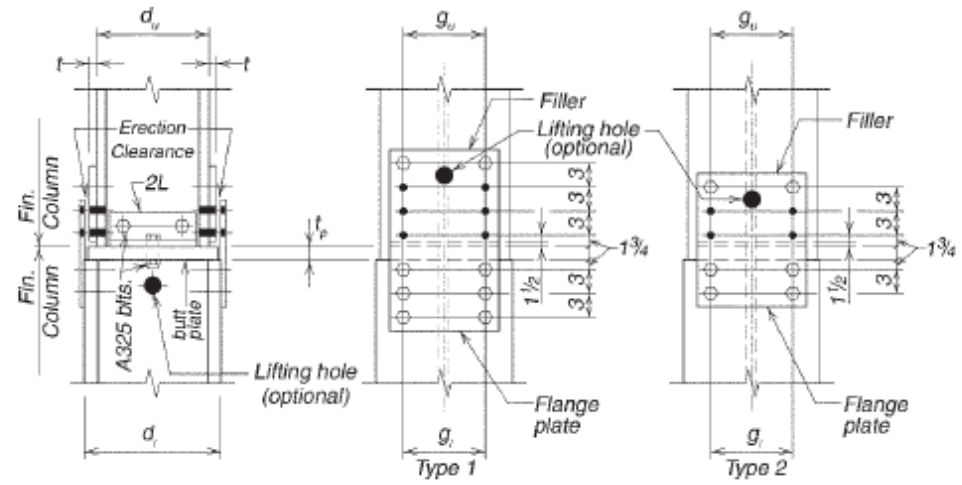

CASE III

2.2.2 Snijder and Hoenderkamp: Experimental Tests on Spliced Columns for Splice Strength and Stiffness Requirements [6]

Snijder and Hoenderkamp's 2006 study investigates variations of stiffness and strength across splice variations [6]. Their research has proved invaluable in column research, with numerous papers further exploring and building on their findings.

In their study, based on columns and column splices designed for second-order bending moments, shear forces, and axial loads, strength and stiffness requirements are derived from stability requirements stated in the Eurocode. The column stiffness is modeled with a 5% reduction in the Euler Buckling Load for an imperfect column. Joints and splices were viewed as rigid elements if the ultimate resistance of the column was not affected by 5% of that of a fully rigid joint.

The strength requirement derived from the study is illustrated as model (a) in Figure 2.1, depicting the splice location as a distance x from the base of the column. Meanwhile, the stiffness requirement, modeled using the Euler buckling load of a spliced column by combining two systems (Fe1 and Fe2), is shown as model (b) in Figure 2.1.

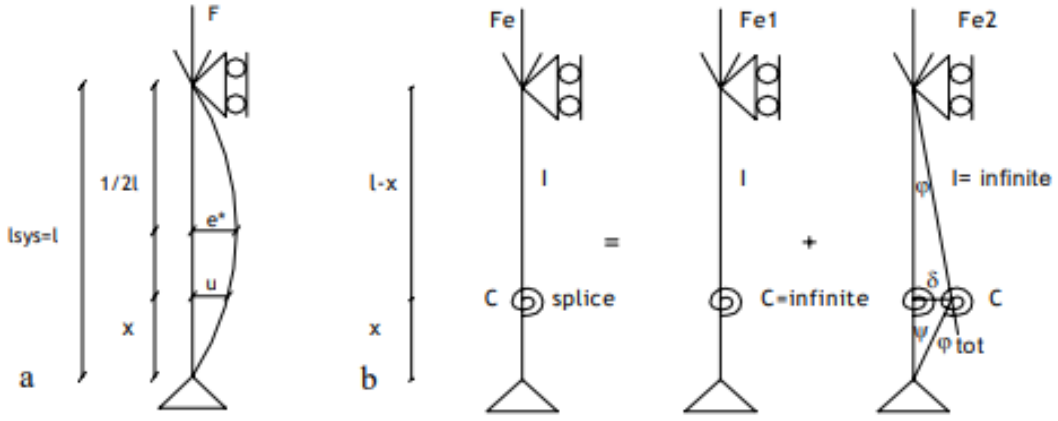

Figure 2.1: Strength (a) and stiffness (b) requirement model for columns and column splices [6].

Experimental testing was conducted based on the modeled stiffness and strength requirements, involving the modeling, analyzing, and testing of three distinct column splices along with an unspliced column for comparison. The test program was developed for lightweight sections to mitigate failure loads.

Figure 2.2 depicts the three splice models, designated as Splice A, Splice B, and Splice C, which were designed with HEA steel section HE100A. Splice A incorporated 12 mm bolted end plates, while Splice B featured 6 mm end plates. In contrast, Splice C connected the column using cover plates bolted over the web, reducing initial rotational stiffness.

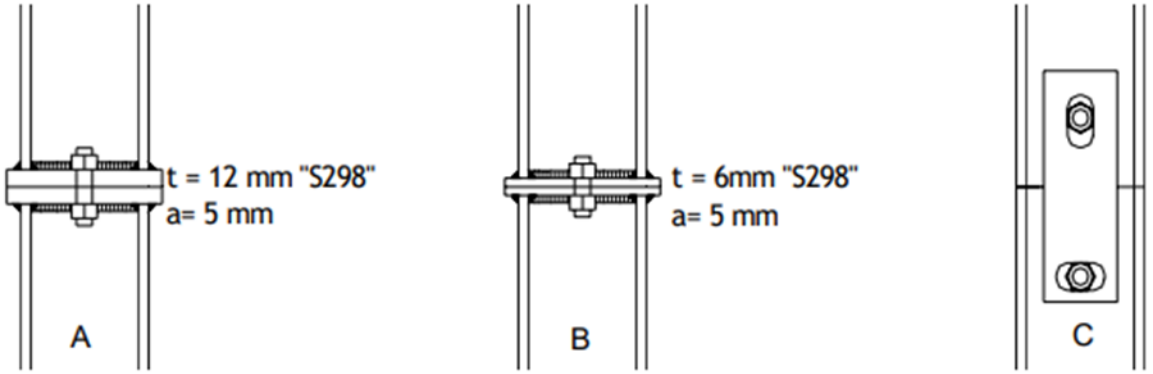

Figure 2.2: Column splices tested by Snijder and Hoenderkamp for stiffness and strength [6].

Experimental testing revealed that the column without a splice exhibited the highest stiffness, as expected, contrasting with Splice A's relatively high stiffness, Splice B's intermediate stiffness, and Splice C's minimum stiffness. The stiffness of the three splice connections did not satisfy the stiffness requirements stipulated in the Eurocode, and it was anticipated that the column's bearing capacities would be affected due to the inclusion of a splice. Additionally, the failure loads for an unspliced column were more significant than those with a splice.

In summary, Snijder and Hoenderkamp concluded that the experimental failure loads of columns exceeded those calculated from frictionless buckling curves, and unspliced columns provided higher stiffness values.

Tests also indicated that the stability of column splices using end plates, such as Splice A and Splice B, were not negatively impacted during tensile testing. Based on this, further research and testing was recommended for column splices.

2.2.3 Girao Coelho and Bijlaard: Requirements for the Design of Column Splices [7]

In their 2008 paper, Girao-Coelho and Bijlaard conducted an analytical analysis of the behavior of strength and stiffness for imperfect column splices with varying end restraints and stability

considerations [7]. Their work aimed to expand on previous research conducted by Snijder and Hoenderkamp in their 2006 paper "Experimental tests on spliced columns for splice strength and stiffness requirements" and their 2008 paper "The influence of end plate splices on the loading carrying capacity of columns." [7], [6], [1]

Girao-Coelho and Bijlaard's research delves into the two fundamental column splices: bearing and non-bearing. Both splices are engineered to transmit compressive loads from the upper column to the lower column via different systems. Splices in bearing achieve load transfer through direct bearing contact (Figure 2.3 (a)), while non-bearing splices utilize splice plates and bolts for force conveyance, as the column ends are not in contact (Figure 2.3 (b)). Due to direct bearing capacity, end plate connections provide a more convenient and efficient solution for splices compared to non-bearing splices.

Mandated by the Eurocode, non-bearing slices must have a design moment resistance of 25% of the moment of the weaker section in both the weak and strong axes. This requirement aims to create a structurally robust column that does not allow hinge behavior at the splice. The European code is based on continuous joint column models, categorizing joints as rigidly stiff and specifying that internal forces, eccentric forces, and forces from initial imperfections must also effectively be transferred by the column and splice material.

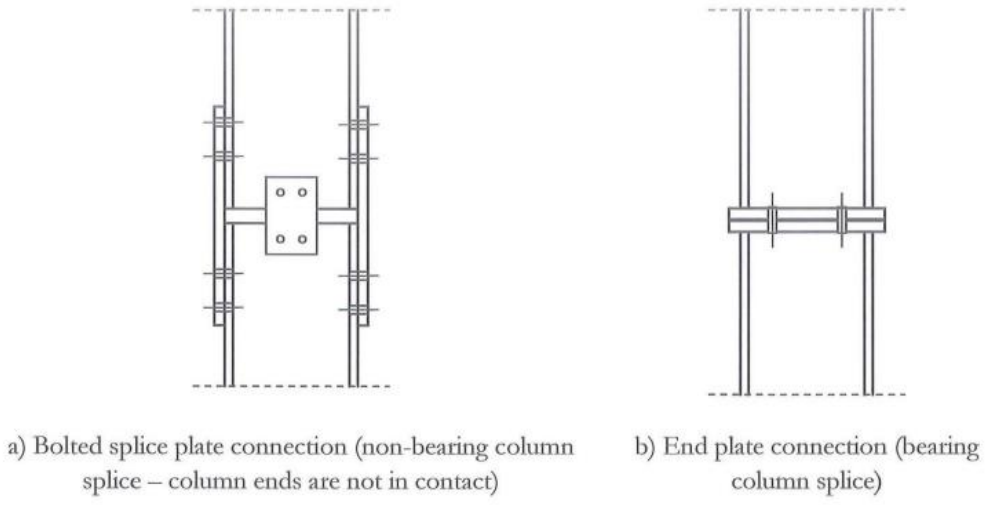

Figure 2.3: Column spice variations considered in research by Girao-Coelho and Bijlaard. [7]

The design framework for the column splices was structured following existing procedures for typical column splices, taking into account framing members using the effective length, the K-

factor. The K-factor is derived from an ideal continuous column with no imperfections. Braced columns fall within the range of $0.5 \leq K \leq 1.0$, while unbraced columns range from $1.0 \leq K \leq \infty$.

As per the Eurocode, bearing spliced columns are mandated to transmit 25% of the maximum compressive force. In contrast, non-bearing column splices are required to transmit internal forces and moments resulting from eccentricity, column imperfections, and second-order deformations. Figure 2.4 displays the column length considerations to determine the K-factor.

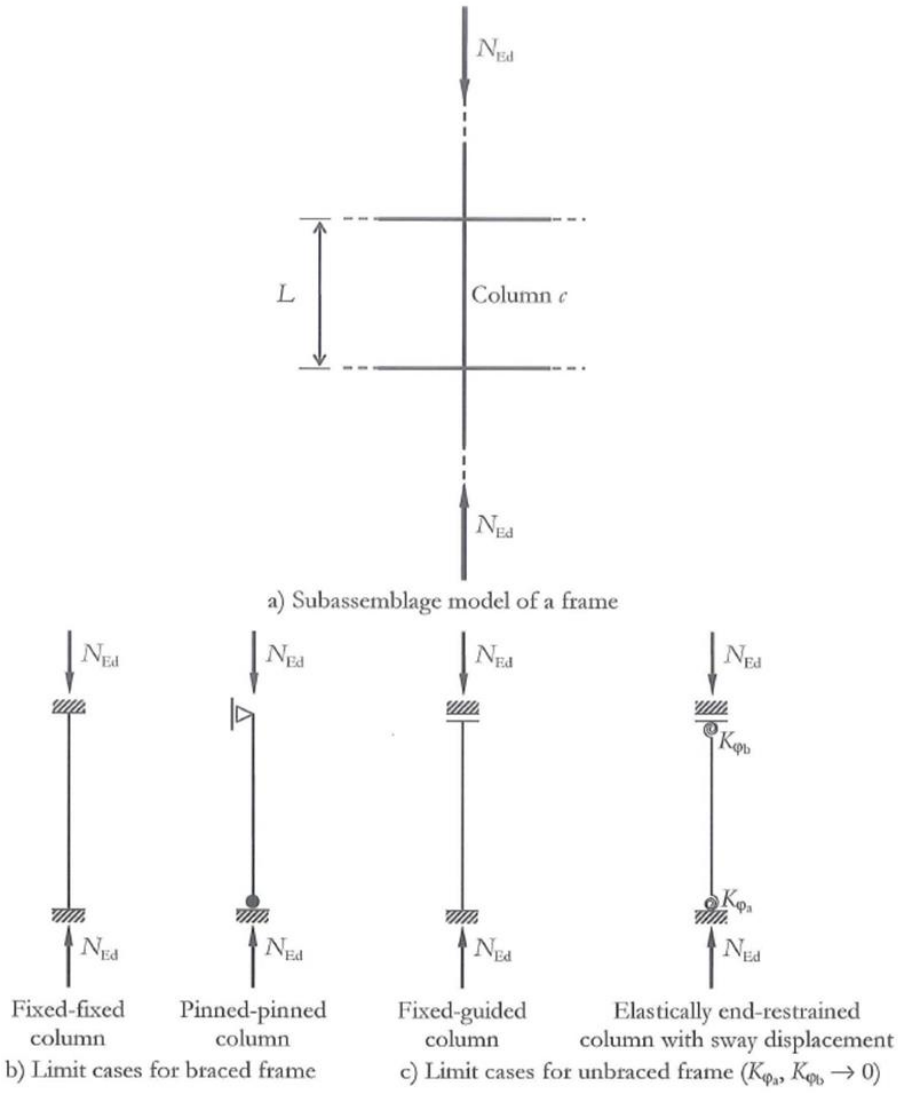

Figure 2.4: Framed column length considerations. [7]

The experimental research emphasized the importance of positioning the column splice away from critical sections and analyzing how the splice location can influence the column behavior

while taking into account the *K*-factor, as depicted in Figure 2.5. Apart from splice location, Girao-Coelho and Bijlaard also considered factors such as the second-order bending moment, column slenderness, and column boundary conditions.

Case	Deflection function	*K*-factor	
		Theoretical	Recommended design value
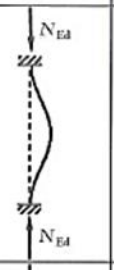	$v = \frac{M_\Delta}{N_{Ed}}\left(1-\cos\frac{2\pi x}{L}\right)$	0.5	0.65
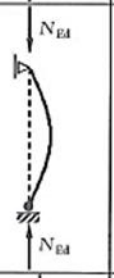	$v = A\sin\frac{\pi x}{L}$	1.0	1.0
	$v = \frac{\Delta}{2}\left(1-\cos\frac{\pi x}{L}\right)$	1.0	1.2
	$v = \Delta\sin\frac{\pi x}{2L}$	2.0	2.0

Figure 2.5: K values for idealized columns. [7]

It was concluded that critical loads for splices should be assessed for each boundary condition, including pinned-pinned, pinned-guided, fixed-pinned, fixed-fixed, and fixed-guided column configurations. This comprehensive approach ensures a thorough understanding of the impact of a splice location and boundary conditions on column behavior.

2.2.4 Lacey et al.: New Interlocking Inter-Module Connection for Modular Steel Buildings: Simplified Structural Behaviors [11]

Lacey, Chen, Hao, and Bi presented their research on interlocking steel column systems for modular buildings in their 2021 paper [11]. Their study aimed to enhance the constructability and performance of modular steel buildings by introducing prefabricated interlocking columns with inter-module connections.

The conventional approach to constructing modular buildings using Square Hollow Steel (SHS) columns with inter-module connections requires site welding and bolting, which can be costly to carry out and raises safety concerns for on-site workers. Previous research has explored various SHS column splice designs, but these designs were not without their concerns. Initial designs faced difficulties maintaining allowable tolerances, especially as additional stories were added, leading to tolerance accumulation and increased slip displacement under extreme lateral loading. Some designs also posed challenges for onsite fabrication due to complex bolt arrangements and inaccessible tension rod placement through the center of the SHS column.

Other concepts presented tolerance and drifting concerns due to the use of adhesive, while other designs increased the presence of onsite work by requiring welding or the use of concrete. Although specific designs demonstrated stable connections, they often came with a significant cost burden for building owners.

During the developmental research for a new concept, the Lacey team noticed an absence of testing standards for prefabricated structural components, highlighting a significant lack of standards for comprehensive structural assessments involving prefabricated components. They recommended continuing research into the structural performance of existing inter-modular connections to deepen their understanding and facilitate the advancement of improved connection systems.

The new design proposed by Lacey et al. suggested the connection of interlocking elements using structural bolts. These bolts would provide the necessary stiffness and slip resistance in the splice. At the same time, the interlocking components would contribute to shear resistance and aid in installation positioning, thereby enhancing construction safety. Figure 2.6 illustrates the proposed connection as a simplified connection between eight modules – four upper and four

lower – featuring a horizontal plate connection and bolted vertical connections. The horizontal plate connection is identified as P2, and the bolted vertical connection is identified as dark grey bolts.

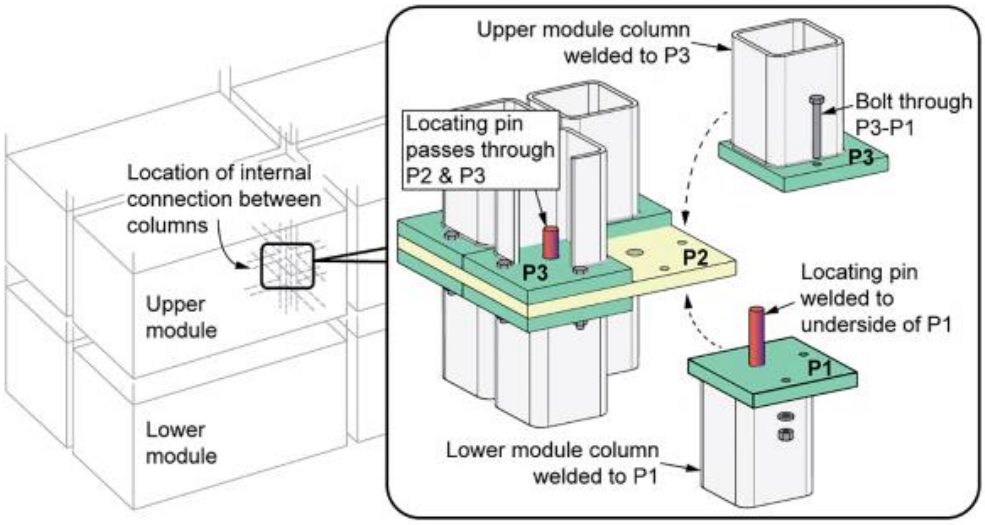

Figure 2.6: Proposed interlocking inter-module connection design. [11]

During the prefabrication phase, the locating pin (highlighted in red) is welded to the underside of the lower local horizontal plate (P1), which is then affixed around the exterior perimeter of the lower column module with welding. Simultaneously, a local horizontal plate (P3) is welded to the exterior perimeter of the upper column module.

During the onsite installation, P2 is positioned over the fixed lower column module and guided by the locating pins. Subsequently, the upper column modules are stacked onto P2 with continuous guidance from the locating pins. Once the column modules are appropriately positioned, P1, P2, and P3 are fastened together with structural bolts, which are tensioned to provide additional column stiffness.

This proposed design offers ease of installation on-site and simplified end-of-life dismantling. By eliminating the need for on-site welding and incorporating locating pins, the design enhances safety for field workers. However, along with its advantages, some drawbacks are considered. For instance, the installation of the P2 plates and bolt assembly and tensioning are necessary on-site, which may add to the complexity of construction. Additionally, securing the bolts on plates external to the column could potentially interfere with desired building aesthetics.

Initial concerns were addressed regarding providing the required installation tolerance without compromising the column's resistance to slip. Further experimental research was conducted to investigate the behavior of shear force slip.

Experimental testing was carried out using a simplified connection between two SHS columns for balanced compressive loading. Adequate bearing and weld clearances were ensured by incorporating a chamfer. The bolts were tensioned before testing. Figure 2.7 illustrates the experimental test drawings with component assignments. Figure 2.8 then provides the setup for testing. The experimental results were then compared with existing connections to evaluate shear behavior.

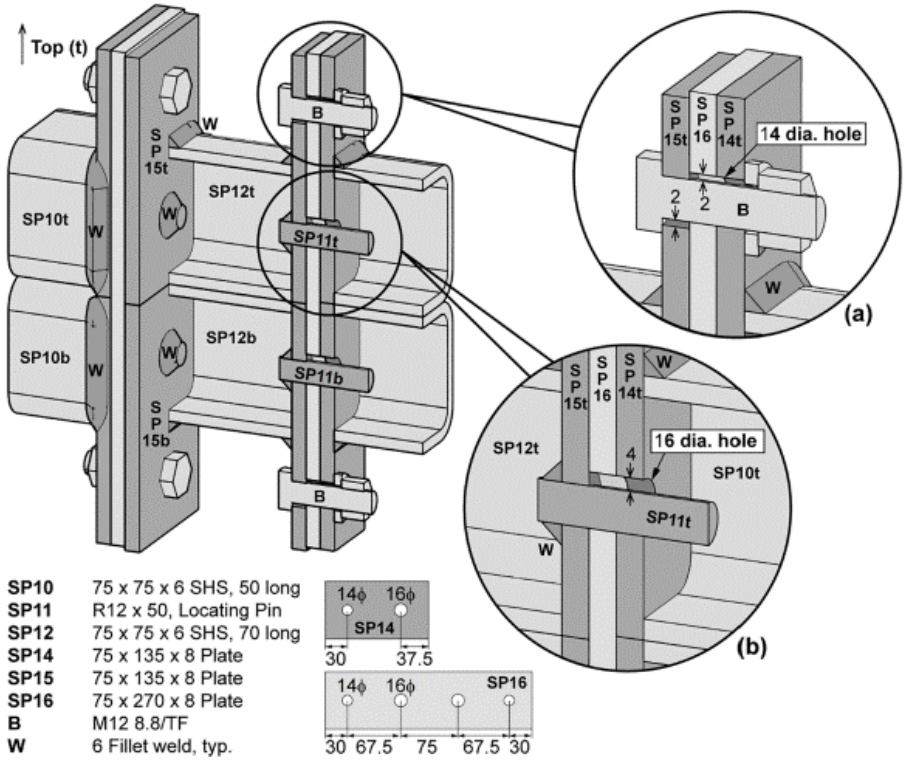

Figure 2.7: Experimental test set up for the inter-module connection design. [11]

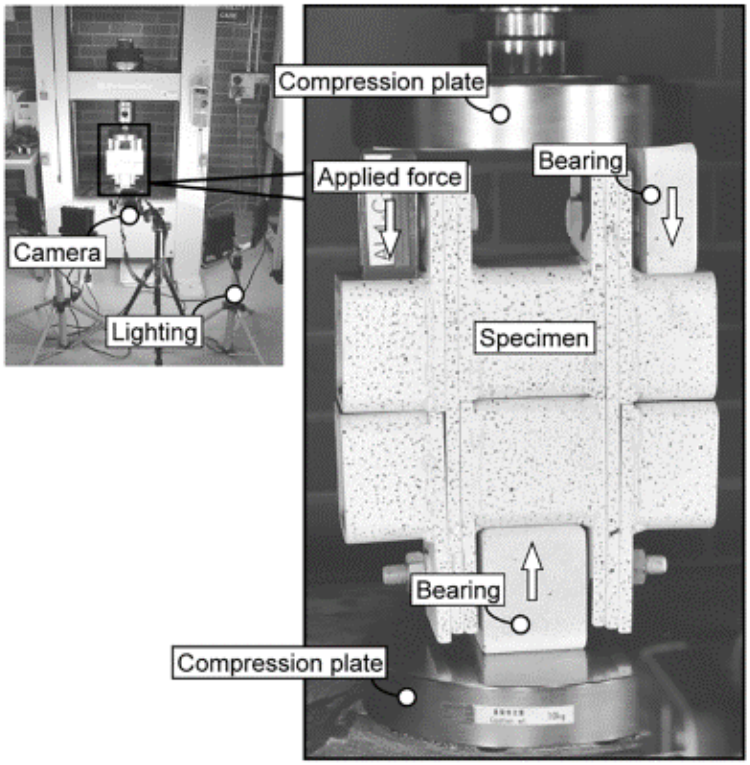

Figure 2.8: Inter-module connection test set up for shear and slip. [11]

Numerical simulations of each component were developed in ABAQUS and were then followed by experimental testing to study slip. The study revealed that slip resistance is influenced by slip factor and the tensioning of the bolts, with the locating pins contributing additional shear resistance after the initial slip occurs. Hole tolerances were found to have a minor impact on slip resistance. Overall, the connection design offered enhanced force-displacement stiffness compared to existing connections.

An empirical model was proposed to describe the shear force-slip behavior. This model was derived from calibrated numerical results and incorporated bearing, failure, friction, and slip.

2.2.4 SnapLocX Design and Considerations from Prior Column Splice Research

The general requirements for the design and required strength, including design bearing strength, of the SnapLocX Connection must be consistent with those outlined in Part 14 of *the Manual*. [13]

Research conducted by Snijder and Hoenderkamp, along with Girao-Coelho and Bijlaard, suggests that additional stability, stiffness, and strength analysis and testing should be conducted

on the spliced column for axial compression and tension, shear force, and bending moment. The SnapLocX Connection would likely need to be identified as a new buckling case, as spliced connections behave differently from unspliced columns. [6], [7]

Limited research has focused on W-shape interlocking steel column splices. However, Lacey, Chen, Hao, and Bi's study on efficient SHS interlocking splices highlights the importance of designs that reduce onsite workload while ensuring high-quality strength. Their research emphasizes that minimizing column slip at the connection splice and considering shear force are critical factors to be addressed. [11]

2.3 Nonlinear Elastic Geometry of Disc Springs

Originally patented in Paris in 1867 by Julein Belleville, disc springs have been found in numerous applications due to their ability to store and release energy, and their capability of implementation in small spaces. Various names include Belleville disc springs, conical washers, and coned disc springs [15]. Engineers have conducted numerous critical studies over the past century to analyze the behavior of disc springs, including the pioneering research by Almen and Laszlo in 1936.

The implementation of disc springs in the design of the SnapLocX Connection allows for the necessary displacements of the Outer Plate during splice assembly without causing the plate to yield. Additionally, the ability to pretension the bolts containing disc springs can enhance plate security after column assembly. The literature on elastic conical disc springs discusses their force-displacement behavior through experimental and numerical analysis and how the force-displacement curves can be manipulated by the spring's geometry to meet specific connection requirements.

2.3.1 Almen and Laszlo: The Uniform-Section Disk Spring [16]

General Motors Corporation research engineers, J. Almen and A. Laszlo, explored the behavior of conical disc springs due to their geometry in their 1936 report undertaking the study due to the lack of analytical behavior formulas in the field at the time [16].

Due to their unique geometric proportions, disc springs offer diverse load-deflection characteristics that typical coil springs cannot. The stiffness of the disc spring can vary based on the free height of the cone (h) relative to its thickness (t). Additionally, the force and

displacement behavior can be modified by the arrangement of disc springs in parallel and/or series.

Almen and Laszlo derived a formula to describe the force-displacement relation of a disc spring based on the spring geometry. They developed this formula using constant-thickness disc springs found in oil cans, as depicted in Figure 2.9, resulting in Equation 2-3. The geometric variables from the disc spring in this equation include the outer diameter ($O.D.$), constant washer thickness (t), inner diameter ($I.D.$), and free height (h), which represents the truncated cone formed by the upper or lower surface of the disc.

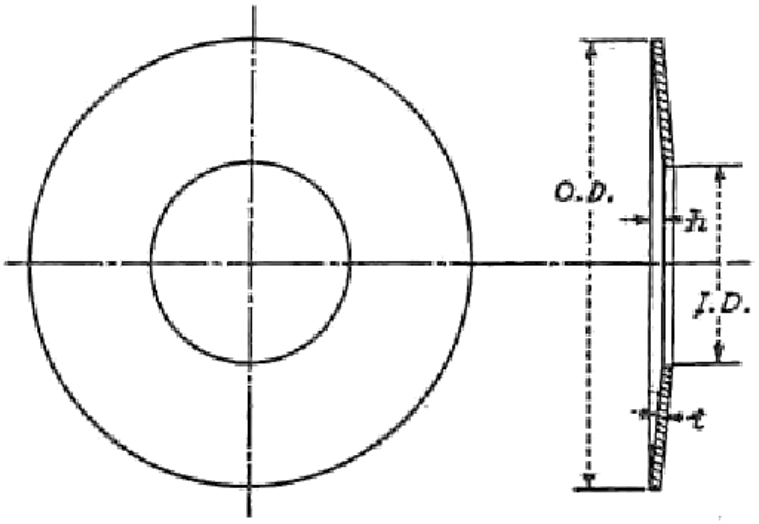

FIG. 2 ANNULAR-DISK SPRING

Figure 2.9: Annular disc spring geometry used to develop a force-displacement relationship. [16]

$$P = \frac{E\delta}{(1-\sigma^2)Ma^2}\left[(h-\delta)\left(h-\frac{\delta}{2}\right)t + t^3\right]$$

Equation 2-3

Equation 2-3 also incorporates additional variables such as a, representing the outside radius and equal to half the diameter; δ, denoting axial deflection; E, signifying the modulus of elasticity; σ, representing Poisson's ratio and M, a constant expressed as a function of the outside diameter and inside diameter ratios.

Initial experimental testing involved determining load-deflection curves from a constant downward force for the disc springs with varying h values plotted in Figure 2.10 and comparing the results to the analytical curves. All other spring dimensions were kept constant throughout this testing process. Results from these tests indicate that as the conical height (h) increased, the allowable disc deflection range increases. Furthermore, the load capacity for deformation increased as h increases.

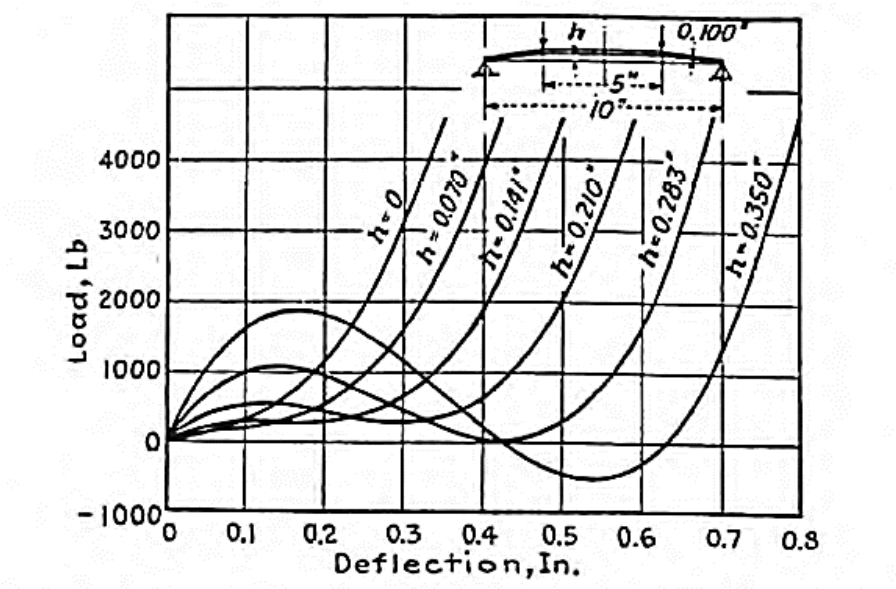

Figure 2.10: Experimental force-displacement curves for disc springs of varying h. [16]

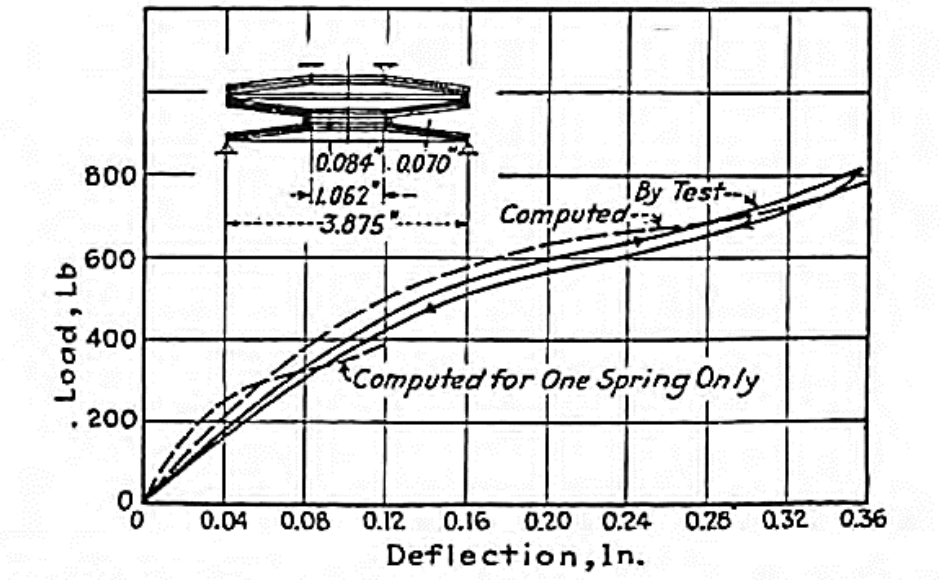

Figure 2.11: Experimental and analytical curves for springs in series and parallel. [16]

In Figure 2.11, additional experimental tests were conducted on disc springs arranged in series and parallel stacks. These tests revealed that the deflection of a single spring tripled when three discs were arranged in series, while the load capacity doubled when two springs were used in parallel. Comparisons between the experimental data and analytical predictions indicated similarities in the curves, demonstrating good agreement between theoretical and practical testing.

The flexibility of a disc spring is influenced by the ratio of the outer diameter to the inner diameter (M), was examined in Figure 2.12. It was observed that at a constant load of 4,000 lbs., the maximum flexibility of the disc spring occurred when the M ratio was approximately two, after which it decreased.

Almen and Laszlo's research on disc springs has provided valuable insights into the behavior and characteristics of these components, verifying numerical results with experimental testing.

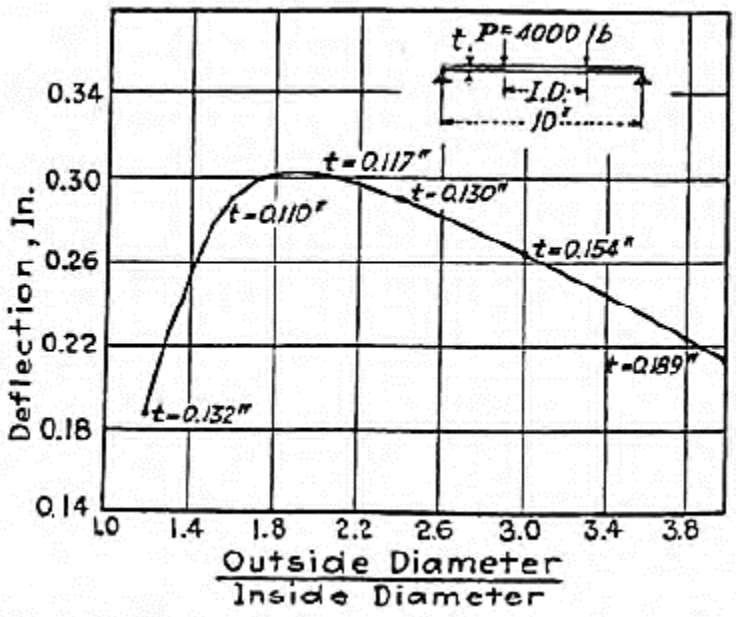

Figure 2.12: Flexibility curve as provided by M. [16]

2.3.2 Bagavathipermual et al.: Elastic Loading Displacement Predictions for Coned Disc Springs Subjected to Axial Loading Using the Finite Element Method [15]

In their 1991 paper, Bagavathiperumal, Chandrasekaran, and Manivasagam expanded upon the work initiated by Almen and Laszlo in 1936 [15]. Their research focused on the analysis of elastic coned disc springs' nonlinear force-displacement relationship obtained through finite element methods (FEM), comparing results to previous experimental testing on disc springs.

Utilizing FEM, Bagavathiperumal et al. developed a computational model to predict stresses and the displacement behavior of a coned disc spring. The dimensions used in their FEM calculations were based on a standard disc spring configuration with constant washer thickness, as outlined in Figure 2.13 below.

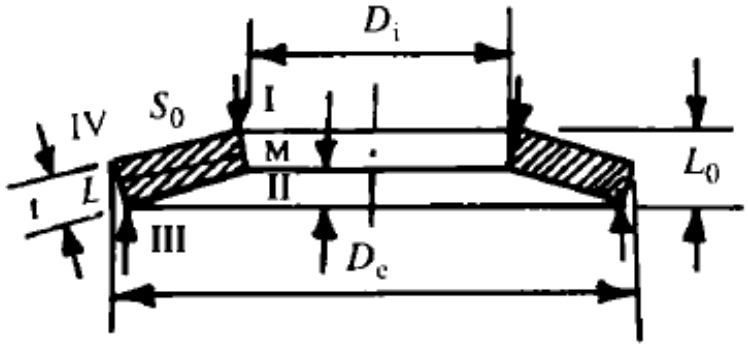

Figure 2.13: Geometric variables used by Bagavathiperumal et al. for a normal disc spring with a constant washer thickness. [15]

Finite element calculations were conducted with uniformly applied axial loads along the upper inner edge, while the lower outer edge was constrained vertically, as indicated by arrows in Figure 2.13. The FEM program developed for this purpose employed an eight-node isoperimetric solid, revolved around the centerline, with two degrees of freedom per node for radial and axial displacements, as depicted in Figure 2.14(a). The stiffness matrix of the disc utilized 2x2 Gauss-Legendre quadrature for numerical integration. It is worth noting that radial constraints were not applied to the joints based on previous research, as their effect was considered negligible. Additionally, friction effects at the supporting points along the outer edge were disregarded.

During the convergence analysis, it was observed that the eight-node isoperimetric model, with one element across the thickness, exhibited excellent convergence. Figure 2.14(b) illustrates the model of an example cross-section using a trapezoidal thickness element layout. A similar model would have been developed for the disc springs with constant cross-sectional thickness.

Small partial load increments were utilized for the nonlinear analysis, with each step increment assumed to be linear. This process continued until the target displacement was achieved, and a nonlinear curve displacement was formed over numerous small linear calculations. The nodal stresses were averaged for the stress analysis, revealing a maximum compressive stress at the upper, inner radius point.

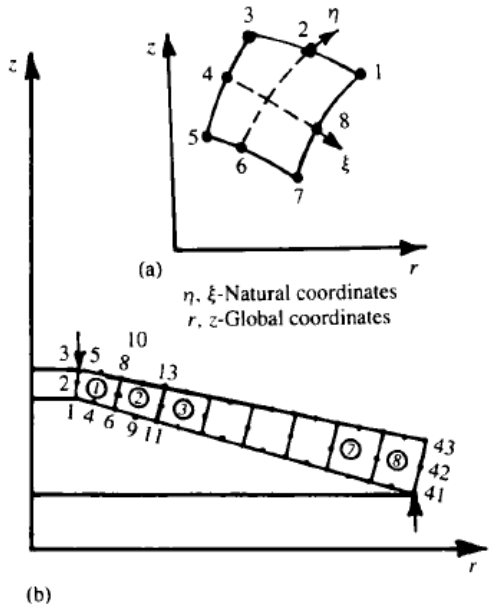

Figure 2.14: (a) 8 node element configuration for FEM. (b) Model element configuration. [15]

Nonlinear load-displacement curves were generated for different geometric parameters and compared to experimental and numerical results obtained by Curti and Almen and Laszlo. Both data sets were plotted in Figure 2.15 for comparison and showcase a close correlation between the curves. This comparison affirmed the validity of the FEM analysis and its ability to accurately predict the behavior of coned disc springs under axial loading.

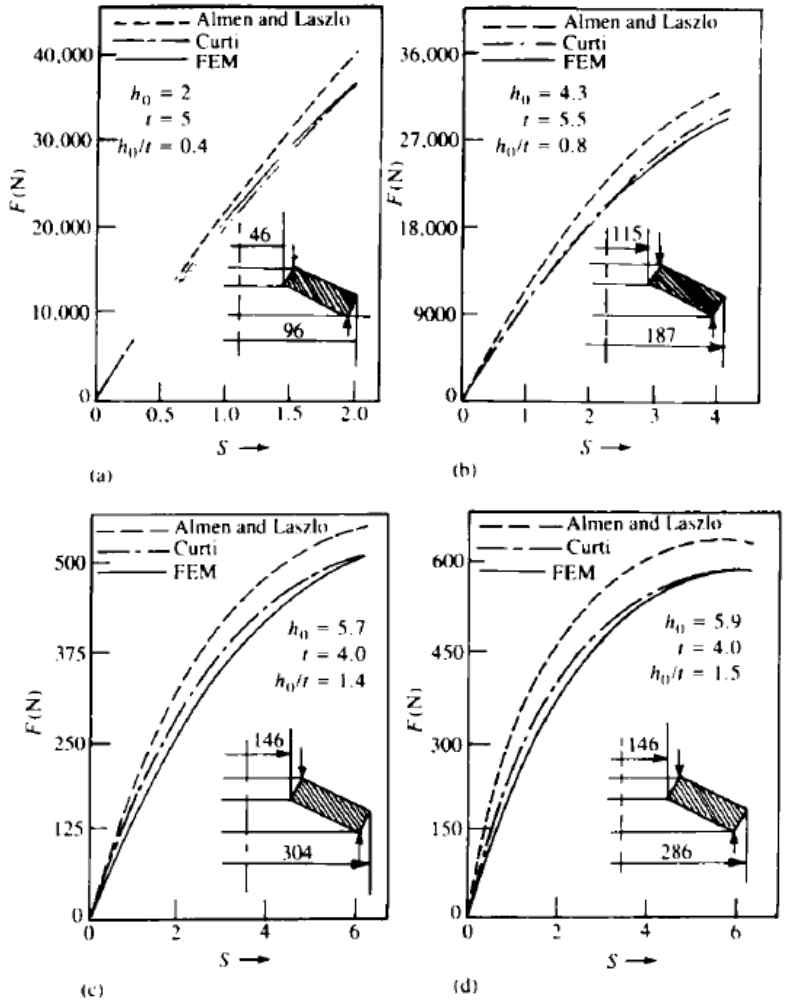

Figure 2.15: Force-displacement curves with differing ratios of conical height to washer thickness, comparing FEM to previous experimental results. [15]

Additional research was conducted to analyze the load-displacement curves of trapezoidal-sectioned coned disc springs. The resulting curves were also compared with prior experimental results.

After confirming the accuracy of the normal spring force-displacement curves using FEM, the study proceeded to investigate stacked spring models in FEM. These stacked disc spring FEM models were designed without accounting for inter-element frictional resistance, assuming no

slippage occurred at the edge interfaces and that the springs would maintain a straight position within the displacement range. Figure 2.16(a) illustrates the stacked springs arranged in a parallel orientation, while Figure 2.16(b) shows the stacked springs arranged in a series orientation.

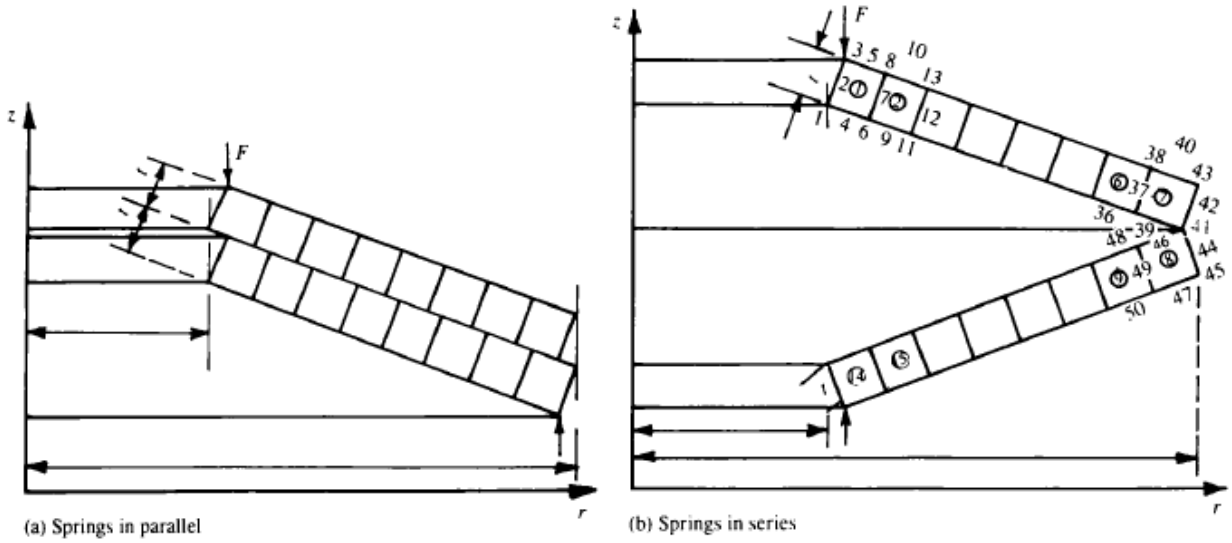

Figure 2.16: FEM model for (a) springs in parallel and (b) springs in series. [15]

The parallel stacked disc springs exhibited characteristics identical to coil springs, where the total stiffness of a parallel arrangement equals the sum of each individual spring's stiffness. Bagavathiperumal et al. adjusted the finite element procedure to accommodate the changing stack stiffness due to the parallel spring stack. Their FEM results successfully reflected the increased load-bearing capacity of parallel springs, aligning closely with the experimental findings produced by Almen and Laszlo for parallel disc stacking. Figure 2.17 contrasts the FEM analysis and experimental curves across two different geometries for two parallel stacks.

In comparison, the study also explored disc springs in a series stacking configuration by modeling stacks of two and three springs in FEM. In the series arrangement, the total spring deflection equals the sum of deflections for each disc spring in the configuration, while the load-carrying capacity for the whole stack is that of a single disc spring. The FEM-modeled results for series stacking closely mirrored the experimental results produced by Almen and Laszlo, further validating the accuracy of the FEM analysis. This validation is proved in Figure 2.18, which compares the curves derived from FEM modeling and experimental results.

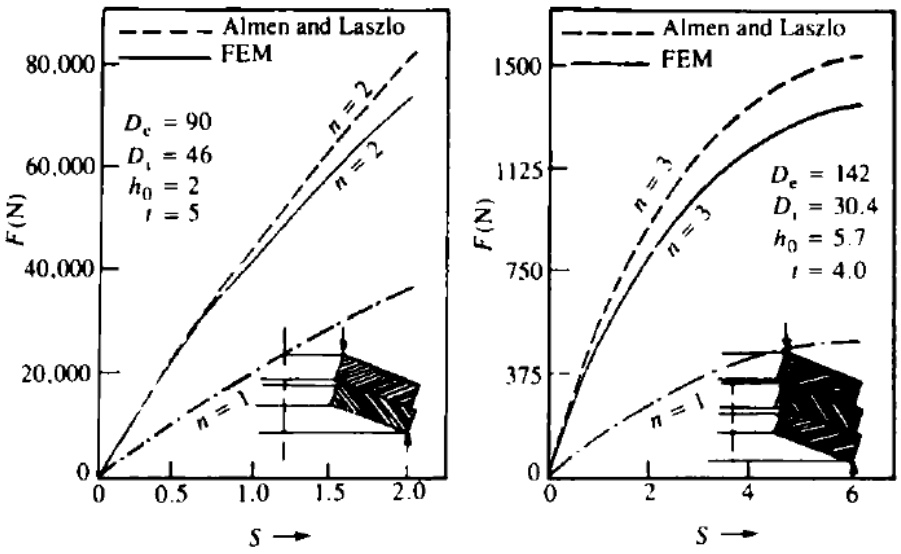

Figure 2.17: FEM results for parallel springs compared to previous experimental results. [15]

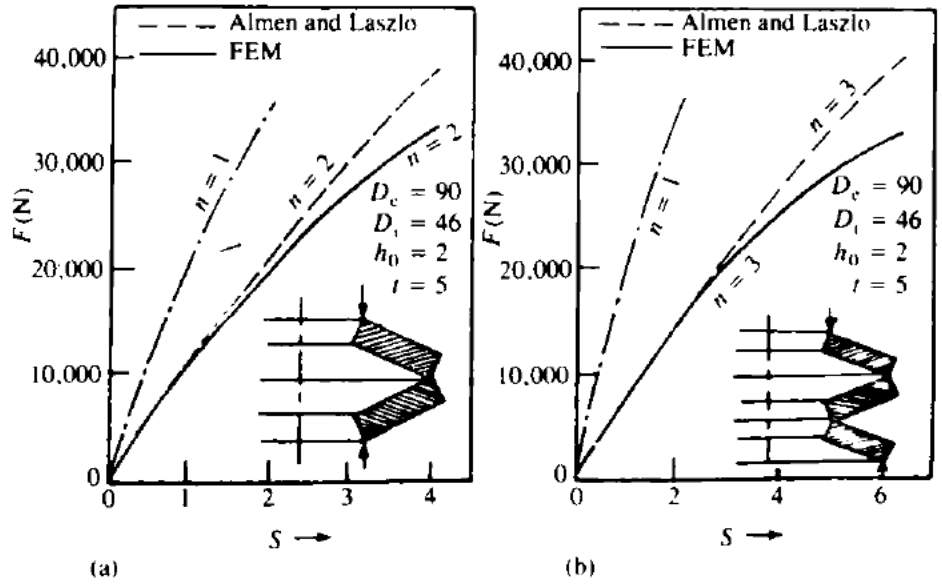

Figure 2.18: FEM results for series springs compared to previous experimental testing. [15]

Bagavathiperumal, Chandrasekaran, and Manivasagam concluded their study on the effectiveness of FEM on disc springs to analyze the nonlinear force-displacement behavior and successfully validated the results against previous numerical and experimental research. Additionally, their research provided a more comprehensive understanding of the properties of parallel and series spring stacks.

2.3.3 SnapLocX Design and Considerations from Prior Disc Spring Research

From the combined research conducted by Almen and Laszlo alongside further research by Bagavathiperumal et al., it is clear that the manipulation of the number and arrangement of disc springs allows for the creation of the desired load capacities and displacements for the Outer Plate at the springs' location.

Chapter 3: Overview of the SnapLocX Connection

The SnapLocX Connection is designed to optimize the onsite assembly of steel column splices. Unlike traditional construction methods that require onsite welding, steel columns would arrive on-site prefabricated with the necessary assembly components attached to the Upper and Lower Column. During column erection, the Upper Column can simply be lowered onto the Lower Column and components to permit the associated plates to snap into place. Pretensioned bolts with disc spring washers assist in holding the snapping plate in place and providing the snapping mechanism, preventing potential shifting. This simplified installation eliminates the need for onsite welding and bolting, leading to increased safety, reduced construction time, and reduced labor costs.

3.1 Overview of the SnapLocX Connection Concept

The conceived SnapLocX Connection is comprised of five individual steel pieces that form a strong snapping connection. These are shown schematically in Figure 3.1, with color coding identities that remain consistent throughout this document. These components, which are delivered attached to the flanges of the Upper and Lower Columns being spliced, include the Inner Plates (IPs), the Outer Plates (OPs), the Shear Keys (SKs), the Upper Lock Plates (ULPs), the Shim Plates (SPs), and the Lower Lock Plates (LLPs) and are described in detail in the following sections. The parts are assembled through a combination of shop welding and bolting, accompanied by disc spring washers on the upper row of bolts. After assembly, the load transfer between the plates fulfills the necessary requirements for moment and shear, ensuring structural integrity and stability.

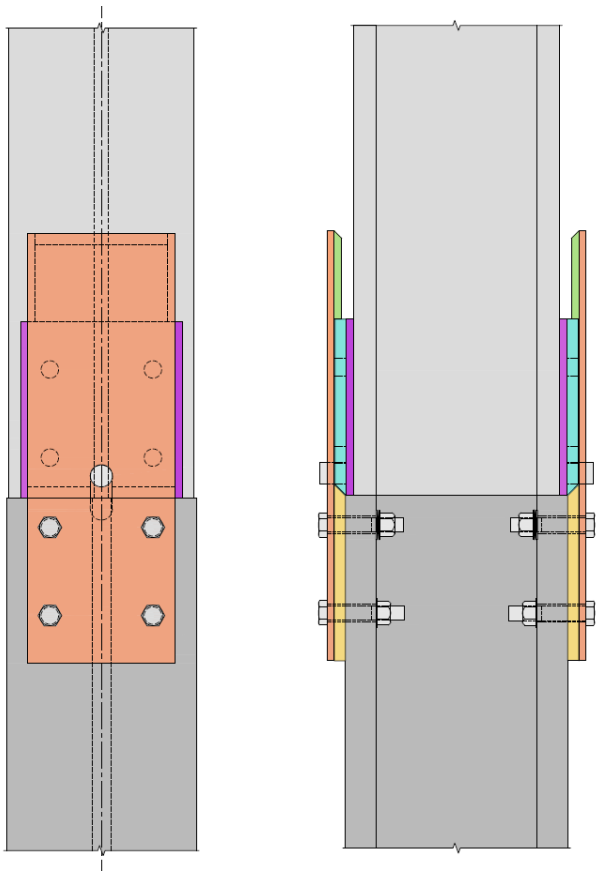

Figure 3.1: Schematic of the final assembled SnapLocX Connection column splice design.

3.1.1 Naming Conventions

Each component's name corresponds to its positional arrangement in the final state of the assembled connection, where the names are provided in Figure 3.2. Positioned in the upper region of the splice represented in blue and green, two plates bear against each other, locking the splice into place, thus termed "lock plates." Bearing between these plates is part of the connection's load path for tension and bending resistance. In the lower section of the assembly, attached to the Lower Column, are the "inner" and "outer" plates, referred to in yellow and orange, respectively. The purple plate of the Upper Column aligns the lower of the two lock plates to the inside plate of the lower column, functioning as a "shim" in cases where the two columns have a significant difference in depth. Additionally, a cylindrical key protrudes through the orange plate and is designed to resist shear in the weak axis direction, acting as a "shear key."

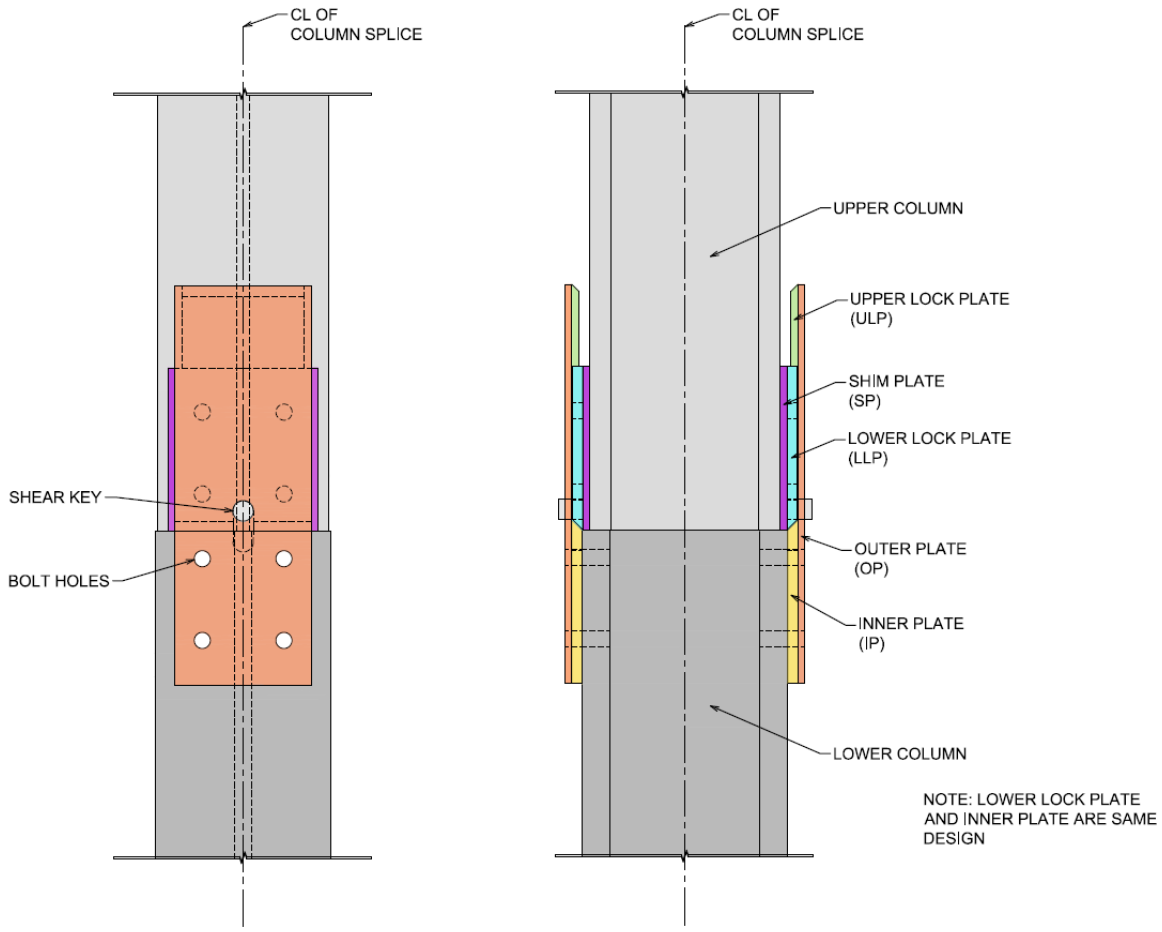

Figure 3.2: Naming conventions for all SnapLocX Connection column splice assembly parts.

3.1.1.1 Lower Lock Plate and Inner Plate

The Lower Lock Plate (*LLP*), highlighted in blue and portrayed in 3D in Figure 3.3, is the central component of the Upper Column assembly. As the crucial part of the locking mechanism, it helps resist moment through bearing and aids in weak and strong-axis shear transfer from the Upper Column to the Lower Column. To improve the efficiency of strong-axis shear transfer, the *LLP* interlocks with the plate below using a beveled edge. The upper edge must be flat to resist moment and tension through bearing effectively. Additionally, for weak-axis shear transfer, the *LLP* features a keyhole for a component of the Outer Plate.

The Inner Plate (*IP*), highlighted in yellow and shown in 3D in Figure 3.3 alongside the *LLP*, is one of the two primary assemblies attached to the Lower Column. The *IP* also features beveled edges to intersect with the *LLP* for strong-axis shear transfer through the thickness of the *IP*.

The *IP* design also requires four bolt holes to allow for the outer snapping plate to be connected to the Lower Column.

To streamline fabrication, the *LLP* and *IP* designs are combined into a single interchangeable plate, incorporating the bolt holes and a shear key slot. Only the weld thickness requirements differ for the respective columns when a plate is assigned as a *LLP* or *IP*. A plate acting as a *LLP* requires two parallel, vertical welds to weld it to the Upper Column components. A plate acting as an *IP* requires a thicker C-shaped weld featuring two parallel, vertical welds and one horizontal weld on the lower edge.

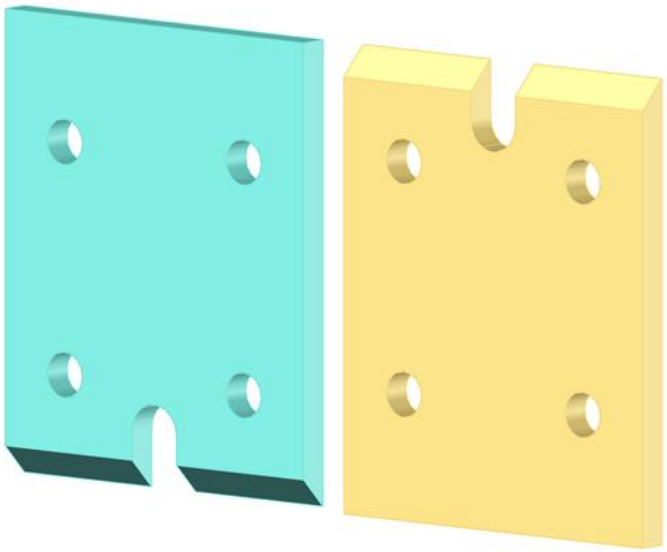

Figure 3.3: 3D view of the LLP (left) and IP (right).

3.1.1.2 Shim Plate and Lower Lock Plate

For column splices with varying depths, the inclusion of Shim Plates (*SP*s) becomes a requirement to align the *LLP*s to the *IP*s and facilitate bearing for strong shear transfers. The *SP*s are specifically designed to compensate for differences in column depth, splitting that difference between one *SP* attached to each Upper (or, in limited cases, Lower) Column flange, ensuring an effectively equal depth for both columns in the splice. This equal column depth then allows for the *LLP*s and *IP*s to engage in bearing and transfer strong-axis shear from the Upper Column to the Lower Column through the beveled edges.

When SPs are required, they are welded to the Upper Column flanges with two parallel, vertical welds. Afterward, the accompanying LLPs are welded to the face of the SPs along its two vertical edges. Figure 3.4 provides a 3D depiction of the LLP and SP assembly, with the LLP depicted in blue and the SP depicted in purple. A complete assembly of the SP and LLP placement on the Upper Column is shown and described later.

The depth difference at each flange of the column splice must exceed 1/16 in., per plate requirements stated in *the Manual*. Accordingly, the minimum SP thickness begins at 1/16 in., increasing in 1/16 in. increments up to 3/8 in., followed by increments increasing by 1/8 in, up to 1 in., and increasing in 1/4 in. increments after that.

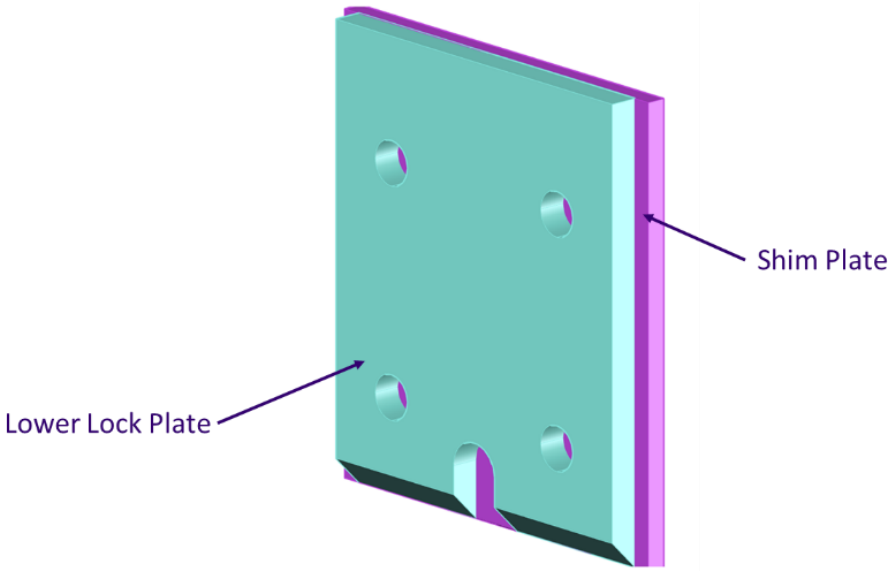

Figure 3.4: Assembly of the LLP welded to the SP.

3.1.1.3 Outer Plate and Components

The functionality of the SnapLocX Connection during assembly is centered around the Outer Plate (OP), highlighted in orange, shown assembled in Figure 3.5. This plate serves as the crucial element that undergoes deformation during assembly and holds the Upper Column to the Lower Column when the connection is subject to moment. The lower portion of the OP rests on the IP and is directly bolted to the Lower Columns. The two lower bolts fix each OP to the Lower Column, while the upper bolts feature disc spring washers that provide nonlinear elastic

deformation during snapping while allowing the bolts to also be pretensioned to inhibit accidental prying of the OP after assembly.

The Upper Lock Plate (ULP) is welded onto the interior face of the OP, oriented towards the Upper Column, using two parallel fillet welds along the vertical edges. After assembly, the lower surface of the ULP bears on the upper face of the LLP, transferring any flexural or tension demands into the OP and into the Lower Column.

Integrated with the OP, the Shear Key (SK) is a cylindrical knob (made from circular steel rod stock) that protrudes through the OP. On the exterior surface, facing away from the column, approximately 1/2 in. of the SK is exposed, allowing for a circumferential weld at the junction of the SK and OP. The SK plays a vital role in transferring weak-axis shear requirements from the Upper Column to the Lower Column through the LLP and into the OP as described later.

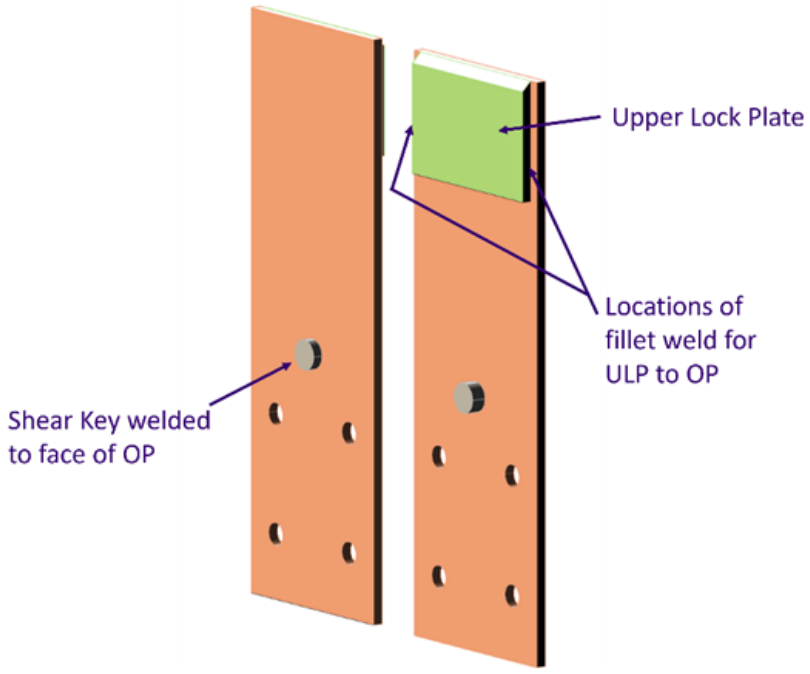

Figure 3.5: OP assembly with the ULP welded to the interior face and the SK welded to the exterior face of the OP.

3.1.1.3(i) Belleville Disc Springs

Steel disc springs, also referred to as Belleville washers or conical spring washers, are cone-shaped washers used in mechanical engineering applications that create loading profiles not feasible with coiled springs or other washers. Chapter 2 reviewed relevant literature related to

their development and behavior, and although not common in steel construction, they are well-understood and mass-produced. As shown in Figure 3.6, disc springs are designed to compress in small deflections with heavy loads on their axis of symmetry. Disc springs can be designed to remain elastic under large loads without undergoing permanent deformation, and this can be achieved through nonlinear geometric deformations [17].

Figure 3.6: Belleville Disc Spring. [18]

The axial force-deformation behavior of a disc spring is heavily influenced by the ratio of the conical disc height (h) to actual washer thickness (t), denoted as h/t. Additional disc spring cross-section variables are shown in Figure 3.7. These include the maximum outer diameter (OD), minimum inner diameter (ID), conical angle (β), overall height (OH), radius from the disc centerline to the bearing edge (R), thickness in the X-axis from the bearing edge to the maximum outer diameter (X or $t * \sin(\beta)$), and vertical height of the thickness when deformed as a cone disc (Y or $t * \cos(\beta)$). [19]

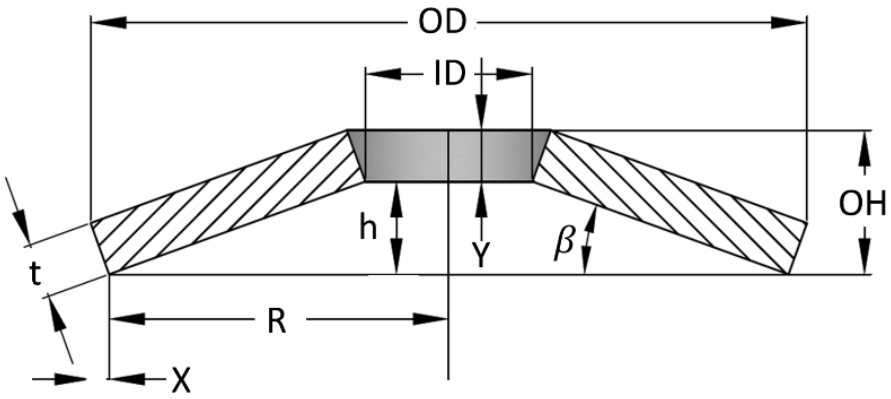

Figure 3.7: Disc spring cross-section and dimensional variables.

The spring force (P_s) relative to the spring deformation (δ) is defined in Equation 3-1 from a disc spring manufacturer, MW Components, and is based on the original spring literature from J.O. Almen and A. Laszlo [19]. Unlike the equation derived by Almen and Laszlo, where R in Figure 3.7 is equal to half the maximum diameter, manufacturers MW Components account for the difference in edge depth for the bearing edge. This causes the bearing edge diameter to be $OD - 2X$, with the outer radius (R) used in Equation 3-1 being half that [19]. Additional calculations are then needed to solve for disc spring dimensions not provided by manufacturers, which can be found in Appendix A.

$$P_s(\delta) = \frac{E*\delta}{(1-\nu^2)*M*R^2} * \left(\left(h - \frac{\delta}{2}\right) * (h-\delta) * t + t^3)\right), \text{ where } 0 \leq \delta \leq h$$

Equation 3-1

Equation 3-1 also includes the elastic modulus of the disc spring material (E) and M, which as defined in Equation 3-2, is a function of α, the ratios of the outer to inner diameter, provided in Equation 3-3.

$$M = \frac{6}{\pi * \ln(\alpha)} * \frac{(\alpha-1)^2}{\alpha^2}$$

Equation 3-2

$$\alpha = \frac{OD}{ID}$$

Equation 3-3

As the ratio of h/t changes, the nonlinear elastic behavior of the spring varies, as exhibited in the force-displacement curves in Figure 3.8. Lower h/t ratios will generate a more linear force-deformation curve, whereas higher h/t ratios will produce a nonlinear curve [16]. Note that Figure 3.8 is given as compressive force normalized by the force required to fully flatten the disc spring versus compressive deflection normalized by the cone height of the disc spring, h.

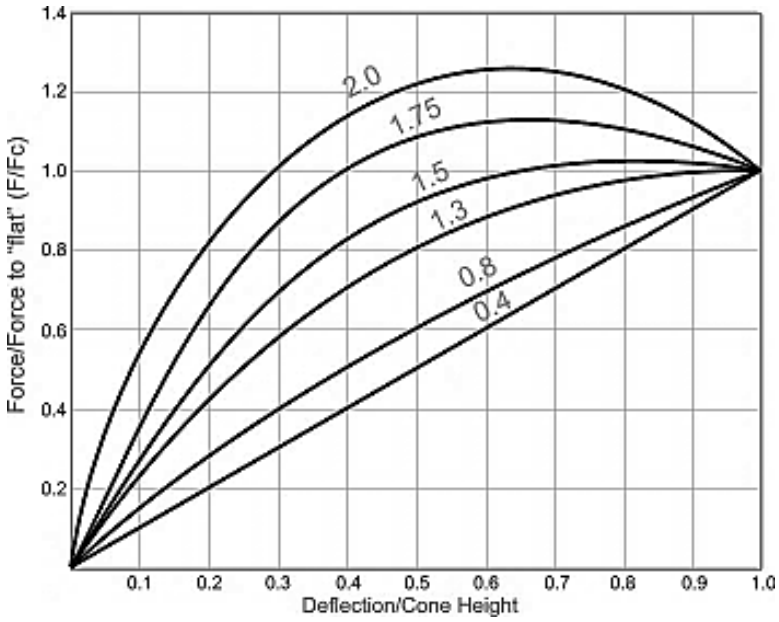

Figure 3.8: Force Deformation curves for different height-to-thickness (h/t) ratios. [20]

In addition to altering the spring stiffness properties through the h/t ratio, disc springs can also be stacked as shown in Figure 3.9 to change their properties. Placing disc springs in series will result in more deformation for the same spring force while placing them in parallel will result in more force for the same deformation. They can also be stacked in combinations of parallel and series springs to increase both the strength and deformation capacity relative to a single spring.

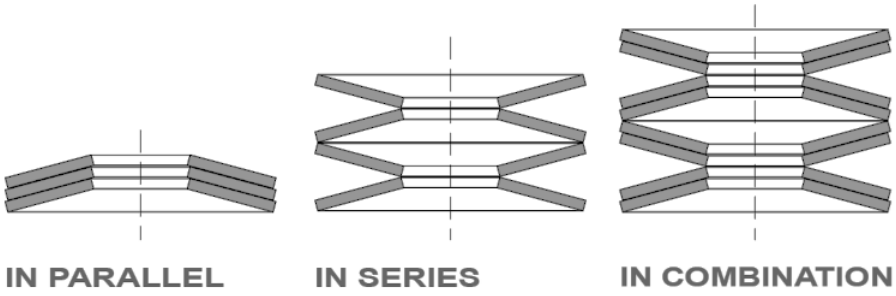

Figure 3.9: Disc spring stacking methods for different load and displacement curves. [21]

The force-deformation behavior of a single spring and two springs placed in parallel are shown in Figure 3.10 using an example washer, AD56-28.5-1.5, from disc spring supplier American Belleville, designed for a standard 1 in. bolt [22]. As shown, disc springs placed in series can accommodate larger deformations, while disc springs placed in parallel accommodate larger forces. As applied in the SnapLocX Connection, disc springs are provided on two bolts connecting the OP to the Lower Column flange, which doubles the clamping force for a given spring deformation similar to two-disc springs in parallel.

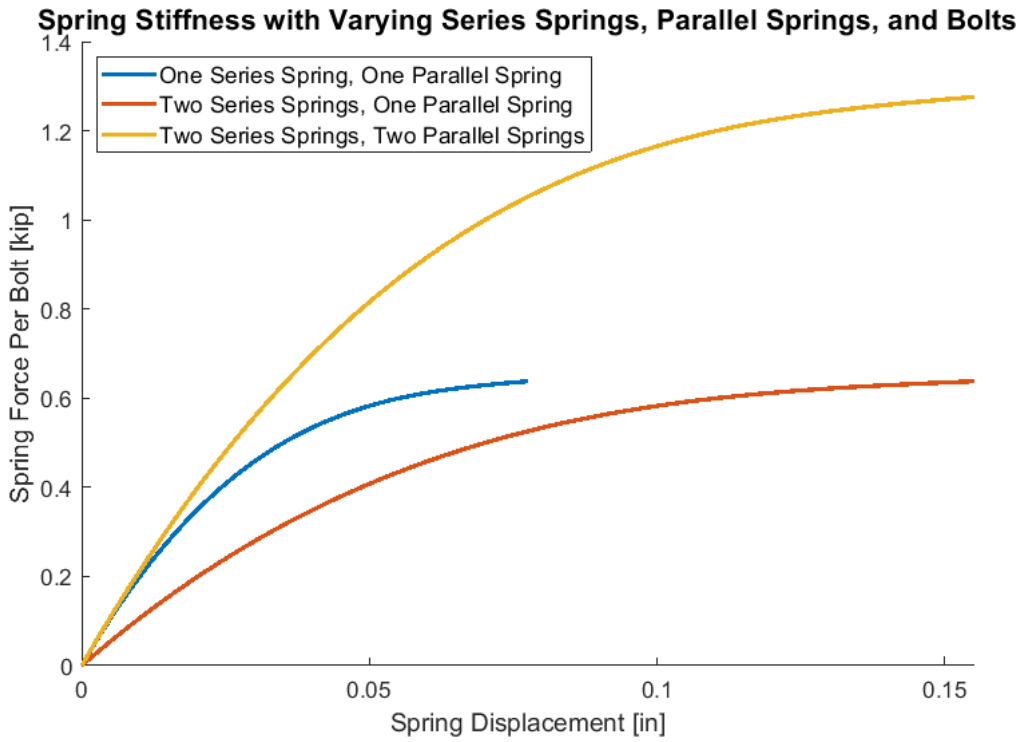

Figure 3.10: Disc spring behavior when placed in series or parallel as compared with the behavior of a single disc spring.

As described below, it is recommended that the bolts using disc spring washers utilized in SnapLocX connections be pretensioned to at least 200 lbs. to safeguard against column displacement and prevent tampering with the OPs post installation. While springs can be pretensioned, they should not be displaced to their full conical height, because they must still be allowed to deform during column installation.

For effective bolt pretensioning based on spring displacement, it may be necessary to use more springs in series than required to accurately measure the spring deflection and loading as reflected in the Figure 3.10 plot.

3.1.1.3(ii) A325 Bolts

Bolts used for connecting the OP and Lower Column in the SnapLocX connections, as designed and discussed in this document, are A325 Bolts, with dimensions and properties corresponding to Table 7-14 in *the Manual*.

3.1.1.3(iii) Nuts

Nuts are used for bolts connecting the OP and the Lower Column, as designed and discussed in this document are A536 Nuts, with dimensions and properties corresponding to Table 7-14 in *the Manual* for the appropriate bolt diameter.

3.1.1.3(iv) Washers

Standard washers used for the A325 bolts in the connections are s F436 Circular Washers, with dimensions and properties corresponding to Table 7-14 in *the Manual* for the appropriate bolt diameter.

3.2 Design Variables

Design variables are established for the dimensions of the various SnapLocX components, and their nomenclature was derived from parameters such as thickness (t), width (b), depth (d), and length (L). The following figure depicts the definitions of each connection component and its accompanying design variables.

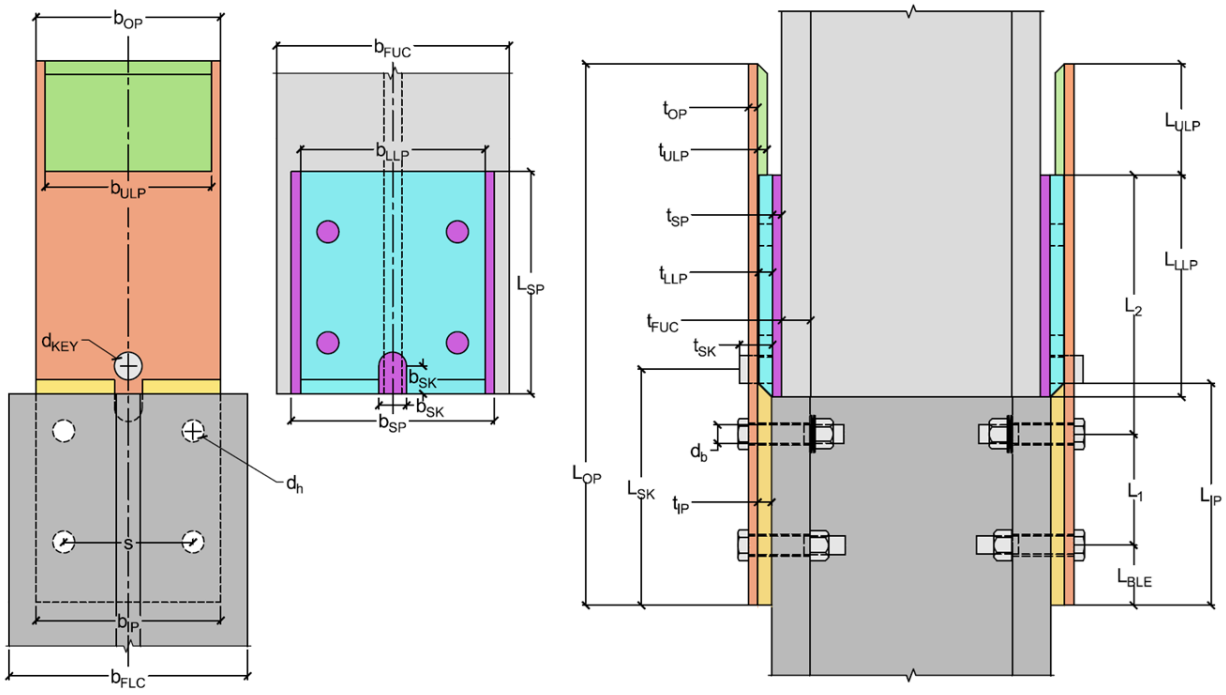

Figure 3.11:Major design variables for the SnapLocX column splice.

As shown in Figure 3.11:

- Variables immediately related to the Outer Plate include b_{OP} as the width of the OP, t_{OP} as the thickness of the OP, and L_{OP} as the length of the OP;
- Variables immediately related to the Inner Plate include b_{IP} as the width of the IP, t_{IP} as the thickness of the IP, and L_{IP} as the length of the IP;
- Variables immediately related to the Shim Plate include b_{SP} as the width of the SP, t_{SP} as the thickness of the SP, and L_{SP} as the thickness of the SP;
- Variables immediately related to the Upper Lock Plate include b_{ULP} as the width of the ULP, t_{ULP} as the thickness of the ULP, and L_{ULP} as the length of the ULP;
- Variables immediately related to the Lower Lock Plate include b_{LLP} as the width of the LLP, t_{LLP} as the thickness of the LLP, L_{LLP} as the length of the LLP, d_{SK} as the diameter of the SK slot, and b_{SK} as the dimension from the lower edge of the LLP to the center of the d_{SK} diameter;
- Variables immediately related to the Shear Key include L_{SK} as the length from the lower end of the OP to the center of the SK, t_{SK} as the thickness of the SK, and d_{KEY} represents the diameter of the face of the SK;

- Bolt variables include d_b as the bolt diameter, d_h is the diameter of the bolt holes, as found in *the Manual*, and L_1 as the distance between the lower, fixed bolt row and the upper disc spring bolt row, with s as the distance between bolt columns; and
- Additional variables used for design calculations include b_{END} as the distance from the lower end of the OP to the center of d_h in the lower bolt row, L_2 as the vertical distance between the upper disc spring bolts to the lower end of the ULP, $t_{f_{UC}}$ as the thickness of the Upper Column flange, $b_{f_{UC}}$ as the width of the Upper Column.

3.2.1 Example Design Variables: W12x170 to W12x230

A column splice connection example is designed in Chapter 5 using a W12x170 shape as the Upper Column and a W12x230 shape as the Lower Column. The dimensions depicted in Figure 3.12 represent the proportions for that design for the design variables identified in Figure 3.11. They are shown to scale to provide a sense of the relative sizes of the components. Note that the dimensions for W-shapes are from Table 1 in *the Manual* and correspond to the detailing dimensions. Additionally, all W-shapes in this document are designed with A992 steel.

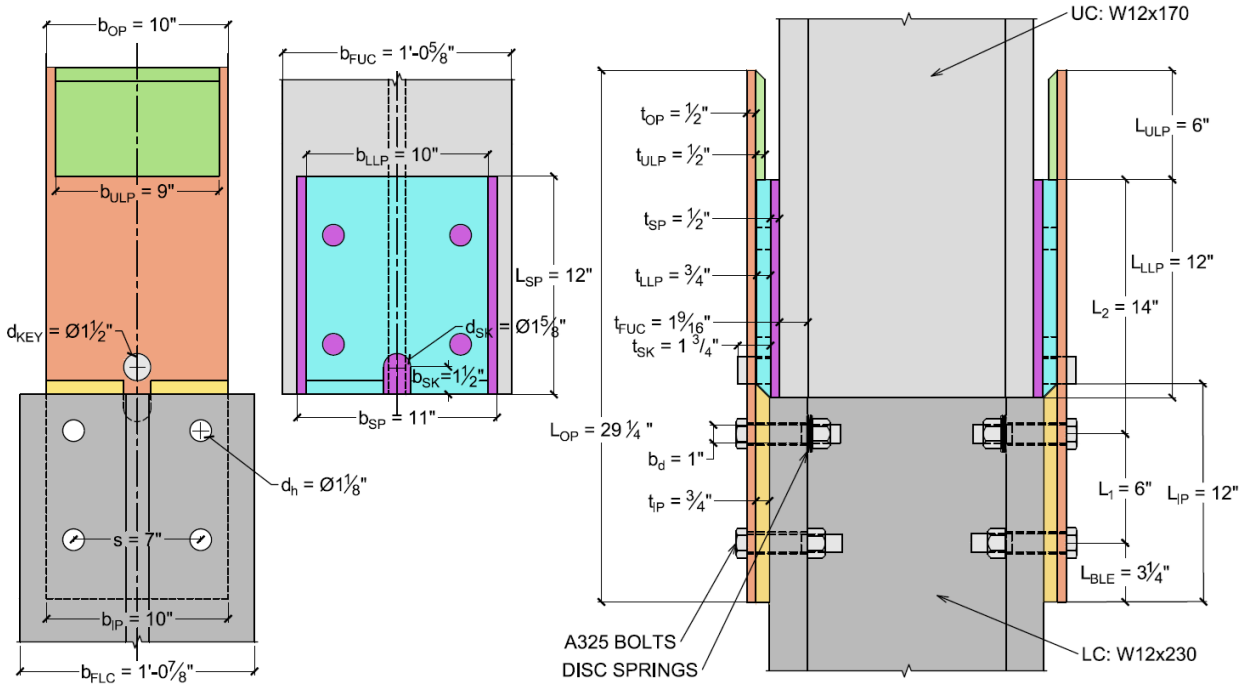

Figure 3.12: Dimensions for the design variables for the example W12x170 to W12x230 column splice as designed in Chapter 5.

3.2.2 Example Design Variables: Final Weld Dimensions

Weld locations and dimensions for the example W12x170 and W12x230 column splice, designed in Chapter 5, are displayed in Figure 3.13 to again provide a sense of proportion of the welds. These weld locations are standardized across all column connection pairings, with the dimensions varying accordingly with plate size.

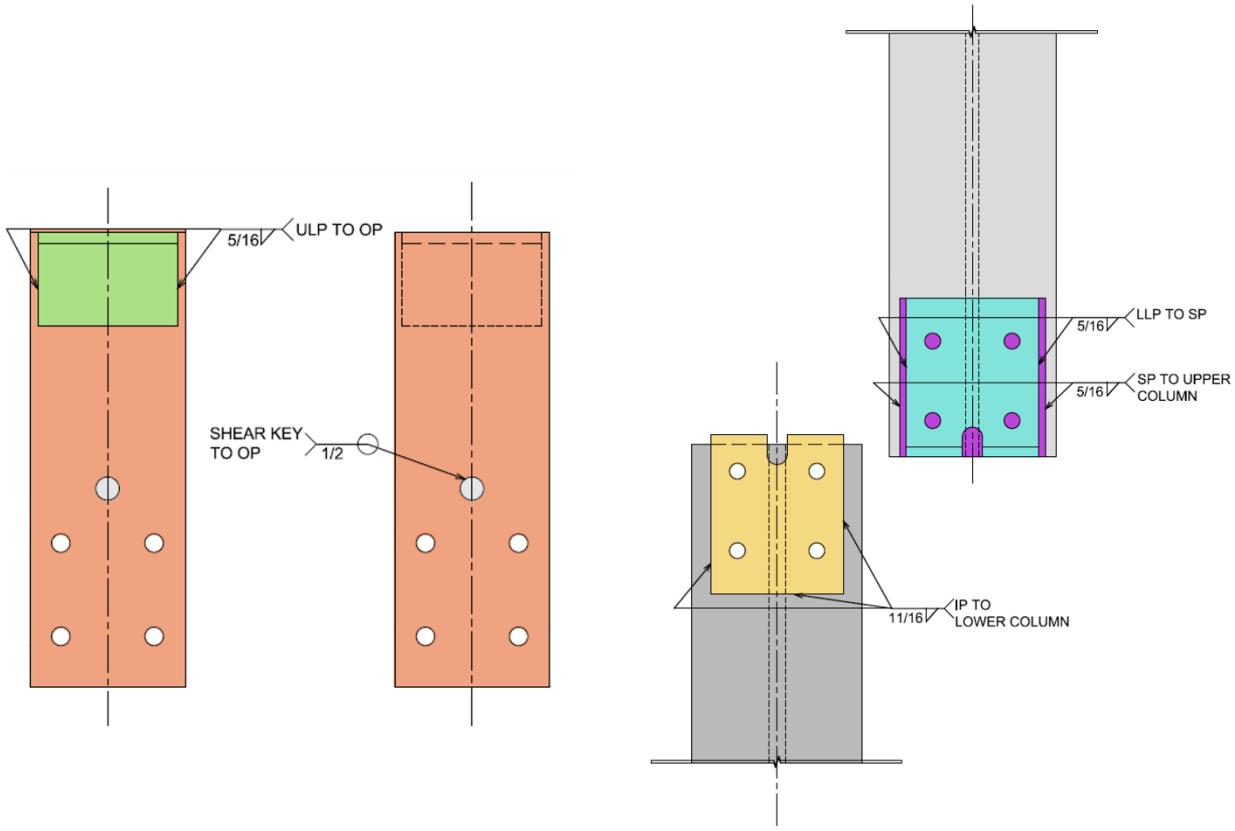

Figure 3.13: Weld locations and dimensions for the example W12x170 to W12x230 design.

3.3 Column Assembly

The primary objective of the SnapLocX Connection is to provide a prefabricated column splice assembly that is easy to install. Prior to column delivery to the construction site, the Upper and Lower Columns are fabricated using their associated SnapLocX components. Onsite assembly of the column splice entails the snapping of the OP as the columns slide together, guided by the SK.

3.3.1 As Delivered Columns

All components are preassembled, welded, and bolted using the required materials for the Upper and Lower Column.

The Upper Column, as delivered, is in Figure 3.14. The SPs, when required, are welded to the flanges of the Upper Column at the welding locations previously shown in Figure 3.13. The LLPs are then welded to the faces of the SPs or directly to the Upper Column flanges when SPs are absent. The weld locations for the LLPs are also identified in Figure 3.13, and the locations of the welds do not change regardless of the presence of the SPs.

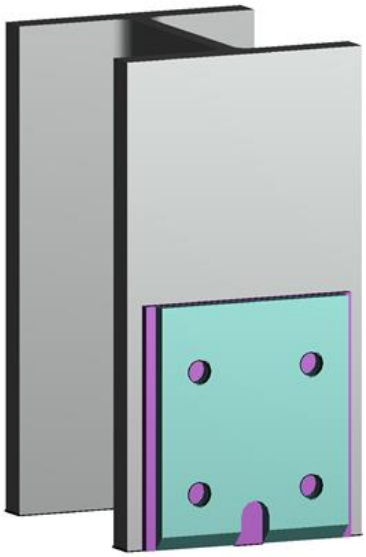

Figure 3.14: Delivered Upper Column assembly with the LLP (blue) welded to the SP (purple) and the SP welded to the Upper Column.

The Lower Column, as delivered, is displayed in Figure 3.15. As shown, the complete Lower Column assembly includes the OP, ULP, SK, and IP, along with disc springs, bolts, nuts, and washers as required. The IP is welded to the Lower Column using a C-shaped weld at locations detailed in Figure 3.13. The OP and its components, including SK and ULP, are assembled separately. The ULP is welded to the interior face of the OP, while the SK is welded to the exterior face of the OP, with locations provided in Figure 3.13. The OP and components are then bolted to the Lower Column through the IP with the necessary bolts, disc springs, washers, and nuts.

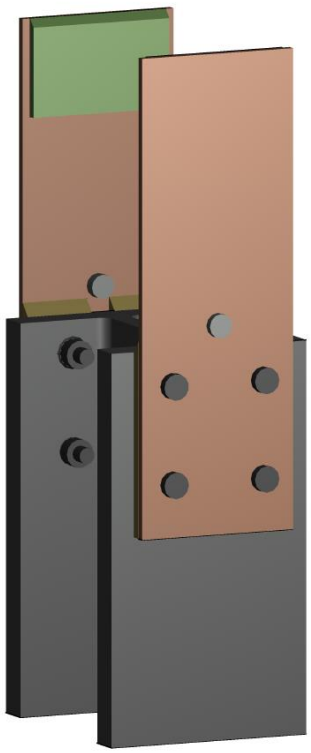

Figure 3.15: Lower Column as delivered with the Inner Plate and Outer Plate with Components attached via fixed bolts and bolts with disc springs.

3.3.2 Initial Condition

Figure 3.16 shows the initial condition of the prepared Upper and Lower Columns before assembly. In preparation for assembly, the disc spring bolts are pretensioned to 0.2 kips, and the lower beveled edge of the *LLP* and upper beveled edge *IP* will guide the Upper Column into alignment with the Lower Column.

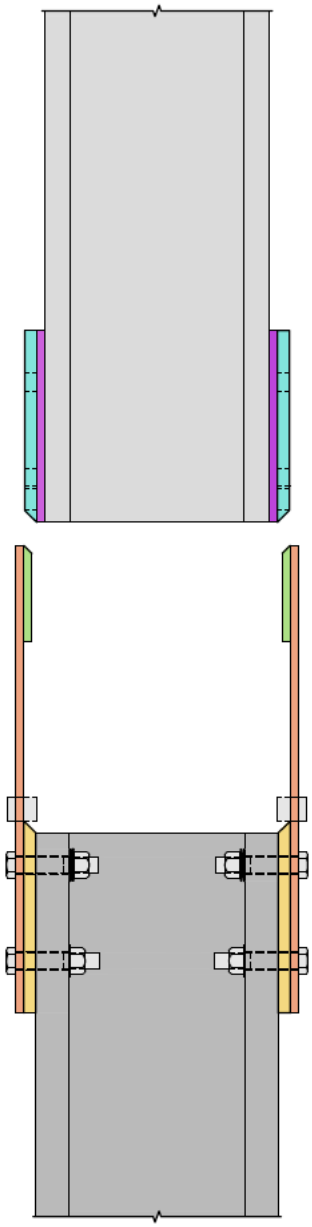

Figure 3.16: Initial condition of a column splice prepared for assembly onsite.

3.3.3 Intermediate Condition

During assembly, the beveled edges of the LLPs and the IPs allow for the two plates to slide past each other, causing the OPs to begin deflecting away from the Lower Column and IPs, depicted in Figure 3.17. This deflection of the OPs leads to further deformation of the disc springs, thereby increasing the force on the OPs at the spring bolts. The maximum deflection of the OPs

and compressive deformation of the disc springs occurs when the lower edge of the ULPs aligns with the upper beveled edge of the LLPs, representing the point of maximum flexure in the OPs.

As the Upper Column approaches the Lower Column, the column alignment is guided by the SKs and SK slots, helping to ensure proper centering of the two columns over each other.

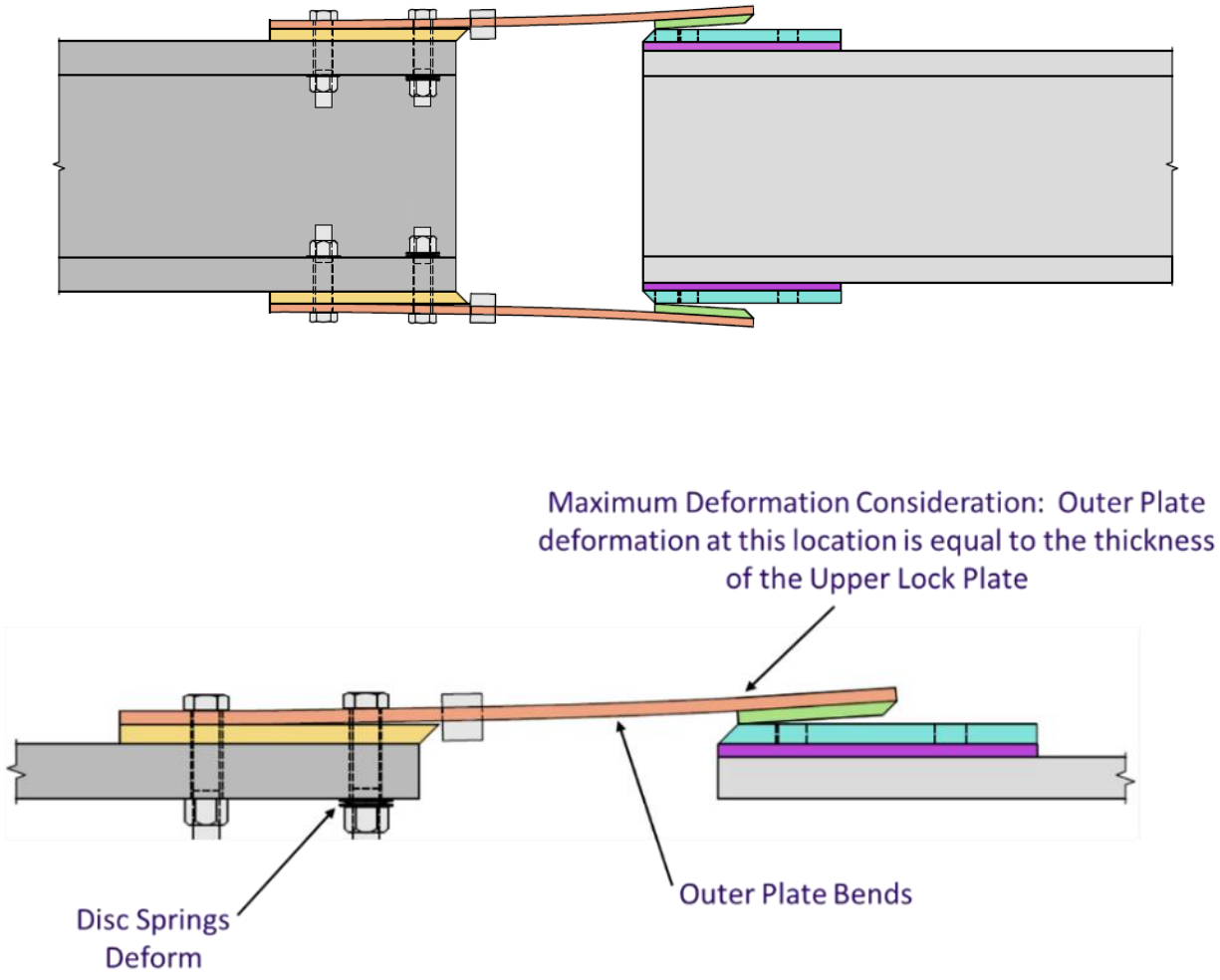

Figure 3.17: Intermediate condition of a column assembly with SnapLocX as the Upper Column slides towards the Lower Column, bending the OP and deforming the disc springs.

3.3.4 Final Condition

As the SK and SK slot guide the connection of the Upper and Lower Columns into the splice, the OP will snap to its initial unbent state, securing the lower face of the ULP over the upper face of the LLP. This plate snap and plates' face interactions effectively lock the Upper Column and its components to the Lower Column and its components, as highlighted in Figure 3.18. Additionally, any deformation and force experienced in the disc springs will return to their original state of 0.2 kips, providing security for the OP alignment.

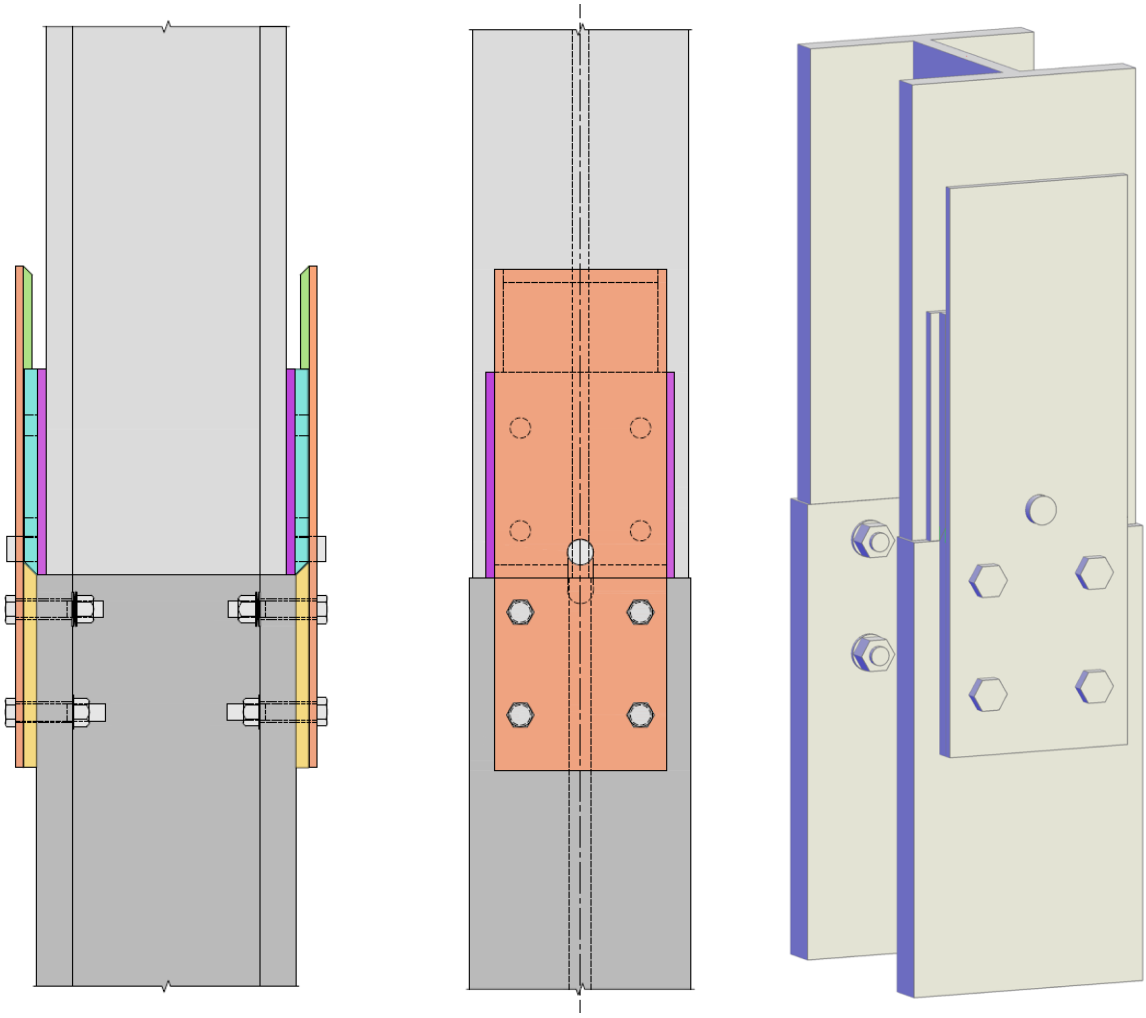

Figure 3.18: Final condition after assembly is complete (left) and 3D rendering of an onsite view after assembly (right).

Chapter 4: Design Considerations

The design of the SnapLocX Connection involves several critical considerations to ensure the structural integrity and optimal performance of the column splice. This chapter provides an in-depth discussion of the detailed design process used to confirm the dimensions in column splice design. [13]. Prior to that, the necessary design provisions and loads will be reviewed. Finally, a comprehensive set of example calculations for the design of a SnapLocX Connection for splicing a W12x170 to a W12x230 is located in Appendix B.

4.1 Design Provisions

The design of column splices must reference standards for computing loads and resistances. For calculating resistances of steel components, this thesis references the content of the Specification for Structural Steel Buildings, ANSI/AISC 360-16, which will be referred to as *the Steel Specification* [14]. Additionally, design aids are used from the 15th edition of the Steel Construction Manual, which will be referred to as *the Manual* [13]. The SnapLocX Connection is intended to be used in gravity framing alongside all types of recognized lateral force systems. Therefore, additional requirements for column splices are referenced from the Seismic Provisions for Structural Steel Buildings, AISC 341-16, which will be referenced as *the* AISC *Provisions* [23].

Other design standards that may be used for steel column splice loading and design requirements include OSHA's Safety Standards for Steel Erection (RIN No. 1218-AA65**)** and ASCE/SEC 7-16 [5], [24].

4.2 Design Loads

Column splices in gravity frames are designed to resist construction loads during assembly, final loads, and extreme events while also considering changes in the column size across the splice. Construction and final loads must consider strong and weak axis direction moment and shear and torsion. Construction loads are set by OSHA at 300 lbs. located 18 in. from the splice (note additional construction loads may need to be considered), and final loads are determined from AISC 341 using an LRFD shear demand [5], [23].

The SnapLocX Connection must be comprised of features to provide necessary resistance in the strong and weak axes. Snap and locking plates (identified as Outer Plate, Upper Lock Plate, and

Lower Lock Plate in Figure 3.2) provide resistance in bearing for strong axis flexure. The Inner Plate and upper column Locking Plate resist strong axis shear. When slotted into the upper column's locking plate, the rounded bars resist weak axis shear and torsion. Additional steel shim plates accompanying the upper column lock plate accommodate column size transitions, continuing the conceptualized resistance paths.

4.3 Design Process

The step-by-step design process used to verify the SnapLocX Connection dimensions is represented in the flow chart provided in Figure 4.1. The following sections move through each design consideration listed in the chart, from initially considering column pairing requirements to post-design calculations of strong axis flexural strength using the limit states.

Throughout the design process, shape detailing dimensions for W-shapes are used for detailing, and precise values are meticulously calculated to ensure the component resistance is accurate.

As shown in Figure 4.1, the required shear strength of the connection in both the column's strong and weak axis directions constitutes a significant design consideration. The SnapLocX design procedure has been developed for gravity framing in buildings with all types of lateral force-resisting systems. As such, the requirements of *the* AISC *Provisions* control the required shear strength in both axes. Section D2.5c of *the* AISC *Provisions* requires that all column splices, even those that are not part of the Seismic Force Resisting System, must have a shear minimum shear strength of at least M_p/H where M_p is the plastic moment strength of the smaller column at the splice in the direction under consideration, and H is the story height.

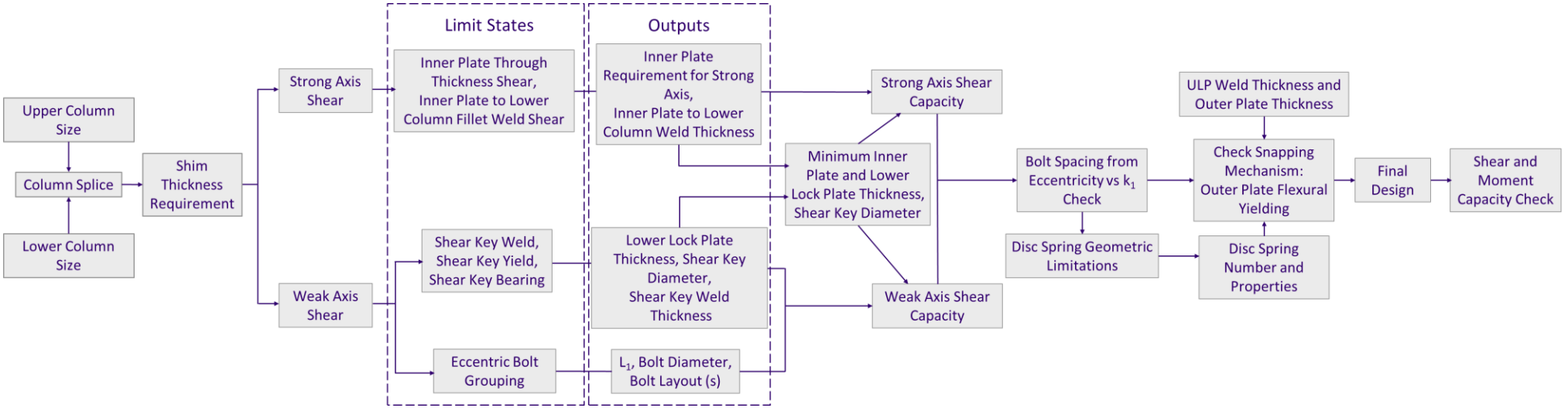

Figure 4.1: Design process flow chart for developing the SnapLocX Connection.

4.4 Column Splice Pairing

The design process is initialized by selecting two column shape sizes to serve as the Upper and Lower Columns. Design considerations include variations in flange widths and column depths to analyze the landing points of the Upper Column flanges. Upon inspecting column pairings, it was observed that some lighter column shapes have a greater depth than those that would act as a Lower Column. For example, creating a splice with a W12x35 Upper Column and W12x50 Lower Column would result in a negative 1/4 in. depth difference at each flange of the Lower Column. Accounting for this consideration, it was assumed that the column shapes spliced with the SnapLocX are to be used within a shape class.

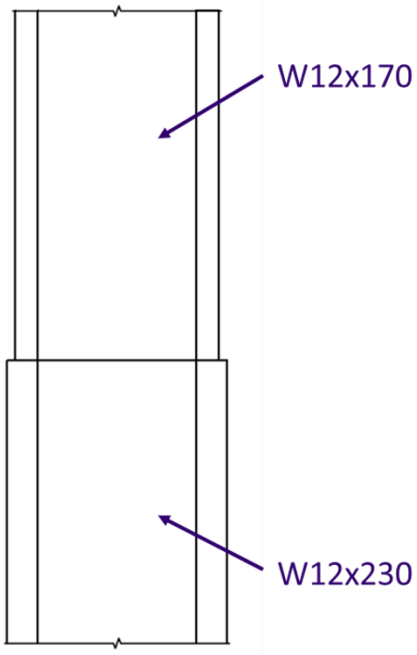

Figure 4.2: SnapLocX Connection example design column pairing selection.

4.4.1 Spliced Column Depth Constraints

For sufficient transfer of column axial force from the Upper Column to the Lower Column, it was assumed that at least half of the flange thickness of the Lower Column ($t_{f_{LC}}$) should support the flange thickness of the Upper Column ($t_{f_{UC}}$) at each flange. Note that the required bearing area must be computed as a function of column axial force, as is done for all column splices. The requirement above is assumed to provide a reasonable range of column splice possibilities for designing standard SnapLocX connections in Chapter 5. Given the varying depth relations

for specific column pairings, two checks were formulated to verify that the Lower Column supported a sufficient amount of upper flange in the absence of a design axial force. Equation 4-1 addresses support for Upper Columns with smaller depths (d_{UC}) than their Lower Column counterpart. Equation 4-2 addresses the less common occurrence of an Upper Column pairing with a smaller Lower Column depth (d_{LC}).

$$Check\ if\ d_{UC} < d_{LC},\ d_{UC} \geq d_{LC} - t_{f_{LC}}$$

Equation 4-1

$$Check\ if\ d_{LC} < d_{UC}: d_{LC} > d_{UC} - t_{f_{UC}}$$

Equation 4-2

4.4.2 Column Bearing Capacity

The full-face column bearing capacity was not considered during the initial analysis, as it was assumed to be significantly greater than the force demanded by the Upper Column. In general, the bearing capacity at the column splice is verified using Equation 4-3 below, in accordance with the requirements for column splices outlined in Part 14 of *the Manual*.

Equation 4-3 uses the bearing capacity resistance factor (ϕ) and nominal bearing strength (R_n) to be greater than the factored axial load (P_u) calculated with the estimated projected bearing area taken from the face of the Upper Column (A_{pb}) and minimum yield stress of the bearing components (F_y).

$$\phi\ R_n = \phi\ 1.8\ F_y\ A_{pb} \geq P_u$$

Equation 4-3

Based on the calculated results for the bearing strength of the example design, the standardized designs in Chapter 5 do not require verification of the bearing capacity of the gravity column pairings.

4.4.3 Shim Plate Design

For column pairings that meet the criteria for acceptable flange support, Shim Plate (SP) requirements are determined for the column splice using Equation 4-4. If the calculated

thickness of the SP (t_{SP}) for each flange exceeds or is equal to 1/16 in., an appropriate plate thickness is assigned, rounded down to the nearest available plate thickness as given in the plate sizing guidelines of *the Manual* under Part 1. Further explanation of plate sizing is located in Appendix B.3. Note that the Shim Plates are not designed to carry bearing loads.

$$t_{SP} = \left| \frac{(d_{LC} - d_{UC})}{2} \right|$$

Equation 4-4

4.5 Strong-Axis Shear

When subject to shear in the strong axis direction (Figure 4.3), the load path within the SnapLocX Connection is provided from the Upper Column to the Lower Column through bearing at the beveled edges of the Lower Lock Plate (LLP) and Inner Plate (IP). Areas of concern as the IP transfers strong axis shear, include yielding through the IP cross-section and failure of the welds connecting the IP to the Lower Column. It is assumed that the bolts connecting the Outer Plate (OP) to the Lower Column do not experience strong axis shear demand or contribute to the strong axis capacity of the connection as the OP is flexible in that direction.

As noted above, the demand for strong axis shear (V_x) comes from Section D2.5c of *the* AISC *Provisions* and uses the minimum design story height (H), plastic section modulus of the Upper Column in the strong axis direction ($Z_{x_{UC}}$), and the nominal yield stress of the Upper Column ($F_{y_{UC}}$). The following subsections detail the various limit states needed to design the SnapLocX components for the required strong axis shear strength, with all associated resistance factors as provided by *the Steel Specification*.

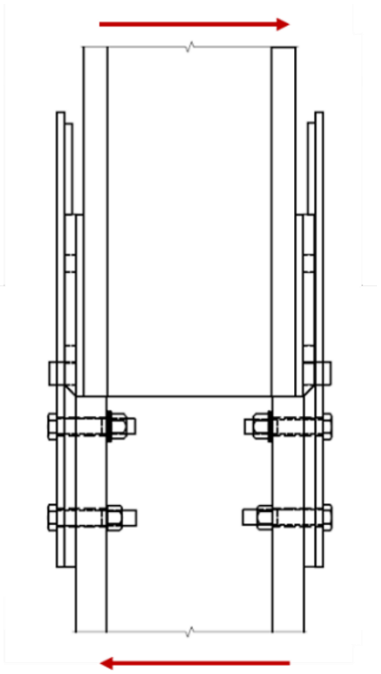

Figure 4.3: Strong axis shear applied to the column splice.

4.5.1 Through Thickness Shear of the Inner Plate

The transfer of strong axis shear through bearing at the 45° edges of the *LLP* and *IP* generates shear stress that occurs across the absolute thickness of the *IP* (t_{IP}), indicated by the black arrow in Figure 4.4.

The capacity of the *IP* to resist shear yielding under strong axis shear can be found using Section J4.2 of *the Steel Specification*. Using that and the required shear demand from *the Provisions* results in the required *IP* thickness, t_{IP}, to prevent shear yielding, as shown in Equation 4-5, where the yield strength of the *IP* is $F_{y_{IP}}$, the width of the *IP* is b_{IP}, the diameter of the shear key slot in the *IP* is d_{SK}, and other terms are previously defined.

$$t_{IP} \geq \frac{Z_{X_{UC}} F_{y_{UC}}}{H} \quad \frac{1}{\phi\, 0.6\, F_{y_{IP}} (b_{IP} - d_{SK})}$$

Equation 4-5

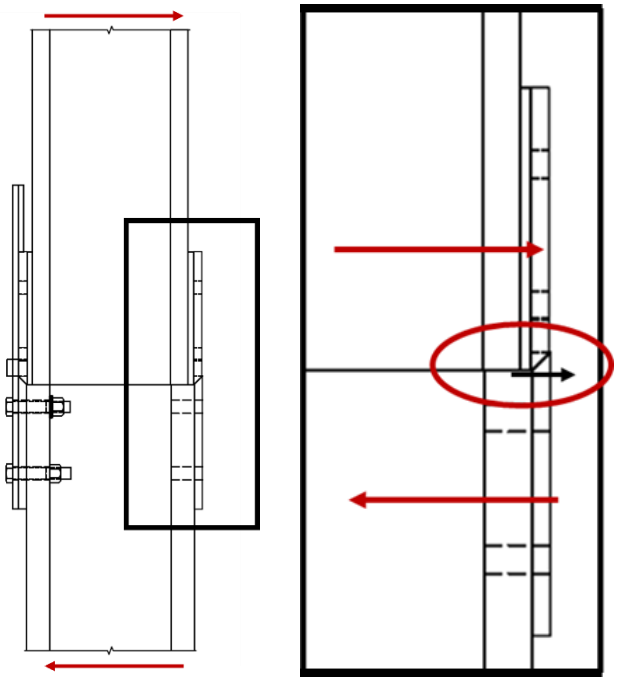

Figure 4.4: Strong axis shear transferred from the LLP to the IP through t_{IP}, with its location circled in red and the cross-section of interest identified with a short black arrow.

4.5.2 Inner Plate to Lower Column Fillet Weld

A C-shaped fillet weld connects the *IP* to the Lower Column along the plate's vertical edges and lower end and transfers the strong axis shear from the *IP* to the Lower Column. The dimension and layout of the weld resisting strong axis shear can be visualized in Figure 4.5. The required weld thickness, $t_{IP_{weld}}$, is found using Equation J2-4 from *the Steel Specification* rearranged as Equation 4-6 below.

$$t_{IP_{weld}} \geq \frac{\sigma_{total}}{\phi 0.6 * 0.707 * F_{EXX}}$$

Equation 4-6

The stress demand in Equation 4-7 is found conservatively using the elastic vector method, where the total stress is taken as the sum of the stress induced by the shear acting perpendicular to the IP and the bending resulting from the eccentricity between where the shear is applied through bearing at the IP's beveled edge and resisted at the centroid of the C-shaped weld. This is summarized in Equation 4-7 through Equation 4-9 below.

$$\sigma_{total} = \sigma_{weld} + \sigma_{bending}$$

Equation 4-7

$$\sigma_{weld} = \frac{P_{weld}}{(2\,L_{weld} + b_{weld})\,t_{IP_{weld_r}}}$$

Equation 4-8

$$\sigma_{bending} = \frac{M_{weld}\,\frac{L_{weld}}{2}}{I_{weld}}$$

Equation 4-9

A detailed example of the elastic vector method used to determine the weld thickness is provided in Section B.4.2 of Appendix B.

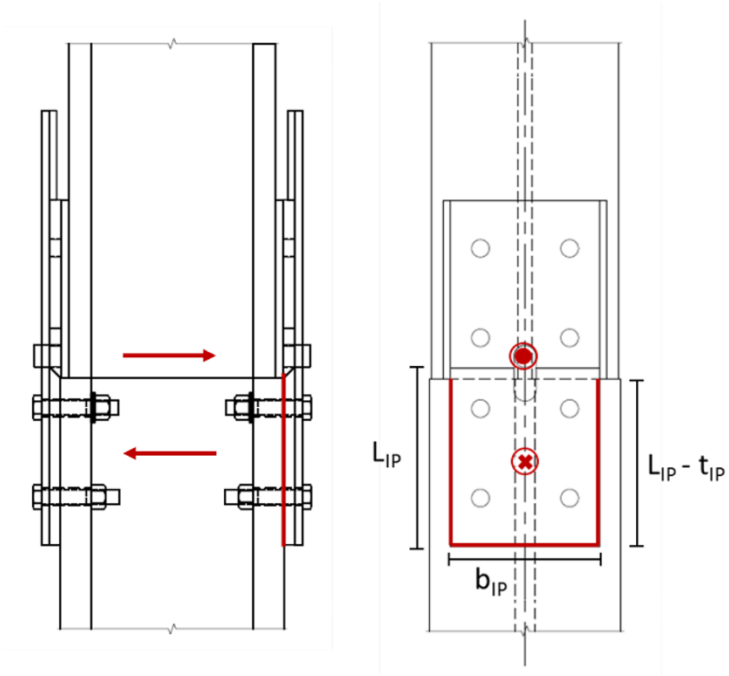

Figure 4.5: Dimensions and layout of IP welds affixed to the Lower Column to prevent strong axis shear.

4.6 Weak-Axis Shear

The weak axis shear, depicted in Figure 4.6, is transferred from the Upper Column and *LLP* through the Shear Key (*SK*), into the *OP*, through the Lower Column bolts, and into the Lower Column itself. Points of concern in that load path include potential yielding of the *SK*, failure of

the weld connecting the SK to the OP, yielding of the LLP due to SK bearing, and the eccentric loading of the bolt grouping.

The weak axis shear demand (V_y) is calculated according to Section D2.5 of *the Provisions* as M_{p_y}/H, where M_{p_y} is the smaller of the weak-axis plastic moment capacities of the columns being spliced, assumed to be the upper column, and *H* is the story height. The plastic moment capacity of the upper column is the plastic section modulus of the Upper Column in the weak axis ($Z_{y_{UC}}$) times the yield stress of the Upper Column ($F_{y_{UC}}$). All limit states checked in the transfer of weak axis shear use the associated resistance factor as given in *the Steel Specification*.

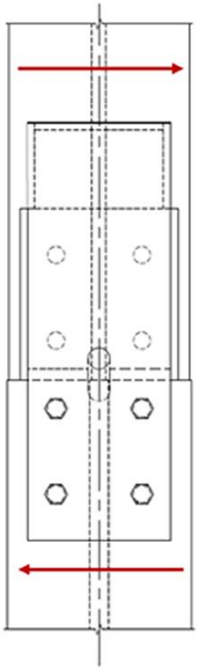

Figure 4.6: Weak axis shear direction through the column splice.

4.6.1 Shear Key Fillet Weld Yield

The SK is affixed to the OP through a circumferential weld on the exterior face of the OP. The design strength of the weld is determined using Section J2 and Equation J2-4 in *the Steel Specification*. The design thickness of the SK weld ($t_{SK_{weld}}$ must exceed the weak axis shear demand divided by the design strength of the weld and is given in Equation 4-10, where n_{KEY} is the number of shear keys (typically two, one on each OP attached to each flange), d_{KEY} is the shear key diameter, and other terms are as previously defined

$$t_{SK_{weld}} \geq \frac{Z_{y_{UC}} F_{y_{UC}}}{H} \frac{1}{n_{KEY} \phi F_{EXX} d_{KEY} \pi}$$

Equation 4-10

4.6.2 Shear Key Cross Section Yield

Yielding of the SK cross-section is governed by the SK cross-sectional area, and therefore, the diameter of the SK (d_{KEY}). The shear yielding capacity based on the area provided by d_{KEY} is calculated using Equation J4-3, located in *the Steel Specification*. Additionally, the number of SKs resisting weak axis shear (n_{KEY}) are taken into account when calculating the design strength. The rearranged equation to solve for the minimum shear key diameter, d_{KEY}, is provided in Equation 4-11.

$$d_{KEY} \geq + \sqrt{\frac{Z_{y_{UC}} F_{y_{UC}}}{H} \frac{4}{n_{KEY} \pi \phi 0.6 F_{y_{KEY}}}}$$

Equation 4-11

4.6.3 Shear Key Slot Bearing

The LLP transfers the weak axis shear to the SK through bearing along the slot in the LLP. Given the cylindrical shape of the SK and the shape of the SK slot in the LLP, only half d_{KEY} is bearing on the thickness of the LLP (t_{LLP}), as shown in Figure 4.7.

Using the previously determined d_{KEY} dimension, the minimum t_{LLP} is found using Equation J7-1 for bearing strength in *the Steel Specification* divided by the weak axis shear demand, as shown in Equation 4-12. To aid in fit-up and ensure the shear key does not get struck during assembly, it is assumed to be fabricated 1/16 in. shorter than the LLP thickness, which reduces the bearing area and is accounted for in Equation 4-12.

$$t_{LLP} - 1/16" \geq \frac{Z_{y_{UC}} F_{y_{UC}}}{H} \frac{1}{n_{KEY} \phi 1.8 F_{y_{LLP}} d_{KEY}}$$

Equation 4-12

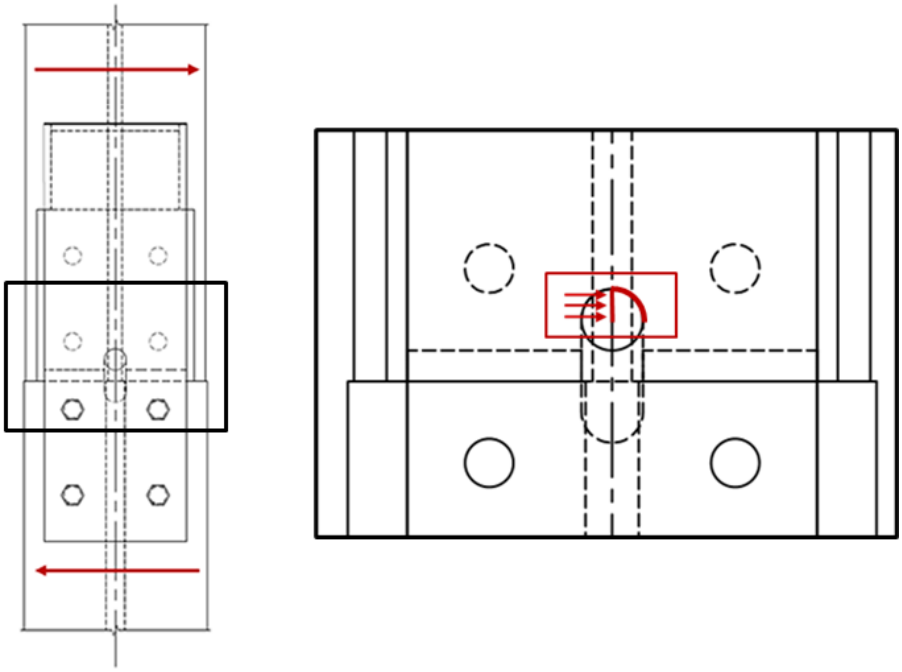

Figure 4.7: Weak axis shear transfer location from the SK to the LLP.

4.6.4 Eccentric Loading on the OP to the Lower Column Bolts

Weak axis shear is transferred from the OPs into the Lower Column through the bolt groups on each flange. These bolt groupings must be capable of withstanding the applied shear. The capacity of a bolt group to resist the force applied is calculated using Table 7-7 found in *the Manual*, which provides Equation 4-13 for bolt group capacity.

$$\phi R_n = C\phi r_n$$

Equation 4-13

Factors considered in determining the eccentrically loaded bolt group coefficient (C) include the bolt row distance (L_1), bolt column spacing (s), and bolt diameters (d_b). The bolt diameter is factored into Equation 4-13 through its available shear strength for the given d_b (r_n).

The horizontal distance from the centroid of the bolt group to the plane of action for the force (e_x), required for the tabulated C, is calculated for the connection design using Equation 4-14. This calculation involves the shear key slot depth (b_{SK}) and distance from the center of the upper bolt row to the upper end of the Lower Column (b_{OFFSET}). Dimensions used to calculate e_x and C are illustrated in Figure 4.8.

$$e_x = \frac{L_1}{2} + b_{top} + b_{OFFSET}$$

Equation 4-14

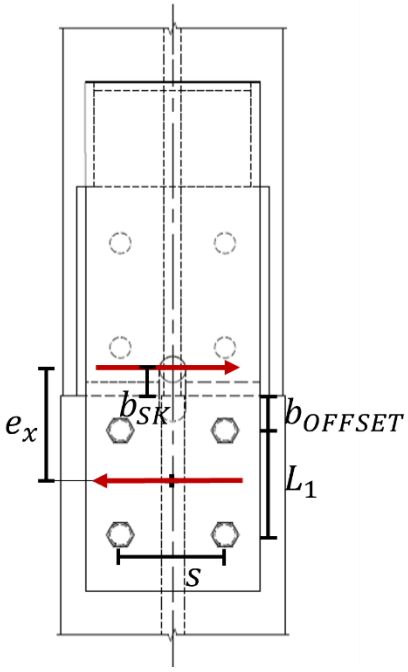

Figure 4.8: Bolt group dimensions for eccentrically loaded bolt groups.

Conservative approximations of e_x and s are used to determine a tabulated C from *the Manual* to ensure the bolt group can resist the weak axis shear demand. Equation 4-15 can be used to determine the upper bound plastic section modulus for the Upper Column in a splice for a given bolt layout with unique bolt properties, n_{bg} is the number of bolt groups resisting the weak axis shear demand (typically two, one on each OP of each column flange).

$$Z_{y_{UC}} \leq n_{bg}\, \phi R_n \, \frac{H}{F_{y_{UC}}}$$

Equation 4-15

4.6.4.1 Bolt Spacing Considerations

Additional considerations for bolt spacing apply to the group's layout on the Lower Column. *The Manual* specifies in Table 7-15 the allowable entering and tightening clearances for the column fillet (C_3) for given bolt diameters. As illustrated in Equation 4-10, C_3 limits the largest

allowable Lower Column size before the web to flange fillet begins to interfere with bolt group spacing considering bolt diameters and OP width for a designed connection.

With the inclusion of the disc spring washers, the outer diameter of the disc spring (OD) must not interfere with the column web to flange fillet while also considering the bolt edge spacing on the OP (b_{EDGE}). The design b_{EDGE} is calculated using the width of the OP (b_{OP}) and s and is provided in Equation 4-16. This must exceed the designated edge distance for bolt diameters as listed in Table J3.4 located in *the Steel Specification*.

$$b_{EDGE} = \frac{b_{OP} - s}{2}$$

Equation 4-16

The maximum OD (OD_{MAX}) of the disc springs is given in Equation 4-17, using the determined b_{EDGE} clearance. The design disc spring OD must not exceed the calculated OD_{MAX}.

$$OD_{MAX} = 2\, b_{EDGE}$$

Equation 4-17

As depicted in Figure 4.9, the maximum fillet size of the Lower Column ($k_{1_{max}}$) can be calculated using Equation 4-18.

$$k_{1_{max}} = \frac{s}{2} - MAX\left(\frac{OD_{max}}{2},\, C_3\right)$$

Equation 4-18

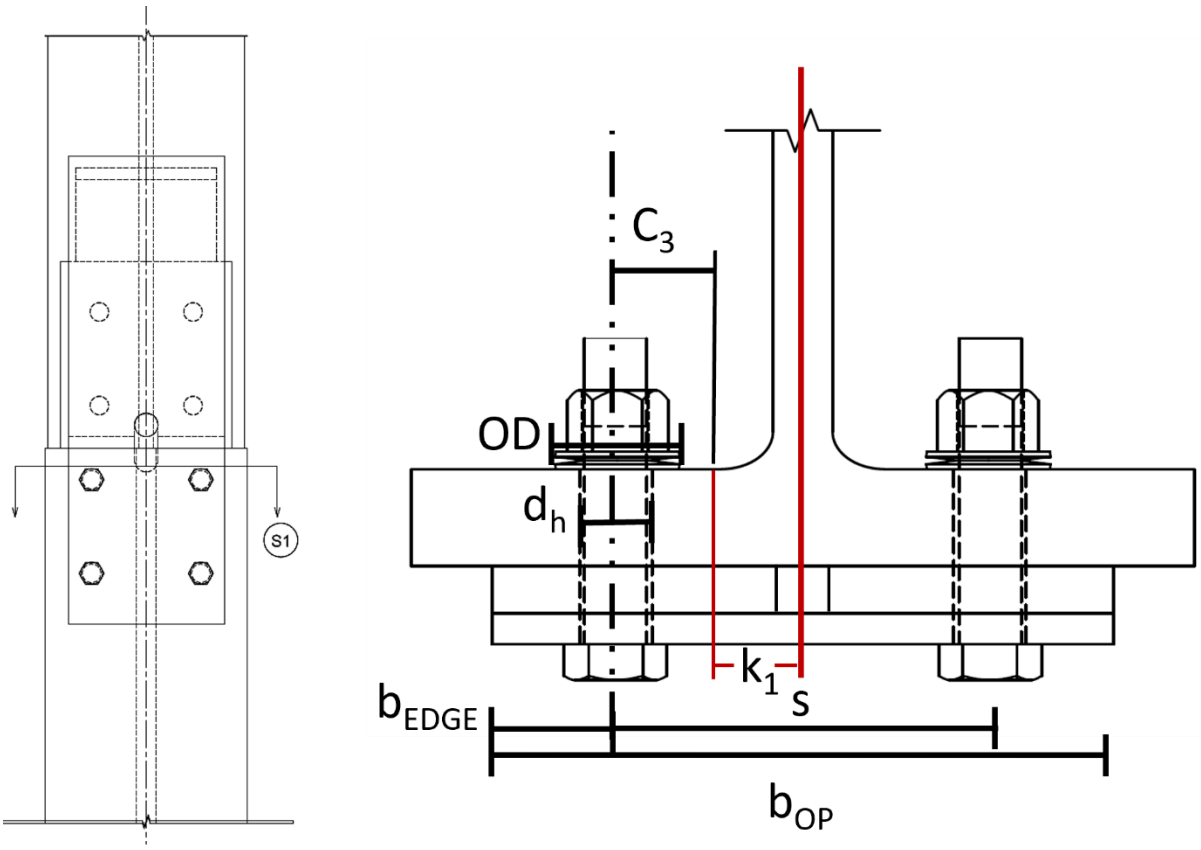

Figure 4.9: Dimensions used to determine the maximum column fillet size of the Lower Column.

4.7 Outer Plate Flexural Yielding

During the SnapLocX assembly, the OP will bend and deform to accommodate sliding the LLP and Upper Column past the ULP, as shown in Figure 4.10. The moment induced in the OP should not exceed its yield moment, as any permanent deformation would reduce the effectiveness of the snapping mechanism. A model of the OP during snaping is proposed in Equation 4-11.

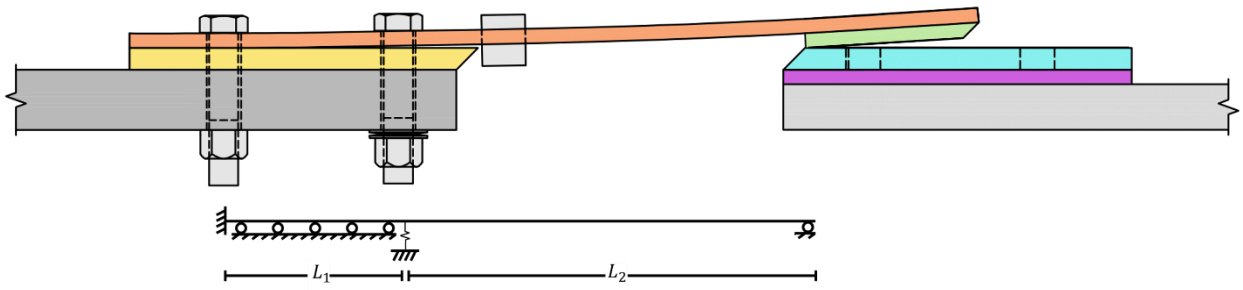

Figure 4.10: Illustration of OP bending and the mathematical model used to check OP yielding and disc spring compression.

The sections of the OP below the lower bolts (left of the bolts in Figure 4.10) and above the lower end of the ULP (right of the ULP and LLP intersection in Figure 4.10) do not experience bending or shear. Therefore, the proportion of the OP considered in the model is located between the lower bolt row and the lower end of the ULP. The maximum OP deformation is equal to the thickness of the ULP (t_{ULP}), as the thickness of the IP (t_{IP}) and thickness of the LLP (t_{LLP}) are designed to be identical. The springs shown in the model represent the disc springs, whose stiffness is much less than that of the bolts. However, the disc spring behavior is nonlinear, which complicates solving the model for moment demand in the OP.

To determine the moment demand in the OP during snapping, the beam model of the OP is analyzed in stages. The results are then superimposed with iterations conducted to include the nonlinear behavior of the disc springs. The steps to calculate the moment demand are as follows:

1. Apply bolt pretensioning to the upper bolts with disc spring washers, as detailed in Section 4.7.1.
2. Compute the displacement at the free end required to initiate uplift at the disc springs and overcome the pretension. The uplift analysis is completed in Section 4.7.2.
3. Use superposition to compute the deformed shape, shear, and moment along the length of the beam from the application of the maximum OP end displacement, excluding displacement from initial uplift at the disc spring and the additional disc spring forces. This process requires multiple iterations due to the nonlinear behavior of the disc springs and is fully outlined under Section 4.7.3.

4.7.1 Pretensioning in the Spring Bolts

The disc springs bolts are pretensioned during the prefabrication of the SnapLocX Connection to prevent OP movement after the splice is assembled. Figure 4.11 shows the beam model used to calculate the plate's moment, shear, and displacement with pretensioned bolts. In this model, the lower bolt row is modeled as a fixed end, while the portion of the OP interacting with the IP modeled as roller supports. The pretensioned spring force (P_{pt}) at the upper bolts is designed to be 0.2 kip.

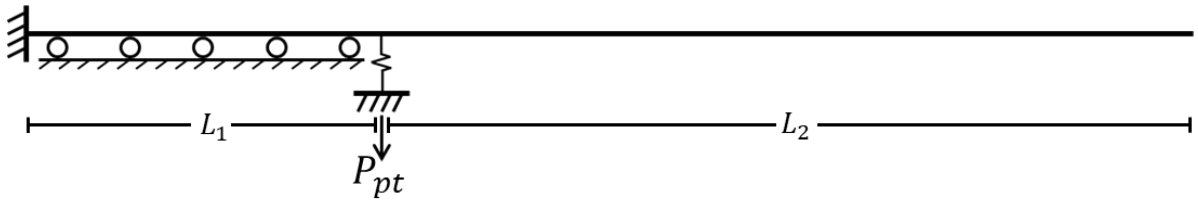

Figure 4.11: Beam mathematical model for pretensioned bolts, occurring before installation.

As described above in Section 3.1.1.3(i), there is a nonlinear force-displacement relationship for disc springs, which is dependent on their geometry. The application of a pretensioned force on the bolts with disc springs results in an initial deformation in the disc springs, as illustrated in Figure 4.12**Error! Reference source not found.**. This initial spring deformation from pretensioning (δ_{s_0}) is determined by considering a disc spring's conical height (h) and the number of springs for each bolt (n_s). The equation provided in Figure 4.12 for total spring height refers to the number of springs in series.

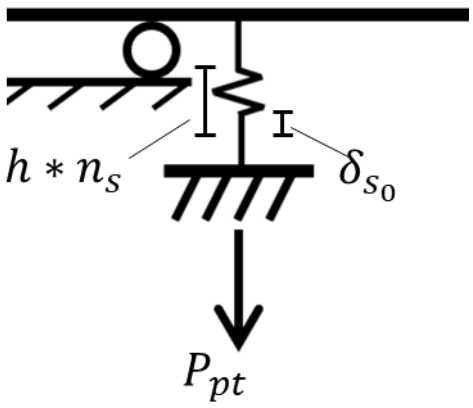

Figure 4.12: Initial disc spring displacement due to pretensioned bolts for single springs for springs in series.

The initial deformation determined is interpolated between two deformation points at the desired pretension force value, as displayed in Equation 4-19.

$$\delta_{s_0} = \delta_{Force}(P_{pt})$$

Equation 4-19

The pretension force and initial spring displacement are shown on the disc spring force-displacement curve in Figure 4.13, and the arrows identify the steps used to solve for δ_{s_0}.

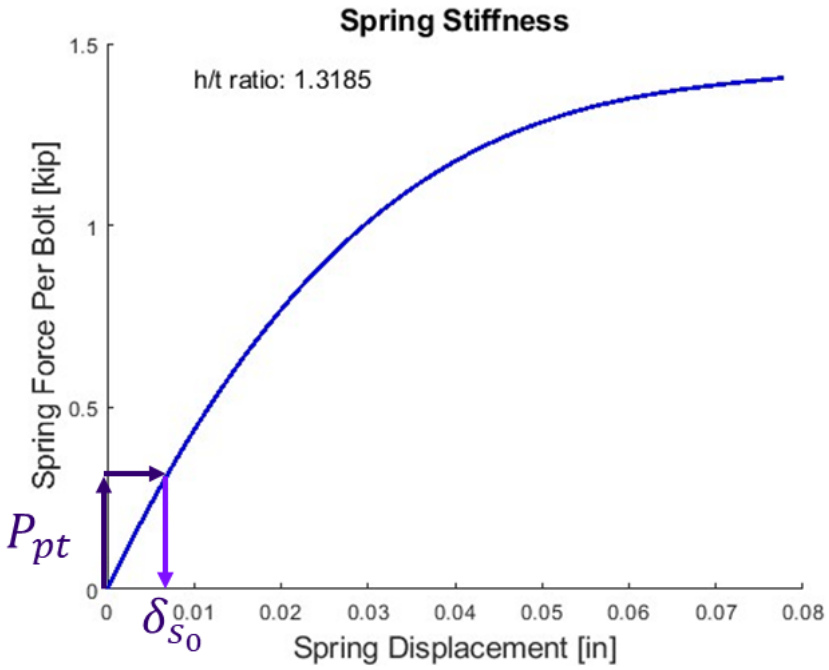

Figure 4.13: Example design force-deformation curve for the assigned disc springs.

4.7.2 OP Uplift at Spring Bolts

The uplift of the OP at the disc springs occurs when the end of the plate is displaced enough to generate an uplift force (F_{up}) equal to the pretensioned force. The beam model of the OP modeling the uplift force is provided in Figure 4.14.

Figure 4.14: Mathematical beam model used for instantaneous uplift at the disc springs (L_1).

The end plate displacement for instantaneous uplift (δ_{up}) is calculated with Equation 4-20 with the known F_{up} along with the Young's Modulus of the OP material (E), moment of inertia for the OP (I_{OP}), and distance between the spring bolts and the lower end of the ULP (L_2).

$$\delta_{up} = \frac{F_{up}\, {L_2}^3}{3\, E\, I_{OP}}$$

Equation 4-20

Since there is no additional force acting on the disc springs, the initial displacement of the washers remains constant, as determined in Equation 4-19.

4.7.3 Post-Uplift Behavior Using Superposition Load Curves

To determine the force exerted by the disc springs at maximum deformation of the OP, two beam models are analyzed and superimposed. One does not include forces from the disc springs, while the other does. The first beam model, Beam 1, provides an initial OP displacement at the disc springs, which is used to calculate the force imposed by the disc springs on the OP. These disc spring forces are then applied to the second beam model, Beam 2, which is used to analyze the beam for just the disc spring force as described in Section 4.7.3.1.

By superimposing the displacement curves from Beams 1 and 2, the combined plate displacement at the disc springs becomes the new spring deformation estimate. Beam 2 calculations are then iterated, and displacements are again superimposed with Beam 1 curves. The process is iterated until the change in spring deformation between iterations is within a predefined tolerance.

4.7.3.1 Beam 1: Cantilever Beam with Displacement at End

Modeled Beam 1 is represented as a cantilever beam with an applied force to achieve the required displacement at the end, shown in Figure 4.15. The lower connection bolts are modeled as a fixed end, and the displacement of the beam needed, without the uplift displacement ($\delta_{1_{end}}$), is modeled as an upward force (F_1). It is assumed that the OP is completely uplifted from the IP and there is no additional support is present along L_1.

Figure 4.15: Mathematical beam model for the OP as a cantilever with end displacement.

The required free-end displacement to determine F_1, $\delta_{1_{end}}$, is calculated using the difference between the maximum deflection at the end from t_{ULP}, δ_{max}, and δ_{up}, as in Equation 4-21.

$$\delta_{1_{end}} = \delta_{max} - \delta_{up}$$

Equation 4-21

The upward force (F_1) is calculated using maximum Beam 1 displacement ($\delta_{1_{end}}$) and the plate stiffness (k_{OP}), shown in Equation 4-22.

$$F_1 = k_{OP}\,\delta_{1_{end}} = \frac{3\,E\,I_{OP}\,\delta_{1_{end}}}{L_{tot}^{\,3}}$$

Equation 4-22

Using standard beam equations, which are provided in Appendix B.6.3.1, the displacement at the location of the disc springs (δ_{s_1}) is determined.

4.7.3.2 Beam 2: Propped Fixed Beam with Disc Spring Force

After identifying the required beam displacement at the disc springs from Beam 1, it serves as an initial guess for the spring force on Beam 2 (P_{s_2}) in the propped fixed beam and displacement force model depicted in Figure 4.16.

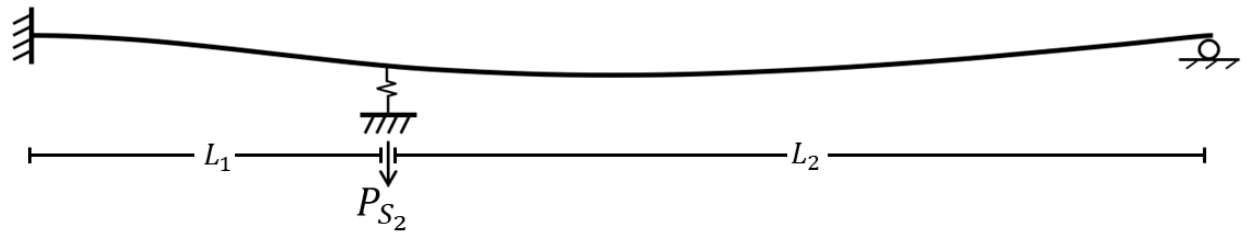

Figure 4.16: Propped cantilever beam model with a displacement force from the disc springs.

By setting δ_{s_1} as the spring deformation of Beam 2 (δ_{s_2}), the total spring deformation ($\delta_{s_{total}}$), seen in Figure 4.17, produces a total disc spring force, including the pretensioned force.

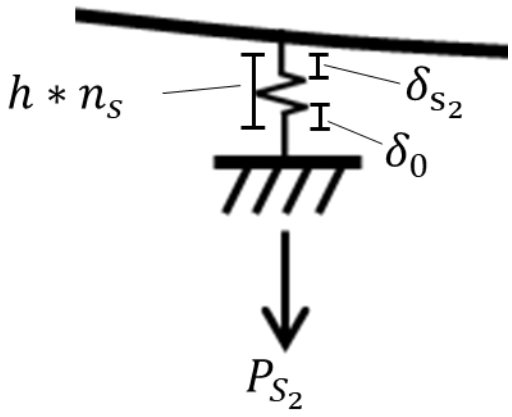

Figure 4.17: Total deformation changes of the disc springs.

$$\delta_{s_{total}} = \delta_{s_2} + \delta_0$$

Equation 4-23

The spring force specific to Beam 2, P_{s_2}, is determined using the nonlinear disc spring force-deformation curve from Chapter 3.1.1.3(i) and Appendix A, excluding P_{pt}, as shown in Equation 4-24. Figure 4.18 illustrates this on the disc spring force-displacement curve, and Equation 4-24 is used to determine the force for loading Beam 2 from δ_{s_2}, $\delta_{s_{total}}$, and P_{δ_s}.

$$P_{s_2} = P_{\delta_s}\left(\delta_{s_{total}}\right) - P_{pt}$$

Equation 4-24

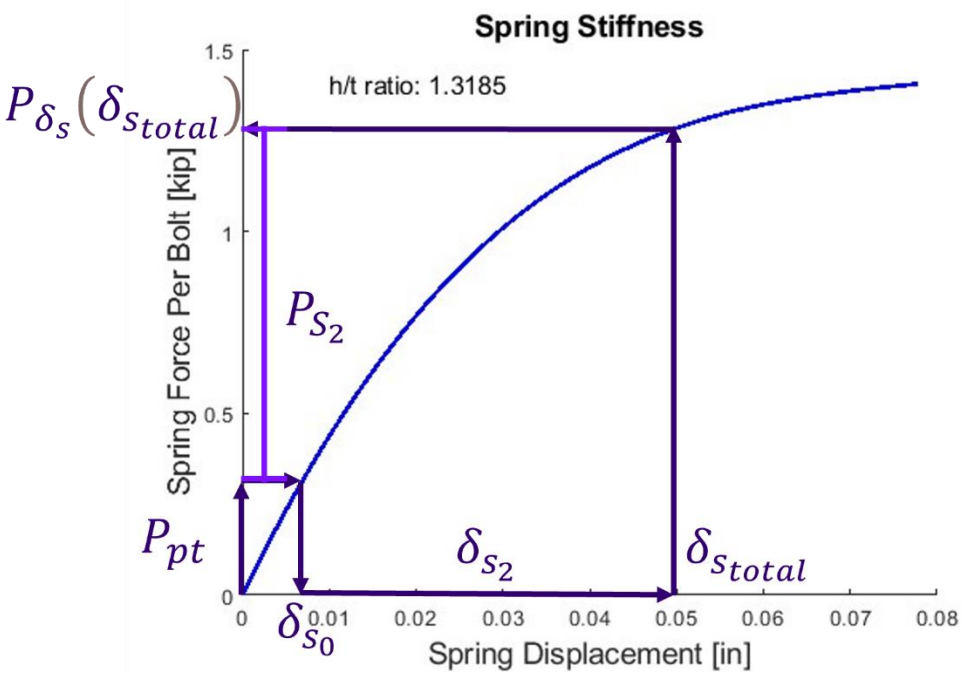

Figure 4.18: The process for calculating the spring force for Beam 2 using the spring force-displacement curve.

The beam equations provided in Section B.6.3.2 of the Appendix are used to develop moment, shear, and displacements along the length of Beam 2.

4.7.3.3 Superimposing Beams 1 and 2 for New Beam Displacement and Applied Spring Force

To understand the complete behavior of the OP Beams 1 and 2 are superimposed. This results in a new beam displacement at L_1 using the combined displacement curves of Beam 1 and Beam 2 (D_{12_0}). Figure 4.19 displays exaggerated displacements along the OP for Beam 1, Beam 2, and the combined case.

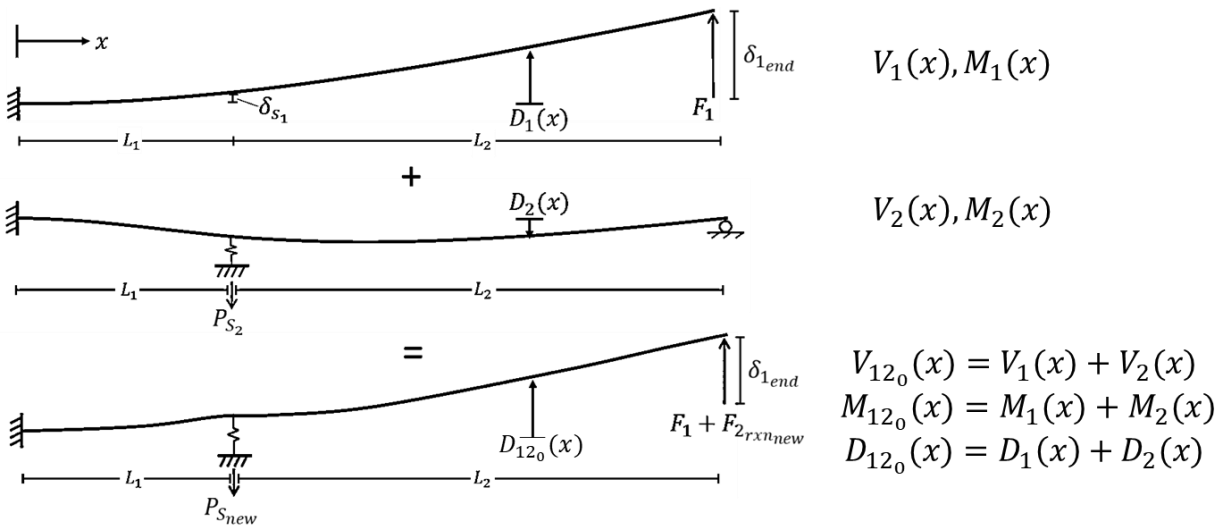

Figure 4.19: Superimposed beams with moment, shear, and deformation.

The displacement of the combined curves at the disc springs is evaluated in Equation 4-25 and compared to the disc spring displacement used to generate the Beam 2 force. The difference between those is checked against a tolerance seen in Equation 4-26.

$$\delta_{next} = D_{12_0}(L_1)$$

Equation 4-25

$$\left|\delta_{next} - \delta_{s_2}\right| \leq 0.000001$$

Equation 4-26

If the tolerance is not satisfied, δ_{next} becomes the new estimate for spring deformation in Beam 2 ($\delta_{s_2 next}$) and Beam 2 is solved again for $M_{2_{next}}$, $V_{2_{next}}$, and $D_{2_{next}}$. These are then superimposed with M_1, V_1, and D_1 to create the following estimate for superimposed curves, $M_{12_{next}}, V_{12_{next}}$, and $D_{12_{next}}$. The displacement at the location of the springs is once again evaluated for a new δ_{next} and compared against the previous spring deformation ($\delta_{s_{2_{next}}}$) used in the new Beam 2 curve calculations. If the tolerance is satisfied, the superimposed curves of Beams 1 and 2 are used to finalize the plate displacement and load demands. If not, the process is repeated until the set tolerance is satisfied.

4.7.4 Finalized Displacement Curve and Load Demands

Upon achieving the tolerance-satisfied $M_{12_{next}}, V_{12_{next}},$ and $D_{12_{next}}$ curves, they are superimposed on the curves from uplift at the disc springs to create the total moment, shear, and displacements for the OP ($D_{total}, V_{total},$ and M_{total}) and determine the maximum moment on the OP during assembly. Figure 4.20 shows the results for the example connection design calculated in Appendix B.

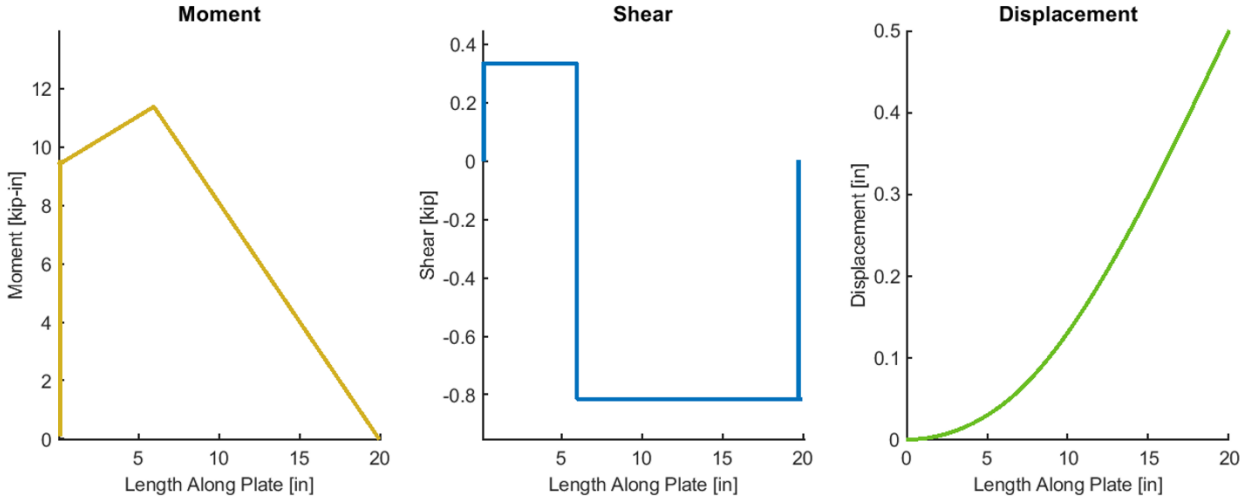

Figure 4.20: Finalized moment, shear, and displacement curves for maximum bending in the OP for the example SnapLocX design in Appendix B.

An algorithm for determining the OP moment demand and disc spring forces during snapping is outlined as follows:

1. Calculate Beam 1 moment, shear, and deflection curves (M_1, V_1, D_1) and determine the beam displacement at L_1 (δ_{s_1}).
2. Apply δ_{s_1} set to the spring deformation of Beam 2 (δ_{s_2}) at L_1 to calculate the initial spring force on Beam 2. Calculate the accompanying moment, shear, and deflection curves (M_2, V_2, D_2).
3. Superimpose curves from Beams 1 and 2, generating initial combined curves:
$$M_{12_0} = M_1 + M_2, \quad V_{12_0} = V_1 + V_2, \quad D_{12_0} = D_1 + D_2$$
4. Determine the displacement of the OP at L_1 from the superimposed displacement curve (D_{12_0}) as:

$$\delta_{next} = D_{12_0}(L_1)$$

5. Iterate Beam 2 spring forces using δ_{next}, so that while $\left|\delta_{next} - \delta_{s_2}\right| \geq$ Tolerance, δ_{next} is used to be the new spring deformation estimate of Beam 2 ($\delta_{s_{2_{next}}}$). Recalculated moment, shear, and displacement curves for Beam 2 ($M_{2_{next}}, V_{2_{next}}$, and $D_{2_{next}}$), and superimpose on Beam 1 curves to create the next estimated curves ($M_{12_{next}}$, $V_{12_{next}}$, and $D_{12_{next}}$), reevaluating the displacement of $D_{12_{next}}$ at the disc springs until the tolerance is satisfied.
6. Once the displacement at the disc springs converges to within the specified tolerance (examples here use a tolerance of 0.000001), combine the iterated curves with the moment, shear, and displacement curves from the initial uplift to provide total beam deflection, shear, and moment equations:

$$D_{total}, V_{total}, \text{ and } M_{total}$$

7. The maximum moment of all curves (max (M_{total})) represents the moment demand for the OP.

4.7.4.1 Elastic Limit Check

The maximum moment demand on the OP during installation is established from the total moment curve. The point along the plate where the maximum moment demand occurs is directly over the disc springs. At this location, the moment capacity of the OP is reduced due to the presence of the bolt holes. The moment resistance is limited to the yield moment of the OP, $M_{y_{OP}}$, to prevent any permanent deformation and is calculated in Equation 4-27, considering the yield strength of the OP ($F_{y_{OP}}$), total OP moment of inertia (I_{OP}), and reduced I_{OP} from the bolt holes (d_h) and thickness of the OP (t_{OP}).

$$M_{y_{OP}} = \frac{F_{y_{OP}} \left(I_{OP} - 2\frac{d_h\, t_{OP}^3}{12}\right)}{\frac{t_{OP}}{2}}$$

Equation 4-27

The demanded moment from the total curves during bending must not exceed $M_{y_{OP}}$.

4.8 Snapping Friction Check

For the OPs to deform during assembly, the weight of the upper column (W) must exceed the shear force at the end of the two OPs ($V_{total}(L_{tot})$) determined in Section 4.7, and the coefficient of friction (μ). This relationship is expressed in Equation 4-28, and the value for the coefficient of friction is identified in Equation 4-29.

$$W \geq 2\,\mu\,V_{total}(L_{tot})$$

Equation 4-28

$$\mu = 0.3$$

Equation 4-29

4.9 Limit States for Strong Axis Flexural Capacity

It may be necessary to compute the column splice flexural capacity for certain applications. While columns in gravity framing do not generally have flexural demands, and the requirements from the *Provisions* concerned with deformation compatibility for seismic loads specify only a shear strength requirement, there may be cases where the flexural capacity must be computed. In the design example of Appendix B, the flexural capacity is not treated as a design constraint but instead is calculated for the designed connection. Further, the standardized connections described in Chapter 5 do not consider flexural strength as a design constraint. Nonetheless, this section describes the limit states that should be considered for computing the strong axis flexural capacity of a SnapLocX splice.

Figure 4.21 illustrates an applied moment over the column splice. In tension, the left side of the figure expands the SnapLocX connection to demonstrate the transfer of force from one component to another. The right side of the image shows flange bearing transferring the compression component of the moment. Limit states considered for each numbered location can be identified in the caption of Figure 4.21.

Example calculations for limit state flexural capacity are provided in Appendix B.8: “Limit States for Strong Axis Flexural Capacity.” All limit state design strengths include the accompanying resistance factor as defined for each state in *the Steel Specification*.

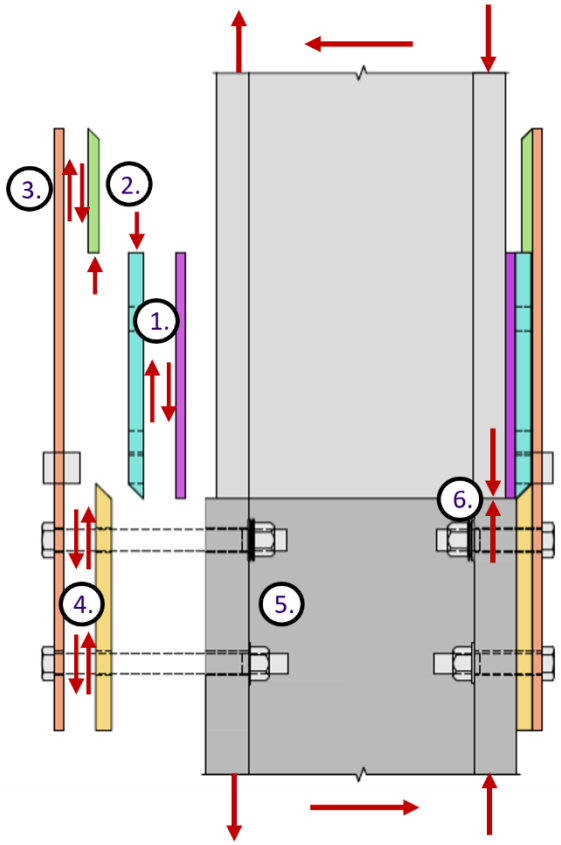

Figure 4.21: Locations of the column splice analyzed for flexural limit states:
1. LLP fillet weld to Upper Column, 2. ULP bearing on LLP, 3. ULP weld to OP, 4. OP limit states from bolts, 5. Bolt limit states, 6. Column flange bearing.

4.9.1 Upper Column Flange to Shim Plate to Lower Lock Plate: Fillet Weld

The minimum fillet weld strength connecting the *LLP* to the Upper Column occurs at the *LLP* to *SP* welds or the *LLP* to Upper Column welds, depending on the *SP* requirement. Fillet weld strength at this location, using a constant weld thickness, is controlled by the length of the weld. *The Steel Specification* defines weld strength as Equation 4-30 using the effective weld area (A_{we}) and nominal weld stress (F_{nw}). This is derived from Section J2 and Equation J2-4 as provided in *the Steel Specification*.

$$\phi R_n = \phi F_{nw} A_{we}$$

Equation 4-30

4.9.2 Lower Lock Plate to Upper Lock Plate: Bearing

The flat bearing strength between the LLP and ULP, shown in Equation 4-31, is provided as Equation J7-1 for bearing strength with finished surfaces from *the Steel Specification*. Equation 4-31 considers the minimum yield stress between the LLP and ULP (F_y) and projected bearing area between the two surfaces (A_{pb}).

$$\phi R_n = \phi 1.8\, F_y\, A_{pb}$$

Equation 4-31

4.9.3 Upper Lock Plate to Outer Plate: Fillet Weld

The fillet weld design strength connecting the ULP to the OP is derived using the same process as denoted in Section 4.9.1.

$$\phi R_n = \phi F_{nw} A_{we}$$

Equation 4-32

4.9.4 Outer Plate Limit States

Four OP limit states are considered during bending and involve the cross-sectional strength and plate strength at the bolts.

4.9.4.1 Bolt Tearout

The available OP strength at the bolts is partially determined using bolt tearout strength, seen in Equation 4-33. This is derived from Section J3.10 and Equation J3-6d in *the Steel Specification* for deformation of the OP and is not considered for design at service load. OP properties considered for bolt tearout include the ultimate stress of the OP (F_u), the thickness of the OP (t), and the clear distance in the direction of the applied load from the bolt holes to adjacent holes and plate end (l_c).

$$\phi R_n = \phi\ 1.5\, F_u\, l_c t$$

Equation 4-33

4.9.4.2 Tensile Yielding

The design strength of the OP for tensile yielding considers the total cross-sectional area of the OP (A_g) as defined in Equation D2-1 from Chapter D of *the Steel Specification*, rewritten as Equation 4-34. In addition to the gross area of the OP, the yield stress of the OP (F_y) is required.

$$\phi P_n = \phi\, F_y A_g$$

Equation 4-34

4.9.4.3 Tensile Rupture

The tensile rupture design strength for the OP considers plate rupture across the bolt holes. Using Chapter D in *the Steel Specification*, design strength for tensile rupture is found in Equations D2-2 and D3-1 and Table D3.1, summarized in Equation 4-35. OP properties used to solve for tensile rupture include the ultimate stress of the OP (F_u), a shear lag factor from Table D3.1 (U), and the net area of the OP through the bolt holes (A_n).

$$\phi P_n = \phi\, F_u U A_n$$

Equation 4-35

4.9.4.4 Block Shear

Block shear design strength incorporates shear and tensile loading from an applied force, using Equation J4-5 in *the Steel Specification.* The lesser design strength of the two methods used determines the capacity of the given mode. The lesser of the two modes is used for block shear design strength.

Equation J4-5, rewritten as Equation 4-36 below, uses the ultimate and yield stress of the OP (F_u, F_y), net area of the OP subject to shear (A_{nv}), net area subject to tension (A_{nt}), and gross area subject to shear (A_{gv}).

$$\phi R_n = \phi 0.6 F_u A_{nv} + U_{bs} F_u A_{nt} \leq \phi 0.6 F_y A_{gv} + U_{bs} F_u A_{nt}$$

Equation 4-36

Two modes of the OP are analyzed for block shear below using Equation 4-36. Each section contains the individual areas for net shear, net tension, and gross shear used to identify the mode capacity.

4.9.4.4 (i) Mode 1

Mode 1 analyzed for block shear, shown in Figure 4.22, projects plate failure at the end and edge of the OP.

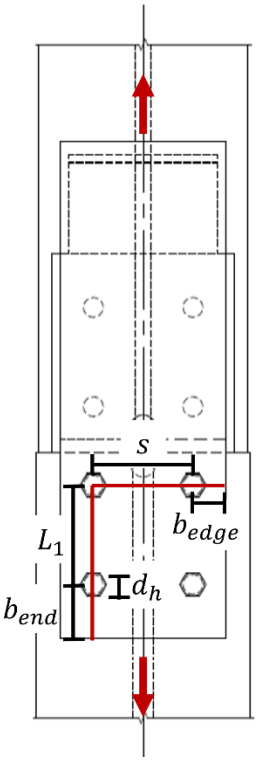

Figure 4.22: Mode 1 for block shear.

Areas considered for Equation 4-36 are listed below in Equation 4-37 through Equation 4-39 and solved for using the OP dimensions provided in Figure 4.22.

$$A_{nv} = t_{OP}\left(L_1 - d_h + b_{END} - \frac{d_h}{2}\right)$$

Equation 4-37

$$A_{nt} = t_{OP}\left(s + b_{EDGE} - 1\frac{1}{2}\,d_h\right)$$

Equation 4-38

$$A_{gv} = t_{OP}\left(L_1 + b_{END}\right)$$

Equation 4-39

4.9.4.4 (ii) Mode 2

Block shear analyzed under Mode 2 is provided in Figure 4.23, with two points of failure projecting to the end of the OP.

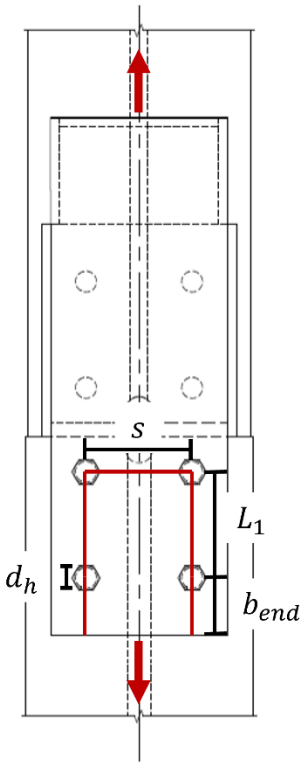

Figure 4.23: Mode 2 for block shear.

Areas considered for block shear in Equation 4-36 use the following area provided in Equation 4-40 through Equation 4-42, using the OP dimensions, as shown in Figure 4.23.

$$A_{nv} = n_{col}\, t_{OP}\, (L_1 - d_h + b_{END} - \frac{d_h}{2})$$

Equation 4-40

$$A_{nt} = t_{OP}\, (s - d_h)$$

Equation 4-41

$$A_{gv} = n_{col}\, t_{OP}\, (L_1 + b_{END})$$

Equation 4-42

4.9.5 Bolt Failure

Design strength for the failure of the bolts connecting the OP to the Lower Column are listed in the following section, considering flange bearing and cross-sectional shear failure.

4.9.5.1 Bolt Bearing of the Outer Plate to the Lower Column Flange

The design strength for the bolt bearing between the OP and Lower Column flange is derived from Equation J3-6a from *the Steel Specification* for bolt deformation when the design considers service load. The design strength, shown in Equation 4-43, considers the number of bolts in tension (n_b), the bolt diameter (d_b), the thickness of the OP (t), and the ultimate strength of the OP (F_u).

$$\phi R_n = n_b \, \phi \, 2.4 \, d_b \, t \, F_u$$

Equation 4-43

4.9.5.2 Bolt Shear

The design strength of bolt shear for a snug-tightened bolt is found using Section J3 with Equation J3-1 from *the Steel Specification*. As provided below in Equation 4-44, bolt shear considers the number of bolts in shear from the applied tension force (n_b), the unthreaded area of the body of the bolt (A_b), and the nominal tensile or shear strength of the bolt (F_n) as identified in Table J3.2.

$$\phi R_n = n_b \, \phi F_n \, A_b$$

Equation 4-44

4.9.6 Column Flange Bearing

The tension component of column bending is observed in column flange bearing. The design strength of flange bearing is determined using Equation J7-1 from *the Steel Specification* and provided in Equation 4-45. Like LLP and ULP bearing from Section 4.9.2, the flat face bearing of the flanges considers the projected bearing area (A_{pb}) and minimum yield stress of the connecting columns (F_y).

$$\phi R_n = \phi \, 1.8 \, F_y \, A_{pb}$$

Equation 4-45

4.9.7 Moment Capacity of the Column Connection

The moment capacity of the SnapLocX Connection is determined using the controlling limit state for the tension component of the moment, T, as expressed in Equation 4-46 since the column flange bearing strength will typically be more significant than most of the tension limit states.

$$T = MIN(\phi\, R_n, \phi\, P_n)$$

Equation 4-46

The strong axis moment is determined using Equation 4-47 from T and the moment arm (d_m) between the centers of the Upper Column flanges.

$$M_n = T\, d_m$$

Equation 4-47

Chapter 5: Development of SnapLocX Connections Families

This chapter describes the complete development and application of standardizing the SnapLocX Connection components customized for column pairings within W14, W12, and W10 shape sizes. Building on the design process described in the preceding chapter, a systematic approach was used to determine families of connection component designs that accommodate wide ranges of column shapes while ensuring satisfactory shear strength and snapping mechanism behavior. The goal for the SnapLocX families is to minimize the number of plate configurations while also providing efficient designs.

5.1 Standardized Designs

The standardized designs for the SnapLocX Connection feature seven different designs for the Outer Plate (OP) combination and nine different designs available for selection for the Lower Lock Plate (LLP) and Inner Plate (IP). To utilize the standardized designs for a specific column pairing, a particular combination of plates is formed, consisting of one lettered OP design and two numbered plates assigned as the LLP and IP. The standardized designs then have a total of nine combinations of Lettered and Numbered Plates exist for the standardized designs. The following sections provide information regarding the development and final dimensions of the lettered and numbered plate groups.

5.1.1 Inner and Lower Lock Plates

To optimize the plate manufacturing process, the essential plate properties for the IP and LLP are integrated into a single design, as required for pairs of Upper and Lower Columns. This integration forms the “Numbered Plates” grouping. A comprehensive layout for the Numbered Plate assignments is illustrated below in Figure 5.1, with the corresponding dimensions provided in Table 5-1.

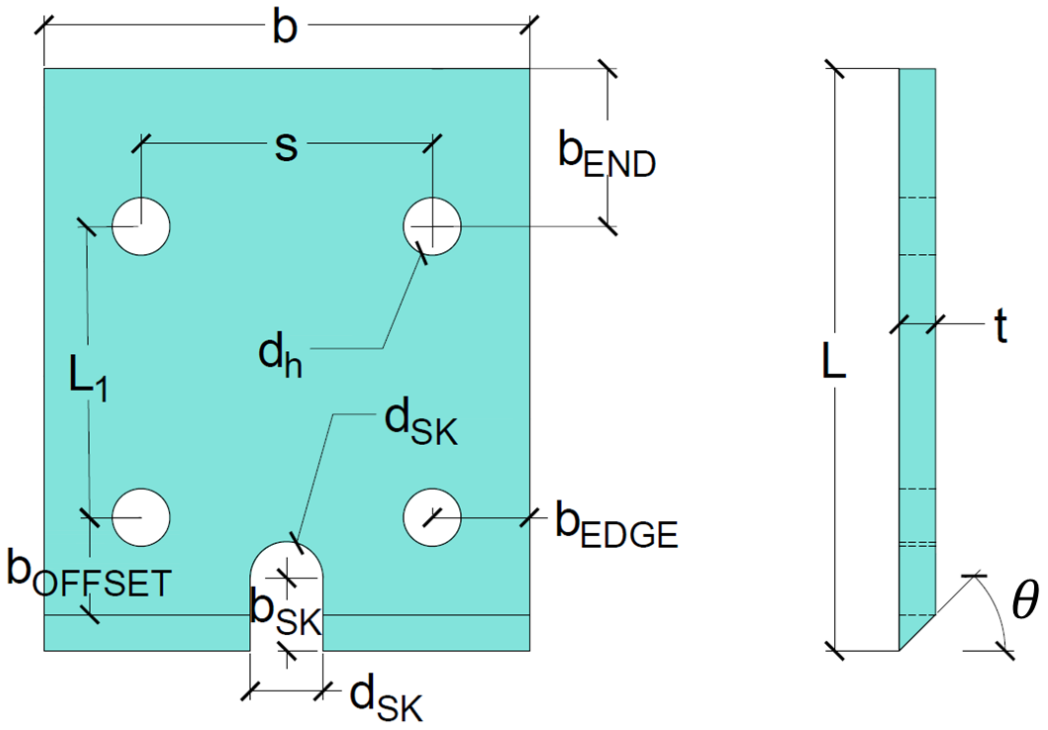

Figure 5.1: Design variables for the Inner Plate and Lower Lock Plate as pertaining to Table 5-1. Subscripts denoting the plate assignment are disregarded as the dimensions are the same for the LLP and IP.

The design variables associated with the standardized *LLP* and *IP* include plate width (b), full plate length (L), and plate thickness (t).

Bolt dimensions and the hole layout dimensions include the distance from the center of the bolt row to the non-beveled end (b_{END}), the distance the bolts are offset from the column splice (b_{OFFSET}), the distance from the center of the bolt columns to the nearest edge (b_{EDGE}), the spacing between bolt columns (s), and distance between bolt rows (L_1). The dimensions for bolt holes (b_h) are determined from Table J3.3 in *the Steel Specification*, based on the assigned bolt diameter. Additionally, all numbered plates beveled end (θ) opposite b_{END}. The angle for the beveled end (θ) is standardized in Equation 5-1.

$$\theta = 45°$$

Equation 5-1

With variables b_{OFFSET} and L_1 designed to be constant across all Numbered Plates, the variable b_{END} can be verified using Equation 5-2.

$$b_{END} = L - \tan(\theta) - b_{OFFSET} - L_1$$

Equation 5-2

The SK slot variables include the slot diameter (d_{SK}) and distance from the beveled end to the center of the slot diameter (b_{SK}). The bottom of the Shear Key cylinder should be positioned immediately above the splice. The values for d_{SK} are calculated using Equation 5-3 below, while b_{SK} measurements are solved using Equation 5-4.

$$d_{SK} = d_{KEY} + 1/8 \ in.$$

Equation 5-3

$$b_{SK} = t \tan(\theta) + \frac{d_{KEY}}{2}$$

Equation 5-4

The dimensions for the Numbered Plate variations are detailed below in Table 5-1, beginning with the largest plate designated as Plate 1. For Numbered Plates, where d_b, d_h, s, L_1, b_{EDGE}, and b_{END} dimensions are not provided, the plate assignment is exclusively designated in a column pairing as a LLP. Similarly, Numbered Plates lacking d_{KEY}, d_{SK} and b_{SK} are exclusively assigned as an IP in the connection.

The weld thickness needed for attaching the IP and LLP to the Upper and Lower Columns depends on the Numbered Plate's assignment as an IP or LLP and is shown in Table 5-2. For plates designated as an LLP and welded to the Upper Column assembly, the weld thickness is a constant 5/16 in. in two parallel lines along the length of the plate, above the beveled at the end. For Numbered Plates lacking an Upper Column weld thickness, the Numbered Plate is exclusively attached to the Lower Column as an IP. Similarly, for plates designated as an IP and welded to the Lower Column, a C-shaped weld connects the plate to the column in varying thicknesses, as denoted in Table 5-2. If a Numbered Plate does not contain a weld dimension for the Lower Column, it is exclusively welded to the Upper Column as an LLP.

Table 5-1: Standardized dimensions for the Inner and Lower Lock Plate designs, listed in inches.

Plate Name	**L**	**t**	**b**	**L_1**	**s**	**b_{EDGE}**	**b_{END}**	**b_{OFFSET}**	**d_{KEY}**	**d_{SK}**	**b_{SK}**	**d_b**	**d_h**	***θ*** [°]
1	20	1	14	6	10	2	11	2	2 1/4	2 3/8	2 1/8	1 1/8	1 1/4	45
2	12	1	14	-	-	-	-	-	2	2 1/8	2	-	-	45
3	15	1	12	6	8	2	6	2	-	-	-	1	1 1/8	45
4	12	1	10	-	-	-	-	-	2	2 1/8	2	-	-	45
5	12	3/4	10	6	7	1.5	3 1/4	2	1 1/2	1 5/8	1 1/2	1	1 1/8	45
6	12	1/2	8	6	6	1	3 1/2	2	1 1/2	1 5/8	1 1/4	3/4	13/16	45
7	12	1/2	6	6	4	1	3 1/2	2	1 1/2	1 5/8	1 1/4	3/4	13/16	45
8	12	1/2	5	6	3	1	3 1/2	2	-	-	-	5/8	11/16	45
9	12	1/2	4	-	-	-	-	-	1	1 1/8	1	-	-	45

Table 5-2: Weld thicknesses for Inner and Lower Lock Plate designs, listed in inches.

Plate Name	Weld Thickness [in]	
	Upper Column	**Lower Column**
	Parallel Weld on L ($t_{LLP_{weld}}$ and $t_{SP_{weld}}$)	C-Shaped Weld on L and Side Without Bevel ($t_{IP_{weld}}$ and $*t_{SP_{weld}}$)
1	5/16	7/8
2	5/16	-
3	-	3/4
4	5/16	-
5	5/16	11/16
6	5/16	3/8
7	5/16	5/16
8	-	5/16
9	5/16	-

(*) Weld for the Shim Plate when assigned to the Lower Column

5.1.2 Outer Plate with Welded Upper Lock Plate and Shear Key

The standardized OP designs are categorized into "Lettered Plates," denoted as A, B, C, etc. Given the load requirements of the LLP and IP, Letter Plates were formed around Numbered Plate dimensions while continuing to meet flexural requirements during assembly. Numbered Plate dimensions that influenced the dimensional layout of the Letter Plates include b_{END}, b_{OFFSET}, L, s, and t.

Each Lettered Plate is assigned a unique Upper Lock Plate (ULP) and Shear Key (SK) pairing for production. Figure 5.2 below provides detailed dimensions for the combined OP, ULP, and SK, including weld dimensions, required for each Lettered Plate, creating a tailored snapping plate for column pairing as described later in the chapter.

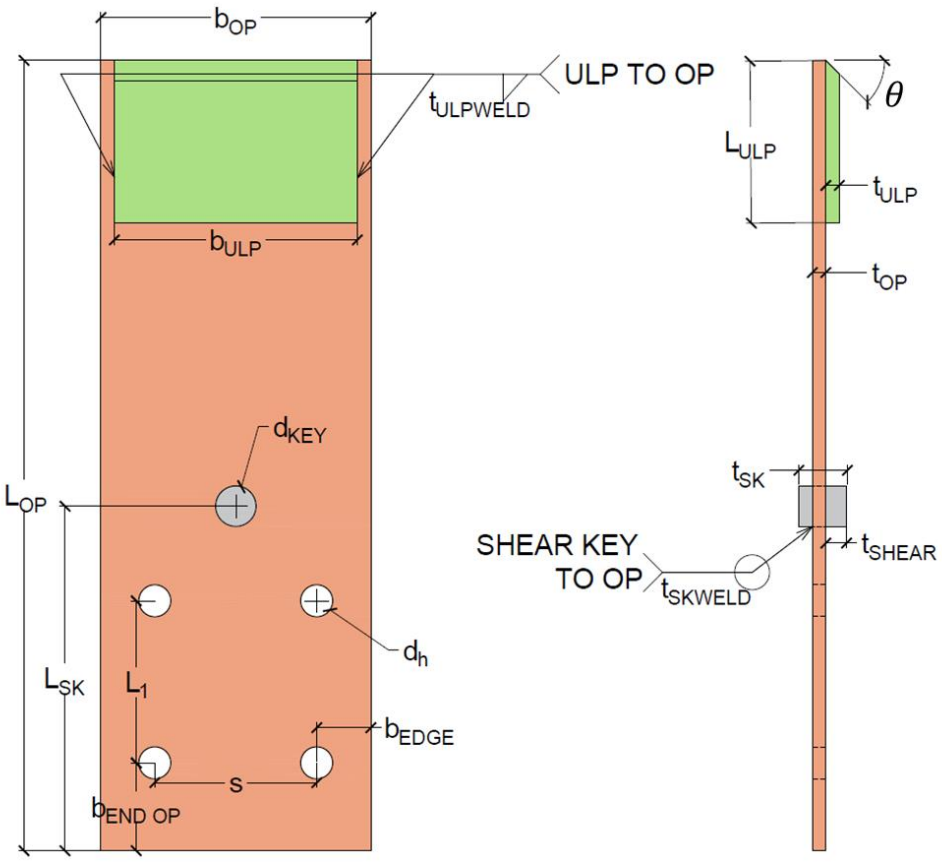

Figure 5.2: Outer Plate design variables as pertaining to Table 5-3.

The design variables associated directly with the OP include the width of the OP (b_{OP}), the length of the OP (L_{OP}), and the thickness of the OP (t_{OP}). The t_{OP} influences the flexural capacity during snapping and remains constant over all plate variations. The b_{OP} was influenced by the b of the IP it would be assigned to. While not required to be equal in width, an OP with a width less than or equal to the IP would ensure the OP would lay flush with the IP after bolting. To guarantee the OP is long enough to perform the snapping action on the LLP, Equation 5-5 solves for the L_{OP} using variables from the assigned LLP, including the length of the Numbered Plate assigned as the LLP (L_{LLP}) and bolt hole offset from the splice (b_{OFFSET}). Variables L_{ULP}, L_1, and $b_{END_{OP}}$ are defined below.

$$L_{OP} = L_{ULP} + L_{LLP} + b_{OFFSET} + L_1 + b_{END\,OP}$$

Equation 5-5

Additionally, dimensions related to spacing on the OP face include the length of the SK from the bottom end of the OP (L_{SK}), the distance from the bottom end of the OP to the center of the

lower bolt row ($b_{END_{OP}}$), the separation between the upper and lower rows of bolt holes (L_1), the spacing between the bolt hole columns (s), and distance from the center of a bolt column to the nearest edge (b_{EDGE}).

In an effort to minimize material costs for the manufacturing of the OP, $b_{END_{OP}}$ slightly varies in its standardization from the associated Numbered Plates' b_{END}. Variations in end length are determined in Equation 5-6.

$$b_{END_{OP}} = \begin{cases} b_{END} & b_{END} \leq 3\frac{1}{2}\ in. \\ 3\ in. & b_{END} > 3\frac{1}{2}\ in. \end{cases}$$

Equation 5-6

The values for b_{EDGE} and $b_{END_{OP}}$ satisfy minimum spacing requirements set in Table J3.4 from *the Steel Specification* for the assigned bolt diameter (d_b). Verified edge distances (b_{EDGE}) are solved for using Equation 5-7.

$$b_{EDGE} = \frac{b_{OP} - s}{2}$$

Equation 5-7

Additionally, bolt hole diameters for the assigned bolts are denoted as d_h for the accompanying d_b, listed in Table 5-3. Furthermore, L_1 remains constant across all plate sizes.

The design variables associated with the SK include the diameter of the SK (d_{KEY}), its total thickness (t_{SK}), the portion of the SK protruding through the inner face of the OP and resisting weak axis shear (t_{SHEAR}), and the thickness of the circumferential weld connecting the SK to the OP ($t_{SK_{weld}}$). The assigned $t_{SK_{weld}}$ must satisfy Equation 5-8, shown below. In addition, t_{SHEAR} is equal to the thickness of the Numbered Plate, assigned as the Lower Lock Plate, minus 1/16 in., displayed in Equation 5-9, to ensure the key's acceptance into the SK slot during assembly.

$$t_{SK_{weld}} \leq t_{SK} - t_{OP} - t_{SHEAR}$$

Equation 5-8

$$t_{SHEAR} = t_{LLP} - \frac{1}{16}\ in.$$

Equation 5-9

The vertical position of the center of the Shear Key centered on the OP, is defined as L_{SK} and is solved for in Equation 5-10.

$$L_{SK} = b_{END_{OP}} + L_1 + b_{OFFSET} + t_{OP}\tan(\theta) + \frac{d_{KEY}}{2}$$

Equation 5-10

Design variables for the ULP include the width of the ULP (b_{ULP}), its length (L_{ULP}), and its thickness (t_{ULP}). The width of the ULP must be less than the width of the OP to allow sufficient space for welding along the ULP edges as provided for in Equation 5-11. The weld thickness connecting the ULP to the OP ($t_{ULP_{weld}}$) is also a design consideration.

$$b_{ULP} \leq b_{OP} - 1\ in.$$

Equation 5-11

For all Lettered Plate designs, t_{ULP} remains constant at 1/2 in., L_{ULP} at 6 in., and $t_{ULP_{weld}}$ at 5/16 in. Furthermore, all ULPs in the Lettered Plates have a beveled upper end to accept the LLP and accompanying column during assembly, where the bevel angle (θ) is equal to 45°.

The Lettered Plate variations of the OP are listed below in Table 5-3, including varying plate dimensions. The largest overall plate begins at Plate A, matching the largest column pairings. Corresponding disc spring sizes have been identified for each Lettered Plate in Table 5-4 using the process as denoted in Section 4.9.4, ensuring moment demand on the OP is less than the plate's flexural yield strength.

.

Table 5-3: Dimensions for the standardized design of the Outer Plate, defined in inches.

Plate Name	L_{ULP}	t_{ULP}	b_{ULP}	$t_{ULPweld}$	$b_{END_{OP}}$	b_{EDGE}	b_{OP}	t_{OP}	L_{OP}	d_{KEY}	t_{SHEAR}	t_{SK}	t_{SKweld}	L_{SK}	d_b	d_h	θ [°]
A	6	1/2	13	5/16	3	2	14	1/2	37	2 1/4	15/16	2	1/2	13 1/8	1 1/8	1 1/4	45
B	6	1/2	13	5/16	3	2	14	1/2	29	2	15/16	2	1/2	13	1 1/8	1 1/4	45
C	6	1/2	11	5/16	3	2	12	1/2	29	2	15/16	2	1/2	13	1	1 1/8	45
D	6	1/2	9	5/16	3 1/4	1.5	10	1/2	29 1/4	1 1/2	11/16	1 3/4	1/2	12 3/4	1	1 1/8	45
E	6	1/2	7	5/16	3 1/2	1	8	1/2	29 1/2	1 1/2	7/16	1 1/2	5/16	12 3/4	3/4	13/16	45
F	6	1/2	5	5/16	3 1/2	1	6	1/2	29 1/2	1 1/2	7/16	1 1/2	5/16	12 3/4	3/4	13/16	45
G	6	1/2	4	5/16	3 1/2	1	5	1/2	29 1/2	1 1/2	7/16	1 1/2	5/16	12 3/4	5/8	11/16	45

5.1.2.1 Disc Springs Required for Standardized Outer Plates

The example disc springs allocated to each Lettered Plate in Table 5-4 were sourced from catalogs provided by American Belleville and Key Belleville manufacturers [25], [26]. The information in Table 5-4 also provides details on the minimum number of springs required in series to achieve the necessary displacement of the OP at the spring bolts during assembly, and it lists the predetermined number of parallel springs used to determine flexural capacity, provided as a reference.

Additionally, splice manufacturers must perform bolt pretensioning with the disc springs during column splice prefabrication in the shop. The pretensioning of the bolts with the disc springs is based on the required minimum initial spring deformation for bolt pretensioning, which is set at 0.2 kips for the example problem, as previously determined in Chapter 3.1.1.3(i) and Chapter 4.7. The tightening rotation for pretensioning is calculated in Equation 5-12 as a percentage full rotation, with inputs including the initial spring deformation for pretensioning (δ_{s_0}) and the thread pitch per inch.

$$Tightening\ Rotation\ \% = (\delta_{s_0} * \frac{thread\ pitch}{inch}) * 100\%$$

Equation 5-12

For a standard A325 bolt with a thread pitch of 8 threads per 1 in., or thread length of 0.125 in., the determined δ_{s_0} and rotation percentage are also provided in Table 5-4.

Figure 5.3 and Figure 5.4 display dimensional variables provided by American Belleville and Key Belleville manufacturers, respectively. These figures provide additional information on the dimensions and properties of the disc springs from each manufacturer used in the design of the SnapLocX Connection.

Table 5-4: Example disc spring selection for standardized Outer Plate designs with the minimum required springs in series and initial spring deformation for pretensioning.

Outer Plate	Manufacturer	Part #	# Parallel	# Series	δ_{s_0} [in.]	Rotation [%]
A/B	American Belleville	AD60-30.5-2.5	1	1	0.001988	1.59
	American Belleville	AD70-30.5-2.5	1	1	0.002321	1.86
	American Belleville	AD70-30.5-3	1	1	0.001706	1.36
	American Belleville	AD80-31-3	1	1	0.002031	1.62
	American Belleville	AD80-31-2.5	1	1	0.002677	2.14
	American Belleville	AD63-31-3	1	1	0.00142	1.14
	American Belleville	AD63-31-2.5	1	1	0.0023	1.84
	American Belleville	AD63-31-1.8	1	1	0.003454	2.76
	Key Belleville	K2500-M-080	1	1	0.003223	2.58
C/D	American Belleville	AD56-28.5-1.5	1	1	0.004722	3.78
	American Belleville	AD56-28.5-2	1	1	0.003141	2.51
	American Belleville	AD56-28.5-2.5	1	1	0.001782	1.43
	American Belleville	AD56-28.5-3	1	2	0.002507	2.01
	Key Belleville	K2250-L-073	1	1	0.003347	2.68
E	American Belleville	AD45-22.4-1.25	1	1	0.005652	4.52
	American Belleville	AD45-22.4-1.75-301	1	2	0.00617	4.94
	American Belleville	AD50-22.4-2	1	1	0.002657	2.13
	American Belleville	AD45-22.4-2.5-301	1	2	0.003024	2.42
	Key Belleville	K1750-J-057	1	1	0.004545	3.64
	Key Belleville	K1750-J-085	1	2	0.004115	3.29
F	American Belleville	AD45-22.4-1.25	1	1	0.005652	4.52
	American Belleville	AD45-22.4-1.75	1	1	0.003279	2.62
	Key Belleville	K1750-J-057	1	1	0.004545	3.64
	Key Belleville	K1750-J-085	1	2	0.004115	3.29
G	American Belleville	AD31.5-16.3-0.8	1	2	0.024973	19.98
	American Belleville	AD31.5-16.3-1.25	1	2	0.009088	7.27
	American Belleville	AD31.5-16.3-1.5	1	2	0.00568	4.54
	American Belleville	AD34-16.3-1.5	1	2	0.006377	5.10
	Key Belleville	K1375-H-044	1	2	0.01283	10.26
	Key Belleville	K1375-H-067	1	2	0.005222	4.18

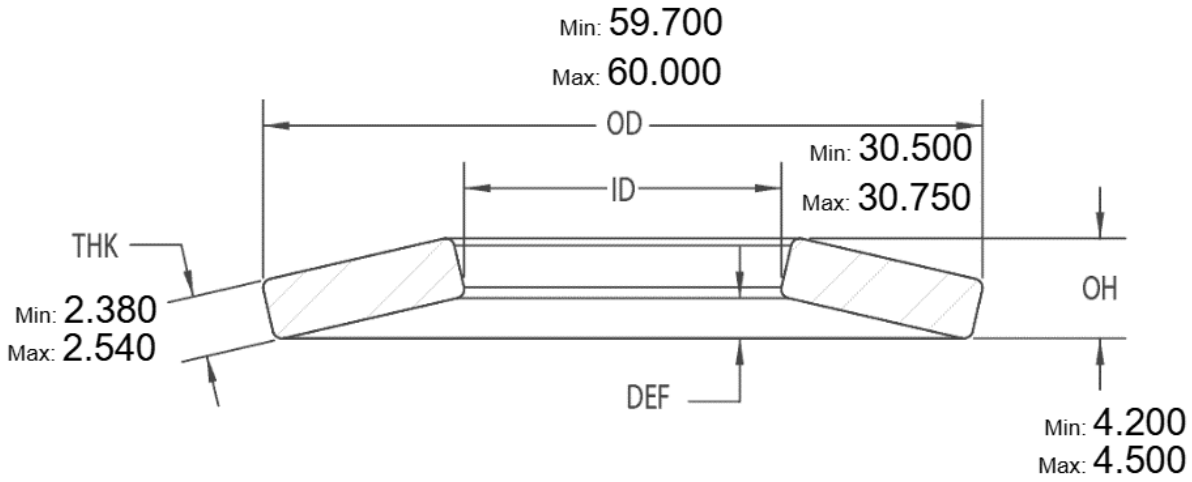

Figure 5.3: Given dimension variables from American Belleville for example disc spring AD60-30.5-2.5. [27]

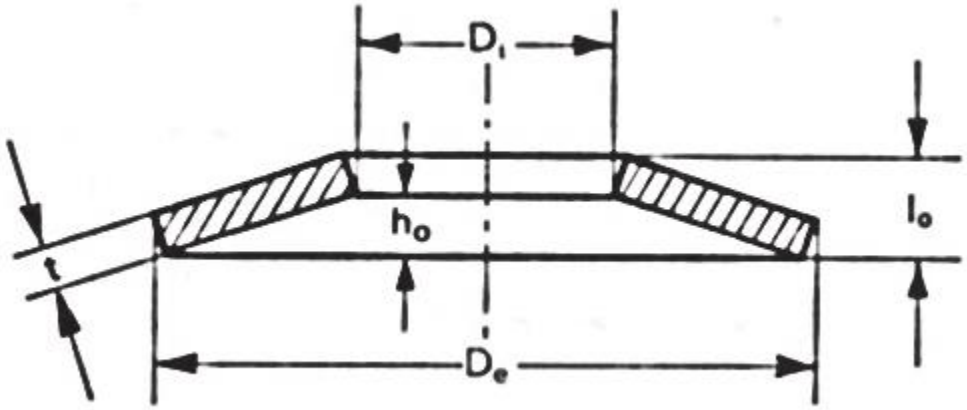

Figure 5.4: Given disc spring dimensions from Key Belleville. [28]

To simplify assembly and ensure adequate snapping behavior, additional disc springs may be added in series due to the small initial displacements required for bolt pretensioning and accompanying nut rotations. This approach provides easily measured rotations while still maintaining the desired pretensioning force for the upper row of bolts.

The new spring deformation during bolt tightening for the required pretensioned force ($\delta_{s_{0_{new}}}$) can be determined using the original spring deformation (δ_{s_0}) multiplied by the new number of springs in series ($n_{s_{s_{new}}}$) and divided by the original number of springs in series (n_{s_s}), as shown in Equation 5-13.

$$\delta_{s_{0_{new}}} = \delta_{s_0} * \frac{n_{s_{s_{new}}}}{n_{s_s}}$$

Equation 5-13

The new tightening rotation of the nut during assembly is then determined with Equation 5-14.

$$Tightening\ Rotation\ \% = (\delta_{s_{0_{new}}} * \frac{thread\ pitch}{inch}) * 100\%$$

Equation 5-14

It is recommended that the tightening rotation for bolt pretensioning be at least a quarter of a turn during assembly. Standard thread pitches for A325 bolts are 8, where one rotation corresponds to a 0.125 in. displacement of a nut. The following table, Table 5-5, provides a comprehensive overview based on information provided in Table 5-4 adjusted for the recommended number of springs in series with their exact spring deformations and assembly rotations to achieve the minimum quarter turn (25%) requirement.

Table 5-5: Example available Disc Spring selection for standardized Outer Plate designs with the number of springs in series to achieve the recommended quarter of a turn for bolt pretensioning.

Outer Plate	Manufacturer	Part #	# Parallel	# Series	$\delta_{s_{0_{new}}}$ [in.]	Rotation [%]
A/B	American Belleville	AD60-30.5-2.5	1	16	0.031809	25.45
	American Belleville	AD70-30.5-2.5	1	14	0.032493	25.99
	American Belleville	AD70-30.5-3	1	19	0.032408	25.93
	American Belleville	AD80-31-3	1	16	0.0325	26.00
	American Belleville	AD80-31-2.5	1	12	0.032126	25.70
	American Belleville	AD63-31-3	1	23	0.03267	26.14
	American Belleville	AD63-31-2.5	1	14	0.032207	25.77
	American Belleville	AD63-31-1.8	1	10	0.034536	27.63
	Key Belleville	K2500-M-080	1	10	0.032232	25.79
C/D	American Belleville	AD56-28.5-1.5	1	7	0.033051	26.44
	American Belleville	AD56-28.5-2	1	10	0.031415	25.13
	American Belleville	AD56-28.5-2.5	1	18	0.032075	25.66
	American Belleville	AD56-28.5-3	1	25	0.031338	25.07
	Key Belleville	K2250-L-073	1	10	0.033473	26.78
E	American Belleville	AD45-22.4-1.25	1	6	0.033909	27.13
	American Belleville	AD45-22.4-1.75-301	1	11	0.033937	27.15
	American Belleville	AD50-22.4-2	1	12	0.031885	25.51
	American Belleville	AD45-22.4-2.5-301	1	21	0.031753	25.40
	Key Belleville	K1750-J-057	1	7	0.031816	25.45
	Key Belleville	K1750-J-085	1	16	0.032921	26.34
F	American Belleville	AD45-22.4-1.25	1	6	0.033909	27.13
	American Belleville	AD45-22.4-1.75	1	10	0.032787	26.23
	Key Belleville	K1750-J-057	1	7	0.031816	25.45
	Key Belleville	K1750-J-085	1	16	0.032921	26.34
G	American Belleville	AD31.5-16.3-0.8	1	3	0.037459	29.97
	American Belleville	AD31.5-16.3-1.25	1	7	0.031808	25.45
	American Belleville	AD31.5-16.3-1.5	1	12	0.034082	27.27
	American Belleville	AD34-16.3-1.5	1	10	0.031887	25.51
	Key Belleville	K1375-H-044	1	5	0.032076	25.66
	Key Belleville	K1375-H-067	1	12	0.03133	25.06

5.1.3 Shim Plates

The Shim Plate (SP) is designed as a simple rectangular plate with no beveled edges. When the depth of the Upper Column is less than that of the Lower Column, the required SP is welded to the Upper Column. Conversely, if the depth of the Upper Column exceeds that of the Lower Column, the required SP is welded to the Lower Column before the IP. The SP width (b_{SP}) is intended to be at least 1 in. less than the width of the column it is connected to and 1 in. greater than the width of the LLP or IP welded to it.

Plates located on the Upper Column have a length equal to the associated LLP and do not require bolt or Shear Key holes to be drilled. On the other hand, plates needed for the Lower Column are 1 in. longer than the associated IP to accommodate the C-shaped welds around the SP and IP. Additionally, the SP on the Lower Column requires mirrored bolt holes from the IP to be drilled, with the first row of bolts centered b_{OFFSET} from the upper end of the SP.

The thickness of the SP is unique for each column pairing and is determined in Chapter 4 using Equation 4-4.

5.1.4 Column Fabrication

To prepare the Lower Column for prefabrication, holes for the bolt groups must be drilled into the upper end of each flange. The bolt dimensions and layout align with those of the numbered IP assigned to the column pairing, with the center of the first row of bolts offset b_{OFFSET} from the end of the column.

No preparation is required for the Upper Column before the SnapLocX Connection prefabrication process begins.

5.2 Standardized Design Combinations and Tables

Standardized Designs for column splice pairings are derived from combinations of the lettered OPs and numbered LLPs and IPs. Table 5-6 displays plate combinations of one Lettered Plate and two Numbered Plates with an associated color used for identification in the following tables: Table 5-7, Table 5-8, and Table 5-9.

Table 5-6 also lists the width of the accompanying SP. If a column pairing in Table 5-7, Table 5-8, or Table 5-9 includes an asterisk (*), the SP is welded to the Lower Column and uses the

width as denoted in the last column of Table 5-6. If no asterisk is provided, the connection is standard with the *SP* welded to the Upper Column and width from the standard column in Table 5-6.

Table 5-6: Color-coded Standardized Design Table used for W-Shapes: 10, 12, and 14.

Outer Plate	Inner Plate	Lower Lock Plate	SP Width	(*) SP Width
A	1	1	15 in.	-
B	1	2	13 in.	-
C	3	4	11 in.	-
D	5	5	11 in.	-
E	6	6	9 in.	9 in.
F	7	7	7 in.	-
E	6	7	7 in.	-
G	8	9	5 in.	6 in.
F	7	9	5 in.	7 in.

Using Table 5-6 and capacity requirements specified in Chapter 4, a standardized design is assigned to all column pairs, as displayed in Table 5-7, Table 5-8, and Table 5-9 for column shapes W14, W12, and W10, respectively. Allowable Lower Column sizes are listed in the first column on the left, and allowable Upper Column sizes are listed in the top row of each table. The color displayed at the intersection of the two columns in a splice corresponds to Table 5-6 and indicates the required thickness of the *SP*. The presence of an asterisk attached to the number for *SP* thickness indicates that the *SP* is welded to the Lower Column instead of the standard placement on the Upper Column. Combinations of column pairs blacked out in the tables identify splices that require non-standardized designs.

5.2.1 W14 Column Splices

Spliced columns for W14-shaped columns range from W14x873 to W14x30 for the Lower Columns and W14x398 to W14x30 for the Upper Columns. Available column connections for W14 shapes are displayed in Table 5-7.

5.2.2 W12 Column Splices

Spliced columns for W12-shaped columns range from W12x366 to W12x26 for the Lower Columns and W12x279 to W12x26 for the Upper Columns. Available column connections for W12 shapes are displayed in Table 5-8.

5.2.3 W10 Column Splices

Spliced columns for W10-shaped columns range from W10x112 to W10x22 for the Upper and Lower Columns. Available column connections for W10 shapes are displayed in Table 5-9.

Table 5-7: W14 shape assignment and shim plate thickness.

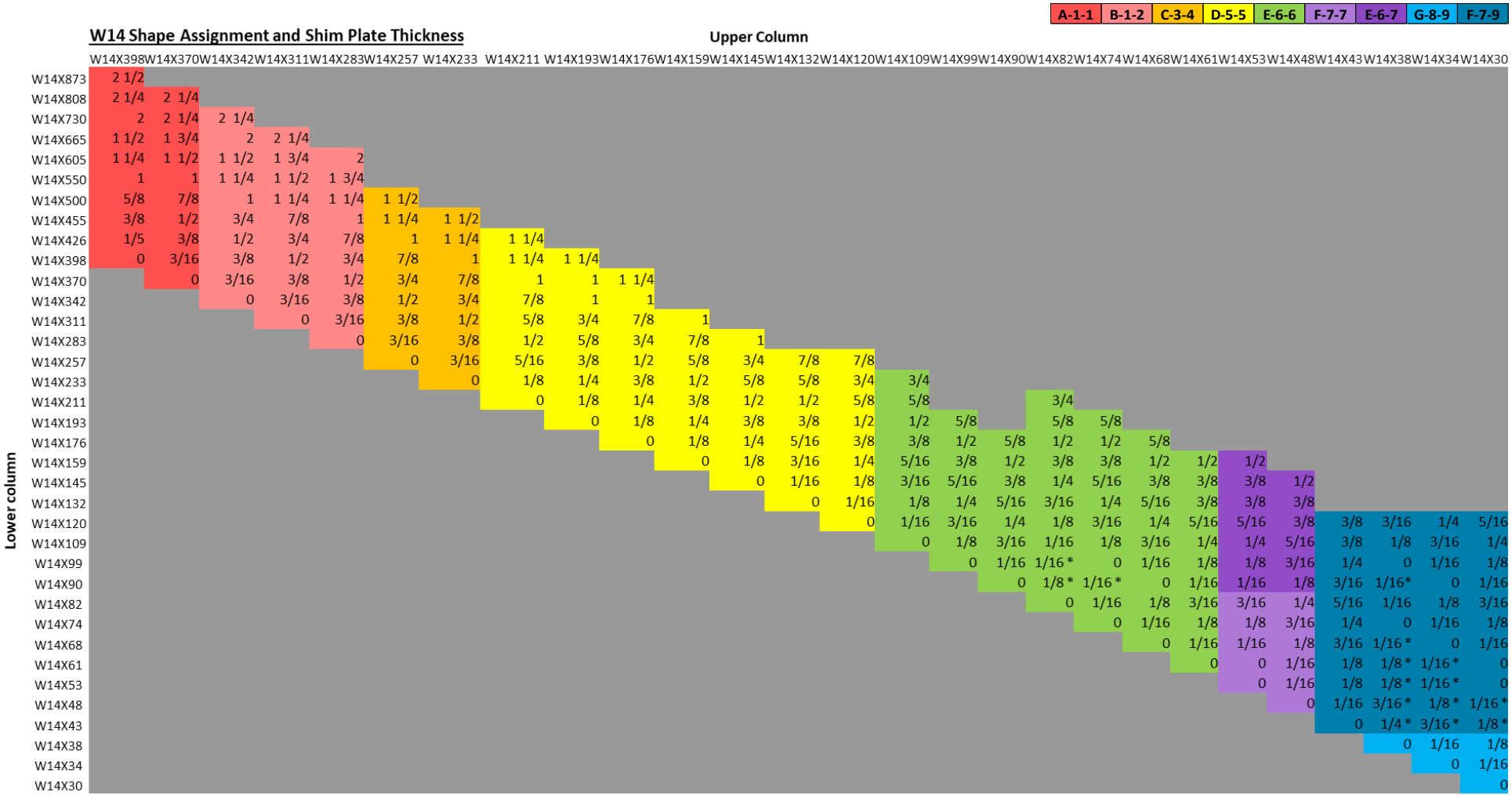

W14 Shape Assignment and Shim Plate Thickness

A-1-1 | B-1-2 | C-3-4 | D-5-5 | E-6-6 | F-7-7 | E-6-7 | G-8-9 | F-7-9

Upper Column

Lower column	W14X398	W14X370	W14X342	W14X311	W14X283	W14X257	W14X233	W14X211	W14X193	W14X176	W14X159	W14X145	W14X132	W14X120	W14X109	W14X99	W14X90	W14X82	W14X74	W14X68	W14X61	W14X53	W14X48	W14X43	W14X38	W14X34	W14X30
W14X873	2 1/2																										
W14X808	2 1/4	2 1/4																									
W14X730	2	2 1/4	2 1/4																								
W14X665	1 1/2	1 3/4	2	2 1/4																							
W14X605	1 1/4	1 1/2	1 1/2	1 3/4	2																						
W14X550	1	1	1 1/4	1 1/2	1 3/4																						
W14X500	5/8	7/8	1	1 1/4	1 1/4	1 1/2																					
W14X455	3/8	1/2	3/4	7/8	1	1 1/4	1 1/2																				
W14X426	1/5	3/8	1/2	3/4	7/8	1	1 1/4	1 1/4																			
W14X398	0	3/16	3/8	1/2	3/4	7/8	1	1 1/4	1 1/4																		
W14X370		0	3/16	3/8	1/2	3/4	7/8	1	1	1 1/4																	
W14X342			0	3/16	3/8	1/2	3/4	7/8	1	1																	
W14X311				0	3/16	3/8	1/2	5/8	3/4	7/8	1																
W14X283					0	3/16	3/8	1/2	5/8	3/4	7/8	1															
W14X257						0	3/16	5/16	3/8	1/2	5/8	3/4	7/8	7/8													
W14X233							0	1/8	1/4	3/8	1/2	5/8	5/8	3/4	3/4												
W14X211								0	1/8	1/4	3/8	1/2	1/2	5/8	5/8		3/4										
W14X193									0	1/8	1/4	3/8	3/8	1/2	1/2	5/8	5/8	5/8									
W14X176										0	1/8	1/4	5/16	3/8	3/8	1/2	5/8	1/2	1/2	5/8							
W14X159											0	1/8	3/16	1/4	5/16	3/8	1/2	3/8	3/8	1/2	1/2	1/2					
W14X145												0	1/16	1/8	3/16	5/16	3/8	1/4	5/16	3/8	3/8	3/8	1/2				
W14X132													0	1/16	1/8	1/4	5/16	3/16	1/4	5/16	3/8	3/8	3/8				
W14X120														0	1/16	3/16	1/4	1/8	3/16	1/4	5/16	5/16	3/8	3/8	3/16	1/4	5/16
W14X109															0	1/8	3/16	1/16	1/8	3/16	1/4	1/4	5/16	3/8	1/8	3/16	1/4
W14X99																0	1/16	1/16 *	0	1/16	1/8	1/8	3/16	1/4	0	1/16	1/8
W14X90																	0	1/8 *	1/16 *	0	1/16	1/16	1/8	3/16	1/16*	0	1/16
W14X82																		0	1/16	1/8	3/16	3/16	1/4	5/16	1/16	1/8	3/16
W14X74																			0	1/16	1/8	1/8	3/16	1/4	0	1/16	1/8
W14X68																				0	1/16	1/16	1/8	3/16	1/16 *	0	1/16
W14X61																					0	0	1/16	1/8	1/8 *	1/16 *	0
W14X53																						0	1/16	1/8	1/8 *	1/16 *	0
W14X48																							0	1/16	3/16 *	1/8 *	1/16 *
W14X43																								0	1/4 *	3/16 *	1/8 *
W14X38																									0	1/16	1/8
W14X34																										0	1/16
W14X30																											0

Table 5-8: W12 shape assignment and shim plate thickness.

W12 Shape Assignment and Shim Plate Thickness

Lower column \ Upper Column	W12X279	W12X252	W12X230	W12X210	W12X190	W12X170	W12X152	W12X136	W12X120	W12X106	W12X96	W12X87	W12X79	W12X72	W12X65	W12X58	W12X53	W12X50	W12X45	W12X40	W12X35	W12X30	W12X26
W12X336	1/2	3/4	7/8	1	1 1/4	1 1/4																	
W12X305	1/4	1/2	5/8	3/4	1	1	1 1/4																
W12X279	0	1/4	3/8	1/2	3/4	7/8	1																
W12X252		0	3/16	5/16	1/2	5/8	3/4	1	1														
W12X230			0	1/8	5/16	1/2	5/8	3/4	7/8														
W12X210				0	3/16	3/8	1/2	5/8	3/4	7/8													
W12X190					0	3/16	5/16	1/2	5/8	3/4	3/4												
W12X170						0	1/8	5/16	3/8	1/2	5/8	3/4											
W12X152							0	3/16	5/16	3/8	1/2	5/8	5/8										
W12X136								0	1/8	1/4	5/16	3/8	1/2	1/2	5/8	1/2							
W12X120									0	1/8	3/16	5/16	3/8	3/8	1/2	3/8							
W12X106										0	1/16	3/16	1/4	5/16	3/8	5/16	3/8	5/16	3/8	3/8	3/16	1/4	5/16
W12X96											0	1/8	3/16	1/4	5/16	1/4	3/8	1/4	3/8	3/8	1/8	3/16	1/4
W12X87												0	1/16	1/8	3/16	1/8	1/4	1/8	1/4	1/4	0	1/16	1/8
W12X79													0	1/16	1/8	1/16	3/16	1/16	3/16	3/16	1/16 *	0	1/16
W12X72														0	1/16	0	1/8	0	1/8	1/8	1/8 *	1/16 *	0
W12X65															0	1/16 *	1/16	1/16 *	1/16	1/16	3/16 *	1/8 *	1/16 *
W12X58																0	1/8	0	1/8	1/8	1/8 *	1/16 *	0
W12X53																	0	1/8 *	0	0	1/4 *	3/16 *	1/8 *
W12X50																		0	1/8	1/8	1/8 *	1/16 *	0
W12X45																			0	0	1/4 *	3/16 *	1/8 *
W12X40																				0	1/4 *	3/16 *	1/8 *
W12X35																					0	1/16	1/8
W12X30																						0	1/16
W12X26																							0

A-1-1 B-1-2 C-3-4 D-5-5 E-6-6 F-7-7 E-6-7 G-8-9 F-7-9

Table 5-9: W10 shape assignment and shim plate thickness.

W10 Shape Assignment and Shim Plate Thickness

A-1-1	B-1-2	C-3-4	D-5-5	E-6-6	F-7-7	E-6-7	G-8-9	F-7-9

Upper Column

Lower column

	W10X112	W10X100	W10X88	W10X77	W10X68	W10X60	W10X54	W10X49	W10X45	W10X39	W10X33	W10X30	W10X26	W10X22
W10X112	0	1/8	1/4	3/8	1/2	1/2	5/8		5/8			3/8	1/2	5/8
W10X100		0	1/8	1/4	3/8	3/8	1/2		1/2			5/16	3/8	1/2
W10X88			0	1/8	1/4	5/16	3/8	3/8	3/8			3/16	1/4	3/8
W10X77				0	1/8	3/16	1/4	5/16	1/4	3/8		1/16	1/8	1/4
W10X68					0	1/16	1/8	3/16	1/8	1/4	5/16	1/16 *	0	1/8
W10X60						0	1/16	1/8	1/16	3/16	1/4	1/8 *	1/16 *	1/16
W10X54							0	1/16	0	1/8	3/16	3/16*	1/8 *	0
W10X49								0	1/16 *	1/16	1/8	1/4 *	3/16*	1/16 *
W10X45									0	1/8	3/16	3/16*	1/8 *	0
W10X39										0	1/16			1/8 *
W10X33											0			
W10X30												0	1/16	3/16
W10X26													0	1/8
W10X22														0

5.3 Using Design Tables and Manufacturing Column Splice

The following section illustrates using the tables provided above to design an example SnapLocX Connection.

5.3.1 Selecting Columns to Splice

For the example design, a W12x230 is used as the Lower Column, and a W12x170 is used as the Upper Column.

5.3.2 Identifying Colored Plate Assignment and Shim Plate Thickness

Using a modified version of Table 5-8, Figure 5.5 calls out the intersection of the selected Upper and Lower Columns, marked with a red circle. In the figure, the corresponding color for the column pairing is yellow, displaying 1/2.

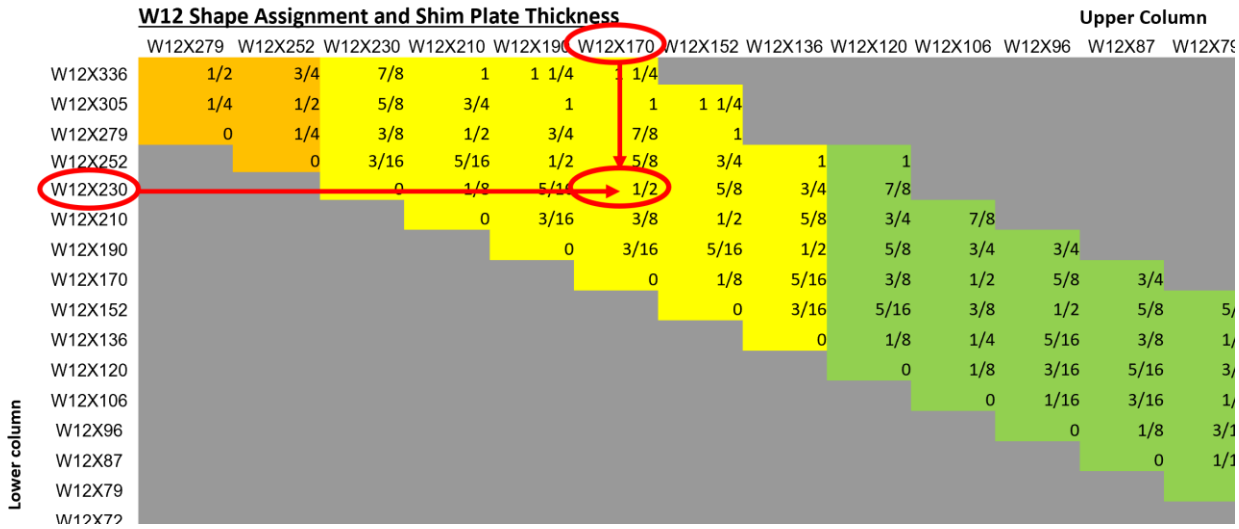

Figure 5.5: Cropped figure of Table 5-8, identifying the intersection of W12x230 and W12x170.

The yellow rectangle at the intersection of W12x230 and W12x170 references back to Table 5-6, indicating the standardized design of plate combinations for the selected splice is D-5-5, as circled in Figure 5.6.

Outer Plate	Inner Plate	Lower Lock Plate	SP Width	(*) SP Width
A	1	1	15 in.	-
B	1	2	13 in.	-
C	3	4	11 in.	-
D	5	5	11 in.	-
E	6	6	9 in.	9 in.
F	7	7	7 in.	-
E	6	7	7 in.	-
G	8	9	5 in.	6 in.
F	7	9	5 in.	7 in.

Figure 5.6: Called out plate combination assignment for the example design from Table 5-6.

The yellow identifier also denotes a Shim Plate width of 11 in., circled in Figure 5.7. The absence of an asterisk at the intersection of the spliced columns in Figure 5.7 specifies the standard location of the SP welded to the Upper Column within the column splice.

Outer Plate	Inner Plate	Lower Lock Plate	SP Width	(*) SP Width
A	1	1	15 in.	-
B	1	2	13 in.	-
C	3	4	11 in.	-
D	5	5	11 in.	-
E	6	6	9 in.	9 in.
F	7	7	7 in.	-
E	6	7	7 in.	-
G	8	9	5 in.	6 in.
F	7	9	5 in.	7 in.

Figure 5.7: Called out SP width and column location within the splice from above Table 5-6.

The provided measurement of 1/2 represents the required 1/2 in. thickness for the SP, required to achieve equal depths between the Upper Column and Lower Column.

5.3.3 Manufacturing the Column Splice

Based on the information provided in Figure 5.5, Figure 5.6, and Figure 5.7, the example column is prepared for prefabrication. The Lower Column is fabricated with bolt holes using dimensions s, b_h, and L_1as indicated from IP and OP centered on the flanges, with the center of the first row of holes located b_{OFFSET} from the location of the column splice.

On the Upper Column, a SP, with a thickness of 1/2 in. and width of 11 in., is aligned with the center of the column flanges. It is then welded to the Upper Column using vertically parallel fillet welds of 5/16 in. over a length of 12 in., as mentioned in Table 5-2 and Section 5.1.2, respectively. The inclusion of the welded SP on the Upper Column is illustrated in Figure 5.8.

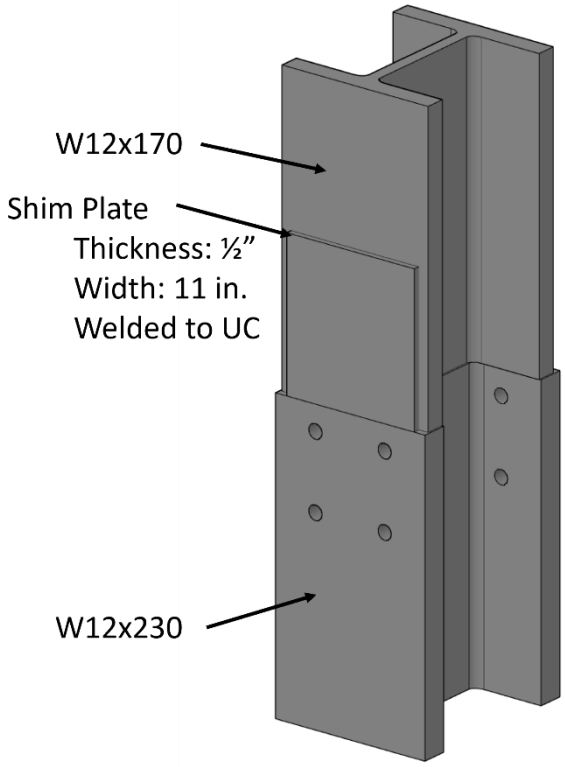

Figure 5.8: Inclusion of the SP in the connection assembly for the example design.

Following the welded attachment of the SP to the Upper Column, the LLP, identified as Plate 5 with dimensions highlighted in Table 5-10, is welded to the SP with two parallel vertical welds on its edges. The length of the weld begins at the upper end of the LLP at ends at the beginning of the beveled face. The length of the weld is expressed in Equation 5-15 and is equal to 11.75 in. for the example design. The weld thickness for the LLP example design is listed in Table 5-11 as 5/16 in.

$$L_{LLP_{weld}} = L_{LLP} - t_{LLP}\cos(\theta)$$

Equation 5-15

The placement of the LLP on the SP and the Upper Column can be viewed in Figure 5.9.

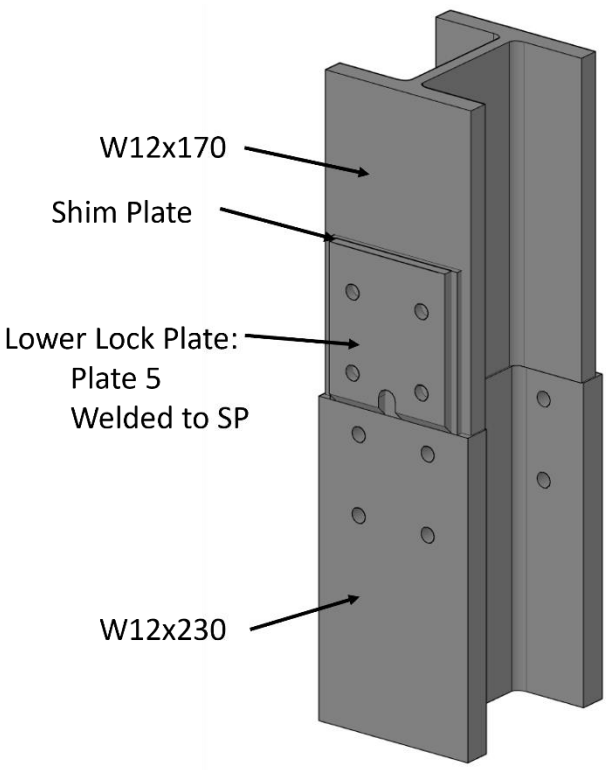

Figure 5.9: Inclusion of the LLP attached to the SP for the Upper Column component.

Table 5-10: Plate dimensions for Plate 5 from Table 5-1 are highlighted for the example design.

Plate Name	**L**	**t**	**b**	**L_1**	**s**	**b_{EDGE}**	**b_{END}**	**b_{OFFSET}**	**d_{KEY}**	**d_{SK}**	**b_{SK}**	**d_b**	**d_h**	***θ*** [°]
1	20	1	14	6	10	2	11	2	2 1/4	2 3/8	2 1/8	1 1/8	1 1/4	45
2	12	1	14	-	-	-	-	-	2	2 1/8	2	-	-	45
3	15	1	12	6	8	2	6	2	-	-	-	1	1 1/8	45
4	12	1	10	-	-	-	-	-	2	2 1/8	2	-	-	45
5	12	3/4	10	6	7	1.5	3 1/4	2	1 1/2	1 5/8	1 1/2	1	1 1/8	45
6	12	1/2	8	6	6	1	3 1/2	2	1 1/2	1 5/8	1 1/4	3/4	13/16	45
7	12	1/2	6	6	4	1	3 1/2	2	1 1/2	1 5/8	1 1/4	3/4	13/16	45
8	12	1/2	5	6	3	1	3 1/2	2	-	-	-	5/8	11/16	45
9	12	1/2	4	-	-	-	-	-	1	1 1/8	1	-	-	45

Table 5-11: Required weld thicknesses for the assigned welding column from Table 5-2, highlighting Plate 5.

Plate Name	Weld Thickness [in]	
	Upper Column	**Lower Column**
	Parallel Weld on L ($t_{LLP_{weld}}$ or $t_{SP_{weld}}$)	C-shaped weld on L and side without bevel ($t_{IP_{weld}}$)
1	5/16	7/8
2	5/16	-
3	-	3/4
4	5/16	-
5	5/16	11/16
6	5/16	3/8
7	5/16	5/16
8	-	5/16
9	5/16	-

The assembly of the Lower Column is initiated with the welding of the *IP* to the Lower Column, as depicted in Figure 5.10. For a W12x230 to W12x170 splice, the *IP* is designated as Plate 5, with dimensions detailed in Table 5-10. The *IP* is aligned in the center of the Lower Column flanges and its beveled end offset to the thickness of the *IP* above the end of the column.

The weld thickness connecting the *IP* to the Lower Column is specified as 11/16 in., as indicated in Table 5-11 for a plate welded to the Lower Column. Unlike the weld locations for the *LLP*, the *IP* is welded to the Lower Column with a C-shaped weld, situated on the two vertical, parallel edges where the Lower Column and *IP* overlap, as well as the lower horizontal end.

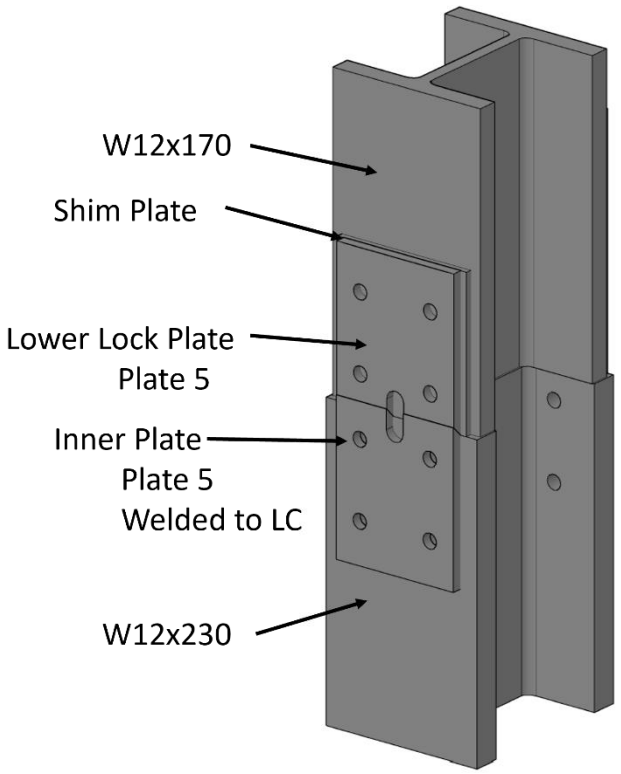

Figure 5.10: Assembly of the IP welded to the Lower Column, identified as Plate 5.

Plate D is selected for the OP, with the plate dimensions outlined in Table 5-12. The OP is positioned over the IP and aligned with the bolt group. The OP has the ULP, welded to it with a 5/16 in. weld on the interior face. The ULP has a width of 9 in. The SK, with a 1 1/2 in. diameter and total thickness of 1 3/4 in., is attached to the exterior face of the OP with a 1/2 in. weld. Figure 5.11 shows the OP resting on the IP.

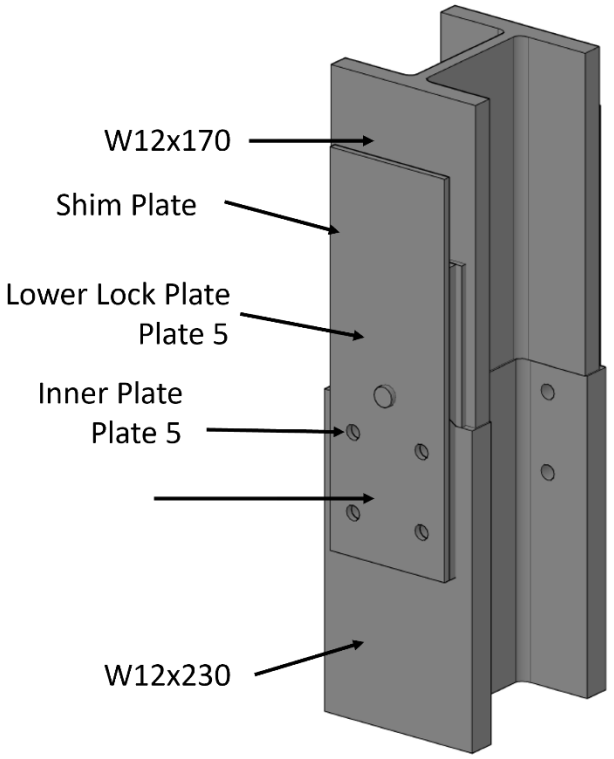

Figure 5.11: OP alignment with the IP, before disc springs and bolts are added.

Table 5-12: Highlighted dimensions for Plate D from a modified Table 5-3.

Plate Name	b_{ULP}	$t_{ULPweld}$	$b_{END_{OP}}$	b_{EDGE}	b_{OP}	t_{OP}	L_{OP}	d_{KEY}	t_{SHEAR}	t_{SK}	t_{SKweld}	L_{SK}	d_b	d_h
A	13	5/16	3	2	14	1/2	37	2 1/4	15/16	2	1/2	13 1/8	1 1/8	1 1/4
B	13	5/16	3	2	14	1/2	29	2	15/16	2	1/2	13	1 1/8	1 1/4
C	11	5/16	3	2	12	1/2	29	2	15/16	2	1/2	13	1	1 1/8
D	9	5/16	3 1/4	1.5	10	1/2	29 1/4	1 1/2	11/16	1 3/4	1/2	12 3/4	1	1 1/8
E	7	5/16	3 1/2	1	8	1/2	29 1/2	1 1/2	7/16	1 1/2	5/16	12 3/4	3/4	13/16
F	5	5/16	3 1/2	1	6	1/2	29 1/2	1 1/2	7/16	1 1/2	5/16	12 3/4	3/4	13/16
G	4	5/16	3 1/2	1	5	1/2	29 1/2	1 1/2	7/16	1 1/2	5/16	12 3/4	5/8	11/16

5.3.3.1 Final Shop Assembly with Disc Springs and Bolts

The OP is secured to the Lower Column through the welded IP, using 1 in. bolts, as assigned in Table 5-12 under d_b. The dimensions for the accompanying nuts and washers for a 1 in. bolt are determined as provided in *the Manual* under Table 7-14

Instead of exclusively using standard washers from Table 7-14 in *the Manual* for the upper row of bolts, disc spring washers are selected from the available disc spring list, detailed in Table 5-13 for Plate D. The disc spring interacting with the Lower Column is positioned with its Outer Diameter on the flange surface and Inner Diameter facing towards the nut [28]. Figure 5.12 illustrates the stacking order of multiple discs in series.

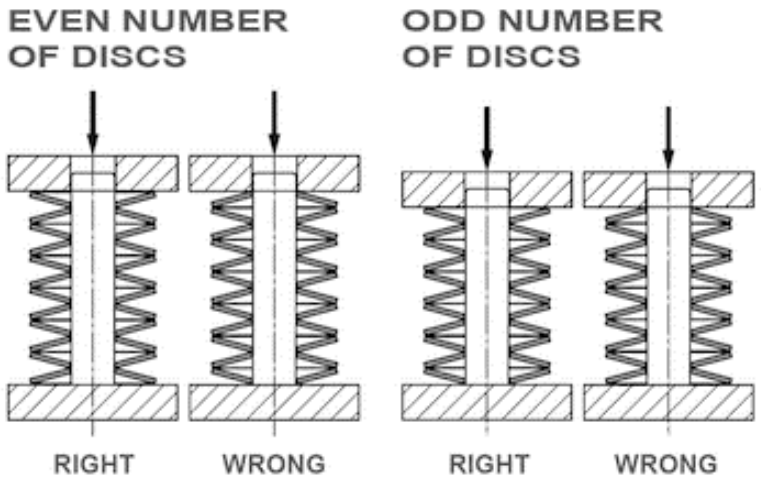

Figure 5.12: Even and odd series spring orientations. [28]

For arranging springs required in series and/or parallel in Table 5-13, refer to Figure 3.9 in Chapter 3 for guidance on placement and orientation after placing the first spring. To provide stable disc deformation during OP bending, a standard washer is required between the nut and the last disc spring.

Table 5-13: Disc Spring washers available from American and Key Belleville from Table 5-4 for Plates C and D.

Outer Plate	Manufacturer	Part #	# Parallel	# Series	δ_{s_0} [in.]	Rotation [%]
C/D	American Belleville	AD56-28.5-1.5	1	1	0.004722	3.78
	American Belleville	AD56-28.5-2	1	1	0.003141	2.51
	American Belleville	AD56-28.5-2.5	1	1	0.001782	1.43
	American Belleville	AD56-28.5-3	1	2	0.002507	2.01
	Key Belleville	K2250-L-073	1	1	0.003347	2.68

The minimum required initial spring displacement for the example design of one spring is $\delta_{s_0} = 0.0047$ in. As stated above, it is recommended to have the minimum tightening rotation be a quarter of a turn to accurately pretension the bolts to their desired load.

Using a standard A325 bolt with 8 threads per inch, and the example washer selected from Table 5-13 as American Belleville AD56-28.5-1.5 with one spring in series and parallel and citing an initial deformation (δ_{s_0}) of 0.004722 in. for a bolt pretension of 0.2 kips, the minimum number of springs in series required to necessitate a spring deformation of 0.03125 in., 25% of 0.125 in., is seven springs on each bolt. The new number of springs required in series, exact new displacements, and rotations for the example springs assigned to Plate D are provided in Table 5-14.

Table 5-14: Recommended number of disc springs in series for the example assembly, taken from Table 5-5.

Outer Plate	Manufacturer	Part #	# Parallel	# Series	$\delta_{s_{0_{new}}}$ [in.]	Rotation [%]
C/D	American Belleville	AD56-28.5-1.5	1	7	0.033051	26.44
	American Belleville	AD56-28.5-2	1	10	0.031415	25.13
	American Belleville	AD56-28.5-2.5	1	18	0.032075	25.66
	American Belleville	AD56-28.5-3	1	25	0.031338	25.07
	Key Belleville	K2250-L-073	1	10	0.033473	26.78

With the completion of the column prefabrication as separate columns, the columns are prepared for onsite assembly. The prefabricated and assembled example design with SnapLocX Connection D-5-5 is illustrated in Figure 5.13.

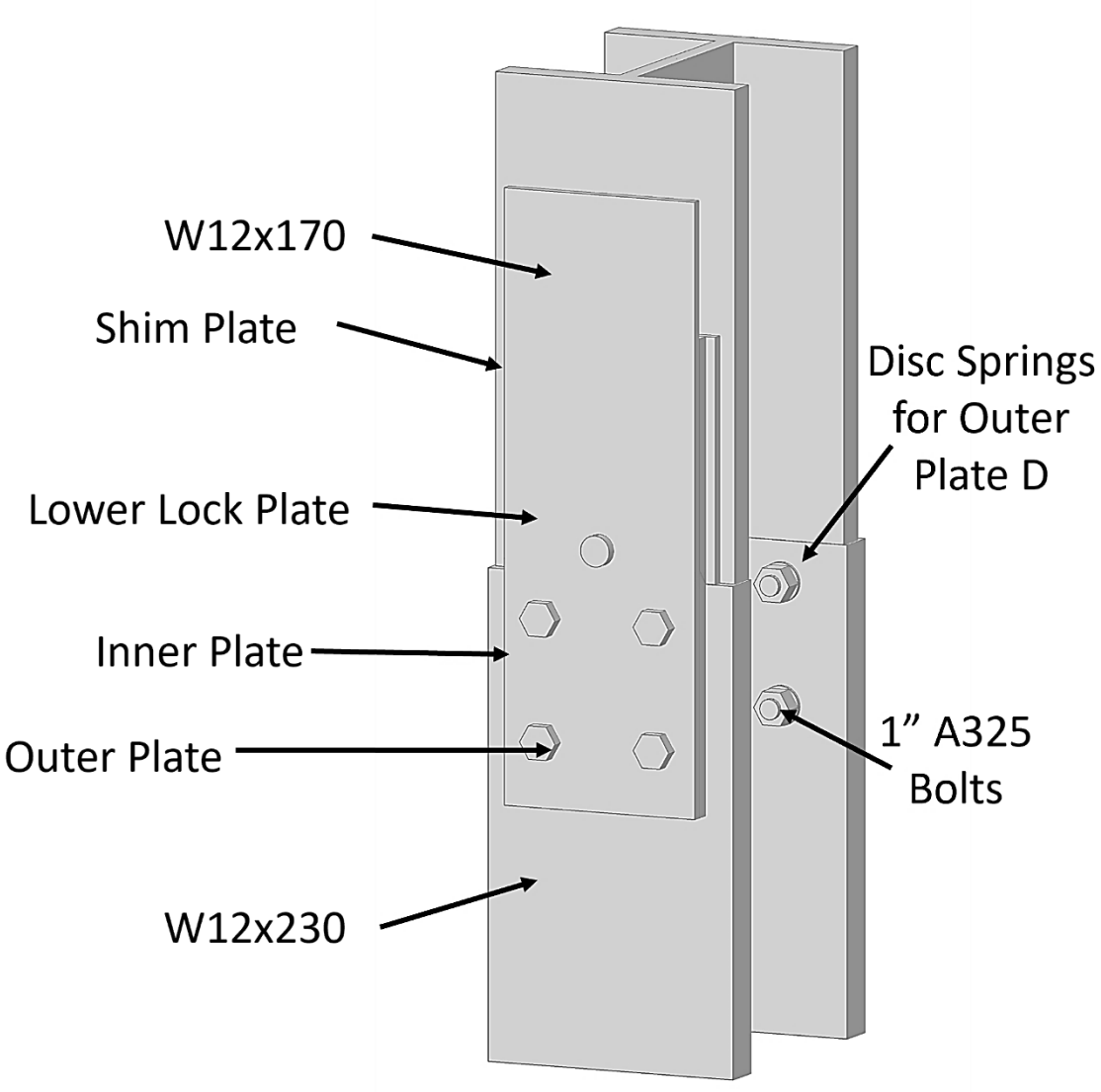

Figure 5.13: The prefabricated and assembled column splice.

Chapter 6: Recommendations and Conclusions

Funded by the American Institute of Steel Construction (AISC), this report presents the initial phase of a multi-phase research project aimed at designing, testing, and implementing a prefabricated, interlocking gravity column splice connection for rapid assembly. The first phase of the project involves the design of a SnapLocX Connection evaluated according to the design provisions stated in ANSI/AISC 360-16, the Steel Construction Manual, AISC 341, OSHA's Safety Standards for Steel Erection (RIN No. 1218-AA65) and ASCE/SEC 7-16. The following sections of this chapter summarize the research conducted, highlight the major research findings, and provide recommendations for future and ongoing research.

6.1 Summary of Research Performed

In preparation for the design of the SnapLocX Connection, a comprehensive evaluation of relevant previous research was conducted. Column splice safety requirements from OSHA were reviewed to ensure both structural compliance and worker safety. Identified gaps in current research on column splices, particularly in designs for prefabricated W-shape rapid assembly columns, indicated a lack of strength and stiffness checks for future design concepts. Existing research into prefabricated column splice designs for rapid assembly was considered, highlighting efficient and practical approaches and providing a foundation for developing new designs. Additionally, the use of nonlinear, elastic disc springs and their performance under loading was evaluated as a method to increase the deformation at which the flexural yielding occurs in the Outer Plate during assembly.

The SnapLocX Connection, a novel column splice system, was designed for prefabrication to enable rapid, on-site assembly. This innovative splice system was assigned naming conventions and design variables for use during loading analyses as dictated by AISC and OSHA. The connection was modeled to scale in 2D and 3D, facilitating comprehensive analysis and visualization. This approach was designed to aid in the precise planning and implementation of the SnapLocX Connection for use in steel construction projects.

In addition to analyzing the overall splice post-assembly, for design strength and compliance with OSHA limits, the Outer Plate was specifically evaluated for flexural yielding under AISC requirements. To ensure flexural yielding does not occur during assembly, the force-deformation

behavior of nonlinear, elastic disc springs was assessed based on their geometric properties. This assessment ensured that the flexural demand on the Outer Plate during assembly remained below the plate's yield capacity. By leveraging the properties of the disc springs, the Outer Plate design could effectively manage the stress encountered during assembly, thereby enhancing both the performance and safety of the SnapLocX Connection.

Through the column design process, the column splice components were standardized to be applied across allowable W14, W12, and W10 column pairings. Each column pairing was assigned a specific plate set from a compiled catalogue to streamline the selection process. Nine different plate sets were created, comprised of seven size variations of Lettered Plates, which included the Outer Plate, Upper Lock, Plate, and Shear Key, and nine variations of Numbered Plates, which are designated as an Inner Plate and/or Lower Lock Plate. Efforts were made to minimize the number of Lettered and Numbered Plates that need to be fabricated, optimizing efficiency and reducing production costs. Additionally, each column pairing was assigned a specific Shim Plate thickness, with the width correlated to the assigned plate set, further standardizing the design and assembly process.

An example SnapLocX Connection was designed to splice W12x170 and W12x230 column shapes together using the standardized designs. This design was evaluated for the required design loads of a column splice. In particular, the required shear strength considering the upper, W12x170 column in the strong and weak axis directions, governed many of the dimensional criteria of the splice components. An evaluation of the Outer Plate's flexural yielding capacity, using the studied example disc spring behavior, was also examined during snapping. It was determined that the example Outer Plate design could accommodate the necessary deflections of the Outer Plate during assembly, enhancing the plate's performance and increasing its flexure. The example splice design was also evaluated under the limit states required by OSHA and successfully passed all criteria.

6.2 Research Conclusions

The primary conclusion is that the SnapLocX Connection appears to be a viable alternative for a column splice connection. It can be used for splicing a variety of wide flange column shapes, and the developed standardized designs meet all minimum strength requirements for column splices in gravity frames.

The following specific observations and conclusions regarding the SnapLocX Connection research were drawn based on the analytical methods used:

- **Compliance Standards**: The SnapLocX Connection design meets all required minimum strength requirements and safety standards outlined by AISC in the ANSI/AISC 360-16, the Steel Construction Manual, and AISC 341, and OSHA's standards stated in Safety Standards in Steel Erection.
- **Upper Column Shape Constraint**: For a given standardized design of plate sets, the maximum column shape, to be assigned as the Upper Column, is constrained by the strength of the C-shaped fillet weld attaching the Inner Plate to the Lower Column. The weld connecting the Inner Plate to the Lower Column is critical for transferring strong axis shear from the Lower Lock Plate through the Inner Plate down into the Lower Column.
- **Inner Plate Thickness Constraint**: The thickness of the Inner Plate is constrained by the thickness of the C-shaped weld connecting it to the Lower Column. This weld is evaluated using the elastic vector method, which initially increased the thickness of the Inner Plate and, subsequently, the Lower Lock Plate.
- **Eccentric Loading from Strong Axis Shear Governs the Bolt Design**: The eccentric load partially constrained the bolt layout and heavily influenced the required bolt diameters and their available shear strength for the standardized designs.
- **Lower Column Shape Constraint**: For a given standardized design of plate sets, the maximum shape of the Lower Column is constrained by the maximum distance from the center of the web to the flange toe of the fillet (k_1). This distance is influenced by the bolt spacing, entering and tightening clearances, and disc spring diameters of a connection.
- **Shim Plate Solution for Heavier Columns**: Column pairings of a Lower Column with a larger weight but smaller depth than the Upper Column require a unique solution. Welding Shim Plates to the Lower Column, rather than the initial Upper Column, assists in aligning the Inner Plate with the Lower Lock Plate for strong axis shear transfer. Plates attached to the Lower Column must then be evaluated for sufficient clearance for

C-shaped welds attaching the Inner Plate to the Shim Plate and the Shim Plate to the Lower Column.

- **Adjustments for Larger W14 Shapes**: The standardized designs needed adjustments for larger W14 shapes. These shapes require a longer Inner Plate and Lower Lock plate to effectively transfer the required shears, which in turn necessitates a longer Outer Plate.
- **Capability of Disc Springs**: A numerical analysis of conical disc springs proved that they would be a viable solution for allowing increased flexure of the Outer Plate due to plate deformation during assembly. However, their unique properties require analysis of each spring to determine compatibility and proper functionality with the Outer Plate.
- **Disc Spring Pretensioning**: The disc spring deformations required for pretensioning the bolts may be so small that additional springs may need to be added in series to normalize the amount of rotation necessary to pretension the bolts. Additionally, more springs in series can assist in safeguarding against over-pretensioning and preventing the Outer Plate from yielding in flexure.
- **Optimized Plate Designs**: Successful efforts were made to reduce the number of plates needed to be manufactured for the SnapLocX Connection, reducing the required plates from unique plates for each connection to seven Lettered Plates, representing the Outer Plates, Shear Keys, and Upper Lock Plates, and nine Numbered Plates, representing the Lower Lock Plates and Inner Plates.
- **Standardized Plate Groupings**: The optimized plates were able to be consolidated into standardized plate groupings presented in a catalogue for future use by engineers and manufacturers.
- **Governing Limit State for In-Plate Bending**: The in-plane flexural capacity of the splice is governed by the fillet weld connecting the Upper Lock Plate to the Outer Plate. The fillet weld connecting the Upper Lock Plate to the Outer Plate is critical for maintaining the structural integrity of the connection under OSHA strong axis flexural loads.

6.3 Recommendations for Future Research

The objective of this research was to evaluate a novel interlocking W-shaped column splice design intended for rapid assembly. Results from analytical research, based on loading requirements from AISC and OSHA, have produced a viable design.

With the creation of a practical splice design, certain assumptions were made during the design process, including a 12-foot story height minimum. To enhance the versatility of the SnapLocX Connection for broader industry implementation, it is recommended to reanalyze the splice behavior in shear for a reduced minimum story height of 10 ft. Lowering the minimum story height from 12 feet. to 10 feet would increase the shear demand at the column splice in both the strong and weak axis directions. This shear demand increase could potentially exceed the design strength capacities of the analyzed states in this report. Key design strengths identified from the shear demands would likely impact the design strength in the strong and weak axes, respectively, and include the design strength of the fillet welds connecting the Inner Plate to the Lower Column, which controls the thickness of the particular weld, and the design strength of the shear key bearing on the Lower Lock Plate, influencing the thickness of the Lower Lock Plate.

Additional assumptions were made about the behavior of the lower row of bolts connecting the Outer Plate to the Lower Column as the plate undergoes flexure during assembly. It was assumed that the lower bolt row would act as a fixed end condition for the observed plate length. However, further research may be warranted to evaluate the actual behavior of the bolt row. An additional potential avenue for further study of the Outer Plate's flexural behavior is to model and analyze the plate as having a pinned connection at the lower bolts. This analysis would provide additional insight into how the bolts and their connections respond to the applied loads from assembly and whether the fixed-end assumption holds accurate and controls under different scenarios. Understanding the actual behavior of the lower bolt row in flexural conditions can lead to improvements in the design approach.

Concluding the current stage and design of the SnapLocX Connection, future design investigations could focus on evaluating force transfer from torsion across the splice to confirm that torsional demands do not control the splice. It is unlikely that torsion would control the splice due to the insignificant rotations expected of gravity columns. However, it could be used to assess the strength of the Shear Key and fillet welds and the bearing of the Lower Lock Plate

on the Inner Plate, optimizing performance and versatility for various additional steel construction applications.

One demand not considered in the SnapLocX development was the necessary weak-axis flexural strength. The demands are small and governed by the OSHA requirements, but a process for calculating the strength should be developed.

A suggestion for future improvement of the Standardized Splice Catalogue includes redesigning the tables and catalogues to enhance accessibility for readers. This can be achieved by assigning a letter or number key to the current-colored standardized plate pairing, facilitating more straightforward interpretation, navigation, and duplication of the information presented.

Material optimization could occur in addition to optimization of plate variation. Many of the standardized plate dimensions were conservative, according to requirements from OSHA and AISC. Specific dimensions could be minimized with additional development.

Additional features should be added to the engineering drawings, including, but not limited to, bolt holes at the upper end of columns for lifting during assembly and a guiding feature at the splice of the Lower Column to ensure proper alignment of all plates.

Due to limitations during the current research phase, finite element analysis (FEA) of the SnapLocX Connection was not conducted. However, it is strongly recommended to perform FEA to verify the load path assumptions used throughout. The analysis of the connection using FEA can verify that load and flexural capacities are satisfied during and post-assembly for the shear, flexure, and torsion requirements of the column and its plates.

Future research should conduct experimental studies and analyses to investigate the SnapLocX Connection's behavior further. Mock-up models of the splice should be fabricated, assembled, and subjected to shear and flexure testing to evaluate the splice design strength and identify limit states. The loading protocol for the column splice tests could be derived from the requirements outlined for moment frame connection tests defined in AISC 341-16. This protocol could include testing for axial loading and moment to assess the SnapLocX Connection's performance under different loading types. The tested splice pairings will adhere to previous assumptions and will be selected to test within shape classes. Data on column and column splice behaviors can be collected during testing through video observations and 3D position tracking. This data

collection could be used to identify how the connection responds to applied loads, including deformations and stress distributions.

Overall, future research should combine experimental testing and data collection to further validate and enhance the understanding of the SnapLocX Connection’s performance and behavior under field conditions.

References

[1] H. Snijder and J. Hoenderkamp, "Influence of end plate splices on the load carrying capacity of columns," *Journal of Constructional Steel Research,* vol. 64, no. 7-8, pp. 845-853, 2008.

[2] A. Girao Coelho, P. Simao, and F. Bijlaard, "Stability design criteria for steel column splices," *Journal of Constructional Steel Research,* vol. 66, no. 10, pp. 1261-1277, 2010.

[3] S. Boulanger, C. Drucker, L. Kruth, D. Miller and T. Meyer, "The Splice is Right," in *NASCC: The Steel Conference*, Orlando, 2016.

[4] F. Marino, "Steel Erection: One of the Top 10 Most Hazardous Occupations," Compliance Management International, 2022.

[5] OSHA, "Safety Standards for Steel Erection," US Department of Labor, Washington D.C., 2001.

[6] B. H. Snijder and H. J. Hoenderkamp, "Experimental Tests on Spliced Columns for Splice Strength and Stiffness," in *Stability and Ductility of Steel Structures*, Lisbon, 2006.

[7] A. M. Girao Coelho and F. S. Bijlaard, "Requirements for the Design of Column Splices," TUDelft, 2008.

[8] D. Papastergiou, "Connections by Adhesion, Interlocking, and Friction for Steel-Concrete Composite Bridges under Static and Cyclic Loading," *EPFL*, 2012.

[9] V. Noorhidana and J. Forth, "An Experimental Study on Precast Concrete Beam-to-Column Connection Using Interlocking Bars," *II International Conference on Concrete Sustainability- ICCS16,* pp. 229-240, 2016.

[10] Y. Yang, L. Sneed, A. Morgan, M. Saiid and A. Belarbi, "Repair of RC bridge columns with interlocking spirals and fractured longitudinal bars – An experimental study," *Construction and Building Materials,* vol. 78, pp. 4056-420, 2015.

[11] A. Lacey, Chen, Wensu, H. Hao and K. Bi, "New interlocking inter-module connection for modular steel buildings: Experimental and numerical studies," *Engineering Structures*, vol. 198, 2019.

[12] S. Al-Sabah, D. Laefer, L. T. Hong, M. P. Huynh, J.-L. Le, T. Martin, P. Matis, P. McGetrick, A. Schults, M. E. Shemshadian and R. Dizon, "Introduction of the Intermeshed Steel Connection—A New Universal Steel Connection," *Buildings*, vol. 10, no. 3, 2020.

[13] AISC, Steel Construction Manual, Chicago: American Institute of Steel Construction, 2017.

[14] P. Bagavathiperumal, K. Chandrasekaran and S. Manivasagam, "Elastic load-displacement predictions for coned disc springs subjected to axial loading using the finite element method," *The Journal of Strain Analysis for Engineering Design*, vol. 26, no. 3, pp. 147-152, 1991.

[15] J. O. Almen and A. Laszlo, "The Uniform-Section Disk Spring," in *Transactions of the American Society of Mechanical Engineers*, Detroit, 1936.

[16] C. K. Dharan and J. A. Bauman, "Composite disc springs," *ScienceDirect*, vol. Composites: Part A 38, no. 2511-2516, 2007.

[17] S. S. Industries, "Round Belleville Spring Washers, Size: 12 mm," IndiaMART, [Online]. Available: https://www.indiamart.com/proddetail/belleville-spring-washers-21192891755.html?pos=1&pla=n.

[18] "Precision Disc Springs," MW Components, Charlotte, 2021.

[19] B. Springs, "Disc Spring Characteristics," Belleville Springs, [Online]. Available: https://www.bellevillesprings.com/disc-spring-characteristics/.

[20] D. Snell, "How to Determine the Proper Disc Spring Stack Configuration," Assembly, April 2021. [Online]. Available: https://digitaledition.assemblymag.com/april-2021/assembly-how-to-spirol/.

[21] "AD56-28.5-1.5," American Belleville, [Online]. Available: https://americanbelleville.com/products/disc-springs/disc-spring/?id=AD56-28.5-1.5&uom=Inch.

[22] AISC, Specification for Structural Steel Buildings, Chicago: American Institute of Steel Construction, 2016.

[23] AISC, Seismic Design Manual, Chicago: American Institute of Steel Construction, 2018.

[24] ASCE, Minimum Design Loads and Associated Criteria for Buildings and Other Structures (7-16), Reston: American Society of Civil Engineers, 2017.

[25] "Disc Spring Products," American Belleville, 2024. [Online]. Available: https://americanbelleville.com/products/disc-springs/.

[26] "Sample Catalog," Key Belleville, [Online]. Available: https://keybellevilles.com/bellevilles/sampleCatalog.

[27] "AD60-30.5-2.5," American Belleville, 2024. [Online]. Available: https://americanbelleville.com/products/disc-springs/disc-spring/?id=AD60-30.5-2.5&uom=Metric.

[28] "Terms & Symbols," Key Belleville, [Online]. Available: https://keybellevilles.com/engineering/terms.

[29] SPIROL, "How to Determine the Proper Disc Spring Stack Configuration," Design Engineering, 1 June 2022. [Online]. Available: https://www.design-engineering.com/how-to-determine-the-proper-disc-spring-stack-configuration-1004038694/.

[30] Solon, "Stackable Belleville DIN & Disc Springs," Solon Manufacturing Co. , [Online]. Available: https://www.solonmfg.com/belleville-spring-washers/din-and-disc-springs.

[31] N. Mastricola and R. Singh, "Nonlinear load-deflection and stiffness characteristics of coned springs in four primary configurations," *Mechanism and Machine Theory,* vol. 116, pp. 513-528, 2017.

Appendix

Table of Contents

List of Figures

Appendix A: Force-Deformation Curves of Disc Springs

A.1 Overview

This appendix includes all detailed calculations related to solving the force-deformation curve for the disc springs, as described in Chapter 3. Dimensions used reference those listed in the cross-sectional view of Figure 4.7. This is necessary as manufacturers do not provide sufficient dimensions to fully determine the force-deformation behavior of disc springs. Additional parameters must be estimated from those given by the manufacturers. Further complicating this is that different manufacturers provide different dimensions.

A.2 Calculating Unprovided Dimension Variables

This section outlines the process for calculating the necessary dimensions required to construct a force-displacement curve. With limited dimensions provided by manufacturers, iterative calculations are performed to approximate the correct values used to determine the force curve (P_s) in relation to spring deformation (δ). Considering the actual disc thickness (t) angled to produce a conical washer, adjustments in the X and Y-axis, using the coordinate system as defined in Figure A.1, are used to compute accurate dimensions of the radius (R) needed for P_s as it is measured from the centerline of the washer to the bearing edge.

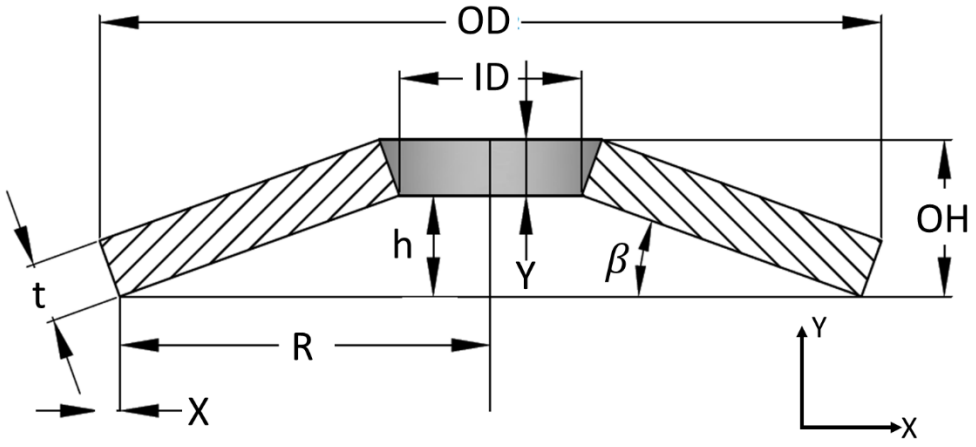

Figure A.1: Disc spring geometry and coordinate system.

Dimensions regularly provided by a manufacturer include t, the minimum inner diameter (ID), the maximum outer diameter (OD), and either the overall height (OH) or the conical height of the disc (h). Notably, the OD extends beyond the bearing edge used for the radius to include the

projection of the disc spring thickness in the X-axis direction (X). The OD then drives the requirement for calculating adjustments of t in the X and Y-axis directions.

Given the incomplete disc spring dimensions, the initial calculations to obtain an accurate R for the force-displacement formula, measured from the centerline of the spring to the bearing outer edge, begins with an estimated conical angle (β). The initial estimation is denoted as $\beta_{initial}$. The initial t projections in the X and Y-axis are computed with $\beta_{initial}$, shown in Equation A-1 for $X_{initial}$ and Equation A-2 for $Y_{initial}$.

$$X_{initial} = t\ \sin\left(\beta_{initial} * \frac{\pi}{180}\right)$$

Equation A-1

$$Y_{initial} = t \cos\left(\beta_{initial} * \frac{\pi}{180}\right)$$

Equation A-2

Two processes to calculate R based on β are needed because available manufacturers specify disc spring height differently. If OH is provided and not h, calculations used to idealize β follow the process completed with Approach 1 in A.2.1. If OH is not provided, but h is, β is approximated following Approach 2 in A.2.2.

A.2.1 β Approach 1: Using OH

Solving for β using the OH begins with determining a radius constant ($R_{constant}$) as given by Equation A-3, which is used in approximating R [18]. After determining the constant and using the previously calculated initial thickness in the X-direction ($X_{initial}$), the initial R ($R_{initial}$) is calculated with Equation A-4.

$$R_{constant} = \begin{cases} \frac{OH}{150} & t \geq \frac{8}{25.4} \\ \frac{t}{6} & t < \frac{8}{25.4} \end{cases}$$

Equation A-3

$$R_{initial} = \frac{OD}{2} - X_{initial} - R_{constant}$$

Equation A-4

To calculate the first iteration of h ($h_{initial}$), the previously estimated conical angle ($\beta_{initial}$) and calculated thickness in the Y-axis ($Y_{initial}$) are used in Equation A-5.

$$h_{initial} = OH - Y_{initial}$$

Equation A-5

Next, an updated estimate of β (β_{solved}) can be calculated using $R_{initial}$ and $h_{initial}$ with Equation A-6.

$$\beta_{solved} = \text{atan}\left(\frac{h_{initial}}{R_{initial} - \frac{ID}{2}}\right) * \frac{180}{\pi}$$

Equation A-6

Comparing the new estimate, β_{solved}, to the original estimate, β_{intial}, it can be determined if the new estimate is appropriate based on a specified tolerance, as given in Equation A-7.

$$|\beta_{sovled} - \beta_{initial}| \leq 0.00001$$

Equation A-7

If the tolerance is met, β_{solved} is the value used to calculate R. If the tolerance is not met, the process must be reiterated by setting $\beta_{initial} = \beta_{solved}$ and producing new values in Equation A-8 through Equation A-13 for X, Y, h, and R, respectively as X_{new}, Y_{new}, h_{new}, and R_{new}. The new β_{solved} must be compared to the current, most recent $\beta_{initial}$ to determine if it satisfies the tolerance from Equation A-7.

$$\beta_{initial} = \beta_{solved}$$

Equation A-8

$$X_{new} = t \ \sin(\beta_{initial} * \frac{\pi}{180})$$

Equation A-9

$$Y_{new} = t\ \cos\left(\beta_{initial} * \frac{\pi}{180}\right)$$

Equation A-10

$$h_{new} = OH - Y_{new}$$

Equation A-11

$$R_{new} = \frac{OD}{2} - X_{new} - R_{constant}$$

Equation A-12

$$\beta_{sovled} = \text{atan}\left(\frac{h_{new}}{R_{new} - \frac{ID}{2}}\right) * \frac{180}{\pi}$$

Equation A-13

Equation A-8 through Equation A-13 are repeated until the tolerance is met.

A.2.2 β Approach 2 Using h

When h is provided, the OH variable must be calculated to determine the $R_{constant}$ value. Iterative calculations, separate from Approach 1, must be completed to solve for OH and R. As in Approach 1, the initial values $X_{initial}$ and $Y_{initial}$ are used to initialize the process, with an initial OH ($OH_{initial}$) in Equation A-14 using the provided h dimension and previously calculated $Y_{initial}$.

$$OH_{initial} = h + Y_{initial}$$

Equation A-14

An initial constant for the R equation ($R_{constant_{initial}}$) is solved for using the initial estimate of the overall height ($OH_{initial}$), as seen in Equation A-15. This is then used to calculate an initial R ($R_{initial}$) in Equation A-16.

$$R_{constant_{initial}} = \begin{cases} \frac{OH_{initial}}{150} & t \geq \frac{8}{25.4} \\ \frac{t}{6} & t < \frac{8}{25.4} \end{cases}$$

Equation A-15

$$R_{initial} = \frac{OD}{2} - X_{initial} - R_{constant_{initial}}$$

Equation A-16

Using $R_{initial}$, a newly estimated β angle (β_{solved}) can be equated using Equation A-6. Similar to Approach 1, β_{solved} must be compared to $\beta_{initial}$ to satisfy the tolerance set in Equation A-7. If the tolerance is not satisfied, new values for X, Y, OH, and R, respectively as X_{new}, Y_{new}, OH_{new}, and R_{new} must be determined to identify a more approximate β. After resetting $\beta_{initial}$ to β_{solved}, X_{new} and Y_{new} are calculated using Equation A-9 and Equation A-10, respectively. Solutions for OH_{new}, $R_{constant_{new}}$, R_{new}, and β_{solved} are as follows, with β_{solved} using Equation A-13:

$$OH_{new} = h + Y_{new}$$

Equation A-17

$$R_{constant_{new}} = \begin{cases} \frac{OH_{new}}{150} & t \geq \frac{8}{25.4} \\ \frac{t}{6} & t < \frac{8}{25.4} \end{cases}$$

Equation A-18

$$R_{new} = \frac{OD}{2} - X_{new} - R_{new_{constant}}$$

Equation A-19

This process is iterated until the tolerance, Equation A-7, is satisfied.

Example Conical Angle Calculation for AD56-28.5-1.5

American Belleville

Disc Dimensions

Outer Diameter	OD =	2.2	in.
Inner Diameter	ID =	1.122	in.
Absolute Thickness	t =	0.059	in.
Overall Height	OH =	0.136	in.

Estimations

Conical Angle	β =	20	°

Initial Values for Thickness in the X and Y-Axis

Initial Thickness Estimation in the X-Axis	X_{intial} =	0.0202	in.	Equation A-1
Initial Thickness Estimation in the Y-Axis	$Y_{initial}$ =	0.0554	in.	Equation A-2

Initial Estimations for β Using A.2.1

Constant Radius Factor	$R_{constant}$ =	0.0098	in.	Equation A-3
Initial Radius Estimation	$R_{initial}$ =	1.0700	in.	Equation A-4
Initial Height Estimation	$h_{initial}$ =	0.0806	in.	Equation A-5
New beta Estimation	β_{solved} =	8.9937	°	Equation A-6

Initial Tolerance for $\beta_{initial}$ and β_{solved}

$\lvert\beta_{solved} - \beta_{initial}\rvert \leq 0.00001$	= 11.0063	FALSE	Equation A-7

New Estimations

New β Estimation	$\beta_{initial}$ =	8.9937	°	Equation A-8
New Thickness Estimation in the X-Axis	X_{new} =	0.0092	in.	Equation A-9
New Thickness Estimation in the Y-Axis	Y_{new} =	0.0583	in.	Equation A-10
New Height Estimation	h_{new} =	0.0777	in.	Equation A-11
New Radius Estimation	R_{new} =	1.0809	in.	Equation A-12
New beta Estimation	β_{solved} =	8.5021	°	Equation A-13

New Tolerance for $\beta_{initial}$ and β_{solved}

$\lvert\beta_{solved} - \beta_{initial}\rvert \leq 0.00001$	= 0.4916	FALSE	Equation A-7

New Estimations are Repeated Until Tolerance is Satisfied

Final Calculated Values After Tolerance is Satisfied

Disc Thickness in the X-Axis	X =	**0.0087**	**in.**
Disc Thickness in the Y-Axis	Y =	**0.0584**	**in.**
Conical Disc Height	h =	**0.0776**	**in.**
Radius from the Centerline to the Bearing Edge	R =	**1.0815**	**in.**
Conical Disc Angle	β =	**8.4852**	°

A.3 Compressive Force-Deformation Curve of a Disc Spring

Upon completing the iterative calculations to determine β using the set tolerance, the most recent R_{new} calculation becomes R and the most recent h_{new} becomes h, when moving forward with calculations to determine the force-deformation curve. For a single disc spring, the force-deformation relationship is as stated in Equation A-20, where E is the Modulus of Elasticity, ν is Poisson's Ratio, and M is the ratio factor of α calculated in Equation A-21, using α as the ratio of the outer and inner diameters, from Equation A-22.

$$P_s(\delta) = \frac{E\ \delta}{(1-\nu^2)\ M\ R^2}\left(\left(h-\frac{\delta}{2}\right)\ (h-\delta)\ t + t^3\right) \text{ where } 0 \leq \delta \leq h$$

Equation A-20

$$M = \frac{6}{\pi\ \ln(\alpha)} * \frac{(\alpha-1)^2}{\alpha^2}$$

Equation A-21

$$\alpha = \frac{OD}{ID}$$

Equation A-22

Example Compressive Force Displacement Calculation for AD56-28.5-1.5

American Belleville

Material Variables

Young's Modulus	E =	29,000	ksi
Poisson's Ratio	ν =	0.3	

Disc Dimensions

Outer Diameter	OD =	2.2	in.
Inner Diameter	ID =	1.122	in.
Conical Height	h =	0.0776	in.
Absolute Thickness	t =	0.059	in.
Radius	R =	1.0815	in.

$$P_s(\delta) = \frac{29000\ \delta}{(1-0.3^2) * 0.6810 * 1.0815^2} * \left(\left(0.0778 - \frac{\delta}{2}\right) * (0.0778 - \delta) * 0.059 + 0.059^3\right)$$

Equation A-23

$$P_s(\delta) = 74300.66\ \delta \left(\left(0.0776 - \frac{\delta}{2}\right) * (0.0776 - \delta) * 0.059 + 0.000205\right)$$

Equation A-24

$$P_s(\delta) = 0.05581\delta^3 - 0.0658\delta^2 + 0.000173\delta$$

Equation A-25

A.4 Force-Displacement Curve for Springs in Series and/or Parallel

The required disc spring deformation at the location of the spring along a beam may be greater than the allowable spring deformation from h of a single spring. Springs in series can be utilized to provide additional deformation for a given load. Equation A-26 identifies the formula used to determine the number of springs in series (n_{s_s}) required to satisfy the displacement demand of the attached object. Using the provided example design, δ_{beam} is the displacement curve of the OP at location x = L_1, divided by the conical height, and rounded up to the whole spring conical height.

$$n_{s_s} = ceiling\left(\frac{\delta_{beam}(L_1)}{h}\right)$$

Equation A-26

This increases the range for δ to:

$$0 \leq \delta \leq h\, n_{s_s}$$

Parallel disc springs are accounted for on each bolt they occupy in the parallel spring configuration, as seen in Figure 4.9. Both the number of bolts with springs (n_{s_b}) and the number of parallel springs on each bolt (n_{s_p}) increase the force for a given spring deformation.

The final P_s force must be multiplied by the number of bolts with springs on them and the number of springs in parallel, both provided in the boundary conditions. Therefore, the total spring force experienced per total disc deformation is:

$$P_{s_{total}}(\delta) = P_s(\delta)\, n_{s_p}\, n_{s_b}$$

Equation A-27

The finalized force-displacement graph for the example spring, AD56-28.5-1.5, is shown in Figure A.2, where $n_{s_b} = 2$, $n_{s_s} = 1$, and n_{s_p}= 1.

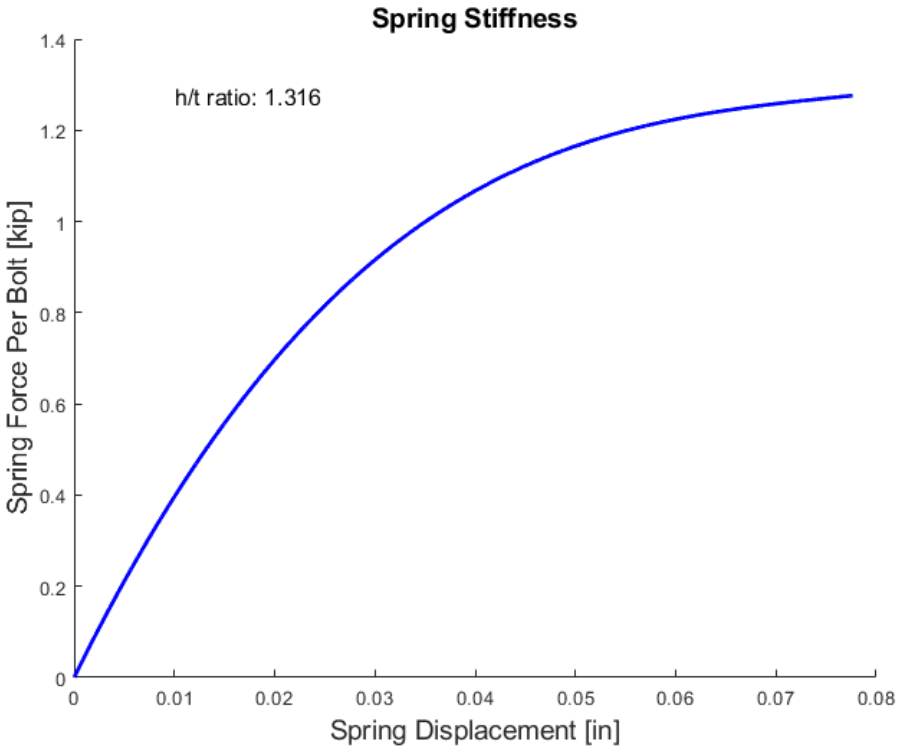

Figure A.2: Example disc spring washer force-deformation curve modeled.

Appendix B: Design Considerations

B.1 Overview

Appendix B provides a comprehensive discussion on design variable derivation given dimension and load requirements. After a detailed discussion of the design centered around the requirements, each section is followed by a sample calculation for the SnapLocX example design.

B.2 Checking Column Splice Pairings

To ensure adequate support of the Upper Column by the Lower Column, it is recommended that at least half the flange thickness of the Lower Column ($t_{f_{LC}}$) should provide support for the Upper Column at each flange. Equation B-1 performs the support check if the Lower Column has a greater depth (d_{LC}) than the Upper Column (d_{UC}).

$$Check\ if\ d_{UC} < d_{LC},\ d_{UC} \geq d_{LC} - t_{f_{LC}}$$

Equation B-1

Alternatively, if the Upper Column has a greater depth, Equation B-2 is applied, with at least half of the thickness of each flange of the Upper Column ($t_{f_{UC}}$) supported by the Lower Column.

$$Check\ if\ d_{LC} < d_{UC},\ \ d_{LC} > d_{UC} - t_{f_{UC}}$$

Equation B-2

Most column connections will utilize Equation B-1 for the check.

Allowable Splice Column Depth Verification

Column Dimensions

Depth of the Upper Column (W12x170)	d_{UC} =	14	in.
Depth of the Lower Column (W12x230)	d_{LC} =	15	in.
Flange Thickness of the Lower Column (W12x230)	$t_{f_{LC}}$ =	2 1/16	in.

For $d_{UC} < d_{LC}$:

$$d_{UC} \geq d_{LC} - t_{f_{LC}}$$ **TRUE** **Equation B-1**

B.2.1 Column Bearing Capacity Check

The Upper Column must bear on the Lower Column without yielding. The bearing capacity is determined with Equation J7-1 from *the Steel Specification*, rewritten in Equation B-3. Variables used to determine the nominal bearing strength (R_n) require the specified minimum yield stress (F_y) and the projected bearing area (A_{pb}). The design strength requires the bearing strength resistance factor (ϕ), shown in Equation B-4.

$$R_n = 1.8\, F_y\, A_{pb}$$

Equation B-3

$$\phi = 0.75$$

Equation B-4

The bearing area should be sufficient to transfer the factored (k) axial compression (P_u) in the upper column to the lower column, as displayed through the design strength in in Equation B-5.

$$\phi\, R_n \geq\ k\, P_u$$

Equation B-5

Example Design Column Bearing Strength

Resistance factor for bearing capacity	ϕ =	0.75		Equation B-4
Column Properties				
Upper Column (W12x170) X-Axis Plastic Section	$Z_{x_{UC}}$ =	275	in.^{3}	
Story Height	H =	144	in.	
Upper Column Nominal Stress	$F_{y_{UC}}$ =	50	ksi	
Upper Column Bearing Area	A_{pb} =	50	in.^{2}	
Column Shear Demand				
Shear Demand in the X-Axis	P_u =	95.49	kip	
Percent of Axial Strength of the Column	k =	30	%	
Bearing Capacity				
Nominal bearing capacity	R_n =	4500	kip	Equation B-3
Bearing Strength	ϕR_n =	3375	kip	

Design Satisfied

$\boldsymbol{\phi R_n \geq k P_u}$	**TRUE**	**Equation B-5**

B.3 Determining Shim Plate Requirement

When the column depths are not equal, a Shim Plate (SP) is welded between the Upper Column flange and the Lower Lock Plate (LLP). The required thickness of the SP (t_{SP}) is determined in Equation B-6.

$$t_{SP} = \left| \frac{(d_{LC} - d_{UC})}{2} \right|$$

Equation B-6

Shim Plates are only included when $t_{SP} \geq 1/16$ in. to accommodate plate sizing requirements stated in *the Manual* from Part 1. According to *the Manual*, available plate sizes increase in increments of 1/16 in. up to plate thicknesses of 3/8 in. Following plate sizes increase by 1/8 in. increments up to 1 in. Plates greater than 1 in. increase in increments of 1/4 in. thereafter. The sizing of SPs used in the SnapLocX connection design follows the requirements stated in *the Manual*, rounding the calculated t_{SP} down to the nearest available plate size.

Example Design Shim Plate Thickness Requirement

Column Dimensions

Depth of the Upper Column (W12x170)	d_{UC} =	14	in.
Depth of the Lower Column (W12x230)	d_{LC} =	15	in.

Calculated Thickness

Shim Plate Thickness	$\boldsymbol{t_{SP}}$ =	**0.5**	**in.**	**Equation B-6**

B.4 Strong Axis Shear

When the designed column splice is subject to shear in the strong axis, the path of shear transfers from the Upper Column to the Lower Column through the IP and IP welds. The required cross-sectional thickness of the IP (t_{IP_r}) and IP weld thickness ($t_{IP_{weld_r}}$) are established in the following sections and compared with example design to be less than or equal to the design dimension. The design strength from LRFD Load Combinations (R_u) is computed using the nominal strength (R_n) and resistance factor (ϕ) for the given design criteria, ensuring it is equal to or greater than the demand.

The required strong axis shear strength (V_x) is expressed in Equation B-7, derived from the plastic moment of the Upper Column in the strong axis (M_{p_x}) and the assumed story height of the column (H) using methods stated in Section D2.5c for column splices from *the* AISC *Provisions*. The moment is calculated as the product of the plastic section of the Upper Column in the strong axis ($Z_{x_{UC}}$) and the yield stress of the Upper Column ($F_{y_{UC}}$).

$$V_x = \frac{M_{p_x}}{H} = \frac{Z_{x\,UC}\,F_{y_{UC}}}{H}$$

Equation B-7

B.4.1 Inner Plate Through Thickness Requirement

To establish the required thickness for the IP (t_{IP_r}) to prevent IP yielding, the strength of the IP in shear is calculated using Equation J4-3 from *the Steel Specification*, seen in Equation B-8. The design strength ($\phi\ R_n$) of the plate is determined by using the gross cross-sectional area subject to shear (A_{gv}) and the nominal yield strength of the IP material ($F_{y_{IP}}$).

$$\phi R_n = \ \phi\ 0.6\ A_{gv}\ F_{y_{IP}}$$

Equation B-8

The cross-sectional area of the IP used for design shear strength, identified in Figure B.1, is found with the product of the required through thickness of the IP (t_{IP_r}) and the width of the IP (b_{IP}), considering the removed width for the Shear Key slot (d_{SK}) in the through shear plane, shown in Equation B-9.

$$A_{gv} = t_{IP_r}\,(b_{IP} - d_{SK})$$

Equation B-9

The strong axis shear demand of the Upper Column, calculated from V_x, is constrained to be less than or equal to the shear yield design strength determined in Equation B-8 and rewritten in Equation B-10.

$$V_x \leq \phi\ 0.6\ F_{y_{IP}}\ t_{IP_r}\ (b_{IP} - d_{SK})$$

Equation B-10

The minimum t_{IP_r} is solved for in Equation B-11 after reformatting Equation B-10.

$$t_{IP_r} \geq V_x\ \frac{1}{\phi\ 0.6\ F_{y_{IP}}(b_{IP} - d_{SK})}$$

Equation B-11

The solved-for required thickness of the IP (t_{IP_r}) must not exceed the thickness of the IP (t_{IP}) used in the SnapLocX Connection design for specific column pairings, provided in Equation B-12.

$$t_{IP} \geq t_{IP_r}$$

Equation B-12

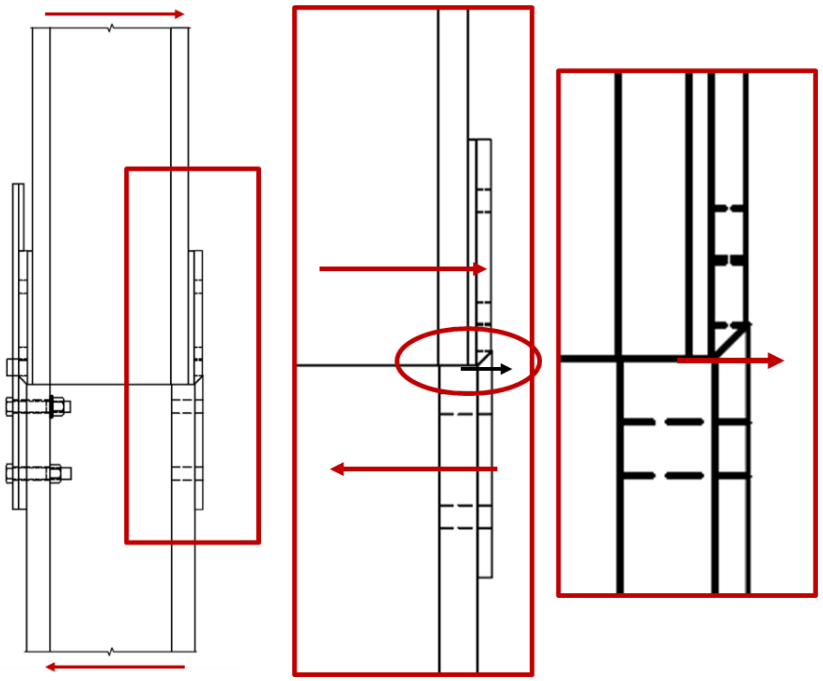

Figure B.1: Area of interest in shear transfer through the Inner Plate.

Example Design Through Shear of the Inner Plate

Inner Plate Properties

IP Nominal Strength (A572)	$F_{y_{IP}}$ =	50	ksi	
IP Width	b_{IP} =	10	in.	
Design *IP* Thickness	t_{IP} =	3/4	in.	

Shear Key Properties

SK Slot Diameter	d_{SK} =	1 5/8	in.	

Column Properties

Upper Column Nominal Strength (A992)	$F_{y_{UC}}$ =	50	ksi	
Story Height	H =	144	in.	
Upper Column X-Axis Plastic Section (W12x170)	$Z_{x_{UC}}$ =	275	$in.^3$	

Shear Yielding Capacity of the Inner Plate

Resistance Factor for Shear Yielding of the *IP*	ϕ =	1.00		

Shear Thickness Requirement from the Upper Column

Shear Demand from the Upper Column	V_x =	95.49	kip	Equation B-7
Inner Plate Thickness Requirement	t_{IP_r} =	0.51	in.	Equation B-11

Design Satisfied

$t_{IP} \geq t_{IP_r}$	**TRUE**	**Equation B-12**

B.4.2 Inner Plate to Lower Column Weld

The IP is secured to the Lower Column through fillet welds. The required thickness of the IP fillet weld ($t_{IP_{weld_r}}$) is calculated using equations from Section J2 of *the Steel Specification* and total stress from the weld and bending moments using the elastic vector method. The weld connection joining the IP to the Lower Column features a C-shaped weld around the edges and lower end of the IP. The IP edge weld length (L_{weld}) is set from the length of the IP (L_{IP}) and accounts for the upper beveled end, determining L_{weld} to be equal to Equation B-13 using the t_{IP}. A visualization of the weld location is shown in Figure B.2.

$$L_{weld} = L_{IP} - t_{IP} \tan(45°)$$

Equation B-13

The expected force experienced by the weld (P_{weld}) is set to be the shear demand in the strong axis direction, as seen in Equation B-14.

$$P_{weld} = V_x$$

Equation B-14

The stress demand experienced by the weld (σ_{weld}) is computed by dividing P_{weld} by the total area of the weld, using weld dimensions of L_{weld}, b_{weld}, and the required IP weld thickness ($t_{IP_{weld_r}}$), explained in Equation B-15.

$$\sigma_{weld} = \frac{P_{weld}}{(2\,L_{weld} + b_{weld})\,t_{IP_{weld_r}}}$$

Equation B-15

The centroid of the IP welds ($\bar{y}$) is calculated in Equation B-16 for use in the bending moment (M_{weld}).

$$\bar{y} = \frac{L_{weld}^2}{2\,L_{weld} + b_{weld}}$$

Equation B-16

Equation B 18 solves the moment demand on the welds using strong axis shear demand and the weld centroid.

$$M_{weld} = V_x\ (L_{weld} - \bar{y})$$

Equation B-17

The moment of inertia of the IP welds (I_{weld}) is calculated in Equation B-18 using weld dimensions.

$$I_{weld} = 2 * \left(\frac{t_{IP_{weld_r}}\ L_{weld}^3}{12} + L_{weld}\ t_{IP_{weld_r}} \left(\frac{L_{weld}}{2} - y_{bar} \right)^2 \right) + t_{IP_{weld_r}}\ b_{weld}\ \bar{y}^2$$

Equation B-18

The bending stress ($\sigma_{bending}$) on the welds is then computed in Equation B-19.

$$\sigma_{bending} = \frac{M_{weld}\ \frac{L_{weld}}{2}}{I_{weld}}$$

Equation B-19

The total stress (σ_{total}) is found through combining Equation B-15 and Equation B-19.

$$\sigma_{total} = \sigma_{weld} + \sigma_{bending}$$

Equation B-20

The weld capacity (σ_{cap}) is equivalent to the nominal stress of the weld (F_{nw}) which corresponds to the resistance factor of metal welds (ϕ), the filler metal classification strength (F_{EXX}), and weld throat factor from Equation J2-5 in *the Steel Specification*.

$$\sigma_{cap} = F_{nw} = \phi\ 0.6\ F_{EXX}\ 0.707$$

Equation B-21

The weld capacity must meet or exceed the total weld stress demand, as indicated in Equation B-22. By substituting the previous equation and rearranging the terms to produce Equation B-23, the $t_{IP_{weld_r}}$ can be determined.

$$\sigma_{cap} \geq \sigma_{total}$$

Equation B-22

$$t_{IP_{weld_r}} = \frac{\sigma_{total}}{\phi\ 0.6\ F_{EXX}\ 0.707}$$

Equation B-23

The design weld thickness ($t_{IP_{weld}}$) must meet or exceed $t_{IP_{weld_r}}$, as verified in Equation B-24.

$$t_{IP_{weld}} \geq\ t_{IP_{weld_r}}$$

Equation B-24

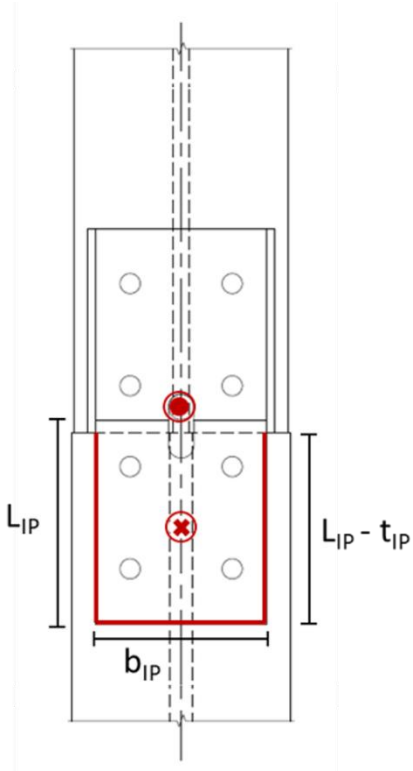

Figure B.2: Location of the welds attaching the Inner Plate to the Lower Column.

Example Design Required Thickness of the Inner Plate to Lower Column Weld

Column Properties				
Upper Column (W12x170) X-Axis Plastic Section	$Z_{x_{UC}}$ =	275	in.^{3}	
Story Height	H =	144	in.	
Upper Column Nominal Strength (A992)	$F_{y_{UC}}$ =	50	ksi	
Weld Properties				
Vertical Length of the *IP* Weld	L_{weld} =	11.25	in.	
Horizontal Width of the *IP* Weld	b_{weld} =	10	in.	
Filler Metal Classification Strength	F_{EXX} =	70	ksi	
Weld Strength Resistance Factor	ϕ =	0.75		
Design Weld Thickness	t_{weld} =	11/16	in.	
Column Shear Demand				
Shear Demand in the X-Axis	V_x =	95.49	kip	Equation B-7
Weld Shear Capacity				
Centroid of Welds	$\bar{y}$ =	3.89	in.	Equation B-16
Moment of Inertia of welds/ $t_{IP_{weld_r}}$	I_{weld}/t_{weld_r} =	456.36	in.^{3}	Equation B-18
Force Demand	P_{weld} =	95.49	kip	Equation B-14
Stress Capacity/ $t_{IP_{weld_r}}$	σ_{weld}/t_{weld_r} =	2.94	kip/in^3	Equation B-15
Moment Capacity of Weld	M_{weld} =	702.37	kip-in.	Equation B-17
Maximum Allowable Bending Stress	$\sigma_{bending}/t_{weld_r}$ =	8.66	kip/in^3	Equation B-19
Total Stress	$\sigma_{total}/t_{weld_r}$ =	11.60	kip/in^3	Equation B-20
Required Weld Thickness	t_{weld_r} =	0.49	in.	Equation B-23

Design Satisfied

$$t_{weld} \geq t_{weld_r}$$ **TRUE** **Equation B-24**

B.5 Weak Axis Shear

Weak axis shear capacity is influenced by several factors, including the cross-sectional area of the Shear Key (SK), the key's weld to the OP, and its area of bearing on the LLP. Additionally, eccentrically loaded bolt groups' nominal strength contributes to the weak axis shear capacity.

The weak axis shear demand (V_y) is determined in Equation B-25, using methods stated in Section D2.5c for column splices from *the* AISC *Provisions*. The weak axis demand is found using the Upper Column plastic moment, as the product between the plastic section in the y-axis ($Z_{y_{UC}}$) and the Upper Column material yield strength ($F_{y_{UC}}$), and the minimum story height (H).

$$V_y = \frac{Z_{y_{UC}} F_{y_{UC}}}{H}$$

Equation B-25

B.5.1 Shear Key Fillet Weld Yield

The required strength capacity of the SK weld can be assessed using Section J2 in *the Steel Specification*, as outlined in Equation B-26. The nominal stress of the fillet weld (F_{nw}) and effective area of the weld on the SK (A_{we}) are determined in Equation B-27 and Equation B-28, respectively. These equations utilize the SK diameter (d_{KEY}) and the filler metal classification strength of the weld (F_{EXX}) to determine the required thickness of the SK weld ($t_{SK_{weld_r}}$).

$$\phi R_n = \phi\ F_{nw}\ A_{we}$$

Equation B-26

$$A_{we} = t_{SK_{weld_r}}\ d_{KEY}\pi$$

Equation B-27

$$F_{nw} = 0.6\ F_{EXX}\ 0.707$$

Equation B-28

To establish the $t_{SK_{weld_r}}$, the shear demand (V_y) is set to be less than or equal to the strength of the weld (ϕR_n) factored by the number of shear keys with welds (n_{KEY}) acting in the direction of the weak axis shear, as per Equation B-29.

$$V_y \leq n_{KEY}\, \phi R_n$$

Equation B-29

In solving for the $t_{SK_{weld_r}}$, Equation B-29 can be rearranged so that $t_{SK_{weld_r}}$ is to be greater than or equal to the weak axis shear demand divided by the required strength and shear key factor, shown in Equation B-30.

$$t_{SK_{weld_r}} \geq V_y \frac{1}{n_{KEY}\, \phi\, F_{EXX}\, d_{KEY}\, \pi}$$

Equation B-30

The computed required thickness must be verified to ensure it is less than or equal to the designed SK weld thickness ($t_{SK_{weld}}$) using Equation B-31.

$$t_{SK_{weld}} \geq t_{SK_{weld_r}}$$

Equation B-31

Example Design Required Thickness of Shear Key Fillet Weld

Column Properties

Upper Column (W12x170) Y-Axis Plastic Section	$Z_{y_{UC}}$ =	126	in.^{3}	
Story Height	H =	144	in.	
Upper Column Nominal Strength (A992)	$F_{y_{UC}}$ =	50	ksi	

Outer Plate Properties

Width of OP	b_{OP} =	10	in.	
Diameter of SK	d_{KEY} =	1.5	in.	

Weld Properties

Design Weld Thickness	$t_{SK_{weld}}$ =	0.5	in.	
Filler Metal Classification Strength	F_{EXX} =	70	ksi	
Number of SK Welds in the Direction of Shear	n_{KEY} =	2	keys	
Resistance Factor of Fillet Weld	ϕ =	0.75		

Column Shear Demand

Shear Demand of the Upper Column (W12x170)	V_y =	43.75	kip	Equation B-25

Required Shear Key Weld Thickness

Required Weld Thickness	$t_{SK_{weld_r}}$ =	0.208	in.	Equation B-30

Design Satisfied

$$t_{SK_{weld}} \geq t_{SK_{weld_r}}$$ **TRUE** **Equation B-31**

B.5.2 Shear Key Cross Section Yield

To prevent SK yield, the required diameter of the SK (d_{KEY_r}) is compared to the design SK diameter (d_{KEY}), using Equation J4-3 from *the Steel Specification*. This verification involves solving for the design strength for the key yield (ϕR_n) in Equation B-32, with the nominal material strength of the SK ($F_{y_{KEY}}$) and gross area of the SK subject to shear (A_{gv}) as described in Equation B-33.

$$\phi R_n = \phi \; 0.6 \; F_{y_{KEY}} \; A_{gv}$$

Equation B-32

$$A_{gv} = \frac{d_{KEY_r}^2}{4} \pi$$

Equation B-33

The weak axis shear demand is constrained to be less than or equal to the yield capacity of the SK, specified in Equation B-34 and factored by the number of shear keys (n_{KEY}) resisting weak axis shear. This is rearranged into Equation B-35 to solve for the minimum required diameter.

$$V_y \leq n_{KEY} \; \phi R_n$$

Equation B-34

$$d_{KEY_r} \geq \; + \sqrt{V_y \frac{4}{n_{KEY} \; \pi \; \phi \; 0.6 \; F_{y_{KEY}}}}$$

Equation B-35

The required diameter solved for in Equation B-35 must be less than or equal to the designed SK diameter (d_{KEY}), confirmed with Equation B-36.

$$d_{KEY} \geq d_{KEY_r}$$

Equation B-36

Example Design Shear Key Cross Section Yield Shear Key Diameter Requirement

Shear Key Properties

Resistance Factor for Shear Yield	ϕ =	1.00		
Design *SK* Diameter	d_{KEY} =	1.5	in.	
SK Nominal Strength (A572)	$F_{y_{KEY}}$ =	50	ksi	
Number of *SK*s in the Direction of Weak Axis Shear	n_{KEY} =	2	keys	

Column Properties

Upper Column (W12x170) Y-Axis Plastic Section	$Z_{y_{UC}}$ =	126	$in.^3$	
Story Height	H =	144	in.	
Upper Column Nominal Strength (A992)	$F_{y_{UC}}$ =	50	ksi	

Column Shear Demand

Shear Demand of the Upper Column (W12x170)	V_y =	43.75	kip	Equation B-25

Required Diameter

Required *SK* Diameter	d_{KEY_r} =	0.96	in.	Equation B-35

Design Satisfied

$$\boldsymbol{d_{KEY} \geq d_{KEY_r}}$$ **TRUE** **Equation B-36**

B.5.3 Shear Key Bearing on the Lower Lock Plate

The SK bears on the LLP to transfer weak axis shear from the Upper Column to the Lower Column. The design strength for the portion of the SK interfacing with the LLP is calculated in Equation B-37, using the minimum yield strength (F_y) between the SK and LLP and the projected bearing area between the SK and LLP. The equation for bearing capacity is found using Equation J7-1, which pertains to the bearing capacity for finished surfaces and is located in *the Steel Specification.*

$$\phi R_n = \phi \; 1.8 \; F_y \; A_{pb}$$

Equation B-37

The projected bearing area (A_{pb}) is identified as the area parallel to the direction of the shear force on which the SK and LLP act on each other, shown in Figure B.3. Given the geometry of the SK slot in the LLP and the cylindrical SK, half the SK diameter (d_{KEY}) will bear on the LLP. Due to the curved surface of the cylinder, A_{pb} can be calculated as half the diameter multiplied by the required bearing thickness on the LLP (t_{LLP_r}), as described in Equation B-38.

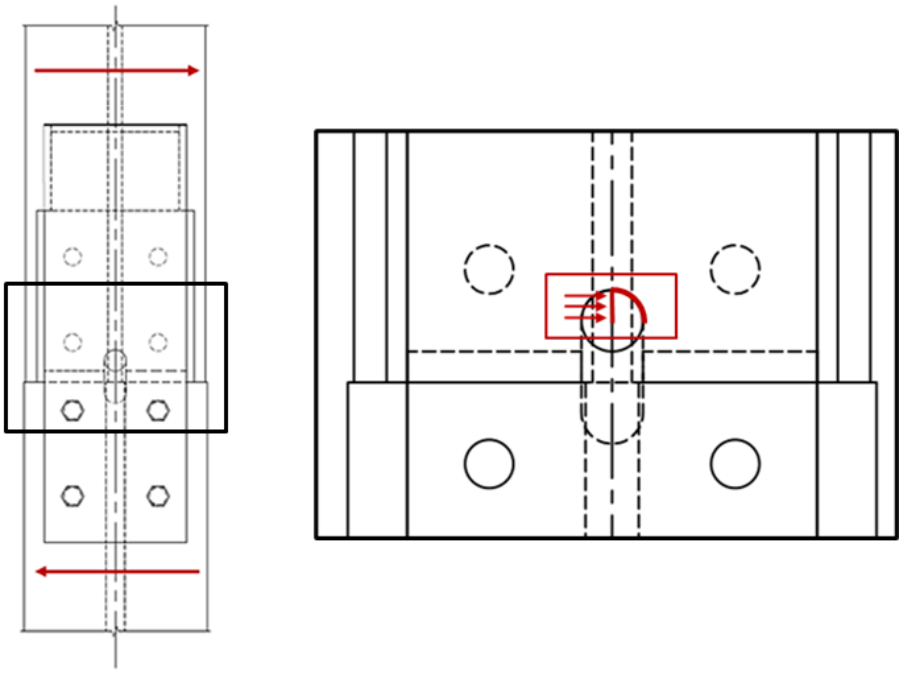

Figure B.3: Area of interest where the Shear Key bears on the Lower Lock Plate.

$$A_{pb} = \frac{d_{KEY}}{2} t_{LLP_r}$$

Equation B-38

The shear demand must be less than or equal to the required shear strength, factored by the number of keys (n_{KEY}) acting in the direction of the shear force, shown in Equation B-39.

$$V_y \leq n_{KEY}\, \phi R_n$$

Equation B-39

Required bearing thickness on the LLP can be calculated with Equation B-40 by substituting and rearranging Equation B-39 to produce Equation B-40.

$$t_{LLP_r} \geq V_y \frac{1}{n_{KEY}\, \phi\, 1.8\, F_{y_{LLP}}\, d_{KEY}}$$

Equation B-40

Equation B-41 then verifies the design thickness of the LLP (t_{LLP}) and t_{LLP_r} by considering the estimated 1/16 in. difference between the actual thickness of the LLP and SK bearing in the SK slot due to manufacturing.

$$t_{LLP} \geq t_{LLP_r} + {}^{1}/_{16}{}''$$

Equation B-41

Example Design Shear Key Slot Bearing on Lower Lock Plate Thickness Requirements

Shear Key Properties

Resistance Factor for Bearing Strength	ϕ =	0.75		
Design *SK* Diameter	d_{KEY} =	1.5	in.	
SK Nominal Strength (A572)	$F_{y_{KEY}}$ =	50	ksi	
Number of *SK* in the Direction of Weak Axis Shear	n_{KEY} =	2	keys	

Lower Lock Plate Properties

LLP Nominal Strength (A572)	$F_{y_{LLP}}$ =	50	ksi	
Design *LLP* Thickness	t_{LLP} =	0.75	in.	

Column Properties

Upper Column (W12x170) Y-Axis Plastic Section	$Z_{y_{UC}}$ =	126	$in.^3$	
Story Height	H =	144	in.	
Upper Column Nominal Strength (A992)	$F_{y_{UC}}$ =	50	ksi	

Column Shear Demand

Shear Demand of the Upper Column (W12x170)	V_y =	43.75	kip	Equation B-25

Required Thickness

Required *LLP* Thickness	t_{LLP_r} =	0.43	in.	Equation B-40

Design Satisfied

$t_{LLP} \geq t_{LLP_r} + 1/16"$	**TRUE**	**Equation B-41**

B.5.4 Eccentric Bolt Groupings

The eccentric load capacity of a bolt group for connecting the OP to the Lower Column, was determined using Table 7-8, with reference to Table 7-1, from *the Manual*.

Design variables used to calculate eccentric bolt design capacity include design bolt column spacing (s), the designed vertical distance from the centroid of the bolt group to the horizontal plane of loading (e_x), the tabulated eccentrically loaded bolt group coefficient (C), and the nominal design strength per bolt (r_n).

Due to the tabulated values for C from predetermined values in Table 7-8 from *the Manual*, conservative tabulated values must be selected for the design variables listed above in order to determine the capacity of the bolt group. Selected conservative values include the tabulated bolt column spacing (s_e), which must be less than or equal to s, the provided bolt row spacing (r_e) must be less than or equal to the design bolt row spacing (L_1), and the tabulated values of the vertical distance from the centroid of the bolt group to the plane of loading (e_{x_e}) must be greater than or equal to e_x.

Calculations to determine e_x, shown in Equation B-42 with the dimensional layout in Figure B.4, utilize L_1, the vertical distance between the center of the upper row of bolts to the upper end of the Lower Column (b_{offset}), and the center of the SK down to the column splice (b_{SK}).

$$e_x = \frac{L_1}{2} + b_{offset} + b_{SK}$$

Equation B-42

The factored available strength (ϕR_n) uses the tabulated C coefficient and available bolt shear strength (ϕr_n) of a given bolt diameter with a Group A designation for A325 bolts, using the "N" condition with threads included in the shear plane and assuming single shear "S" loading. Using the previous constraints of $s \geq s_e$, $L_1 \geq 5\ 1/2"$, and $e_x \leq e_{x_e}$, the C coefficient can be estimated and used in Equation B-43.

$$\phi R_n = C\ \phi r_n$$

Equation B-43

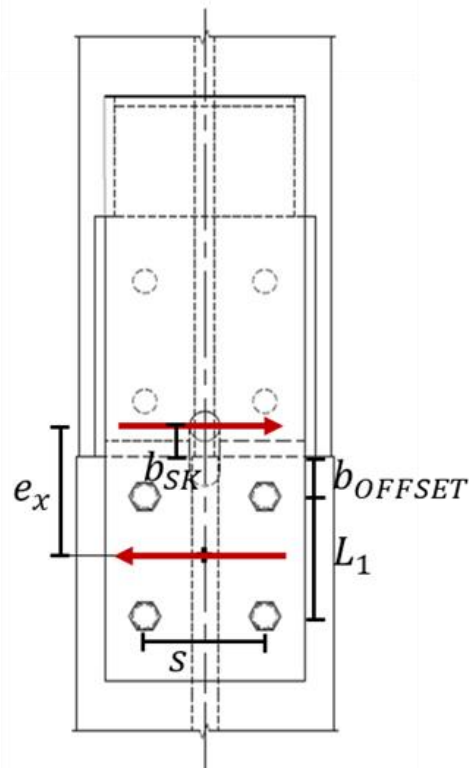

Figure B.4: Dimensional layout used to determine eccentricity.

Example Design Eccentrically Loaded Bolt Groups

Outer Plate Properties

OP Plate Width	b_{OP} =	10	in.	
Distance Between Bolt Rows	L_1 =	6	in.	
Number of Bolt Columns	n_{col} =	2		
Distance Between Bolt Columns	s =	7	in.	
Center of Upper Bolt Row to Upper End of Lower Column	b_{top} =	2	in.	
Center of SK to Lower End of Upper Column	b_{SK} =	1.5	in.	
Number of Bolt Groups in Direction of Shear	n_{bg} =	2	groups	

Bolt Properties

Column Splice Bolt Diameter	d_b =	1	in.	
Bolt Hole Diameter	d_h =	1.125	in.	
Available Shear Strength for 1" Bolts	ϕr_n =	31.8	kip	
Design Vertical Distance from the Centroid of the Bolt Group to Column Shear Transfer (Center of SK)	e_x =	6.5	in.	Equation B-42

Column Properties

Upper Column (W12x170) Y-Axis Plastic Section	$Z_{y_{UC}}$ =	126	in.^{3}	
Story Height	H =	144	in.	
Upper Column Nominal Strength (A992)	$F_{y_{UC}}$ =	50	ksi	

Tabulated Eccentrically Loaded Coefficients

Tabulated Eccentric Distance from Centroid of Bolt Group to Line of Action	e_{x_e} =	7	in.	
Tabulated Bolt Column Spacing	s_e =	6	in.	
Tabulated Bolt Row Spacing	r_e =	5.5	in.	
Coefficient Tabulated from similar s_e, e_{x_e}, and n_{col}	C =	1.8		

Verification of Values

$L_1 \geq r_e$	TRUE
$s \geq s_e$	TRUE
$e_x \leq e_{x_e}$	TRUE

Available Strength from Splice Bolt Group ϕR_n = **57.24 ksi** **Equation B-43**

B.5.4.1 Spacing Considerations

In conjunction with bolt sizes and spacing for bolt grouping strength, allowable tightening and entering clearances must be met for the bolts on the Lower Column. This, combined with the outer diameter of the disc spring, must not interfere with the column fillet of the web to flange on the Lower Column.

Using the design values of the OP width (b_{OP}) and bolt column spacing (s), the design edge distance (b_{EDGE}) for a given bolt diameter can be determined and compared to Table J3.4 ($b_{EDGE_{min}}$) for the corresponding bolt diameter in *the Steel Specification*. The edge distance to the OP is used as the width of the Lower Column will never be less than the width of the OP. The calculation to find b_{EDGE} is identified in Equation B-44, with the verification outlined in Equation B-45.

$$b_{EDGE} = \frac{b_{OP} - s}{2}$$

Equation B-44

$$b_{EDGE} \geq b_{EDGE_{min}}$$

Equation B-45

Using the verified b_{EDGE} and subsequent s, the maximum fillet size for the Lower Column ($k_{1_{max}}$) can be calculated using the allowable s and the larger dimension of the maximum outer diameter of the disc spring (OD_{max}) used in design and the clearance for flange-to-web column fillets (C_3) located in Table 7-15 for A325 bolts from *the Manual*, provided in Equation B-46. The resulting maximum fillet size calculated must not be less than the design dimensions for the Lower Column ($k_{1_{LC}}$), defined in Equation B-47 and shown in Figure B.5.

$$k_{1_{max}} = \frac{s}{2} - MAX\left(\frac{OD}{2},\ C_3\right)$$

Equation B-46

$$k_{1_{max}} \geq k_{1_{LC}}$$

Equation B-47

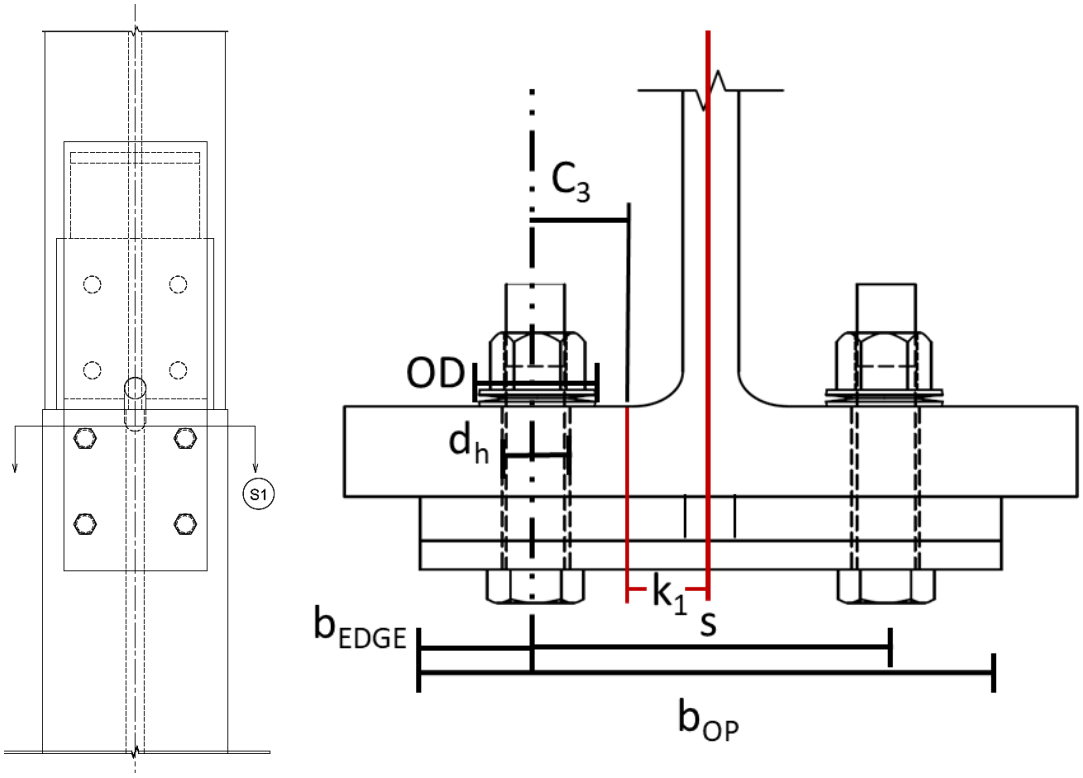

Figure B.5: Dimensional considerations for bolt spacing and Lower Column size.

Example Design Bolt Spacing Considerations of the Outer Plate

Outer Plate Properties

Width of the OP	b_{OP} =	10	in.	
Bolt Column Spacing	s =	7	in.	

Bolt Properties

Bolt Diameter	b_d =	1	in.	
Bolt Hole Diameter	b_h =	1.125	in.	
Minimum Edge Distance Allowed	$b_{EDGE_{min}}$ =	1.25	in.	Table J3.4
Entering and Tightening Clearance for Given Bolt Diameter	C_3 =	1	in.	

Disc Spring Properties

Disc Spring Maximum Outer Diameter	OD =	2.2	in.	

Center to Flange Distance

Center Web to End of Fillet of the Lower Colum	$k_{1_{LC}}$ =	1 1/2	in.	

Edge Verification

Center of Bolt Hole to OP Edge Design	b_{EDGE} =	1.5	in.	Equation B-44
$\boldsymbol{b_{EDGE} \geq b_{EDGE_{min}}}$	**TRUE**			**Equation B-45**

Maximum Shape Size

Maximum Distance from Center of Web to Flange Fillet Toe	$k_{1_{max}}$ =	2 3/8	in.	Equation B-46

Shape Verification

$\boldsymbol{k_{1_{max}} \geq k_{1_{UC}}}$	**TRUE**	**Equation B-47**

B.6 Outer Plate Flexural Yielding

The analysis for maximum Outer Plate flexural bending occurs during the intermediate condition of assembly as the OP deforms around the LLP. When the lower end of the ULP aligns with the face of the LLP before the beveled edge, the OP is at its maximum deformation and experiences its greatest bending moment across the plate.

To analyze the extreme bending moment, there are three points of interest on the OP. First, the lower, fixed bolts behave like a cantilever end of a beam, and the location of interest along the plate is at $x = 0$. Next, the location of the upper, spring bolts is identified at $x = L_1$. The last point of interest occurs at the location of maximum deflection on the beam experiencing shear and moment. This takes place at the lower edge of the ULP and is defined by $x = L_{tot}$. The difference in length between the spring bolts at $x = L_1$ and the edge of the ULP at $x = L_{tot}$ is defined as L_2, with the numerical expression for L_{tot} shown in Equation B-48. The mathematical model used in the analysis, containing the locations of interest, is displayed in Figure B.6 with the CAD rendering portraying the intermediate assembly condition.

$$L_{tot} = L_1 + L_2$$

Equation B-48

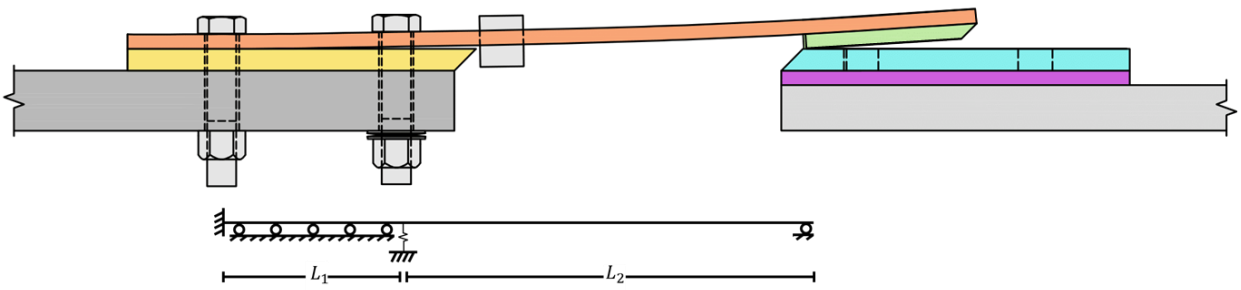

Figure B.6: Mathematical model of the Outer Plate with dimensions along the beam.

The determination of the location of maximum flexure utilizes supplementary equations provided in Equation B-49 and Equation B-50 to calculate the moment of inertia for the OP (I_{OP}) and OP stiffness (k_{OP}). Design variables include OP width (b_{OP}), OP thickness (t_{OP}), and L_{tot}.

$$I_{OP} = \frac{b_{OP}\, t_{OP}^3}{12}$$

Equation B-49

$$k_{OP} = \frac{3\, E\, I_{OP}}{L_{tot}^3}$$

Equation B-50

The following sections of Section B.6 describe a series of equations and iterations used to determine the maximum moment of the OP modeled as a beam.

Example Design General Calculations for Outer Plate Flexural Yielding

Outer Plate Properties				
OP Thickness	t_{OP} =	0.5	in.	
OP Width	b_{OP} =	10	in.	
Length from the Lower Row to the Upper Row of Bolts	L_1 =	6	in.	
Length from the Upper Row of Bolts to the Lower Edge of the Upper Lock Plate	L_2 =	14	in.	
OP Material (A572) Young's Modulus	E =	29,000	ksi	
Total Bending Length Consideration				
Length from Fixed Bolts to Lower Edge of ULP	L_{tot} =	20	in.	Equation B-48
Moment of Inertia				
Moment of Inertia for the OP	$\boldsymbol{I_{OP}}$ =	**0.104**	**in.^{4}**	**Equation B-49**
Plate Stiffness				
Stiffness of the OP	$\boldsymbol{k_{OP}}$ =	**1.133**	**kip/in**	**Equation B-50**

B.6.1 Pretensioning in the Spring Bolts

To ensure column stability and prevent any tampering or movement of the OP after installation, the disc springs on the upper row of bolts are pretensioned to 0.2 kip. The pretension force (P_{pt}) on the bolts remains constant throughout the column's erection life cycle, with force changes only occurring during the initial installation process. To achieve the pretension force, the initial spring deformation (δ_{s_0}) is defined Equation B-51 as it is related to the force-deformation curve of the spring.

$$\delta_{s_0} = \delta_{Force}(P_{pt})$$

Equation B-51

Using the process described in Appendix A.3, the nonlinear curve deformation for the required pretension force is determined by interpolating between two points at P_{pt} = 0.2 from the curve data of change in displacement.

Example Design Disc Deformation for Bolt Pretensioning

Disc Spring Deformation from Bolt Pretensioning	δ_{s_0} =	**0.0047**	**in.**	**Equation B-51**

B.6.2 Instantaneous Plate Uplift at Spring Bolts

The OP deformation during snapping can be analyzed by superimposing three different deformation models. Partial beam deformation is outlined in Section B.6.2, while full beam deformation is determined in Section B.6.3. To initiate the process, the first observation occurs when the upward force at L_{tot} is equal to P_{pt}, written as F_{up} and shown in Equation B-52.

$$F_{up} = P_{pt}$$

Equation B-52

With F_{up} set equal to P_{pt}, there is deformation of the OP from L_1 to L_{tot}. This indicates that the springs exert no further force, and the deformation remains constant from the initial pretensioned deformation. Of the maximum displacement allowable ($\delta_{max} = t_{ULP}$), the initial free end uplift displacement is calculated applying Equation B-53, using the OP Young's Modulus (E), L_2, F_{up}, and I_{OP}.

$$\delta_{up} = \frac{F_{up}\, {L_2}^3}{3\, E\, I_{OP}}$$

Equation B-53

The bending moment (M_{uplift}), shear force (V_{uplift}), and displacement (D_{uplift}) curves along the OP from $0 \le x \le L_{tot}$ from the initial uplift are calculated from Equation B-54 through Equation B-56 and provide an analysis of structural behavior along the plate.

$$M_{uplift}(x) = \begin{cases} F_{up}\, L_2 & 0 \le x < L_1 \\ \vdots & \vdots \\ \dfrac{F_{up}\, L_2\, x}{L_1 - L_{tot}} - \dfrac{F_{up}\, L_2\, L_1}{L_1 - L_{tot}} + F_{up}\, L_2 & L_1 \le x \le L_{tot} \end{cases}$$

Equation B-54

$$V_{uplift}(x) = \begin{cases} 0 & 0 \le x < L_1 \\ \vdots & \vdots \\ -F_{up} & L_1 \le x \le L_{tot} \end{cases}$$

Equation B-55

$$D_{uplift}(x) = \begin{cases} 0 & 0 \le x < L_1 \\ \square & \square \\ F_{up}\,(x - L_1)^2 * \dfrac{3\,L_2 - (x - L_1)}{6\,E\,I_{OP}} & \square \\ & L_1 \le x \le L_{tot} \end{cases}$$

Equation B-56

Example Design Instantaneous Uplift at Spring Bolts

Outer Plate Properties				
OP Thickness	t_{OP} =	0.5	in.	
OP Width	b_{OP} =	10	in.	
Length from the Lower Row to the Upper Row of Bolts	L_1 =	6	in.	
Length from the Upper Row of Bolts to the Lower Edge of the Upper Lock Plate	L_2 =	14	in.	
OP Material (A572) Young's Modulus	E =	29,000	ksi	
Fixed Bolts to Lower Edge of ULP	L_{tot} =	20	in.	Equation B-48
Moment of Inertia				
Moment of Inertia for the OP	I_{OP} =	0.104	$in.^4$	Equation B-49
Forces				
Reaction Force to Pretensioned Bolts at L_{tot}	F_{up} =	0.2	kip	Equation B-52
Displacement of Outer Plate				
Displacement at L_{tot}	δ_{up} =	**0.0606**	**in.**	**Equation B-53**

The generalized equations for instantaneous uplift are specified for the example design dimensions defined in Equation B-57 through Equation B-59. The accompanying curves for the example design are visualized in Figure B.7.

$$M_{uplift}(x) = \begin{cases} 2.8 & 0 \le x < L_1 \\ \square & \square \\ -0.2\,x + 4 & L_1 \le x \le L_{tot} \end{cases}$$

Equation B-57

$$V_{uplift}(x) = \begin{cases} 0 & 0 \le x < L_1 \\ \square & \square \\ -0.2 & L_1 \le x \le L_{tot} \end{cases}$$

Equation B-58

$$D_{uplift}(x) = \begin{cases} 0 & 0 \le x < L_1 \\ \square & \square \\ 0.2\,(x-6)^2 * \dfrac{42-(x-6)}{18{,}125} & L_1 \le x \le L_{tot} \end{cases}$$

Equation B-59

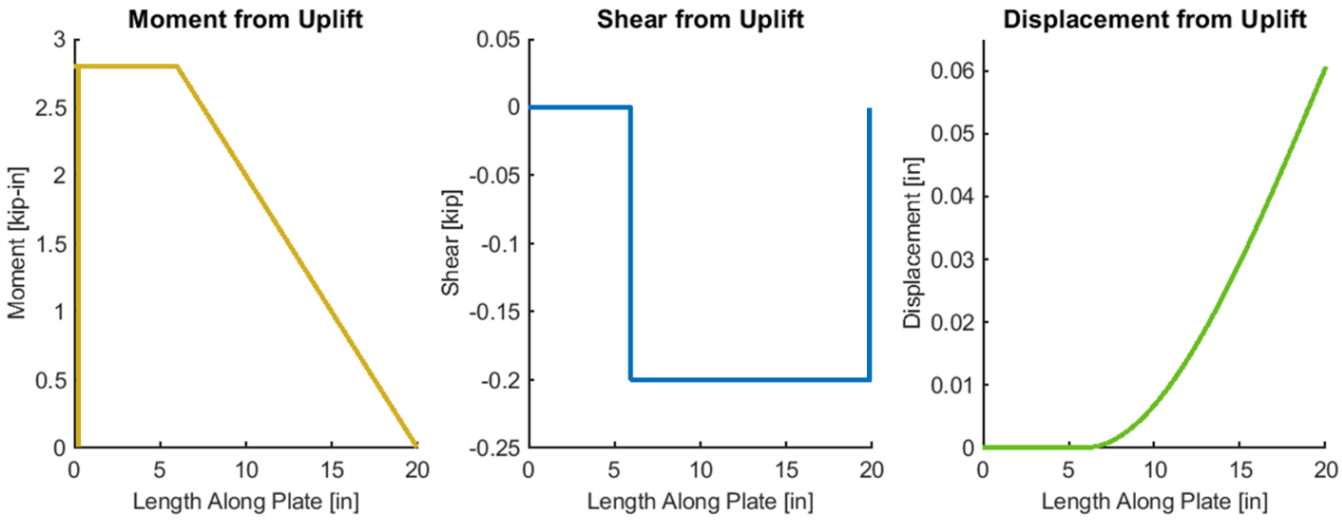

Figure B.7: Moment, velocity, and displacement along the OP using Equation B-57 through Equation B-59.

B.6.3 Using Superposition to Find Forces and Displacements After Uplift

When determining the applied force on the plate from the disc springs caused by the displacement of the OP, two beam models are superimposed. First, the plate is modeled as a cantilever beam with an end displacement from an uplift force. Second, the OP is modeled as a propped, simply supported cantilever with a force applied at the location of the disc springs.

The displacement at the spring location on the OP, modeled as a cantilever beam, initializes the first approximation for the spring deformation (δ_{s_1}) and is used to determine the accompanying spring force approximation (P_{s_2}) used in the second beam model, the propped cantilever. Modeled independently, the second beam model will cause an independent deformation at the disc springs from P_{s_2}. To identify the total deformation of the OP the two beam model deformations are superimposed to determine a new approximated spring deformation at L_1, which will identify a new disc spring force on the OP. This iteration occurs until the new and original spring deformation guesses are within a tolerance of each other.

B.6.3.1 Beam 1: Cantilever Beam with Displacement at End

Starting with the cantilever rendering of the OP, the lower bolts are considered fixed, and a force is applied to L_{tot} to displace the end of the plate the remainder of δ_{max}, equal to $\delta_{1_{end}}$, considering the previously identified δ_{up}, as defined in Equation B-60.

$$\delta_{1_{end}} = \delta_{max} - \delta_{up}$$

Equation B-60

In this beam model, the forces from the disc springs are not considered. Instead, the forces acting on the beam originate from the upward end displacement and the beam's reaction at the fixed bolts. The force required to induce $\delta_{1_{end}}$ at the free end of the plate (F_1) is determined using the previously calculated OP stiffness (k_{OP}) and $\delta_{1_{end}}$ seen in Equation B-61.

$$F_1 = k_{OP}\,\delta_{1_{end}} = \frac{3\,E\,I_{OP}\,\delta_{1_{end}}}{L_{tot}^{\,3}}$$

Equation B-61

The reaction force of Beam 1 at the fixed bolts ($F_{1_{rxn}}$) is equal and opposite to F_1, seen in Equation B-62.

$$F_{1_{rxn}} = -F_1$$

Equation B-62

From the forces occurring on the plate and the OP material properties (E, I_{OP}), the moment curve (M_1), shear curve (V_1), and displacement (D_1) across the plate from the first modeled beam can be determined from Equation B-63 through Equation B-65 below.

$$M_1(x) = -F_{1_{rxn}}(L_{tot} - x)$$

Equation B-63

$$V_1(x) = F_{1_{rxn}}$$

Equation B-64

$$D_1(x) = \frac{F_{1_{rxn}}\, x^3}{6\, E\, I_{OP}} + \frac{F_1\, L_{tot}\, x^2}{2\, E\, I_{OP}}$$

Equation B-65

With a defined displacement curve, the exact displacement of the OP from Beam 1 at the location of the springs is used to determine a first approximate guess for the force that the disc springs will apply on the plate during Beam 2 calculations.

$$\delta_{s_1} = D_1(L_1)$$

Equation B-66

Example Design Superposition of Beam 1

Outer Plate Properties				
OP Thickness	t_{OP} =	0.5	in.	
OP Width	b_{OP} =	10	in.	
Length from the Lower Row to the Upper Row of Bolts	L_1 =	6	in.	
Length from the Upper Row of Bolts to the Lower Edge of the Upper Lock Plate	L_2 =	14	in.	
OP Material (A572) Young's Modulus	E =	29,000	ksi	
Fixed Bolts to Lower Edge of ULP	L_{tot} =	20	in.	Equation B-48
Upper Lock Plate Properties				
Thickness of the ULP	t_{ULP} =	0.5	in.	
Moment of Inertia				
Moment of Inertia for the OP	I_{OP} =	0.104	$in.^4$	Equation B-49
Plate Stiffness				
Stiffness of the OP	k_{OP} =	1.133	kip/in	Equation B-50
Displacement of Outer Plate				
Displacement at L_{tot}	δ_{up} =	0.0606	in.	Equation B-53
Variables for Beam 1 Superposition				
Displacement of Beam 1 at L_{tot}	$\delta_{1_{end}}$ =	0.4394	in.	Equation B-60
Force for L_{tot} Displacement	F_1 =	0.4978	kip	Equation B-61
Reaction Force to F_1	$F_{1_{rxn}}$ =	-0.4978	kip	Equation B-62

Displacement of the Outer Plate

Displacement of the OP at the Disc Springs from Beam 1 δ_{s_1} = **0.0534 in. Equation B-70**

From the example OP design dimensions, the Beam 1 design moment, shear, and displacement behaviors are displayed below in Equation B-67 through Equation B-69. The curve equations are accompanied by Figure B.8, presenting the curves plotted along the analyzed length of the OP.

$$M_1(x) = 0.4978(20 - x)$$

Equation B-67

$$V_1(x) = -0.4978$$

Equation B-68

$$D_1(x) = \frac{-0.498\,x^3}{18{,}125} + \frac{9.956\,x^2}{6{,}041.667}$$

Equation B-69

To estimate the initial deformation of the springs used in Beam 2 calculations, the plate displacement from Beam 1 is taken at L_1, where $L_1 = 6$ in. The solution for beam displacement is seen in Equation B-70.

$$\delta_{S_1} = D_1(L_1) = D_1(6) = \frac{-0.498 * 6^3}{18{,}125} + \frac{9.956 * 6^2}{6{,}041.667} = 0.0534\ in.$$

Equation B-70

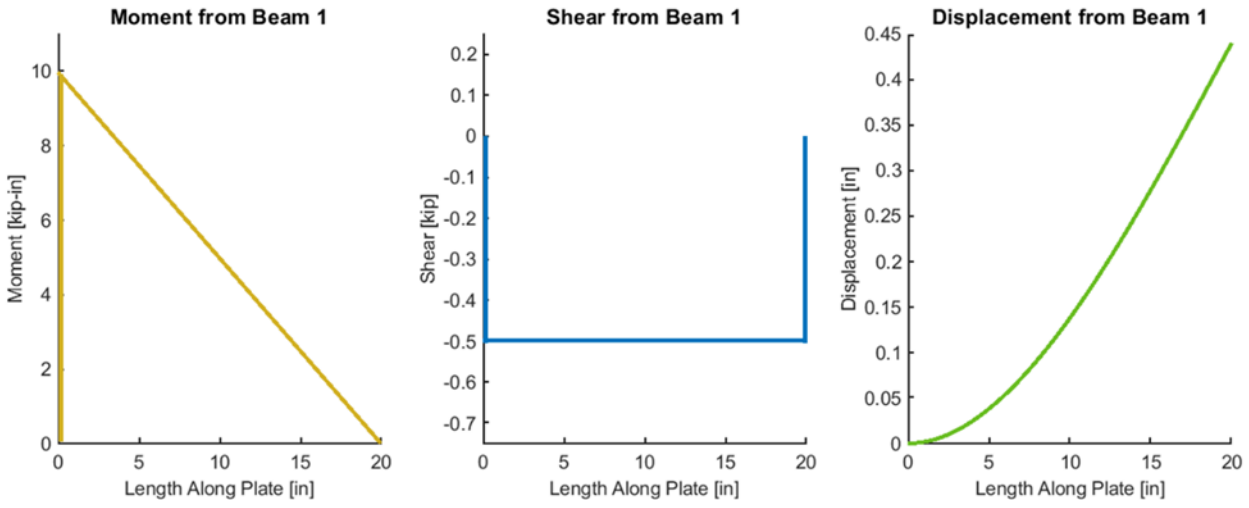

Figure B.8: Moment, shear, and displacement curves for the design dimensions, modeling the curve as a cantilever with an end force from displacement.

B.6.3.2 Beam 2: Propped Fixed Beam with Force from Deformed Springs

The second modeled beam features boundary conditions with one fixed end at $x = 0$ and one simply supported end at $x = L_{tot}$. An applied force is generated by the disc springs at L_1 based on the first model's deformation at the disc springs. The force is determined by setting the deformation of Beam 2 equal to δ_{s_1} (δ_{s_2}), defined in Equation B-71, and adding it to the initial spring deformation from pretensioning to determine the total spring deformation ($\delta_{s_{total}}$), shown in Equation B-72.

$$\delta_{s_2} = \delta_{s_1}$$

Equation B-71

$$\delta_{s_{total}} = \delta_{s_2} + \delta_0$$

Equation B-72

The force exerted on Beam 2 from the springs (P_{s_2}) does not include the pretensioned force (P_{pt}) and must be subtracted from the nonlinear force-displacement projection represented by $\delta_{s_{total}}$ ($P_{\delta_s}\left(\delta_{s_{total}}\right)$), as per Equation B-73. Given that P_{s_2} is acting in the opposite direction of the displacement forces, it is defined as a negative force.

$$P_{s_2} = P_{\delta_s}\left(\delta_{s_{total}}\right) - P_{pt}$$

Equation B-73

The reaction forces and moments of the plate modeled as Beam 2 are determined through Equation B-74 - Equation B-76 using beam equilibrium principles. The reaction force of Beam 2 at its fixed end ($R_{2_{f_0}}$) is defined in Equation B-74, while the reaction force of Beam 2 at its support end ($R_{2_{s_0}}$) is defined in Equation B-75. Equation B-76 describes the reaction moment of Beam 2 at its fixed end ($M_{2_{f_0}}$). All equations use the initial estimate for the force the disc springs exert (P_{s_2}).

$$R_{2f_0} = \frac{-P_{S_2}\, L_2(3\, L_{tot}^2 - L_2^2)}{2\, L_{tot}^3}$$

Equation B-74

$$R_{2_{s_0}} = \frac{-P_{S_2}\, L_1^2\, (L_2 + 2\, L_{tot})}{2\, L_{tot}^3}$$

Equation B-75

$$M_{2_{f_0}} = \frac{P_{S_2}\, L_1\, L_2\, (L_{tot} + L_2)}{2\, L_{tot}^2}$$

Equation B-76

Upon determining the reactions, moment (M_2), shear (V_2), and displacement (D_2) curves for Beam 2 can be formed through beam governing equations, shown in Equation B-77 through Equation B-79 respectively.

$$M_2(x) = \begin{cases} M_{2_{f_0}} + R_{2_{f_0}}\, x & 0 \le x < L_1 \\ \vdots & \vdots \\ R_{2_{s_0}}\, (L_{tot} - x) & L_1 \le x \le L_{tot} \end{cases}$$

Equation B-77

$$V_2(x) = \begin{cases} R_{2_{f_0}} & 0 \le\ x < L_1 \\ \vdots & \vdots \\ R_{2_{f_0}} + P_{S_2} & L_1 \le x \le L_{tot} \end{cases}$$

Equation B-78

$$D_2(x) = \begin{cases} \dfrac{\left((L_{tot} - L_1)\, P_{S_2}\, x^2 * \left(L_{tot}^2\, (6\, L_1 - 2\, x) + L_1^2\, x - L_{tot}\, L_1\, (3\, L_1 + 2\, x)\right)\right)}{12\, L_{tot}^3\, E\, I_{OP}} & 0 \le x < L_1 \\ \vdots & \vdots \\ \dfrac{\left(L_1^2\, (-P_{S_2})\, (L_{tot} - x)\left(2\, L_{tot}^2\, (L_1 - 3x) - L_1\, x^2 + L_{tot}\, x\, (2\, L_1 + 3\, x)\right)\right)}{12 L_{tot}^{\ 3}\, E\, I_{OP}} & L_1 \le x \le L_{tot} \end{cases}$$

Equation B-79

Example Design Superposition of Beam 2

Outer Plate Properties

Length from the Lower Row to the Upper Row of Bolts	L_1 =	6	in.	
Length from the Upper Row of Bolts to the Lower Edge of the Upper Lock Plate	L_2 =	14	in.	
OP Material (A572) Young's Modulus	E =	29,000	ksi	
Length from Fixed Bolts to Lower Edge of ULP	L_{tot} =	20	in.	Equation B-48

Disc Deformation

Disc Spring Deformation from Bolt Pretensioning	δ_{s_0} =	0.0047	in.	Equation B-51

Moment of Inertia

Moment of Inertia for the OP	I_{OP} =	0.104	$in.^4$	Equation B-49

Forces

Spring Force from Pretensioned Bolts	P_{pt} =	0.2	kip	

Calculated Displacements

Displacement of the OP at the Disc Springs from Beam 1	δ_{s_1} =	0.0534	in.	Equation B-70
Spring Deformation Due to OP Displacement	δ_{s_2} =	0.0534	in.	Equation B-71
Total Spring Deformation	$\delta_{s_{total}}$ =	0.1068	in.	Equation B-72

Calculated Forces

Force at L_1 caused by \delta_s_2	P_{s_2} =	-1.0155	kip	Equation B-73
Reaction of Beam 2 at Fixed End for Initial Guess	$R_{2_{f_0}}$ =	0.8921	kip	Equation B-74
Reaction of Beam 2 at Support End for Initial Guess	$R_{2_{s_0}}$ =	0.1234	kip	Equation B-75

Calculated Moments

Moment of Beam 2 at Fixed End for Initial Guess	$M_{2_{f_0}}$ =	-3.6252	kip	Equation B-76

The generalized moment, shear, and displacement curves for Beam 2 are applied from the example design dimensions in Equation B-80 through Equation B-82. The accompanying plotted curve behaviors are shown in Figure B.9 across the length of interest on the OP.

$$M_2(x) = \begin{cases} -3.6252 + 0.8921\,x & 0 \le x < L_1 \\ \vdots & \vdots \\ 0.1234\,(20 - x) & L_1 \le x \le L_{tot} \end{cases}$$

Equation B-80

$$V_2(x) = \begin{cases} 0.8921 & 0 \le x < L_1 \\ \vdots & \vdots \\ -0.1234 & L_1 \le x \le L_{tot} \end{cases}$$

Equation B-81

$$D_2(x) = \begin{cases} \dfrac{\left(-14.217\,x^2\left(400\,(36 - 2\,x) + 36\,x - 120\,(18 + 2\,x)\right)\right)}{290{,}000{,}000} & 0 \le x < L_1 \\ \vdots & \vdots \\ \dfrac{\left(36.557\,(20 - x)\left(800\,(6 - 3\,x) - 6\,x^2 + 20\,x\,(12 + 3\,x)\right)\right)}{290{,}000{,}000} & L_1 \le x \le L_{tot} \end{cases}$$

Equation B-82

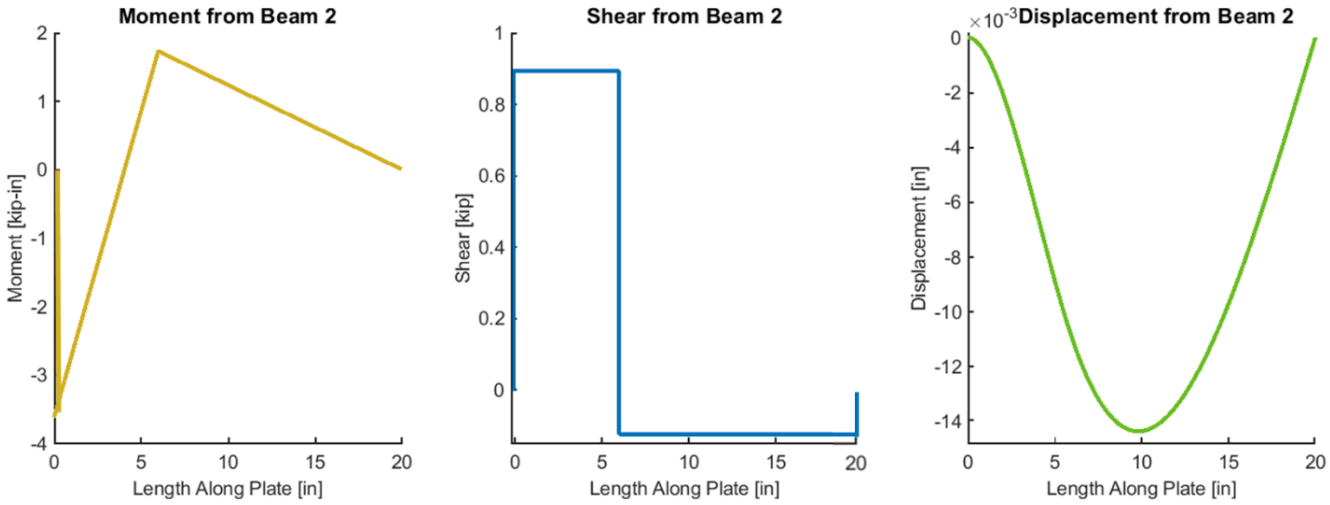

Figure B.9: Moment, shear, and displacement curves of Beam 2 with the initial guessed P_{s_2} originating from δ_{s_1}.

B.6.4 Finalize Displacement Curve and Load Demands

Due to the different deflections of the OP caused by Beams 1 and 2, the deflection curves must be superimposed to predict a more accurate displacement at L_1 during snapping. The initial curve combinations of Beams 1 and 2 produce new moment (M_{12_0}), shear (V_{12_0}), and displacement (D_{12_0}) products used to re-estimate the spring deformation and produce the next spring force guess for Beam 2.

The initial superimposed moment curve (M_{12_0}) combines Equation B-63 from Beam 1 calculations and Equation B-77 from Beam 2 calculations to produce Equation B-83.

$$M_{12_0}(x) = M_1(x) + M_2(x) = \begin{cases} -F_{1_{rxn}}(L_{tot} - x) + M_{2_{f_0}} + R_{2_{f_0}}\, x & 0 \le x < L_1 \\ \vdots & \vdots \\ -F_{1_{rxn}}(L_{tot} - x) + R_{2_{S_0}}\,(L_{tot} - x) & L_1 \le x \le L_{tot} \end{cases}$$

Equation B-83

The initial superimposed shear curve (V_{12_0}) combines Equation B-64 from Beam 1 calculations and Equation B-78 from Beam 2 calculations, creating the combined shear equation shown in Equation B-84.

$$V_{12_0}(x) = V_1(x) + V_2(x) = \begin{cases} F_{1_{rxn}} + R_{2_{f_0}} & 0 \le x < L_1 \\ \vdots & \vdots \\ F_{1_{rxn}} + R_{2_{f_0}} + P_{S_2} & L_1 \le x \le L_{tot} \end{cases}$$

Equation B-84

The initial superimposed displacement curve (D_{12_0}) combines Equation B-65 from Beam 1 calculations and Equation B-79 from Beam 2 calculations, producing Equation B-85.

$$D_{12_0}(x) = D_1(x) + D_2(x)$$

$$= \begin{cases} \frac{F_{1_{rxn}}\, x^3}{6\, E\, I_{OP}} + \frac{F_1\, L_{tot}\, x^2}{2\, E\, I_{OP}} + \frac{\left((L_{tot} - L_1)\, P_{S_2}\, x^2 * \left(L_{tot}^2\,(6\, L_1 - 2\, x) + L_1^2\, x - L_{tot}\, L_1\,(3\, L_1 + 2\, x)\right)\right)}{12\, L_{tot}^3\, E\, I_{OP}} & 0 \le x < L_1 \\ \vdots & \vdots \\ \frac{F_{1_{rxn}}\, x^3}{6\, E\, I_{OP}} + \frac{F_1\, L_{tot}\, x^2}{2\, E\, I_{OP}} + \frac{\left(L_1^2\,\left(-P_{S_2}\right)\,(L_{tot} - x)\,\left(2\, L_{tot}^2\,(L_1 - 3x) - L_1\, x^2 + L_{tot}\, x\,(2\, L_1 + 3\, x)\right)\right)}{12 L_{\ tot}^{\ 3}\, E\, I_{OP}} & L_1 \le x \le L_{tot} \end{cases}$$

Equation B-85

Using the example design dimensions, the initial superimposed moment, shear, and displacement curves are derived in Equation B-86 through Equation B-88. These equations are displayed as plotted curves in Figure B.10.

$$M_{12_0}(x) = \begin{cases} 6.3308 + 0.3943\,x & 0 \le x < L_1 \\ \square & \square \\ 12.424 - 0.6212\,x & L_1 \le x \le L_{tot} \end{cases}$$

Equation B-86

$$V_{12_0}(x) = \begin{cases} 0.3943 & 0 \le\ x < L_1 \\ \square & \square \\ -0.6212 & L_1 \le x \le L_{tot} \end{cases}$$

Equation B-87

$$D_{12_0}(x) = \begin{cases} (0.001048 + 0.00002527\,x)x^2 & 0 \le x < L_1 \\ \square & \square \\ 0.1210 - 0.006051\,x + 0.002056\,x^2 - 0.00003428\,x^3 & L_1 \le x \le L_{tot} \end{cases}$$

Equation B-88

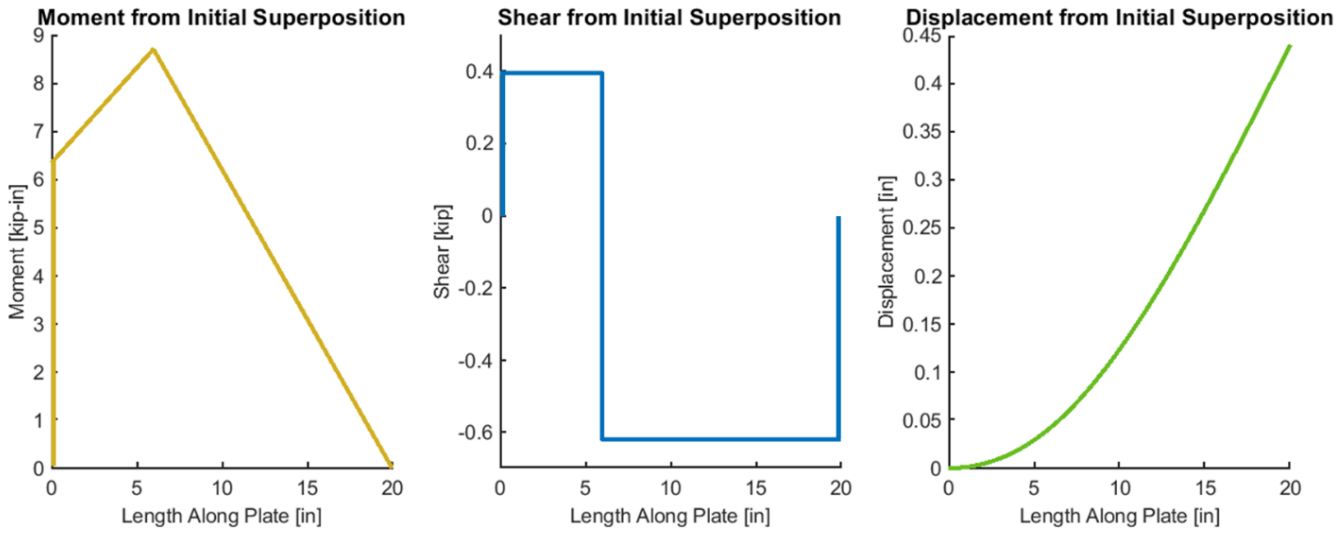

Figure B.10: Initial superposition of Beam 1 and Beam 2 produce combined moment, shear, and displacement curves.

The initial superimposed displacement curve allows for the next spring deformation guess (δ_{next}) at L_1 and can be estimated using Equation B-89. Equation B 95 provides the next spring deformation estimation for the example design dimensions.

$$\delta_{next} = D_{12_0}(L_1)$$

Equation B-89

$$\delta_{next} = D_{12_0}(6) = 0.0424\ in.$$

Equation B-90

To assess the accuracy of the next deformation guess relative to the spring's exact deformation, a tolerance is established to compare the original guess (δ_{s_2}) with the next guess (δ_{next}). If the tolerance is met, no further calculations are necessary to determine the most accurate superimposed curves. The defined tolerance for the example design is provided in Equation B-91. Alternatively, if the tolerance is not met, additional iterative calculations are required to determine a more accurate δ_{next} that complies with the tolerance criteria.

$$\left|\delta_{next} - \delta_{s_2}\right| \leq 0.000001$$

Equation B-91

If the tolerance is not met, the iterative process for the previous calculations is as follows. The iterations begin with Equation B-92, setting the next spring deformation estimate ($\delta_{s_{2_{next}}}$) equal to the superimposed displacement of Beams 1 and 2 at L_1 as derived from Equation B-89 (δ_{next}). By processing the next deformation estimate, the calculations used to determine the moment, shear, and displacement curves of Beam 2 must be repeated. The original calculations for Beam 1 remain unchanged since the spring force is neglected.

$$\delta_{s_{2_{next}}} = \delta_{next}$$

Equation B-92

The total deformation of the disc springs ($\delta_{s_{total_{next}}}$) must be calculated for the next estimated applied force on Beam 2. The $\delta_{s_{total_{next}}}$ is calculated in Equation B-93 by combining the pretensioned initial spring deformation with the $\delta_{s_{2_{next}}}$.

$$\delta_{s_{total_{next}}} = \delta_{s_0} + \delta_{s_{2_{next}}}$$

Equation B-93

Examining $\delta_{s_{total_{next}}}$ in the nonlinear force-deformation curve identifies the total force exerted by the disc springs ($P_{\delta_s}\left(\delta_{s_{total_{next}}}\right)$), which includes the pretensioned force (P_{pt}). As the pretensioned force is already factored into the instantaneous uplift curves, it is not included in estimating the spring force for Beam 2 moment, shear, and displacement curves. This produces the next estimated spring force for Beam 2 ($P_{s_{2_{next}}}$) as explained in Equation B-94.

$$P_{s_{2_{next}}} = P_{\delta_s}\left(\delta_{s_{total_{next}}}\right) - P_{pt}$$

Equation B-94

Using $P_{s_{2_{next}}}$, the next estimations for the reaction forces and reaction moment of Beam 2 are determined. The next estimation for the reaction force at the fixed end of Beam 2 ($R_{2f_{next}}$) is defined in Equation B-95. Similarly, the next estimation for the reaction force at the simply supported end of Beam 2 ($R_{2s_{next}}$) is defined in Equation B-96. The next estimation for the moment reaction at the fixed end of Beam 2 ($M_{2f_{next}}$) is defined in Equation B-97.

$$R_{2f_{next}} = \frac{-P_{S_{2_{next}}} L_2 (3\, L_{tot}^2 - L_2^2)}{2\, L_{tot}^3}$$

Equation B-95

$$R_{2s_{next}} = \frac{-P_{S_{2_{next}}} L_1^2\, (L_2 + 2\, L_{tot})}{2\, L_{tot}^3}$$

Equation B-96

$$M_{2f_{next}} = \frac{P_{S_{2_{next}}} L_1\, L_2\, (L_{tot} + L_2)}{2\, L_{tot}^2}$$

Equation B-97

By employing the next reaction estimations, the new Beam 2 moment ($M_{2_{next}}$), shear ($V_{2_{next}}$), and displacement ($D_{2_{next}}$) curves are modeled as outlined in Equation B-98 through Equation B-100, respectively.

$$M_{2_{next}}(x) = \begin{cases} M_{2_{f_{next}}} + R_{2_{f_{next}}}\, x & 0 \le x < L_1 \\ \vdots & \vdots \\ R_{2_{s_{next}}}\,(L_{tot} - x) & L_1 \le x \le L_{tot} \end{cases}$$

Equation B-98

$$V_{2_{next}}(x) = \begin{cases} R_{2_{f_{next}}} & 0 \le x < L_1 \\ \vdots & \vdots \\ R_{2_{f_{next}}} + P_{S_2} & L_1 \le x \le L_{tot} \end{cases}$$

Equation B-99

$$D_{2_{next}}(x) = \begin{cases} \dfrac{\left((L_{tot} - L_1)\, P_{S_{2_{next}}}\, x^2 * \left(L_{tot}^2\,(6\,L_1 - 2\,x) + L_1^2\, x - L_{tot}\, L_1\,(3\,L_1 + 2\,x)\right)\right)}{12\, L_{tot}^3\, E\, I_{OP}} & 0 \le x < L_1 \\ \vdots & \vdots \\ \dfrac{\left(L_1^2\,\left(-P_{S_{2_{next}}}\right)\,(L_{tot} - x)\left(2\, L_{tot}^2\,(L_1 - 3x) - L_1\, x^2 + L_{tot}\, x\,(2\, L_1 + 3\, x)\right)\right)}{12 L_{tot}^{\,3}\, E\, I_{OP}} & L_1 \le x \le L_{tot} \end{cases}$$

Equation B-100

As previously demonstrated in Equation B-83 through Equation B-85, the curves derived from Beam 2 must be superimposed with the curves from Beam 1, using the next estimations from Beam 2. This process creates the next superimposed moment ($M_{12_{next}}(x)$), shear ($V_{12_{next}}(x)$), and displacement ($D_{12_{next}}(x)$) curve estimations, defined in Equation B-101 through Equation B-103, respectively.

$$M_{12_{next}}(x) = M_1(x) + M_{2_{next}}(x) = \begin{cases} -F_{1_{rxn}}(L_{tot} - x) + M_{2_{f_{next}}} + R_{2_{f_{next}}}\, x & 0 \le x < L_1 \\ \vdots & \vdots \\ -F_{1_{rxn}}(L_{tot} - x) + R_{2_{s_{next}}}\,(L_{tot} - x) & L_1 \le x \le L_{tot} \end{cases}$$

Equation B-101

$$V_{12_{next}}(x) = V_1(x) + V_{2_{next}}(x) = \begin{cases} F_{1_{rxn}} + R_{2_{f_{next}}} & 0 \leq x < L_1 \\ \vdots & \vdots \\ F_{1_{rxn}} + R_{2_{f_{next}}} + P_{S_{2_{next}}} & L_1 \leq x \leq L_{tot} \end{cases}$$

Equation B-102

$$D_{12_{next}}(x) = D_1(x) + D_{2_{next}}(x)$$

$$= \begin{cases} \frac{F_{1_{rxn}}\, x^3}{6\, E\, I_{OP}} + \frac{F_1\, L_{tot}\, x^2}{2\, E\, I_{OP}} + \frac{\left((L_{tot} - L_1)\, P_{S_{2_{next}}}\, x^2 * \left(L_{tot}^2\,(6\, L_1 - 2\, x) + L_1^2\, x - L_{tot}\, L_1\,(3\, L_1 + 2\, x)\right)\right)}{12\, L_{tot}^3\, E\, I_{OP}} & 0 \leq x < L_1 \\ \vdots & \vdots \\ \frac{F_{1_{rxn}}\, x^3}{6\, E\, I_{OP}} + \frac{F_1\, L_{tot}\, x^2}{2\, E\, I_{OP}} + \frac{\left(L_1^2\, \left(-P_{S_{2_{next}}}\right)\, (L_{tot} - x)\left(2\, L_{tot}^2\,(L_1 - 3x) - L_1\, x^2 + L_{tot}\, x\,(2\, L_1 + 3\, x)\right)\right)}{12 L_{\ tot}^{\ 3}\, E\, I_{OP}} & L_1 \leq x \leq L_{tot} \end{cases}$$

Equation B-103

By evaluating $D_{12_{next}}(x)$ at L_1, the next superimposed plate displacement (δ_{next}) can be determined, shown in Equation B-104, and compared against the previous to determine if it meets the required tolerance defined in Equation B-105.

$$\delta_{next} = D_{12_{next}}(L_1)$$

Equation B-104

$$\left|\delta_{next} - \delta_{S_{2_{next}}}\right| \leq 0.000001$$

Equation B-105

Example Design Superposition of Beams 1 and 2 Iteration

Pretensioned Spring Deformation	δ_{s_0} =	0.0047	in.	Equation B-51

Estimated Spring Deformation

Initial Spring Deformation Guess Based on Beam 1 Displacement at Springs	δ_{s_2} =	0.0534	in.	Equation B-71
New Spring Deformation Guess Based on Combined Beam 1 and 2 Displacement Curves	δ_{next} =	0.0424	in.	Equation B-89

Tolerance Met

$$\left|\delta_{next} - \delta_{s_2}\right| \leq 0.000001$$ **FALSE** **Equation B-92**

Next Curve Calculations Based on New Spring Deformation Guess

Next Spring Deformation Guess for Beam 2	$\delta_{s_{2_{next}}}$ =	0.0424	in.	Equation B-93
Total Spring Deformation from Pretensioning and Next Guess	$\delta_{s_{total_{next}}}$ =	0.0471	in.	Equation B-94
Downward Force at Disc Springs for Beam 2	$P_{s_{2_{next}}}$ =	-0.9419	in.	Equation B-95
Reaction of Beam 2 at Fixed End for Next Force Guess	$R_{2_{f_{next}}}$ =	0.8275	kip	Equation B-96
Reaction of Beam 2 at Support End for Next Force Guess	$R_{2_{s_{next}}}$ =	0.1144	kip	Equation B-97
Moment of Beam 2 at Fixed End for Next Force Guess	$M_{2_{f_{next}}}$ =	-3.3626	kip-in	Equation B-97
Superimposed Displacement Curve for Beam 1 and 2	δ_{next} =	0.0432	in.	Equation B-104

Next Tolerance Met

$$\left|\delta_{next} - \delta_{s_{2_{next}}}\right| \leq 0.000001$$ **FALSE** **Equation B-91**

Final Curve Calculations for Allowable Spring Deformation

Downward Force at Disc Springs for Beam 2	$P_{s_{2_{next}}}$ =	**-0.9482**	**kip**	**Equation B-94**
Reaction of Beam 2 at Fixed End for Next Force Guess	$R_{2_{f_{next}}}$ =	**0.822**	**kip**	**Equation B-95**
Reaction of Beam 2 at Support End for Next Force Guess	$R_{2_{s_{next}}}$ =	**0.1152**	**kip**	**Equation B-96**
Moment of Beam 2 at Fixed End for Next Force Guess	$M_{2_{f_{next}}}$ =	**-3.385**	**kip-in**	**Equation B-97**
Superimposed Displacement Curve for Beam 1 and 2 at Disc Springs	δ_{next} =	**0.0431**	**in.**	**Equation B-104**

The following functions use the example design dimensions to compute the finalized superimposed moment ($M_{12_{next}}(x)$), shear ($V_{12_{next}}(x)$), and displacement ($D_{12_{next}}(x)$) curves once the tolerance has been satisfied.

$$M_{12_{next}}(x) = \begin{cases} 0.4978\,(20 - x) - 3.3850 + 0.8330\,x & 0 \le x < L_1 \\ \vdots & \vdots \\ 0.4978\,(20 - x) + \ 0.115203794993404\,(20 - x) & L_1 \le x \le L_2 \end{cases}$$

Equation B-106

$$V_{12_{next}}(x) = \begin{cases} -0.4978 + 0.8330 & 0 \le \ x < L_1 \\ \vdots & \vdots \\ -0.4978 + 0.8330 - 0.9482 & L_1 \le x \le L_2 \end{cases}$$

Equation B-107

$$D_{12_{next}}(x) =$$

$$\begin{cases} \dfrac{-0.4978\,x^3}{18125} + \dfrac{9.9561\,x^2}{6041.667} + \dfrac{\left(-13.2745\,x^2 * \left(400\,(36 - 2\,x) + 36x - 120\,(18 + 2\,x)\right)\right)}{290000000} & 0 \le x < L_1 \\ \vdots & \vdots \\ \dfrac{-0.4978\,x^3}{18125} + \dfrac{9.9561\,x^2}{6041.667} + \dfrac{\left(36.557\ \ (20 - x)\left(800\,(6 - 3x) - 6x^2 + 20\,x\,(12 + 3\,x)\right)\right)}{290000000} & L_1 \le x \le L_2 \end{cases}$$

Equation B-108

Due to minimal deformation changes caused by the minimal tolerance, the curves plotted from the functions above appear nearly identical to Figure B.10.

To fully understand the behavior of the OP during installation as it reaches maximum deflection, the superimposed curves, satisfying the tolerance, must be combined with the curves from instantaneous uplift at the disc springs, identified as Equation B-54 through Equation B-56, to produce Equation B-109 through Equation B-111.

$$M_{total} = M_{12_{next}} + M_{uplift}$$

Equation B-109

$$V_{total} = V_{12_{next}} + V_{uplift}$$

Equation B-110

$$D_{total} = D_{12_{next}} + D_{uplift}$$

Equation B-111

The complete functions for the total moment ($M_{total}(x)$), shear ($V_{total}(x)$), and displacement ($D_{total}(x)$), using the design variables, are displayed below in Equation B-112 through Equation B-114 respectively.

$$M_{total}(x) = \begin{cases} F_{up}\, L_2 \; - \; F_{1_{rxn}}(L_{tot} - x) + \; M_{2_{f_{next}}} + R_{2_{f_{next}}}\, x & 0 \le x < L_1 \\ \vdots & \vdots \\ \dfrac{F_{up}\, L_2\, x}{L_1 - L_{tot}} - \dfrac{F_{up}\, L_2\, L_1}{L_1 - L_{tot}} + F_{up}\, L_2 - \; F_{1_{rxn}}(L_{tot} - x) + \; R_{2_{s_{next}}}\, (L_{tot} - x) & L_1 \le x \le L_2 \end{cases}$$

Equation B-112

$$V_{total}(x) = \begin{cases} F_{1_{rxn}} + R_{2_{f_{next}}} & 0 \le x < L_1 \\ \vdots & \vdots \\ F_{1_{rxn}} + \; R_{2_{f_{next}}} + P_{S_{2_{next}}} - F_{up} & L_1 \le x \le L_2 \end{cases}$$

Equation B-113

$$D_{total}(x) = \begin{cases} \dfrac{F_{1_{rxn}}\, x^3}{6\, E\, I_{OP}} + \dfrac{F_1\, L_{tot}\, x^2}{2\, E\, I_{OP}} + \dfrac{\left((L_{tot} - L_1)\, P_{S_{2_{next}}}\, x^2 * \left(L_{tot}^2\, (6\, L_1 - 2\, x) + L_1^2\, x - L_{tot}\, L_1\, (3\, L_1 + 2\, x)\right)\right)}{12\, L_{tot}^3\, E\, I_{OP}} & 0 \le x < L_1 \\ \vdots & \vdots \\ F_{up}\, (x - L_1)^2\, \dfrac{3\, L_2 - (x - L_1)}{6\, E\, I_{OP}} + \dfrac{F_{1_{rxn}}\, x^3}{6\, E\, I_{OP}} + \dfrac{F_1\, L_{tot}\, x^2}{2\, E\, I_{OP}} + \dfrac{\left(L_1^2\, \left(-P_{S_{2_{next}}}\right)\, (L_{tot} - x)\, \left(2\, L_{tot}^2\, (L_1 - 3x) - L_1\, x^2 + L_{tot}\, x\, (2\, L_1 + 3\, x)\right)\right)}{12 L_{tot}^{\,3}\, E\, I_{OP}} & L_1 \le x \le L_2 \end{cases}$$

Equation B-114

The example design dimensions of the OP produce total moment, shear, and displacement curves as depicted below in Figure B.11. These curves are defined by functions $M_{total}(x)$ in Equation B-115, $V_{total}(x)$ in Equation B-116, and $D_{total}(x)$ in Equation B-117.

$$M_{total}(x) = \begin{cases} 9.371 + 0.3352\,x & 0 \le x < L_1 \\ \vdots & \vdots \\ 16.206 - 0.8103\,x & L_1 \le x \le L_2 \end{cases}$$

Equation B-115

$$V_{total}(x) = \begin{cases} 0.3352 & 0 \le x < L_1 \\ \vdots & \vdots \\ -0.813 & L_1 \le x \le L_2 \end{cases}$$

Equation B-116

$$D_{total}(x) = \begin{cases} (0.0010872 + 0.00001849\,x)x^2 & 0 \le x < L_1 \\ \vdots & \vdots \\ 0.03037 - 0.01240\,x + 0.002691x^2 - 0.00004486\,x^3 & L_1 \le x \le L_2 \end{cases}$$

Equation B-117

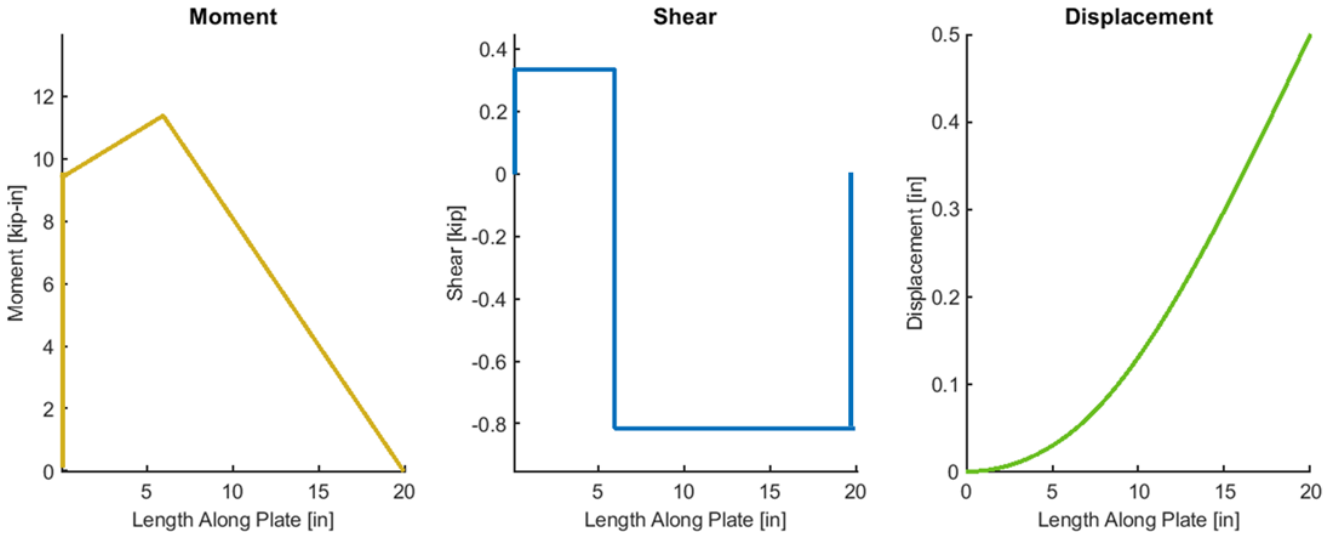

Figure B.11: Finalized moment, shear, and displacement curves of the Outer Plate when it reaches maximum deflection during installation.

B.6.4.1 Elastic Limit Check

By utilizing the final moment function for the OP from Equation B-112, the maximum moment experienced by the plate can be calculated and compared against the lowest moment capacity of the plate. The maximum moment demand, as identified in Equation B-112, occurs at L_1, as shown in Equation B-118.

$$M_{demand} = \max(M_{total}) = M_{total}(L_1)$$

Equation B-118

Comparatively, the minimum moment capacity in the plate also occurs at L_1 due to stress concentrations from the upper bolt holes. The allowable bending moment from the minimum capacity is calculated in Equation B-120, using the centroid around the bending axis, and solved in Equation B-119.

$$c = \frac{t_{OP}}{2}$$

Equation B-119

$$M_{allow} = \frac{F_y \left(I_{OP} - 2\frac{d_h\, t_{OP}^3}{12} \right)}{c}$$

Equation B-120

The moment demand for the OP during column installation must not exceed the moment capacity at the disc springs, as defined in Equation B-121.

$$M_{demand} \leq M_{allow}$$

Equation B-121

Example Design Outer Plate Elastic Limit Check

Outer Plate Properties

Nominal Yield Strength of the OP	$F_{y_{OP}}$ =	50	ksi	
Thickness of the OP	t_{OP} =	0.5	in.	
Bolt Hole Diameter of the Outer Plate	d_h =	1.125	in.	

Moment of Inertia

Moment of Inertia for the OP	I_{OP} =	0.104	$in.^4$	Equation B-49

Minimum Allowable Flexural Moment of the Outer Plate

OP Centroid	c =	0.25	in.	Equation B-119
Allowable Moment at Bolt Holes	M_{allow} =	16.146	kip-in.	Equation B-120

Moment Demand

Maximum Moment Demand Disc Springs	M_{demand} =	11.382	kip-in.	Equation B-118

Elastic Limit Check

$\boldsymbol{M_{demand} \leq M_{allow}}$	**TRUE**	**Equation B-121**

B.7 Snapping Friction Check

During assembly, the weight of the Upper Column (W) must be sufficient to deform the two Outer Plates attached to the Lower Column. The total weight of the column is determined by the column's nominal weight per unit length (w_{col}) and the total length of the column (L_{col}), as shown in Equation B-122.

$$W = L_{col}\, w_{col}$$

Equation B-122

This weight (W) must exceed the shear force at the end of the plates during maximum flexure ($V_{total}(L_{tot})$) and a friction coefficient (μ), as shown in Equation B-123.

$$W \geq 2\, \mu\, V_{total}(L_{tot})$$

Equation B-123

This friction coefficient (μ) is defined in Equation B-124.

$$\mu = 0.3$$

Equation B-124

Example Design Snapping Friction Check

Column Properties

Upper Column Nominal Weight (W12x170)	w_{col} =	0.17	kip/ft.	
Column Length	L_{col} =	30	ft.	
Column Weight	W =	5.1	kip	Equation B-122

Friction

Friction Coefficient	μ =	0.3		Equation B-124

Outer Plate Shear

Total Shear at the End of the OP during Maximum Flexure	$V_{total}(L_{tot})$ =	0.813	kip	

Friction Verification

$\boldsymbol{W \geq 2\,\mu\,V_{total}(L_{tot})}$	**TRUE**	Equation B-123

B.8 Limit States for Flexural Capacity

While there are no operational moment demands on the column splice, the design strengths of the column splice components are required to be compared against the OSHA moment demands. The following sections outline the limit state for all variations of flexural capacity in the SnapLocX connection. This includes the compression component of the moment moving from the Upper Column to the Lower Column through the column flange bearing and the tension component transferring from the Upper Column to the Lower Column through the SnapLocX Connection components. The order of the limit states in Section B.8 follows the tensile force from bending as it transitions from the Upper Column to the Lower Column through the design components, finishing with compressive flange bearing.

B.8.1 Lower Lock Plate to Upper Column Flange Fillet Weld

The first fillet weld analyzed connects the Lower Lock Plate (*LLP*) to the Upper Column. For fillet welds with longitudinal axes parallel to the direction of loading, depicted in Figure B.12, the weld strength is derived from Equation J2-4 in *the Steel Specification*.

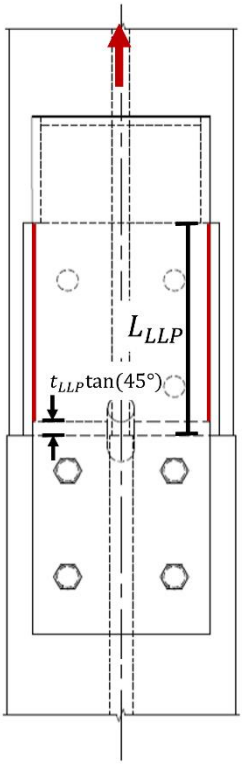

Figure B.12: Weld location for design strength of the LLP to the Upper Column weld.

Depending on the difference in Upper Column and Lower Column depth, a Shim Plate (SP) may need to first be welded to the Upper Column. The process used to calculate design strength for fillet weld is identical between the fillet weld connecting the SP and the Upper Column, the fillet weld connecting the LLP to the SP, or the fillet weld connecting the LLP to the Upper Column. The only alteration between the three variations is the length used for the weld area calculation. Of the three weld scenarios, the welds involving the LLP have the shortest weld length, thereby controlling the fillet weld design capacity between the LLP, SP, and Upper Column. For simplicity in design analysis, only the controlling weld design between the LLP, SP, and Upper Column is analyzed. The minimum design strength for fillet welds ($\phi\ R_n$) is determined in Equation B-125, using the nominal weld strength (F_{nw}), and effective area of the weld (A_{we}).

$$\phi R_n = \phi F_{nw} A_{we}$$

Equation B-125

As there is no angle between the line of action for required force and the weld longitudinal axis, the force calculation from Equation J2-5 in *the Steel Specification* to solve for F_{nw} simplifies to Equation B-126, using a factored filler metal weld classification strength (F_{EXX}).

$$F_{nw} = 0.6F_{EXX}$$

Equation B-126

The weld area (A_{we}), described in Equation B-127, is determined by calculating the weld thickness through the "throat" of the weld, which is achieved by multiplying the predetermined thickness of the weld (t_{weld}) by $\sqrt{2}/2$ or 0.707. Subsequently, the throat of the weld is then multiplied by the weld length (L_{weld}) and number of welds (n_{weld}) in the direction of interest.

$$A_{we} = n_{weld}\ 0.707\ t_{weld}\ L_{weld}$$

Equation B-127

The length of the weld for the LLP excludes the bevel length and is determined using Equation B-128, which involves the difference between the entire length of the LLP (L_{LLP}) and the length of the bevel in the direction of L_{LLP} from the thickness of the LLP (t_{LLP}).

$$L_{weld} = L_{LLP} - t_{LLP} \tan(45\ °)$$

Equation B-128

Design Strength of the Lower Lock Plate to Upper Column Weld for Flexural Capacity

Weld Metal Properties

Resistance Factor of Available Weld Strength	ϕ =	0.75		
Filler Metal Classification Strength	F_{EXX} =	70	ksi	

Lower Lock Plate Properties

Length of the LLP	L_{LLP} =	12	in.	
Thickness of the LLP	t_{LLP} =	0.75	in.	

Weld Dimensions

Design Weld Thickness	t_{weld} =	5/16	in.	
Length of the Weld on the LLP	L_{weld} =	11.25	in.	Equation B-128
Number of Welds on LLP Resisting Bending	n_{weld} =	2	welds	
Nominal Weld Stress	F_{nw} =	42	ksi	Equation B-126
Weld Area	A_{we} =	4.97	in.^{2}	Equation B-127
Design Strength of LLP to Upper Column Weld	$\boldsymbol{\phi R_n}$ =	**156.59**	**kip**	**Equation B-125**

B.8.2 Lower Lock Plate to Upper Lock Plate Flat Face Bearing

The design strength for flat face bearing ($\phi\ R_n$) is calculated using Equation B-129, which is drawn from Equation J7-1 in *the Steel Specification* for local compressive yielding of finished surface bearing strength. The variables used to solve for the design strength include the minimum yield stress (F_y) of the bearing plates, Equation B-130, and the projected bearing area (A_{pb}) of the ULP and LLP, Equation B-131.

$$\phi R_n = \phi 1.8\ F_y\ A_{pb}$$

Equation B-129

The current SnapLocX Connection design incorporates plates made of the same material. However, in scenarios with plates of different metal classifications, the minimum yield stress between the two materials is established as F_y and is defined by Equation B-130.

$$F_y = \min(F_{y_{LLP}}, F_{y_{ULP}})$$

Equation B-130

The exact A_{pb} of the ULP and the LLP is calculated using the smaller of the two plate widths, designated as the width of the ULP (b_{ULP}). The bearing thickness is determined using a difference in the depth between the ULP and LLP. The total Upper Column depth (d_{UC}) from the centerline includes the thickness of the Shim Plate (t_{SP}) and thickness of the LLP (t_{LLP}), providing the total depth from the centerline to the edge of the plates associated with the Upper Column. The depth of the Lower Column (d_{LC}) from the centerline, including the thickness of the Inner Plate (t_{IP}) and removing the thickness of the ULP (t_{ULP},) produces the distance from the inside of the ULP to the Lower Column centerline. Using the upper and lower difference, with b_{ULP}, $A_{pb}$is calculated in Equation B-131.

$$A_{pb} = b_{ULP}\left(\left(\frac{d_{UC}}{2} + t_{SP} + t_{LLP}\right) - \left(\frac{d_{LC}}{2} + t_{IP} - t_{ULP}\right)\right)$$

Equation B-131

A visualization of the location of A_{pb} is provided in Figure B.13.

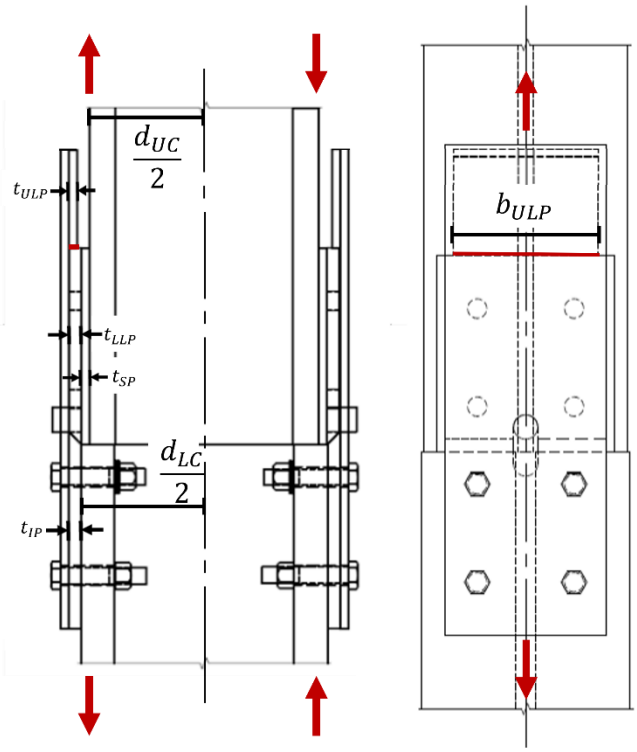

Figure B.13: The locations for the Lower Lock Plate and Upper Lock Plate bearing are denoted in red.

Design Strength of Lower Lock Plate to Upper Lock Plate Flat Face Bearing

Resistance Factor for Bearing Strength	ϕ =	0.75		
Nominal Stresses				
Nominal Stress of the Upper Lock Plate	$F_{y_{ULP}}$ =	50	ksi	
Nominal Stress of the Lower Lock Plate	$F_{y_{LLP}}$ =	50	ksi	
Bearing Dimensions for Area				
Width of the Upper Lock Plate	b_{ULP} =	9	in.	
Depth of the Upper Column	d_{UC} =	14	in.	
Depth of the Lower Column	d_{LC} =	15	in.	
Thickness of the Shim Plate	t_{SP} =	0.5	in.	
Thickness of the Lower Lock Plate	t_{LLP} =	0.75	in.	
Thickness of the Inner Plate	t_{IP} =	0.75	in.	
Thickness of the Upper Lock Plate	t_{ULP} =	0.5	in.	
Projected Bearing Area of the ULP on the LLP	A_{pb} =	4.5	in.^{2}	Equation B-131
Minimum Yield Stress	F_y =	50	ksi	Equation B-130
Design Strength of ULP to LLP Bearing	$\boldsymbol{\phi R_n}$ =	**303.75**	**kip**	**Equation B-129**

B.8.3 Upper Lock Plate to Outer Plate Fillet Weld

Section B.8.3 follows a similar process to calculate the design strength weld strength ($\phi\ R_n$), using Equations J2-4 and J2-5 from *the Steel Specification*, as explained in B.8.1. The significant difference in determining the design strength for a weld parallel to the required force is a change in effective weld area (A_{we}) due to the shorter length of the ULP and consequently resulting in a shorter length of the ULP weld (L_{weld}) and lower design strength.

$$\phi R_n = \phi F_{nw} A_{we}$$

Equation B-132

$$F_{nw} = 0.6 F_{EXX}$$

Equation B-133

$$A_{we} = n_{weld} 0.707\ t_{weld}\ L_{weld}$$

Equation B-134

The length of the weld on the ULP is calculated using Equation B-135 from the length of the ULP (L_{ULP}) and thickness of the ULP (t_{ULP}). The location of the welds is provided in Figure B.14.

$$L_{weld} = L_{ULP} - t_{ULP} \tan(45\ °)$$

Equation B-135

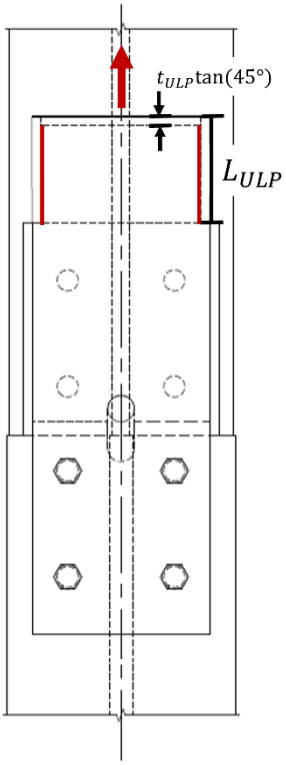

Figure B.14: Location of fillet weld for the ULP to the OP denoted in red.

Design Strength of the Upper Lock Plate to Outer Plate Weld

Weld Metal Properties

Resistance Factor of Available Weld Strength	ϕ =	0.75		
Filler Metal Classification Strength	F_{EXX} =	70	ksi	

Upper Lock Plate Properties

Length of the Upper Lock Plate	L_{ULP} =	6	in.	
Thickness of the Upper Lock Plate	t_{ULP} =	1/2	in.	

Weld Dimensions

Design Weld Thickness	t_{weld} =	5/16	in.	
Length of the Weld on the LLP	L_{weld} =	5 1/2	in.	Equation B-135
Number of Welds on LLP Resisting Bending	n_{weld} =	2	welds	
Nominal Weld Stress	F_{nw} =	42	ksi	Equation B-133
Weld Area	A_{we} =	2.65	in.^{2}	Equation B-134
Design Strength for ULP to OP Weld Strength	$\boldsymbol{\phi R_n}$ =	**76.55**	**kip**	**Equation B-132**

B.8.4 Outer Plate Limit States

To establish the overall design strength of the Outer Plate (OP) the various limit states involving the OP are considered. All limit states involving the OP are encompassed in Section B.8.4.

B.8.4.1 Tearout Strength at the Bolt Holes

Bolt tearout analyzes the shearing of the material of the OP surrounding the bolt hole, called out in Figure B.15. The design tearout strength ($\phi\ R_n$) is determined using Equation J3-6 from *the Steel Specification* for a bolted connection with standardized holes parallel to the direction of force, seen in Equation B-136.

$$\phi R_n = \phi\ 1.5\ F_{u_{OP}}\ l_c\ t_{OP}$$

Equation B-136

The ultimate strength of the connected material ($F_{u_{OP}}$) and connection thickness (t_{OP}) are used to determine design strength, along with the clear distance in the direction of the force (l_c). The l_c represents the distance between the edges of the bolt holes and the edge of the material in the direction of the applied force. The total l_c is determined by using the total of bolt columns in the direction of the force (n_{col}), as seen in Equation B-137 and illustrated in Figure B.15.

$$l_c = n_{col}(\ l_{c_{up}} +\ l_{c_{low}})$$

Equation B-137

The upper clear distance ($l_{c_{up}}$) is calculated as the distance between the upper and lower bolt rows on the OP, provided in Equation B-138. This approach uses the distance from the center of the upper bolt holes to the center of the lower bolt holes (L_1), removing included bolt-hole diameters (d_h).

$$l_{c_{up}} = \mathrm{L}_1 - d_h$$

Equation B-138

The lower clear distance ($l_{c_{low}}$) is calculated as the distance between the lower bolt row to the lower end of the OP, as seen in Equation B-139. This approach uses the distance from the center

of the lower bolt row to the end of the OP (b_{END}), removing included bolt hole diameters (d_h) in b_{END}.

$$l_{c_{low}} = b_{END} - \frac{d_h}{2}$$

Equation B-139

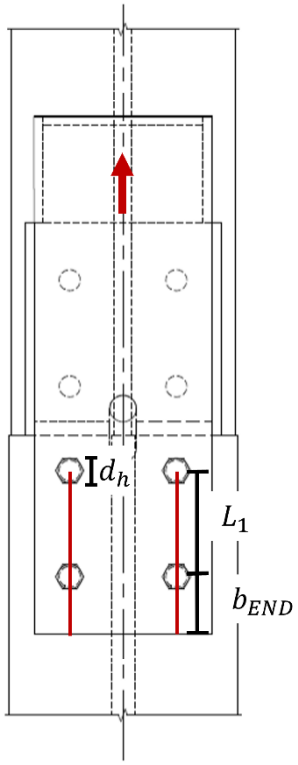

Figure B.15: Location on the OP analyzed for bolt tearout.

Design Strength of Outer Plate Bolt Tearout

Resistance Factor for Bolt Tearout	ϕ =	0.75		
Bolt Properties				
Number of Bolt Columns	n_{col} =	2	columns	
Bolt Hole Diameter	d_h =	1.125	in.	
Outer Plate Properties				
Ultimate Strength of the Outer Plate	$F_{u_{OP}}$ =	65	ksi	
Length of the Upper Lock Plate	L_{ULP} =	6.75	in.	
Thickness of the Outer Plate	t_{OP} =	0.5	in.	
Distance Between the Lower Bolt Row and Upper Bolt Row	L_1 =	6	in.	
Center of Lower Bolt to Lower End of OP	b_{END} =	3.25	in.	
Clear Distances				
Clear Distance from Upper Bolts to Upper Edge	$l_{c_{up}}$ =	4.875	in.	Equation B-138
Clear Distance from Upper to Lower Bolts	$l_{c_{low}}$ =	2.6875	in.	Equation B-139
Total Clear Distance of the Outer Plate	l_c =	15.125	in.	Equation B-137
Design Strength for OP Bolt Tearout	$\boldsymbol{\phi R_n}$ =	**553.008**	**kip**	**Equation B-136**

B.8.4.2 Tensile Yielding

The tensile yield design strength of the OP ($\phi\ P_n$) is calculated using Equation D2-1 from *the Steel Specification* as designed for members in tension, rewritten in Equation B-140. The variables used for $\phi\ P_n$ include the yield strength of the OP ($F_{y_{OP}}$) and the gross area of the OP cross-section (A_g).

$$\phi P_n = \phi\ F_{y_{OP}} A_g$$

Equation B-140

The gross area (A_g) is derived in Equation B-141 and utilizes the gross thickness (t_{OP}) and width (b_{OP}) dimensions of the OP. The dimensions of tensile yielding on the OP can be seen in Figure B.16.

$$A_g = t_{OP} b_{OP}$$

Equation B-141

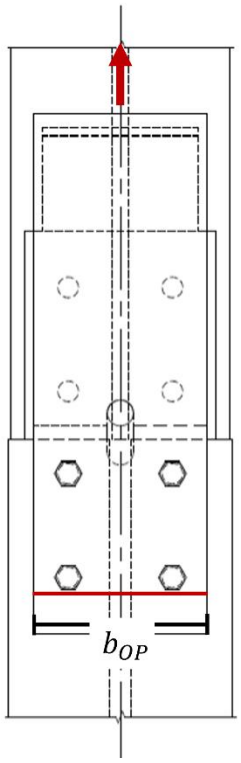

Figure B.16: The cross-section of the OP considered for tensile yielding.

Design Strength of Outer Plate Tensile Yielding

Resistance Factor for Tensile Yielding	ϕ =	0.9		
Outer Plate Properties				
Yield Stress of the OP	$F_{y_{OP}}$ =	50	ksi	
Thickness of the OP	t_{OP} =	0.5	in.	
Width of the OP	b_{OP} =	10	in.	
Gross Area of the Outer Plate	A_g =	5	in.^{2}	Equation B-141
Design Strength for OP Tensile Yielding	$\boldsymbol{\phi P_n}$ =	**225**	**kip**	**Equation B-140**

B.8.4.3 Tensile Rupture

Similar to tensile yielding, tensile rupture considers the OP cross-sectional failure perpendicular to the direction of applied force, as shown in Figure B.17. Derived from Equation D2-2 in *the Steel Specification*, the design strength of tensile rupture ($\phi\ P_n$) considers the bolt holes (d_h) in determining the cross-section for the net effective area of the OP (A_e) and uses the ultimate stress of the OP (F_u), seen in Equation B-142.

$$\phi P_n = \phi\ F_u A_e$$

Equation B-142

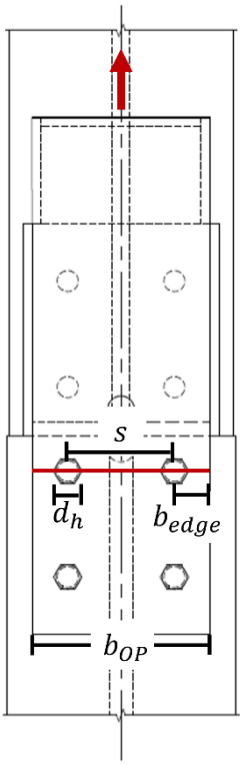

Figure B.17: Net area cross-section identified in tensile rupture.

The effective net area of the OP in tension (A_e), Equation B-143, is calculated in accordance with Equation D3-1 from *the Steel Specification*. The shear lag factor (U) is defined in Table D3.1 from *the Steel Specification*. The shear lag factor considered for the SnapLocX Connection is identified as Case 1 from Table D3.1.

$$A_e = U\ A_n$$

Equation B-143

The calculation for A_e uses the net area of the OP (A_n), as solved for in Equation B-144 with the previously determined gross area (A_g) from Equation B-141 and bolt hole diameter (d_h), accounting for 1/16 in. as damage allowance and 1/16 in. for machining.

$$A_n = A_g - 2\left[d_h + \frac{1}{16} + \frac{1}{16}\right]$$

Equation B-144

Design Strength of Outer Plate Tensile Rupture

Resistance Factor for Tensile Yielding	ϕ =	0.75		
Outer Plate Properties				
Ultimate Stress of the OP	$F_{u_{OP}}$ =	65	ksi	
Thickness of the OP	t_{OP} =	0.5	in.	
Width of the OP	b_{OP} =	10	in.	
Bolt Hole Diameter	d_h =	1.125	in.	
Shear Lag Factor	U =	1		
Area of the OP				
Gross Area of the Outer Plate	A_g =	5	in.^{2}	Equation B-141
Net Area of the OP	A_n =	2.5	in.^{2}	Equation B-144
Effective Net Area of the OP	A_e =	2.5	in.^{2}	Equation B-143
Design Strength for OP Tensile Yielding	$\boldsymbol{\phi P_n}$ =	**121.875**	**kip**	**Equation B-142**

B.8.4.4 Block Shear

Block shear analyzes the main part of the connecting member torn away, considering both tension and shear. Guidelines for evaluating block shear are identified in Section J4.3 and Equation J4-5 in *the Steel Specification.*

In block shear analysis, there are often multiple failure paths to consider. This section examines the two failure paths for the example design OP. Of the two computed design strengths ($\phi\ R_n$) in Equation B-145, the lesser of the two will control the design strength capacity of block shear for the given mode.

Considered variables for solving for block shear design strength include the ultimate stress of the OP (F_u), the yield stress of the OP (F_y), the net area of the OP subject to shear (A_{nv}), the net area of the OP subject to tension (A_{nt}), and the gross area of the OP in shear (A_{gv}). All areas are through the thickness of the OP (t_{OP}). Additionally, a tension stress factor (U_{bs}) is defined as uniform tension stress, equal to 1, for the example design, as opposed to nonuniform tension stress equal to 0.5.

B.8.4.4 (i) Mode 1

The design stress for block shear in Mode 1 is defined in Equation B-145, broken into separate (A) and (B) sections for evaluation in the example calculations. A visualization of Mode 1 block shear can be seen in Figure B.18. Failure for Mode 1 involves three bolts and occurs on one edge and the lower end of the OP.

$$\phi R_n = \phi 0.6 F_u A_{nv} + U_{bs} F_u A_{nt} \leq \phi 0.6 F_y A_{gv} + U_{bs} F_u A_{nt}$$

Equation B-145

$$\phi R_{n_A} = \phi 0.6 F_u A_{nv} + U_{bs} F_u A_{nt}$$

Equation B-145(A)

$$\phi R_{n_B} = \phi 0.6 F_y A_{gv} + U_{bs} F_u A_{nt}$$

Equation B-145(B)

The net area in shear (A_{nv}) for Mode 1, shown in Equation B-146, considers the vertical distance from the center of the upper bolt row to the center of the lower bolt row (L_1) and from the center

of the lower bolt row to the lower end (b_{end}), removing any area including the bolt hole diameter (d_h).

$$A_{nv} = t_{OP}\left(L_1 - d_h + b_{end} - \frac{d_h}{2}\right)$$

Equation B-146

The net area in tension (A_{nt}) for Mode 1, shown in Equation B-147, considers the horizontal distance of one bolt column to the far edge of the OP through the bolt spacing from the center of one column to the center of the other (s) and edge distance from the center of the bolt column to the edge of the OP (b_{edge}), removing any area including d_h.

$$A_{nt} = t_{OP}\left(s + b_{edge} - 1\frac{1}{2}\ d_h\right)$$

Equation B-147

The gross area in shear (A_{gv}) for Mode 1, shown in Equation B-148, considers the vertical distance calculated in Equation B-146, with the inclusion of d_h.

$$A_{gv} = t_{OP}\left(L_1 + b_{end}\right)$$

Equation B-148

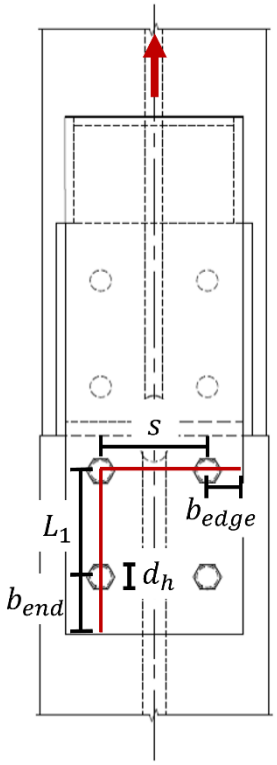

Figure B.18: Mode 1 for block shear design strength of the OP.

Design Strength of Outer Plate Block Shear Mode 1

Resistance Factor for Block Shear	ϕ =	0.75		
Outer Plate Properties				
Ultimate Stress of the OP	$F_{u_{OP}}$ =	65	ksi	
Yield Stress of the OP	$F_{y_{OP}}$ =	50	ksi	
Thickness of the OP	t_{OP} =	0.5	in.	
Bolt Hole to OP Lower End	b_{END} =	3.25	in.	
Bolt Hole to OP Edge	b_{EDGE}=	1.5	in.	
Bolt Hole Diameter	b_h =	1.125	in.	
Bolt Spacing Between Columns	s =	7	in.	
Distance Between the Lower Bolt Row and Upper Bolt Row	L_1 =	6	in.	
Uniform Tension Stress	U_{bs} =	1		
Area of the OP				
Gross Area of the OP Subject to Shear	A_{gv} =	4.625	in.^{2}	Equation B-148
Net Area of the OP Subject to Shear	A_{nv} =	3.78125	in.^{2}	Equation B-146
Net Area of the OP Subject to Tension	A_{nt} =	4.25	in.^{2}	Equation B-147
Design Strength for Block Shear (a)	ϕR_{n_A} =	386.852	kip	Equation B-145(A)
Design Strength for Block Shear (b)	ϕR_{n_B} =	380.3125	kip	Equation B-145(B)
Design Strength for Block Shear	$\boldsymbol{\phi R_n}$ =	**380.3125**	**kip**	**Equation B-145**

B.8.4.4 (ii) Mode 2

Design stress for block shear in Mode 2 is defined in Equation B-145, broken into separate (A) and (B) sections for evaluation in the example calculations. A visualization of Mode 2 block shear can be seen in Figure B.19. Failure for Mode 2 involves all bolts in the bolt group and occurs on the lower end of the OP.

$$\phi R_n = \phi 0.6 F_u A_{nv} + U_{bs} F_u A_{nt} \leq \phi 0.6 F_y A_{gv} + U_{bs} F_u A_{nt}$$

Equation B-145

$$\phi R_{n_A} = \phi 0.6 F_u A_{nv} + U_{bs} F_u A_{nt}$$

Equation B-145(A)

$$\phi R_{n_B} = \phi 0.6 F_y A_{gv} + U_{bs} F_u A_{nt}$$

Equation B-145(B)

The net area in shear (A_{nv}) for Mode 2, shown in Equation B-149, considers the vertical distance between the bolt rows (L_1) and the lower bolt row to the lower OP end (b_{end}), excluding bolt hole diameters (d_h).

$$A_{nv} = n_{col}\, t_{OP}\, (L_1 - d_h + b_{end} - \frac{d_h}{2})$$

Equation B-149

The net area in tension (A_{nt}) for Mode 2, shown in Equation B-150, considers the horizontal distance from one bolt column to the other (s), excluding d_h.

$$A_{nt} = t_{OP}\, (s - b_h)$$

Equation B-150

The gross area in shear (A_{gv}) for Mode 2, shown in Equation B-151, considers the horizontal distance calculated in Equation B-149 with the inclusion of d_h.

$$A_{gv} = n_{col}\, t_{OP}\, (L_1 + b_{end})$$

Equation B-151

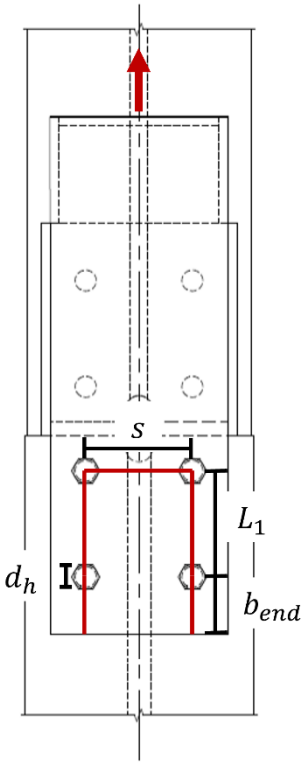

Figure B.19: Mode 2 for block shear design strength of the OP.

Design Strength of Outer Plate Block Shear Mode 2

Resistance Factor for Block Shear	$\phi =$	0.75		
Outer Plate Properties				
Ultimate Stress of the OP	$F_{u_{OP}} =$	65	ksi	
Yield Stress of the OP	$F_{y_{OP}} =$	50	ksi	
Thickness of the OP	$t_{OP} =$	0.5	in.	
Bolt Hole to OP Lower End	$b_{end} =$	3.25	in.	
Bolt Hole Diameter	$d_h =$	1.125	in.	
Bolt Spacing Between Columns	$s =$	7	in.	
Number of Bolt Columns	$n_{col} =$	2	columns	
Distance Between the Lower Bolt Row and Upper Bolt Row	$L_1 =$	6	in.	
Uniform Tension Stress	$U_{bs} =$	1		
Area of the OP				
Gross Area of the OP Subject to Shear	$A_{gv} =$	4.625	in.^{2}	Equation B-151
Net Area of the OP Subject to Shear	$A_{nv} =$	7.5625	in.^{2}	Equation B-149
Net Area of the OP Subject to Tension	$A_{nt} =$	5.875	in.^{2}	Equation B-150
Design Strength for Block Shear (a)	$\phi R_{n_A} =$	603.08	kip	Equation B-145(A)
Design Strength for Block Shear (b)	$\phi R_{n_B} =$	485.938	kip	Equation B-145(B)
Design Strength for Block Shear	$\boldsymbol{\phi R_n} =$	**485.938**	**kip**	**Equation B-145**

B.8.5 Bolt Failure

Bolt failure of the SnapLocX Connection is evaluated in the following section under bolt bearing design strength and bolt shear design strength, connecting the OP to the Lower Column.

B.8.5.1 Bolt Bearing of the Outer Plate to the Lower Column Flange

The bolt bearing design strength ($\phi\ R_n$) of the OP observes deformation at the bolt holes during service load, considering Equation J3-6a from *the Steel Specification*, using standard holes independent of the direction of loading.

To solve for $\phi\ R_n$ in Equation B-152, the number of bolts in a bolt group (n_b), the bolt diameter (d_b), the thickness of the OP (t_{OP}), and the ultimate stress of the OP ($F_{u_{OP}}$) are required.

$$\phi R_n = n_b\ \phi\ 2.4\ d_b\ t_{OP}\ F_{u_{OP}}$$

Equation B-152

Design Strength of Bolt Bearing of the Outer Plate to the Lower Column Flange

Resistance Factor for Bolt Bearing	ϕ =	0.75		
Bolt Properties				
Bolt Diameter	d_b =	1	in.	
Number of Bolts in a Grouping	n_b =	4	bolts	
Outer Plate Properties				
Ultimate Stress of the Outer Plate	$F_{u_{OP}}$ =	65	ksi	
Thickness of the Outer Plate	t_{OP} =	0.5	in.	
Design Strength for Bolt Bearing	$\boldsymbol{\phi R_n}$ =	**234**	**kip**	**Equation B-152**

B.8.5.2 Bolt Shear

The second consideration for bolt failure, bolt shear, can be determined using Equation J3-1 from *the Steel Specification.* Bolt shear is assessed under any tension experienced from the prying action of the applied force leading to the deformation of the connected parts.

The design strength for bolt shear ($\phi\ R_n$), as outlined in Equation B-153, takes into account the number of bolts in a bolt grouping (n_b), the nominal area of the body of the bolt (A_b), and the nominal stress of the bolt (F_n) as nominal tensile stress (F_{nt}) or shear stress (F_{nv}) per Table J3.2 in *the Steel Specification*.

$$\phi R_n = n_b\ \phi F_n\ A_b$$

Equation B-153

To consider bolt shear, F_n is determined for bolts in shear, referencing F_{nv} as of nominal shear in bearing-type connections. For the SnapLocX Connection, Group A (A325) bolts are used threads included in shear planes. From Table J3.2 in *the Steel Specification*, $F_{nv} = 54$ ksi.

$$F_n = F_{nv}$$

Equation B-154

The area of the bolt (A_b) considers the diameter of the bolt (d_b), solved for in Equation B-155.

$$A_b = \frac{d_b^2}{4}\pi$$

Equation B-155

Design Strength of Bolt Shear

Resistance Factor for Bolt Shear	$\phi =$	0.75		
Nominal Bolt Shear Stress	$F_{nv} =$	54	ksi	Equation B-154
Bolt Properties				
Number of Bolts in Grouping	$n_b =$	4	bolts	
Bolt Diameter	$d_b =$	1	in.	
Nominal Unthreaded Area of Bolt	$A_b =$	0.785	$in.^2$	Equation B-155
Design Strength for Bolt Shear	$\boldsymbol{\phi R_n} =$	**127.23**	**kip**	**Equation B-153**

B.8.6 Flange Bearing

The design strength for bearing ($\phi\ R_n$), shown in Equation B-156, evaluates flange capacity using Equation J7-1 in *the Steel Specification* for bearing of finished surfaces in compressive yielding. As the flexural limit states evaluate tension in the column connection components, compression is evaluated in the column flanges using the projected flange bearing area (A_{pb}) and minimum yield stress of the two columns (F_y).

$$\phi R_n = \phi\ 1.8\ F_y\ A_{pb}$$

Equation B-156

The bearing area in Equation B-157 requires the minimum width of the Upper and Lower Columns (b_{UC} and b_{LC}, respectively) and the bearing thickness of the column flanges (t_{f_b}).

$$A_{pb} = t_{f_b} MIN(b_{UC}, b_{LC})$$

Equation B-157

The bearing thickness is determined in Equation B-158 with the difference of the depth of the Upper Column (d_{UC}), depth of the Lower Column (d_{LC}), and thickness of the Lower Column flange ($t_{f_{LC}}$), demonstrated in Figure B.20.

$$t_{f_b} = \frac{d_{UC}}{2} - (\frac{d_{LC}}{2} - t_{f_{LC}})$$

Equation B-158

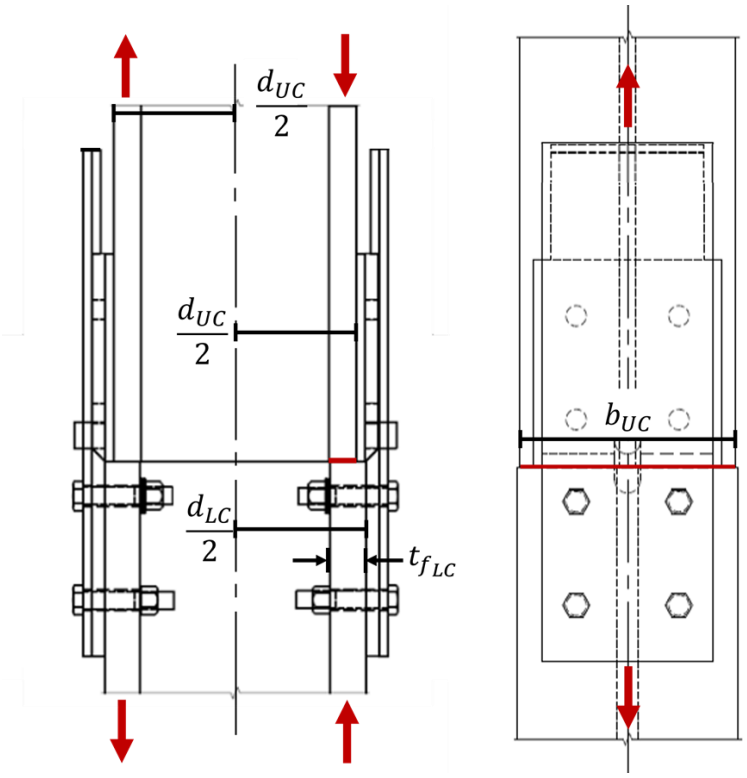

Figure B.20: Location of Upper Column and Lower Column flange bearing design strength from an applied moment.

Design Strength of Flange Bearing

Resistance Factor for Flange Bearing	ϕ =	0.75		
Column Properties				
Nominal Yield Stress of Columns	F_y =	50	ksi	
Upper Column Depth	d_{UC} =	14	in.	
Lower Column Depth	d_{LC} =	15	in.	
Upper Column Flange Thickness	$t_{f_{UC}}$ =	1 9/16	in.	
Lower Column Flange Thickness	$t_{f_{LC}}$ =	2 1/16	in.	
Upper Column Width	b_{UC} =	12 5/8	in.	
Lower Column Width	b_{LC} =	12 7/8	in.	
Bearing Properties				
Thickness of Flange Bearing	t_{f_b} =	1.5625	in.	Equation B-158
Projected Area of Flange Bearing	A_{pb} =	19.73	in.^{2}	Equation B-157
Design Strength of Flange Bearing	$\boldsymbol{\phi R_n}$ =	**1331.543**	**kip**	**Equation B-156**

B.8.7 Moment Capacity of Column Splice Based on Limit States

The nominal moment capacity (M_n) of the column splice is determined using Equation B-159 from the minimum limit state capacity of the connection (T) and moment arm (d_m).

$$M_n = T\ d_m$$

Equation B-159

The minimum capacity is taken from all previously calculated design strengths in the column from $\phi\ R_n$ and $\phi\ P_n$.

$$T = MIN(\phi\ R_n, \phi\ P_n)$$

Equation B-160

To ensure the applied force generated by the moment acts through the center of each flange in the Upper Column, d_m is set using the distance between the center of each flange from the depth of the Upper Column (d_{UC}) and thickness of the Upper Column flange ($t_{f_{UC}}$).

$$d_m = d_{UC} - t_{f_{UC}}$$

Equation B-161

Moment Capacity Using Design Strength

Design Strength from Appendix B.8

B.8.1	LLP to Upper Column Weld Design Strength	$\phi R_n =$	156.59	kip	Equation B-125
B.8.2	LLP to ULP Bearing Design Strength	$\phi R_n =$	303.75	kip	Equation B-129
B.8.3	ULP to OP Fillet Weld Design Strength	$\phi R_n =$	76.55	kip	Equation B-132
B.8.4.1	OP Bolt Tearout Design Strength	$\phi R_n =$	553.01	kip	Equation B-136
B.8.4.2	OP Tensile Yielding Design Strength	$\phi P_n =$	225.00	kip	Equation B-140
B.8.4.3	OP Tensile Rupture Design Strength	$\phi P_n =$	121.88	kip	Equation B-142
B.8.4.4.i	Mode 1 OP Block Shear Design Strength	$\phi R_n =$	380.31	kip	Equation B-145
B.8.4.4.ii	Mode 2 OP Block Shear Design Strength	$\phi R_n =$	485.94	kip	Equation B-145
B.8.5.1	OP Bolt Bearing Design Strength	$\phi R_n =$	234.00	kip	Equation B-152
B.8.5.2	Bolt Shear Design Strength	$\phi R_n =$	127.23	kip	Equation B-153
B.8.5	Flange Bearing Strength	$\phi R_n =$	1331.54	kip	Equation B-156
Design Strength Limit State Capacity		$T =$	76.55	kip	Equation B-160

Upper Column Flange Properties

Depth of the Upper Column	$d_{UC} =$	14	in.	
Flange Thickness of the Upper Column	$t_{f_{UC}} =$	1 9/16	in.	
Moment Arm	$d_m =$	12.44	in.	Equation B-161
Moment Capacity of Column Splice	$\boldsymbol{M_n} =$	**952.15**	**kip-in.**	**Equation B-159**

Appendix C: Standardized Design

This appendix uses the design checks and considerations described in Chapter 4 and Appendix B to standardize SnapLocX designs across many of the possible column pairings that could arise in practice. Generally, the approach uses groups of SnapLocX component designs from which an assessment of the maximum strong and weak axis shear demand for a given connection arrangement is calculated, leading to an upper bound for the Upper Column. Each SnapLocX standardized design uses one of a few defined design dimensions for the Outer Plates (OP), Inner Plates (IP), Shear Keys (SK), Lower Lock Plates (LLP), and Upper Lock Plates (ULP). Additionally, this appendix provides demonstrative calculations for determining the maximum plastic section properties in both the weak and strong axis for the Upper Column given a standard SnapLocX design. The calculations demonstrated are in relation to the example SnapLocX Connection design, classified as SnapLocX Connection D-5-5 of the standardized designs described in Chapter 5.

C.1 Strong Axis Shape Size Capacity

For column splices subjected to shear in the strong axis direction of the spliced columns, the design shear strength of the connection ($\phi\ R_n$) must exceed the strong axis shear demand from the Upper Column ($V_{x_{max}}$), as written out in Equation C-1.

$$V_{x_{max}} \leq \phi\ R_n$$

Equation C-1

The maximum column shape, satisfying Equation C-1, is found based on the plastic section for the column in the strong axis ($Z_{x_{max}}$) using the shear strength requirements for column splices from *the* AISC *Provisions* stated in Section D2.5. The required shear strength is as described previously in Chapter 4.

$$V_{x_{max}} = \frac{Z_{x_{max}} F_y}{H}$$

Equation C-2

The calculated $Z_{x_{max}}$ is subsequently compared against the detailing dimensions of Z_x found in Table 1-1 of *the Manual*, for shape classes W10, W12, and W14. This comparison permits the

assignment of the maximum column shape within each class for the provided standardized design dimensions.

C.1.1 Designed Inner Plate Through Thickness Shear

The process of solving for the maximum Upper Column shape involves substituting the design IP thickness (t_{IP}) into Equation B-10 from Appendix B for the required IP thickness (t_{IP_r}) and solving for $Z_{x_{max}}$. This is expressed in Equation C-3.

$$Z_{x_{max}} = \frac{\phi\ 0.6\ F_{y_{IP}}\ t_{IP}\ (b_{IP} - d_{SK})}{\frac{F_{y_{UC}}}{H}}$$

Equation C-3

Shape Capacity of the Through Shear of the Inner Plate

Inner Plate Properties			
IP Nominal Strength (A572)	$F_{y_{IP}}$ =	50	ksi
IP Width	b_{IP} =	10	in.
Design IP Thickness	t_{IP} =	3/4	in.
Shear Key Properties			
SK Slot Diameter	d_{SK} =	1 5/8	in.
Column Properties			
Upper Column Nominal Strength (A992)	$F_{y_{UC}}$ =	50	ksi
Story Height	H =	144	in.
Shear Yielding Capacity of the Inner Plate			
Resistance Factor for Shear Yielding of the IP	ϕ =	1	

Maximum Upper Column Size Using Design Dimensions

Maximum X-Axis Plastic Section	$Z_{x_{max}}$ =	**542 5/7**	**in.^{3}**	**Equation C-3**
	Maximum W14	**W14x283**		
	Maximum W12	**W12x305**		
	Maximum W10	**W10x112**		

C.1.2 Designed Inner Plate to Lower Column Weld

The maximum Upper Column shape size ($Z_{x_{max}}$) is determined by substituting the design IP weld thickness ($t_{IP_{weld}}$) for the required IP weld thickness ($t_{IP_{weld_r}}$) in Equation B-15 and Equation B-18 of Appendix B. This provides a $Z_{x_{max}}$, as seen in Equation C-4.

$$Z_{x_{max}} = \frac{\phi\ 0.6\ F_{EXX}\ 0.707}{\frac{F_{y_{UC}}}{H}\left(\frac{1}{t_{weld}\ (2\ L_{weld} + b_{weld})} + \frac{(L_{weld} - \bar{y})\left(\frac{L_{weld}}{2}\right)}{I_{weld}}\right)}$$

Equation C-4

Shape Capacity of the Thickness of the Inner Plate to Lower Column Weld

Column Properties

Story Height	H =	144	in.	
Upper Column Nominal Strength (A992)	$F_{y_{UC}}$ =	50	ksi	

Weld Properties

Vertical Length of the IP Weld	L_{weld} =	11.25	in.	
Horizontal Width of the IP Weld	b_{weld} =	10	in.	
Filler Metal Classification Strength	F_{EXX} =	70	ksi	
Resistance Factor	ϕ =	0.8		
Design Weld Thickness	t_{weld} =	11/16	in.	

Weld Shear Capacity

Centroid of Welds	$\bar{y}$ =	3.89	in.	Equation B-16
Moment of Inertia of Welds	I_{weld} =	456.36	in.^{4}	Equation B-18

Maximum Upper Column Size Using Design Dimensions

Maximum X-Axis Plastic Section	$\boldsymbol{Z_{x_{max}}}$ =	**387.33**	**in.^{3}**	**Equation C-4**
	Maximum W14	**W14x193**		
	Maximum W12	**W12x230**		
	Maximum W10	**W10x112**		

C.2 Weak Axis Shear Size Capacity

The column splice's weak axis shear capacity ($\phi\ R_n$) must exceed the weak axis shear demand from the Upper Column. The maximum shear demand ($V_{y_{max}}$) is limited by the factored capacity of the connection in the column's weak axis direction, as determined in Equation C-5.

$$V_{y_{max}} \leq \phi R_n$$

Equation C-5

The maximum plastic column section in the weak axis ($Z_{y_{max}}$) is determined by rearranging Equation C-5 as stated in *the* AISC *Provisions*. This calculation includes the minimum story height (H) and yield stress of the Upper Column material ($F_{y_{UC}}$) as displayed in Equation C-6.

$$V_{y_{max}} = \frac{Z_{y_{max}}\, F_{y_{UC}}}{H}$$

Equation C-6

The calculated $Z_{y_{max}}$ is then compared against the detailing dimensions of Z_y in Table 1-1 from *the Manual* for shape classes W10, W12, and W14 to determine each maximum column shape within each class.

C.2.1 Designed Shear Key Fillet Weld to Outer Plate

The maximum Upper Column shape, based on the fillet weld connecting the SK to the OP, replaces the required SK weld thickness ($t_{SK_{weld_r}}$) from Equation B-27 in Appendix B with the design SK weld thickness ($t_{SK_{weld}}$). Using additional design variables from the SK and OP, the maximum allowable weak axis plastic section ($Z_{y_{max}}$) is determined in Equation C-7.

$$Z_{y_{max}} = \frac{n_{key}\ \phi\ 0.6\ F_{EXX}\ 0.707\ t_{SK_{weld}}\, d_{KEY}\ \pi}{\frac{F_{y_{UC}}}{H}}$$

Equation C-7

Shape Capacity of the Thickness of Shear Key Fillet Weld

Column Properties

Story Height	H =	144	in.
Upper Column Nominal Strength (A992)	$F_{y_{UC}}$ =	50	ksi

Outer Plate Properties

Width of OP	b_{OP} =	10	in.
Diameter of SK	d_{KEY} =	1.5	in.

Weld Properties

Design Weld Thickness	$t_{SK_{weld}}$ =	0.5	in.
Filler Metal Classification Strength	F_{EXX} =	70	ksi
Number of SK Welds in the Direction of Shear	n_{KEY} =	2	keys
Resistance Factor of Fillet Weld	ϕ =	0.75	

Maximum Upper Column Size Using Design Dimensions

Maximum Y-Axis Plastic Section	$Z_{y_{max}}$ =	**302.25**	**in.^{3}**	**Equation C-7**
	Maximum W14	**W14x283**		
	Maximum W12	**W12x336**		
	Maximum W10	**W10x112**		

C.2.2 Designed Shear Key Cross-Section Yield

The maximum Upper Column shape size can be calculated in Equation C-8 by substituting d_{KEY} for the required SK diameter (d_{KEY_r}).in Equation B-33 of Appendix B and solving for the maximum allowable weak axis plastic section ($Z_{y_{max}}$).

$$Z_{y_{max}} = n_{KEY} \frac{\phi \; 0.60 \; F_{y_{key}} \; d_{slot}^2 \; \pi}{4 \; \frac{F_{y_{col}}}{H}}$$

Equation C-8

Shape Capacity of the Shear Key Cross Section

Shear Key Properties			
Resistance Factor for Shear Rupture	ϕ =	1.00	
Design SK Diameter	d_{KEY} =	1.5	in.
SK Nominal Strength (A572)	$F_{y_{KEY}}$ =	50	ksi
Number of SKs in the Direction of Weak Axis Shear	n_{KEY} =	2	keys
Column Properties			
Story Height	H =	144	in.
Upper Column Nominal Strength (A992)	$F_{y_{UC}}$ =	50	ksi

Maximum Upper Column Size Using Design Dimensions

Maximum Y-Axis Plastic Section	**$Z_{y_{max}}$ =**	**229.02**	**in.^{3}**	**Equation C-8**
	Maximum W14	**W14x211**		
	Maximum W12	**W12x279**		
	Maximum W10	**W10x112**		

C.2.3 Designed Shear Key Bearing on Lower Lock Plate Key Slot

The maximum shape size of the Upper Column can be achieved by solving for the plastic section in the y-axis ($Z_{y_{max}}$), as shown in Equation C-9. This computation uses the design thickness of the LLP (t_{LLP}). Equation C-9 accounts for the difference between the t_{LLP} and bearing depth of the SK.

$$Z_{y_{max}} = n_{KEY} \frac{\phi \; 1.8 \; F_{y_{LLP}} \; (t_{LLP} - {}^{1}/_{16}) \frac{d_{slot}}{2}}{\frac{F_{y_{col}}}{H}}$$

Equation C-9

Shape Capacity of the Shear Key Slot Bearing on the Lower Lock Plate

Shear Key Properties			
Resistance Factor for Bearing Strength	ϕ =	0.75	
Design SK Diameter	d_{KEY} =	1.5	in.
SK Nominal Strength (A572)	$F_{y_{KEY}}$ =	50	ksi
Number of SK in the Direction of Weak Axis Shear	n_{KEY} =	2	keys
Lower Lock Plate Properties			
LLP Nominal Strength (A572)	$F_{y_{LLP}}$ =	50	ksi
Design LLP Thickness	t_{LLP} =	0.75	in.
Column Properties			
Upper Column (W12x170) Y-Axis Plastic Section	$Z_{y_{UC}}$ =	126	in.^{3}
Story Height	H =	144	in.
Upper Column Nominal Strength (A992)	$F_{y_{UC}}$ =	50	ksi

Maximum Upper Column Size Using Design Dimensions

Maximum Y-Axis Plastic Section	$Z_{y_{max}}$ =	**200.475**	**in.^{3}**	**Equation C-9**
	Maximum W14	**W14x211**		
	Maximum W12	**W12x252**		
	Maximum W10	**W10x112**		

C.2.4 Designed Eccentrically Loaded Bolt Grouping

Column size verification for bolt grouping from Section B.5.4 is applied to the standardized designs in Equation C-10 for the design strength of eccentrically loaded bolt groups.

$$Z_{y_{max}} = n_{bg}\, C\, \phi r_n \frac{H}{F_{y_{UC}}}$$

Equation C-10

Shape Capacity of Eccentrically Loaded Bolt Groups

Outer Plate Properties				
OP Plate Width	b_{OP} =	10	in.	
Distance Between Bolt Rows	L_1 =	6	in.	
Number of Bolt Columns	n_{col} =	2		
Distance Between Bolt Columns	s =	7	in.	
Center of Upper Bolt Row to Upper End of Lower Column	b_{top} =	2	in.	
Center of SK to Lower End of Upper Column	b_{SK} =	1.5	in.	
Number of Bolt Groups in Direction of Shear	n_{bg} =	2	groups	
Bolt Properties				
Column Splice Bolt Diameter	d_b =	1	in.	
Bolt Hole Diameter	d_h =	1.125	in.	
Available Shear Strength for 1" Bolts	ϕr_n =	31.8	kip	
Design Vertical Distance from the Centroid of the Bolt Group to Column Shear Transfer (Center of SK)	e_x =	6.5	in.	Equation B-42
Column Properties				
Story Height	H =	144	in.	
Upper Column Nominal Strength (A992)	$F_{y_{UC}}$ =	50	ksi	
Tabulated Eccentrically Loaded Coefficients				
Coefficient Tabulated from similar s, e_x, and n_{col}	C =	1.8		
Available Strength from Splice Bolt Group	R_n =	57.24	ksi	Equation B-43

Maximum Upper Column Size Using Design Dimensions

Maximum Y-Axis Plastic Section $Z_{y_{max}}$ **= 329.70 in.^{3} Equation C-10**

Maximum W14	**W14x311**
Maximum W12	**W12x336**
Maximum W10	**W10x112**

C.2.4.1 Bolt Spacing through Outer Plate and Lower Column

The design constraints on the maximum Upper Column shape size are caused by shear loading in the strong and weak axis, which contrast with limitations on the Lower Column shape size, enforced by tightening and entering clearance between the bolts and column fillet from the flange to the web. Derived from formulas in Section B.5.4.1, the calculation for the maximum fillet size of the Lower Column ($k_{1_{max}}$) involves the bolt column spacing (s), the more considerable value between the maximum outer diameter of the disc spring (OD_{max}), and clearance for column fillet (C_3) as specified in Table 7-15 for A325 bolts from *the Manual* and expressed in Equation C-11.

$$k_{1_{max}} = \frac{s}{2} - MAX\left(\frac{OD_{max}}{2},\ C_3\right)$$

Equation C-11

Shape Capacity from Bolt Spacing Considerations of the Outer Plate

Outer Plate Properties			
Width of the OP	b_{OP} =	10	in.
Bolt Column Spacing	s =	7	in.
Bolt Properties			
Bolt Diameter	b_d =	1	in.
Bolt Hole Diameter	b_h =	1.125	in.
Minimum Edge Distance Allowed	$b_{EDGE_{min}}$ =	1.25	in.
Entering and Tightening Clearance for Given Bolt Diameter	C_3 =	1	in.
Disc Spring Properties			
Disc Spring Maximum Outer Diameter	OD_{max} =	2.2	in.

Maximum Shape Size

Maximum Distance from Center of Web to Flange Fillet Toe	$k_{1_{max}}$ =	**2 3/8**	**in.**	**Equation C-11**

Maximum W14	**W14x550**
Maximum W12	**W12x336**
Maximum W10	**W10x112**

C.3 Maximum Shape Size for D-5-5

Given the maximum Upper Column shape sizes calculated through $Z_{x_{max}}$ and $Z_{y_{max}}$ for each design constraint, the allowable maximum size is determined as the smallest column size from each column classification.

Additionally, the maximum size of the Lower Column is governed by $k_{1_{max}}$ due to the tightening and entering clearance.

Maximum Column Shape Size for Standardized Design D-5-5

Upper Column Constraints							
Strong Axis					**W14**	**W12**	**W10**
IP Through Thickness	$Z_{x_{max}}$ =	542.71	in.^{3}	Equation C-3	W14x283	W12x305	W10x112
IP to Lower Column Weld	$Z_{x_{max}}$ =	387.33	in.^{3}	Equation C-4	W14x193	W12x230	W10x112
Weak Axis							
SK Weld to OP	$Z_{y_{max}}$ =	302.25	in.^{3}	Equation C-7	W14x283	W12x336	W10x112
SK Cross-Section Yield	$Z_{y_{max}}$ =	229.02	in.^{3}	Equation C-8	W14x211	W12x279	W10x112
SK LLP Bearing	$Z_{y_{max}}$ =	200.48	in.^{3}	Equation C-9	W14x211	W12x252	W10x112
Eccentrically Loaded Bolt Group	$Z_{y_{max}}$ =	329.70	in.^{3}	Equation C-10	W14x311	W12x336	W10x112
Maximum Upper Column Shape					**W14x193**	**W12x230**	**W10x112**
Lower Column Constraints							
Bolt Spacing	$k_{1_{max}}$ =	2 3/8	in.	Equation C-11	W14x550	W12x336	W10x112
Maximum Lower Column Shape					**W14x550**	**W12x336**	**W10x112**

C.4 Outer Plate Capacity

The moment demand of the OP is dependent on the plate displacement resulting from the thickness of the ULP during assembly and the geometric dimensions of the accompanying disc springs. Across all Lettered Plates, the ULP thickness is constant at 1/2 in. Each Lettered Plate category requires unique Belleville washer assignments to allow for the required displacement of the OP at the disc springs without exceeding the plate's moment capacity during assembly.

The moment capacity of the OP relies on factors such as the OP width, thickness, and bolt hole diameters integral to the calculation for the OP's moment of inertia, displayed in Equation B-120 from Section B.6.4.1. Notably, the large the bolt holes will decrease the moment capacity, while a wider OP will increase the moment capacity.

C.5 Snapping Friction Shape Constraints

The minimum Upper Column shape size is constrained by the nominal weight of the column required to overcome friction and the shear of the Outer Plate during assembly. The minimum nominal column weight is determined using the process outlined in Section B.7.

Example Design Snapping Friction Check

Column Properties				
Column Length	L_{col} =	30	ft.	
Friction				
Friction Coefficient	μ =	0.3		Equation B-124
Outer Plate Shear				
Total Shear at the End of the OP during Maximum Flexure	$V_{total}(L_{tot})$ =	0.813	kip	
Minimum Column Weight				
Minimum Total Weight	$\boldsymbol{W}$ =	**0.4878**	**kip**	Equation B-122
Minimum Nominal Weight	$\boldsymbol{w_{col}}$ =	**0.01626**	**kip/ft**	Equation B-123
	=	**16.26**	**lbs/ft**	

Minimum Upper Column Shape

Minimum W14	**W14X22**
Minimum W12	**W12X19**
Minimum W10	**W10X17**

Appendix D: Matlab Code for Example Outer Plate Flexural Capacity

Appendix D provides the Matlab script used to calculate the flexural capacity of the Outer Plate as detailed in Chapter 4 and Appendix B.

D.1 Initial Inputs

D.1.a. Number of Iterations

```
n = 100000;
```

D.1.b. Plate Geometry

Chosen Length 1 - Fixed Bolt to Spring Bolt:

```
L1 = 6; %[in]
```

Chosen Length 2 - Spring bolt to bottom of upper lock plate:

```
L2 = 14; %[in]
```

Total Length of Plate:

```
L_tot = L1 + L2;
```

At some location x:

```
length_x = linspace(0, L_tot, n);
```

Chosen OP thickness:

```
t_OP = 1/2; %[in]
```

Chosen OP width:

```
b_OP = 10; %[in]
```

Shear key diameter:

```
d_sk = 1.625; %[in]
```

ULP thickness:

```
t_ULP = 1/2; %[in]
```

Number of spring bolts:

```
n_s_bolt = 2;
```

D.1.c. Material Properties for Steel (Spring Disks and Columns)

Young's Modulus:

```
E = 29000; %[ksi]
```

Poisson's Ratio:

```
nu = 0.3;
```

D.1.d. Spring Disk Washer Geometry

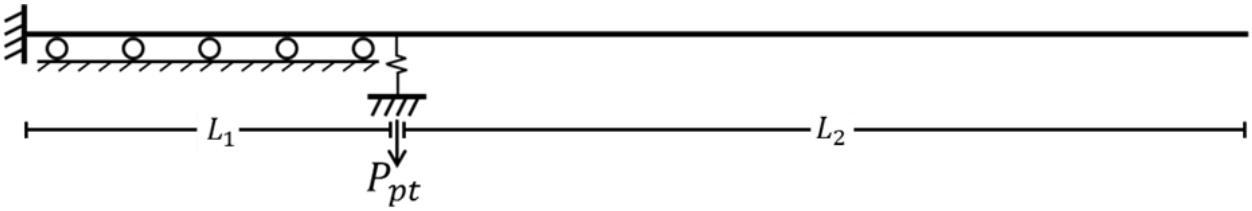

Pretensioned Spring Force:

```
P_pt = -0.2; %[kip]
```

D.1.d(i). F436 Washer Properties:

Example Washer: American Belleville AD56-28.5-1.5

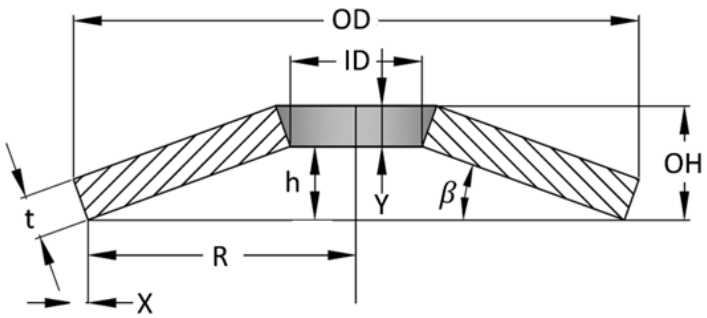

Outer Diameter:

```
OD = 2.2; %[in]
```

Inner Diameter:

```
ID = 1.122; %[in]
```

Washer thickness:

```
t_wash = 0.059; %[in]
```

Catalogues used for disc spring research either provide conical height (h) or overall height (OH).

- The value not provided by manufacturers is entered as 0.

Overall height:

```
OH = 0.136; %[in]
```

Conical height:

```
h = 0.0; %[in]
```

D.2 Initial Calculations Used to Set Up Beam Superposition

D.2.a. Moment of Inertia for the Outer Plate

```
I_OP = (b_OP * t_OP^3)/12; %[in^4]
```

D.2.b. Stiffness of Outer Plate

```
k_OP = 3*E*I_OP/L_tot^3; %[kip/in]
```

D.2.c. Spring Geometry

D.2.c(i). Initial Beta

Initial guess of conical angle

```
beta_initial = 20; %[degrees]
```

Geometry changes in X and Y direction of the thickness at rest:

```
 X_initial = sin(beta_initial*pi/180)*t_wash; %[in] initial
sin(beta)*disc_thickness
 Y_initial = cos(beta_initial*pi/180)*t_wash; %[in] initial
cos(beta)*disc_thickness
```

D.2.c(ii). Solved Beta

The first if condition loops through the angle calculation the conical angle if manufactures provide OH. The else condition uses the provided h value for the accompanying while loop:

```
 if h == 0
```

Initial guess for height from ground to bottom of washer thickness at rest:

```
    h_initial = OH - Y_initial;
    if t_wash >= 8/25.4
        R_constant = OH/150;
    else
        R_constant = t_wash/6;
    end
```

Initial radius guess of radius from centerline to load bearing circle (bottom surface):

- Considers machined flat for OD >= 8 mm and corner radius for OD < 8mm

```
    R_initial = OD/2 - X_initial - R_constant;
```

New beta solved for with the calculated h and R:

```
    beta_solved = atan(h_initial/(R_initial-ID/2))*180/pi;
```

Loop through the previous calculations until the solved for beta is within a tolerance of the most recently solved beta:

```
    while abs(beta_solved - beta_initial) >= 0.00001
        beta_initial = beta_solved;
        X_new = sin(beta_initial*pi/180)*t_wash;
        Y_new = cos(beta_initial*pi/180)*t_wash;
        h_new = OH - Y_new;
        R_new = OD/2 - X_new - R_constant;

        beta_solved = atan(h_new/(R_new - ID/2))*180/pi;
    end
```

Initial guess for the overall height if conical height is given:

```
else
    OH_initial = h + Y_initial;

    if t_wash >= 8/25.4
        R_constant = OH_initial/150;
    else
        R_constant = t_wash/6;
    end
    R_initial = OD/2 - X_initial - R_constant;
    beta_solved = atan(h/(R_initial - ID/2)) * 180/pi;

    while abs(beta_solved - beta_initial) >= 0.00001
        beta_initial = beta_solved;
        X_new = sin(beta_initial*pi/180)*t_wash;
        Y_new = cos(beta_initial*pi/180)*t_wash;
        OH_new = h + Y_new;

        if t_wash >= 8/25.4
            R_new_constant = OH_new/150;
        else
            R_new_constant = t_wash/6;
        end

        R_new = OD/2 - X_new - R_new_constant;
        beta_solved = atan(h/(R_new - ID/2)) *180/pi;
    end
end
```

Ratio of Diameters (OD/ID) - recommended to be between 1.75 and 2.5 - MW Components

```
alpha = OD/ID; %[unitless]
```

Ratio factor of alpha

```
M = 6/(pi*log(alpha))*(alpha-1)^2/alpha^2; %[unitless]
```

D.3 Superposition

D.3.a. Cantilever at Instant Uplift

Force required for displacement:

```
F_up = -P_pt;
```

Displacement of OP while displacement at spring = 0:

```
delta_uplift = F_up*L2^3/(3*E*I_OP);
```

Moment, Shear, and Displacement Curves for Instantaneous Uplift at Spring Bolts:

```
for ii = 1:n
    if length_x(ii) >= 0 && length_x(ii) < L1
        M_uplift(ii) = F_up*L2; %moment constant from 0 to L1
        V_uplift(ii) = 0;
        D_uplift(ii) = 0;
    else
        V_uplift(ii) = -F_up;
        M_uplift(ii) = F_up*L2*(length_x(ii))/(L1-L_tot) -
F_up*L2*L1/(L1-L_tot) + F_up*L2;
        D_uplift(ii) = F_up*(length_x(ii)-L1)^2 * (3*L2 - (length_x(ii)-
L1))/ (6*E*I_OP);
    end
end
```

D.3.b. SUPERPOSITION 1: Fixed with Free End

(Superposition #1 - 1 denotes superposition number [M1])

Force from free end:

```
F1 = k_OP * (t_ULP-delta_uplift); %[kip]
```

Reaction force at free end:

```
F1_rxn = -F1; %[kip]
```

Shear, Moment, and Displacement Curves for Beam 1:

```
for ii = 1:n
    V1(ii) = F1_rxn;
    M1(ii) = -V1(ii)*(L_tot-length_x(ii));
    D1(ii) = F1_rxn*length_x(ii)^3/(6*E*I_OP) +
F1*L_tot*length_x(ii)^2/(2*E*I_OP) + (length_x(ii)/(E*I_OP))*(((t_ULP-
delta_uplift)*E*I_OP/L_tot)- F1*L_tot^2/3);
end
```

D.3.c. SUPERPOSITION 2: Beam Fixed at One End with a Point Load at the Other

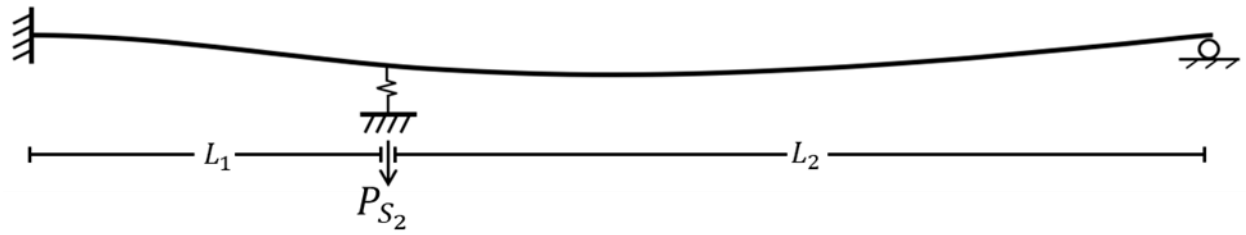

D.3.c(i). Disc Spring Load Curve Used to Determine Force from Springs (P_{s2})

Number of springs in parallel:

```
n_s_p = 1;
```

Spring displacement with no load applied:

```
disp_spring_initial = 0; %[in]
```

Identifying the conical height:

```
if h > 0
    h_final = h;
else
    h_final = h_new;
end
```

Ratio of cone height to thickness:

- Recommended to be between 0.4 and 1.3

```
h_t = h_final/t_wash;
```

Maximum disc spring displacement:

- Solved using the conical height

```
disp_spring_max = h_final; %[in]
```

Spring displacement array for one disc spring using the provided the parameters:

```
for i = 1:n-1
    delt_spring_disp1(1) = disp_spring_initial;
    delt_spring_disp1(i+1) = (disp_spring_max-disp_spring_initial)/n +
delt_spring_disp1(i);
end
```

Spring force array:

- Calculated from the displacement array

```
for i = 1:n
    P_spring1(i)= E*delt_spring_disp1(i) / ((1- nu^2)*M*R_new^2)
*((h_final -delt_spring_disp1(i)/2)*(h_final -
delt_spring_disp1(i))*t_wash + t_wash^3);
end
```

Number of springs in series needed for required displacement of D1(L1):

```
n_s_s = ceil(D1(ceil((L1/L_tot)*n))/h_final);
```

```
disp(['WARNING: Number of Springs Needed In Series: ', num2str(n_s_s)]);
```

```
WARNING: Number of Springs Needed In Series: 1
```

Total force array including the number of springs in parallel and the number of bolts with disc springs:

```
P_spring = P_spring1*n_s_p;
P_spring_tot = P_spring*n_s_bolt;
```

Total displacement array including the required number of springs in series:

```
delta_disp = delt_spring_disp1 * n_s_s;
```

Plot of the force-displacement curve for the example disc springs:

```
figure
hold on
plot(delta_disp, P_spring_tot, "LineWidth", 2, "Color", 'b')
xlabel('Spring Displacement [in]', 'FontSize', 14)
ylabel('Spring Force Per Bolt [kip]', 'FontSize', 14)
xPos = 0.01;
yPos = max(P_spring_tot);
title('Spring Stiffness', 'FontSize', 14)
text(xPos, yPos, ['h/t ratio: ' num2str(h_t)], 'FontSize', 12)
hold off
```

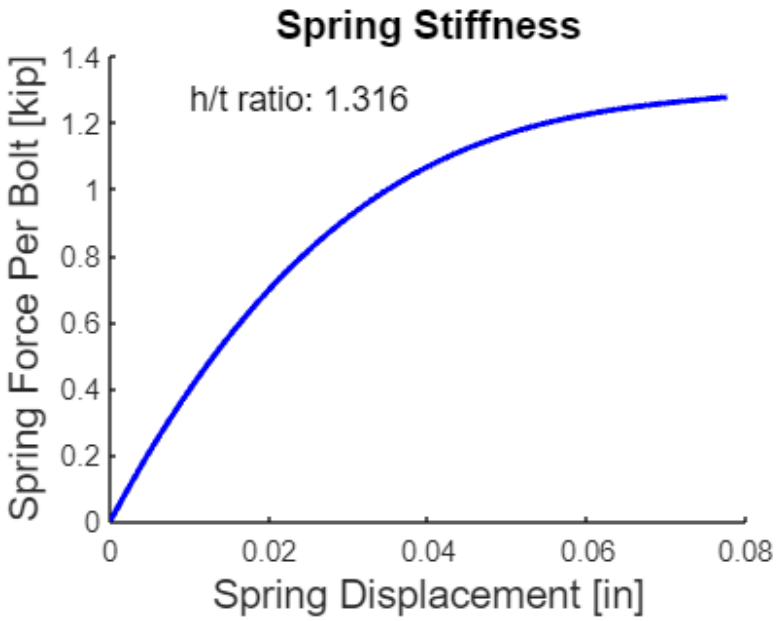

D.3.c(ii). Identifying Initial Force of Springs from the Initial Displacement

Find the displacement offput caused by the pretension force before solving for actual spring deformation.

Difference between pretension load and spring load array:

```
abs_diff = abs(P_spring_tot - abs(P_pt));
```

Find at which point in the array where difference ~ 0:

```
P_spring_pt_loc = find(abs_diff == min(abs_diff));
```

Displacement caused by pretensioned spring Ps:

```
delta_s0 = delta_disp(P_spring_pt_loc);
```

Initial displacement of spring taken from the displacement at L1 from the first superposition array:

```
delta_s_1 = D1(ceil((L1/L_tot)*n));
```

Account for hypothetical displacement from pretensioning:

- Actual displacement required = initial total - disp_pt

```
delta_s_total = delta_s0 + delta_s_1;
```

Linear interpolation for the required force of the spring given the displacement needed:

```
Ps_guess = -1*interp1(delta_disp, P_spring_tot, delta_s_total,
'linear');
```

Force exerted by springs in Beam 2 model:

```
Ps_2 = -1*interp1(delta_disp, P_spring_tot, delta_s_total, 'linear') -
P_pt;
```

Beam 2 reactions caused by Ps_2:

- Force at fixed end given the guessed force from the spring:

```
Fixed_rxn2_initial = -Ps_2* L2 * (3*L_tot^2-L2^2) / (2*L_tot^3); %[kip]
```

- Reaction force at the fixed bolts:

```
Support_rxn2_initial = -Ps_2 * L1^2 * (L2+2*L_tot) / (2*L_tot^3); %[kip]
```

- Moment at the fixed bolts given the guessed spring force

```
MFixed2_initial = Ps_2 * L1 * L2 *(L_tot+L2)/(2*L_tot^2);  %[kip-in]
```

Shear, moment, and displacement curves for the guessed spring load of Beam 2:

```
 for ii = 1:n

     if length_x(ii) >=0 && length_x(ii) < L1
         V2(ii) = Fixed_rxn2_initial;
         M2(ii) = MFixed2_initial + Fixed_rxn2_initial*length_x(ii);
         D2(ii) = ((L_tot-L1)*Ps_2*length_x(ii).^2*(L_tot^2*(6*L1 -
2*length_x(ii))+L1^2*length_x(ii) -
L_tot*L1*(3*L1+2*length_x(ii))))/(12*L_tot^3*E*I_OP); %P force is
positive down and doesn't need a sign adjustment
     else
         V2(ii) = Fixed_rxn2_initial + Ps_2;
         M2(ii) = Support_rxn2_initial*(L_tot-length_x(ii));
         D2(ii) = (L1^2*(-Ps_2)*(L_tot-length_x(ii))*(2*L_tot^2*(L1-
3*length_x(ii))-
L1*length_x(ii).^2+L_tot*length_x(ii)*(2*L1+3*length_x(ii))))/(12*L_tot^3
*E*I_OP);
     end
 end
```

D.4 Total Force, Shear, Moment, and Displacement for the Initial for Superposition of Beam 1 and Beam 2

```
M12_0 = M1 + M2; %[kip-in]
V12_0 = V1 + V2; %[kip]
D12_0 = D1 + D2; % [in]
```

Superposition values will have to go through a loop to adjust for the force P given the total displacement and will converge determine the stiffness of the springs.

The next spring deformation estimate using the total displacement for the initial superposition:

```
delt_next = D12_0(ceil((L1/L_tot)*n));
```

Iterate through previous equations for Beam 2 and total beam superposition unitl a set tolerance is met:

```
while abs(delta_s_total-delt_next) >= 0.000001

    delta_s_total = delt_next;

    delta_guess = delta_s_total + delta_s0; %includes the displacement
from Pt

    Ps_new = -interp1(delta_disp, P_spring_tot, delta_guess, "linear") -
P_pt; %take away Pt force to find curves  :  Isn't adding
disp_P_spring_pt in then taking P_spring_pt out repetitive

    Fixed_rxn2 = -Ps_new* L2 * (3*L_tot^2-L2^2) / (2*L_tot^3);
    Support_rxn2 = -Ps_new * L1^2 * (L2+2*L_tot) / (2*L_tot^3);
    MFixed2 = Ps_new * L1 * L2 *(L_tot+L2)/(2*L_tot^2);

    for ii = 1:n
        if length_x(ii) >=0 && length_x(ii) < L1
            V2_new(ii) = Fixed_rxn2;
            M2_new(ii) = MFixed2 + Fixed_rxn2 *length_x(ii);
            D2_new(ii) = -((L_tot-L1)*(-
Ps_new)*length_x(ii).^2*(L_tot^2*(6*L1 -
2*length_x(ii))+L1^2*length_x(ii) -
L_tot*L1*(3*L1+2*length_x(ii))))/(12*L_tot^3*E*I_OP);
        else
            V2_new(ii) = Fixed_rxn2 + Ps_new;
            M2_new(ii) = Support_rxn2*(L_tot-length_x(ii));
            D2_new(ii) = (L1^2*(-Ps_new)*(L_tot-
length_x(ii))*(2*L_tot^2*(L1-3*length_x(ii))-
L1*length_x(ii).^2+L_tot*length_x(ii)*(2*L1+3*length_x(ii))))/(12*L_tot^3
*E*I_OP);
        end
    end
    M12_next = M1 + M2_new; %[kip-in]
    V12_next = V1 + V2_new; %[kip]
    D12_next = D1 + D2_new; % [in]

    delt_next = D12_next(ceil((L1/L_tot)*n));
end
```

D.5 Combine Beam Superposition and Uplift Curves for Final Plate Behavior in Moment, Shear, and Displacement

```
M_final = M12_next + M_uplift;
V_final = V12_next + V_uplift;
D_final = D12_next + D_uplift;
```

D.6 Flexural Limits

Nominal yield strength of the OP:

```
Fy = 50; %[ksi]
```

Maximum moment through the OP cross section:

```
c = t_OP/2; %[in]
```

Bolt hole diameter:

```
d_h = 1+1/8;
```

Moment capacity of the OP at the Bolt Holes (and location of maximum flexure):

```
M_allow = Fy*(I_OP - 2*d_h*t_OP^3/12)/c;
```

Maximum moment demand of the OP:

```
M_max = max(M_final); %[kip-in] maximum moment associated with input
variables on the outer plate
```

Flexure Check:

```
if M_allow < M_max
    disp('FAILED: Outer Snap-Plate Moment Capacity Exceeded')
else
    disp('Moment Limit State: PASSED')
end
```

```
Moment Limit State: PASSED
```

D.7 Final Moment, Shear, and Displacement Plots of the *OP*

```
figure
```

```
set(gcf, 'Position', [100, 100, 1500, 500]);
set(gca, 'FontSize', 30, 'LineWidth', 3)
subplot(1,3,1)
hold on
set(gca, 'FontSize', 14, 'LineWidth', 1.5)
title('Moment','FontSize',16)
plot(length_x, M_final, 'linewidth', 3, 'Color', '#D3B123')
xlabel('Length Along Plate [in]','FontSize',14)
ylabel('Moment [kip-in]','FontSize',14)
hold off

subplot(1,3,2)
hold on
set(gca, 'FontSize', 14, 'LineWidth', 1.5)
title('Shear','FontSize',16)
plot(length_x, V_final,'linewidth', 3)
xlabel('Length Along Plate [in]','FontSize',14)
ylabel('Shear [kip]','FontSize',14)
hold off

subplot(1,3,3)
hold on
set(gca, 'FontSize', 14, 'LineWidth', 1.5)
title('Displacement', 'FontSize', 16)
plot(length_x, D_final,'linewidth', 3, 'color', '#6ABF23')
xlabel('Length Along Plate [in]','FontSize',14)
ylabel('Displacement [in]','FontSize',14)
hold off
```

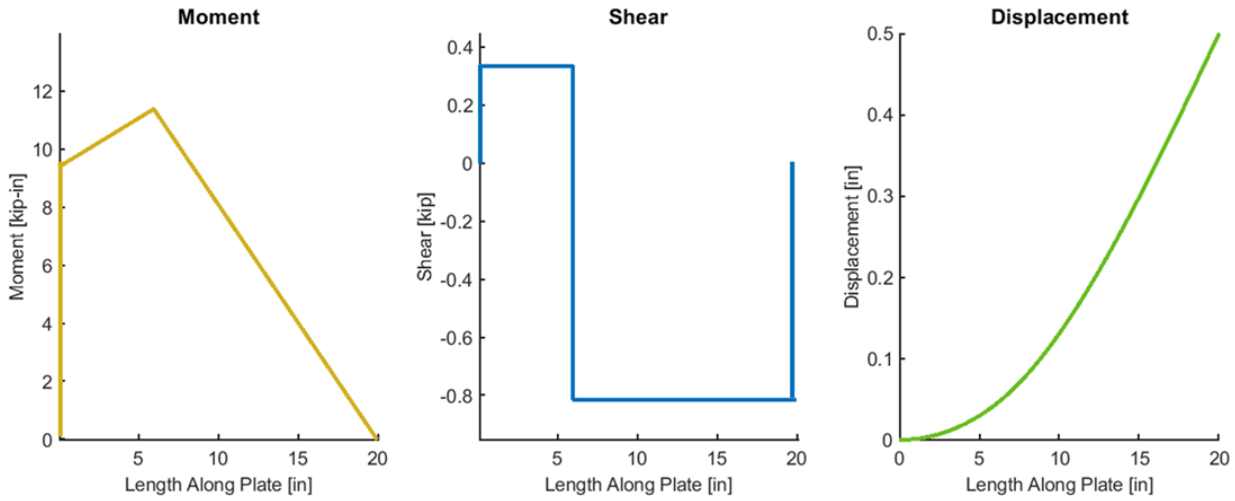

Appendix E: SnapLocX Engineering Drawings

Snap Conditions

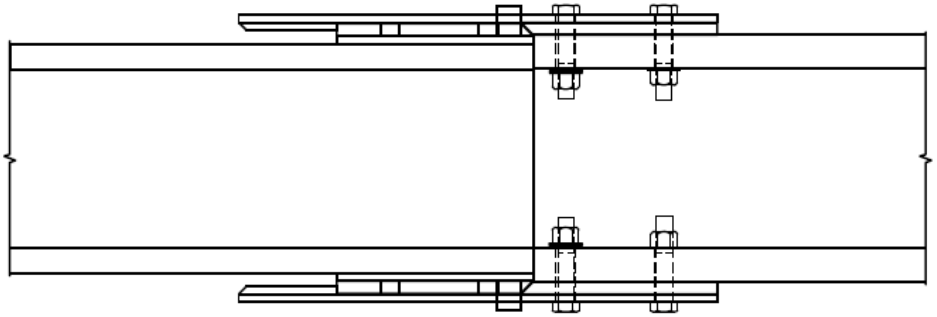

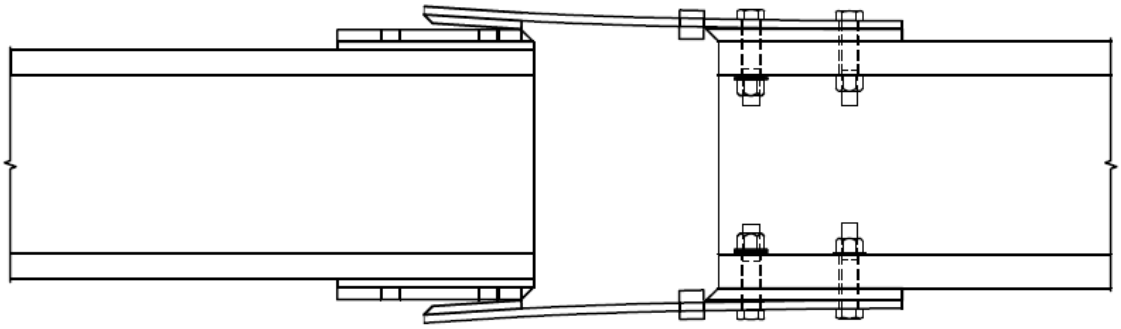

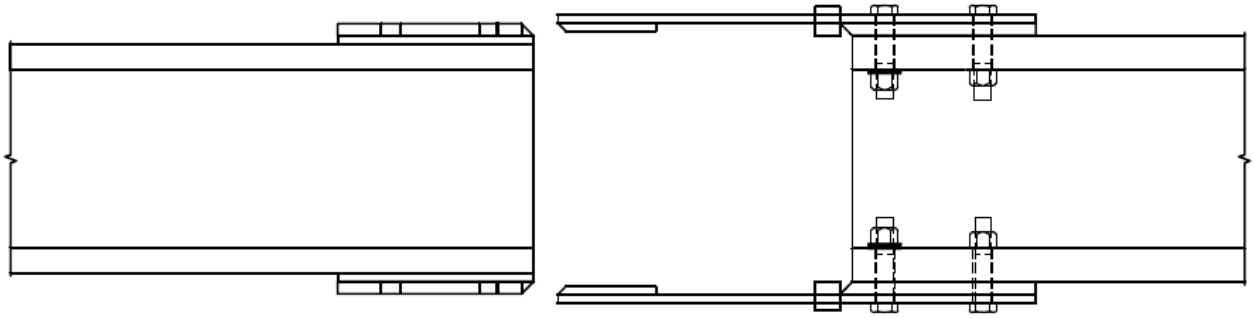

Standardized SnapLocX Nomenclature

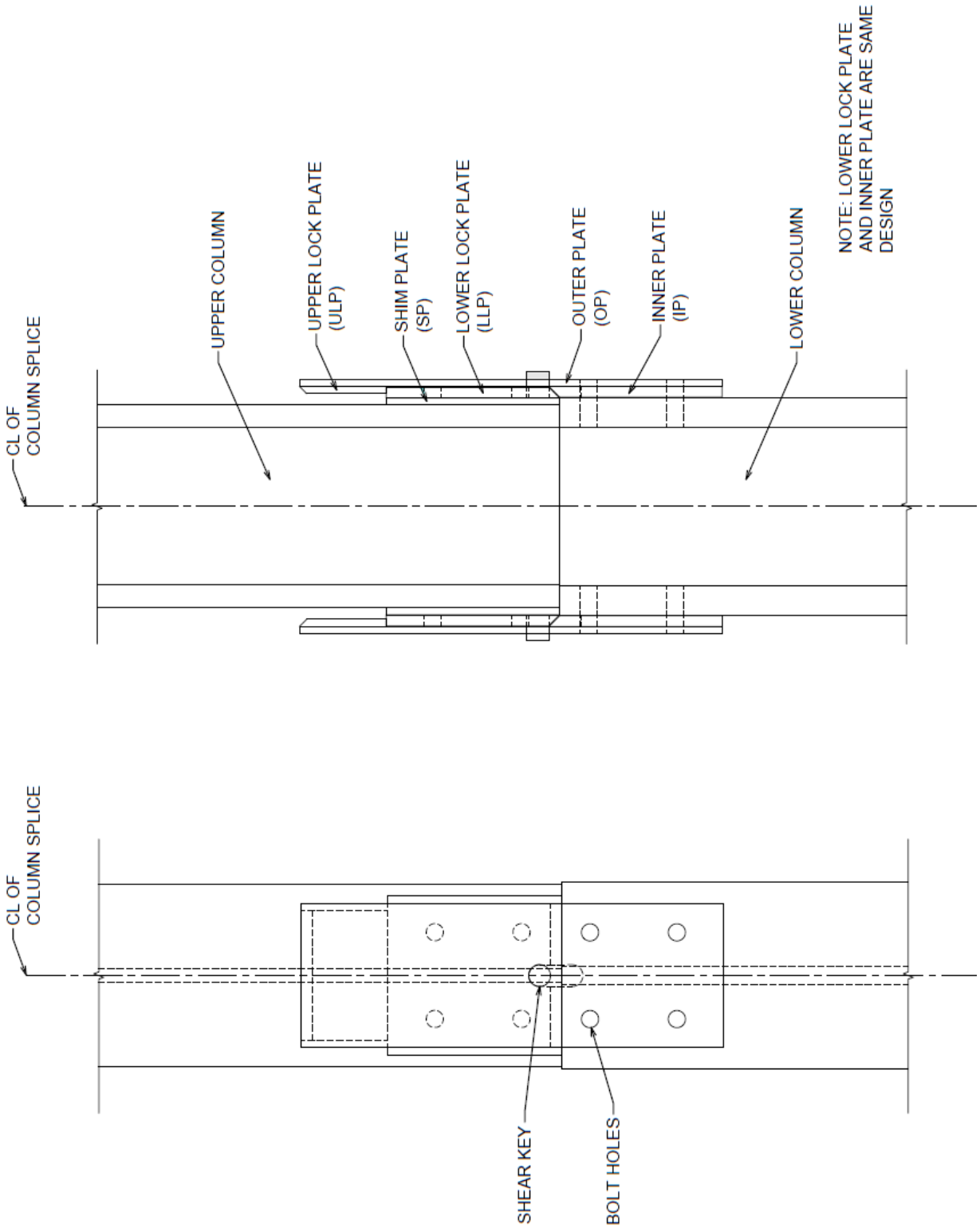

Delivered Preassembled Columns

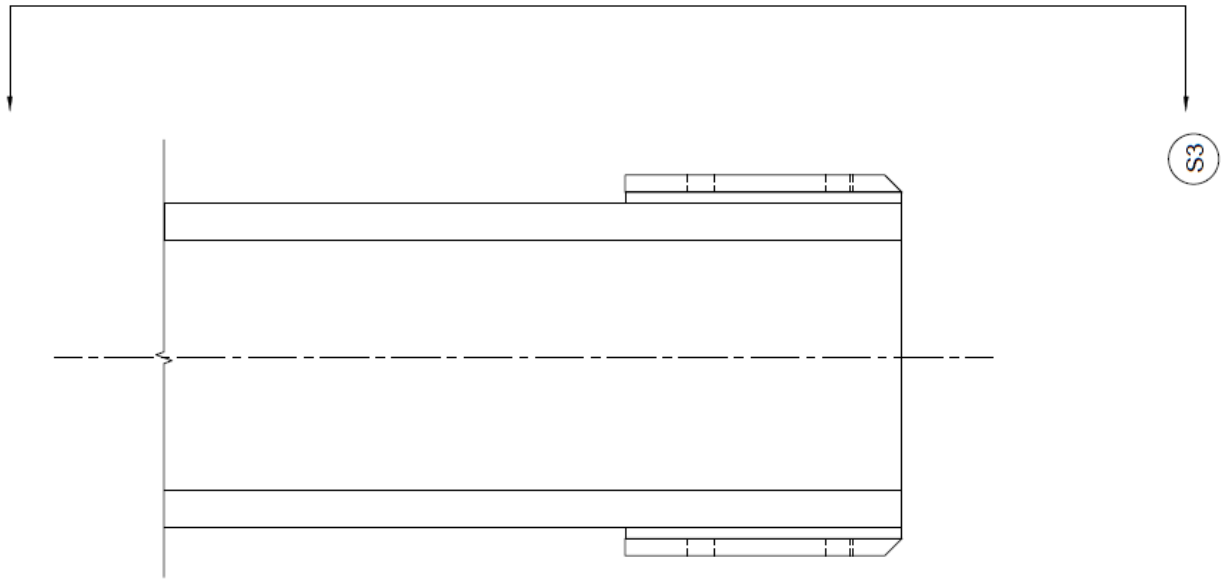

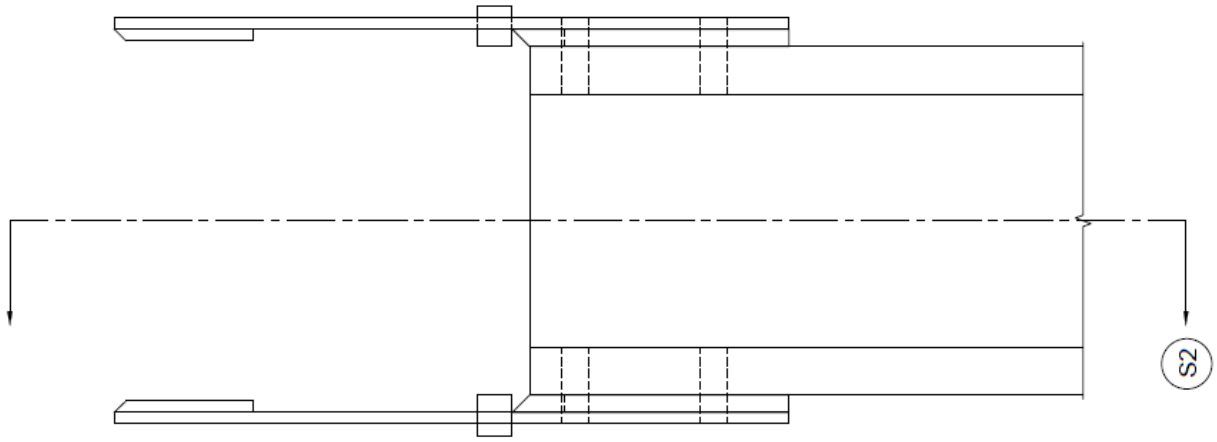

Standardized Design Variables

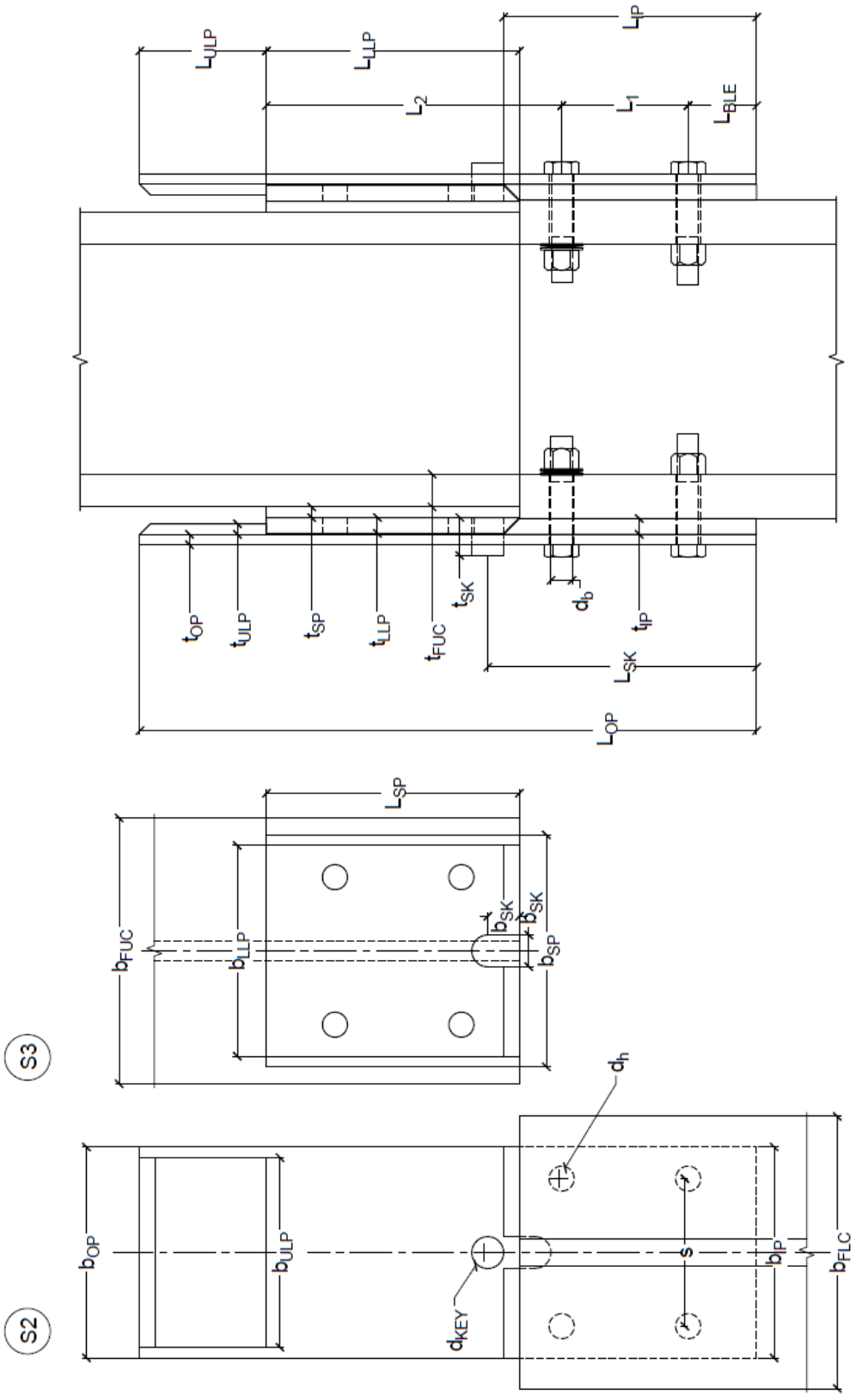

Example Design Variable Dimensions

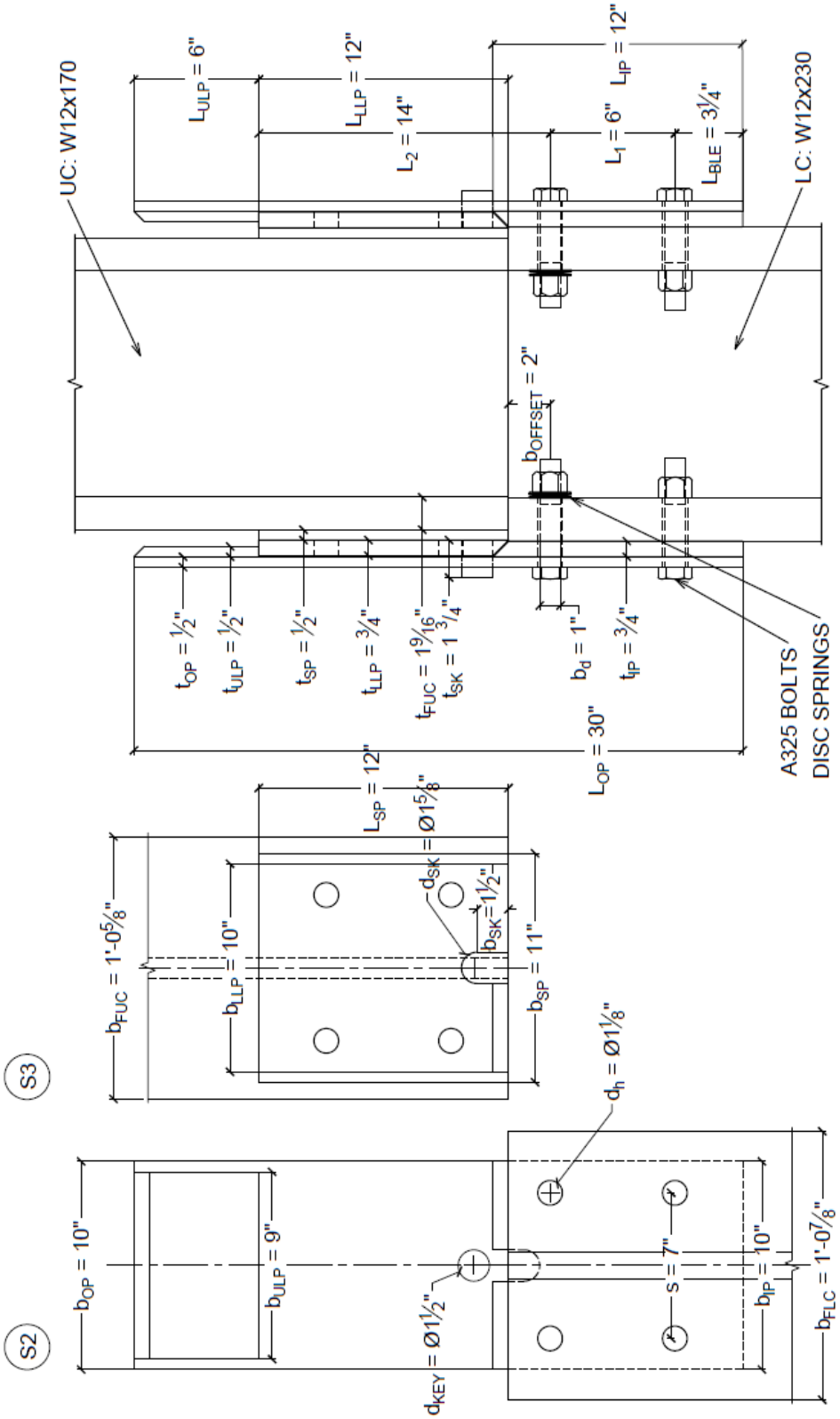

Standardized Weld Placements

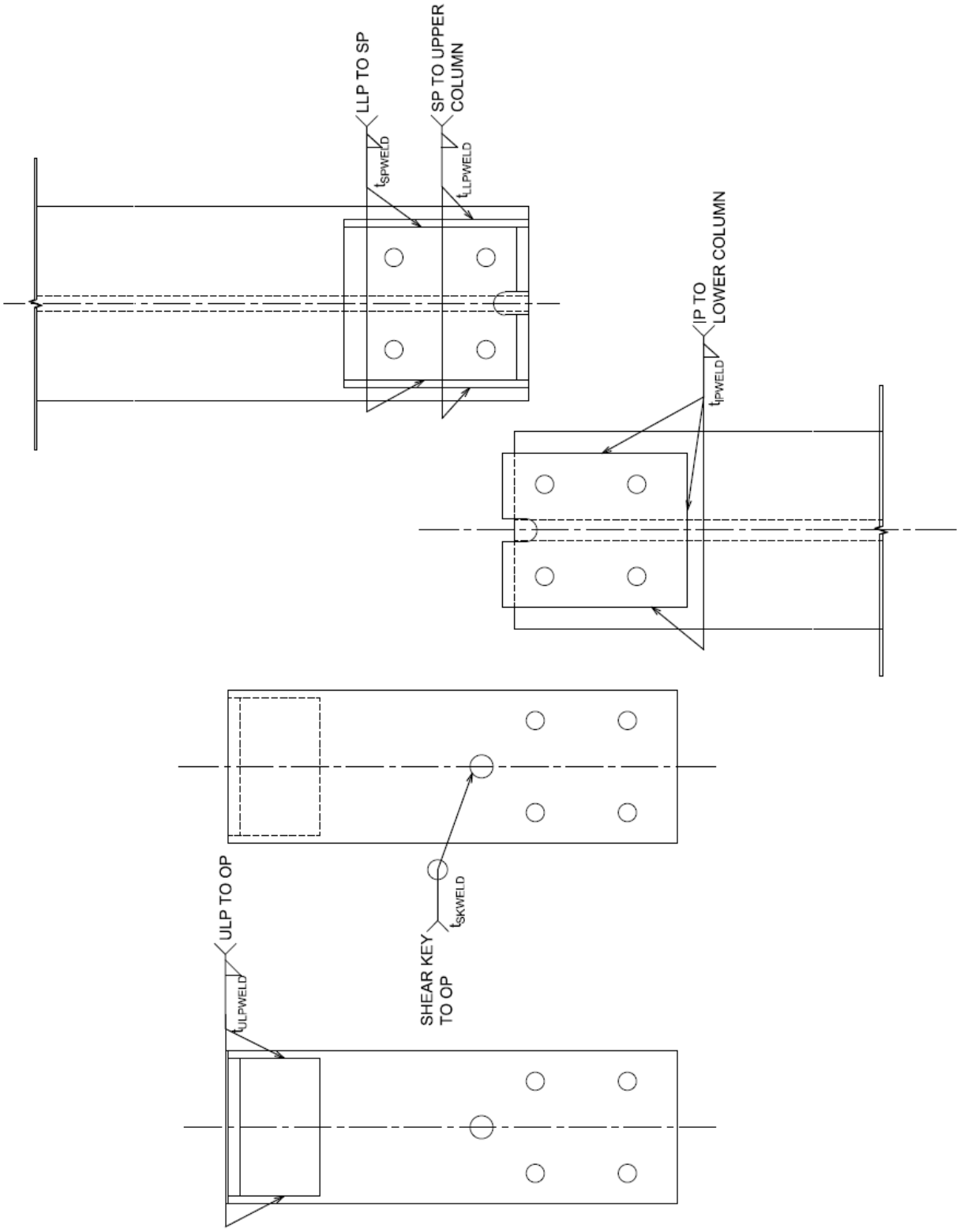

Example Design Weld Dimensions

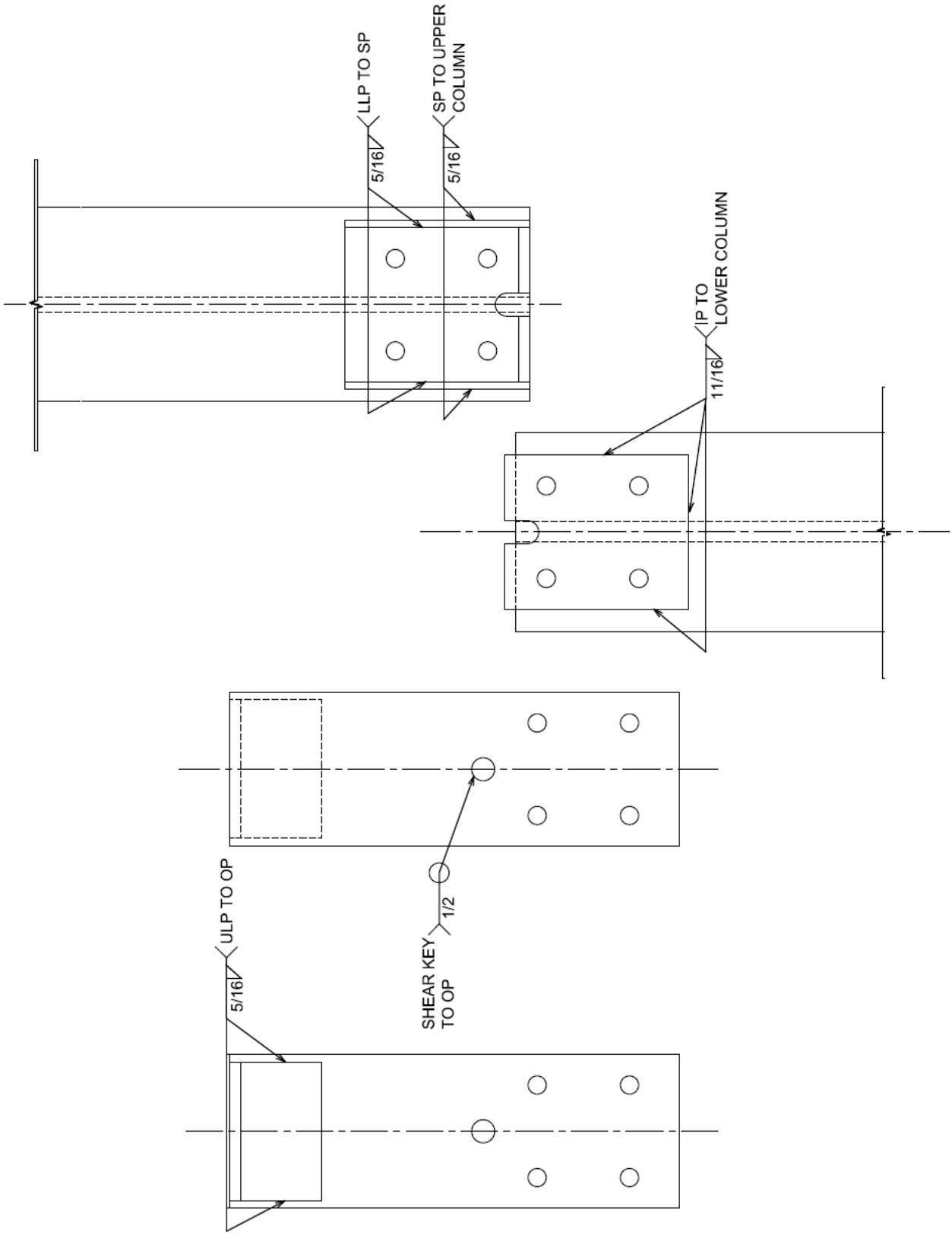

Standardized Numbered Plate Design Variables

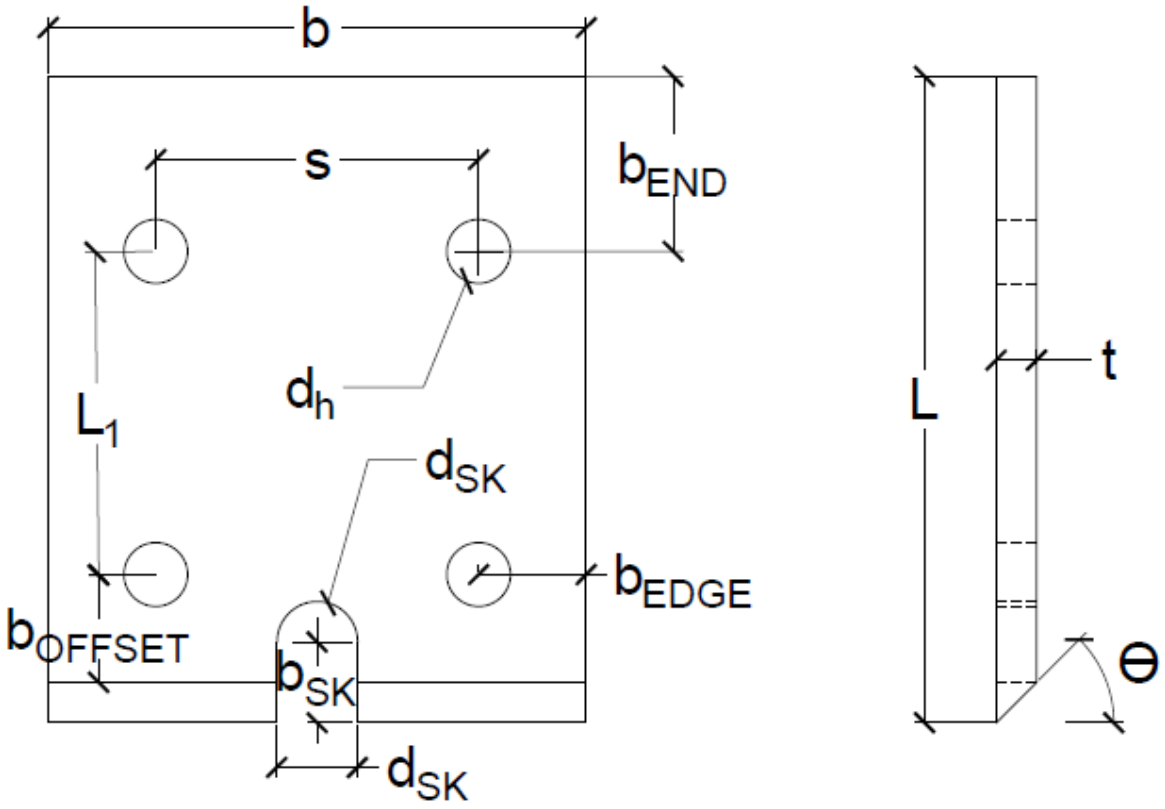

Numbered Plate Engineering Drawings

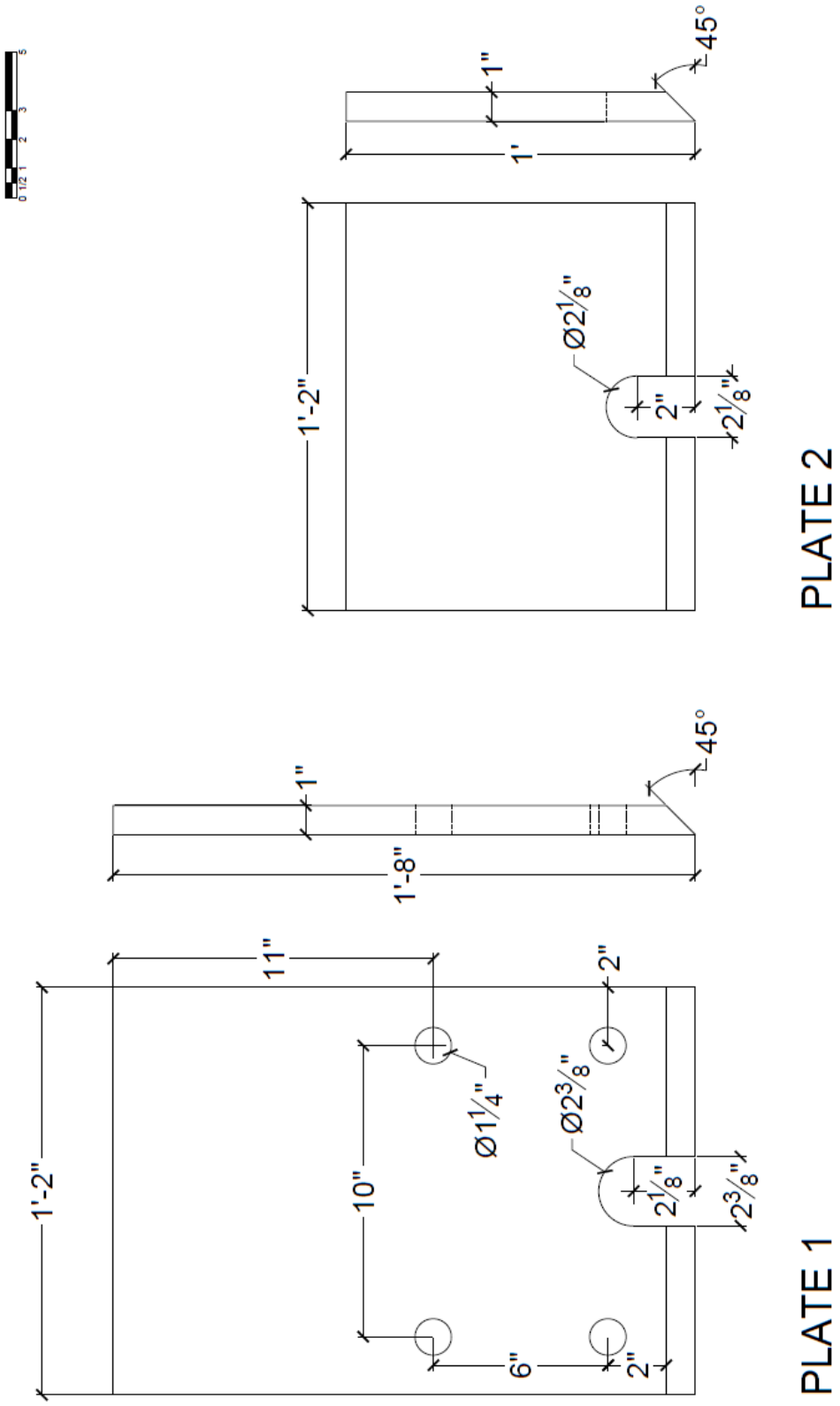

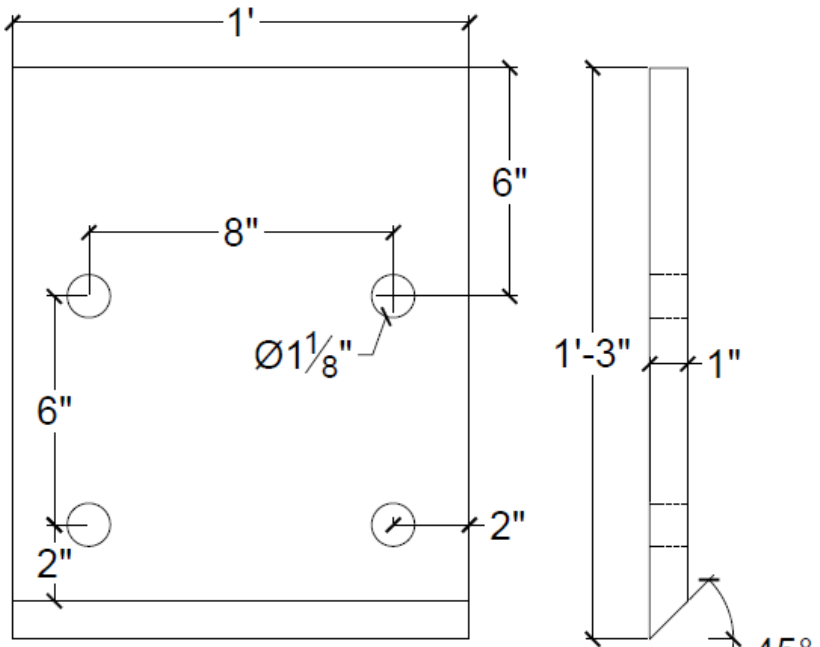

PLATE 3

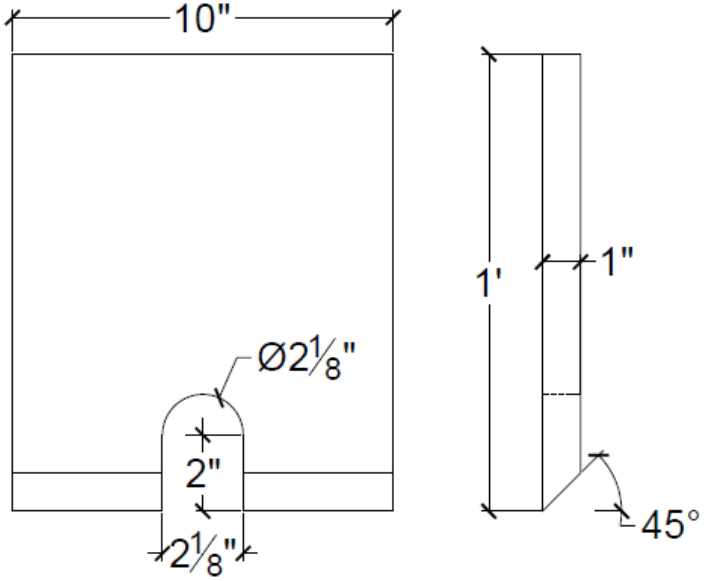

PLATE 4

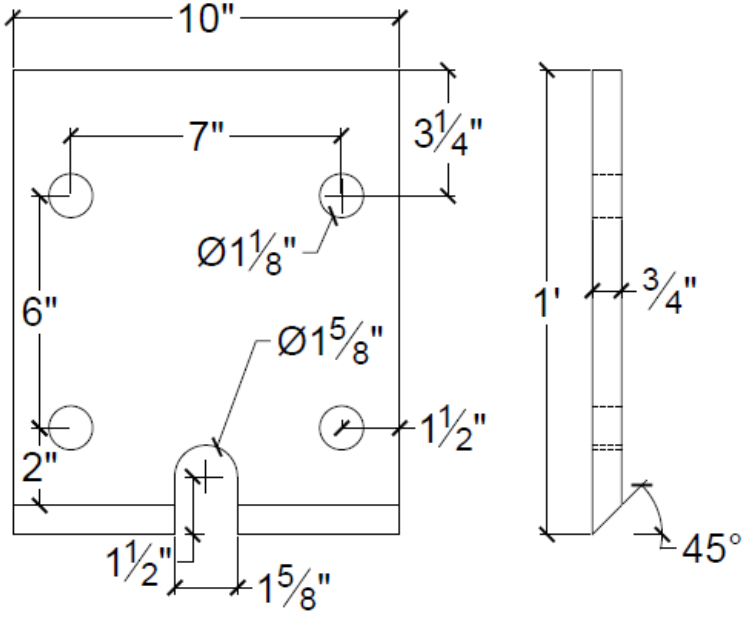

PLATE 5

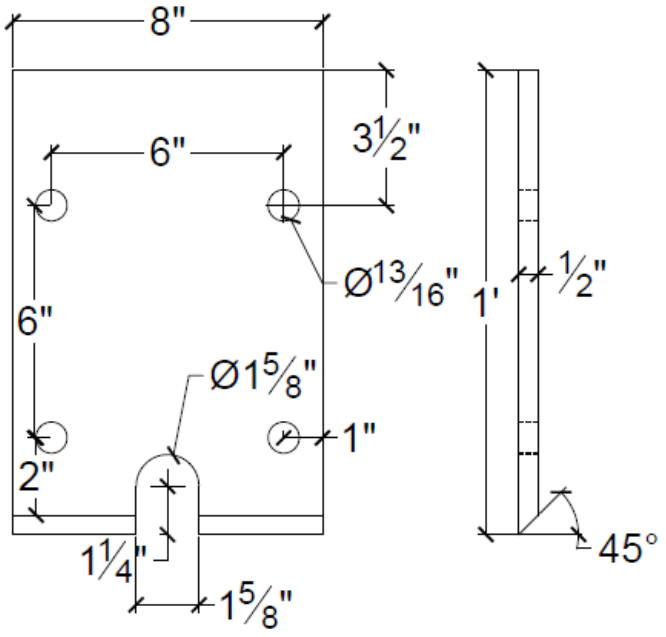

PLATE 6

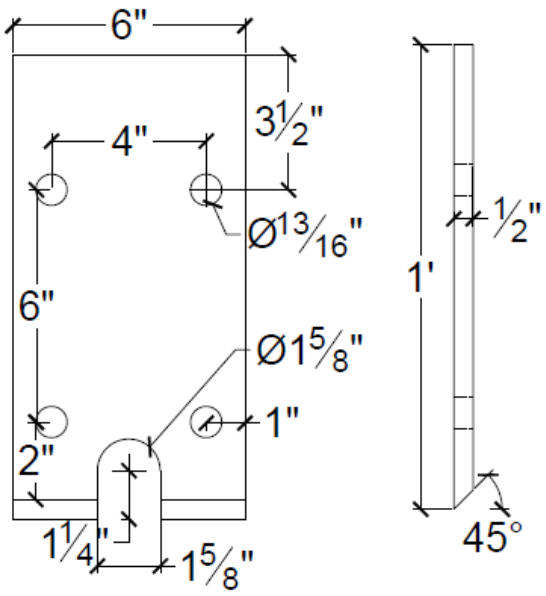

PLATE 7

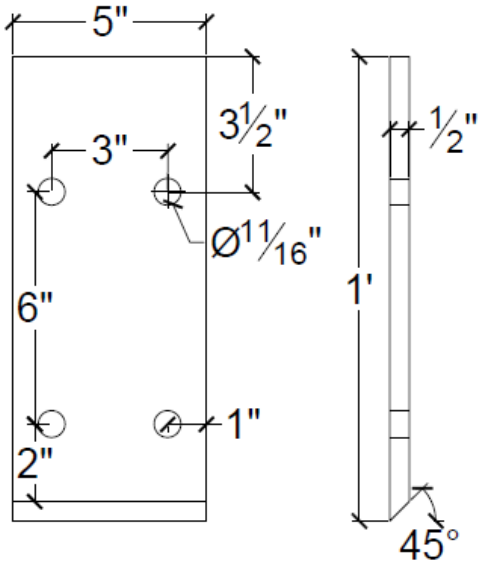

PLATE 8

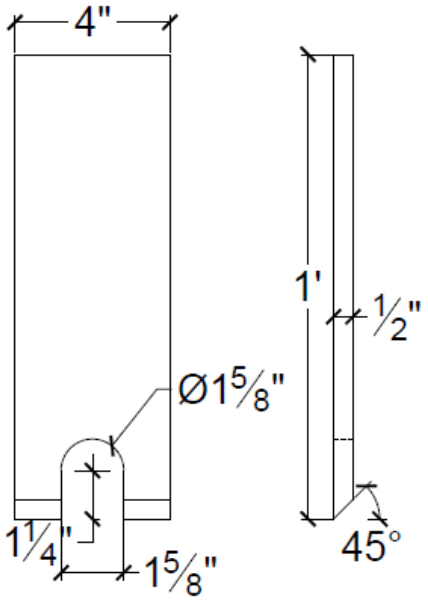

PLATE 9

Standardized Lettered Plate Design Variables

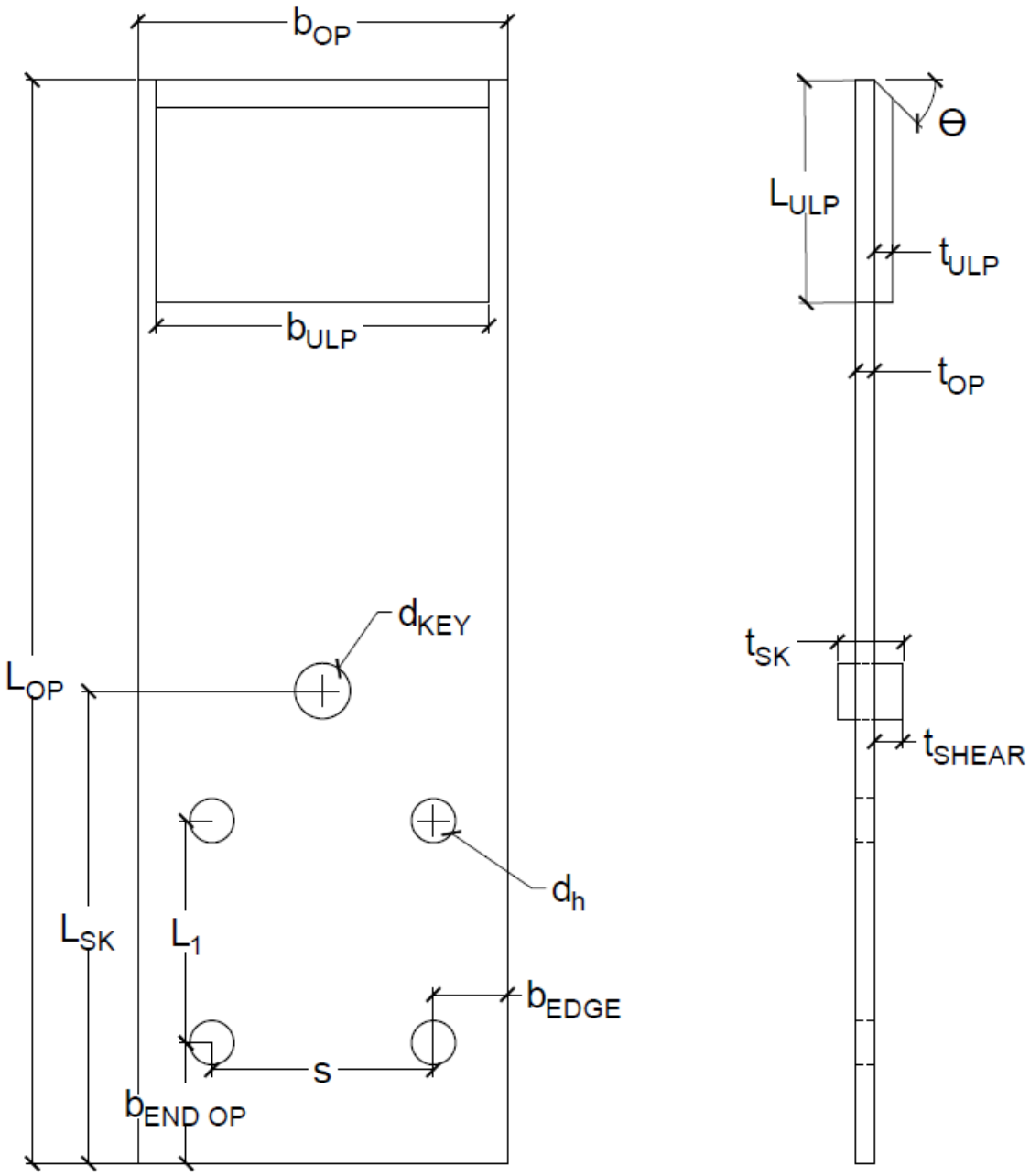

Lettered Plate Engineering Drawings

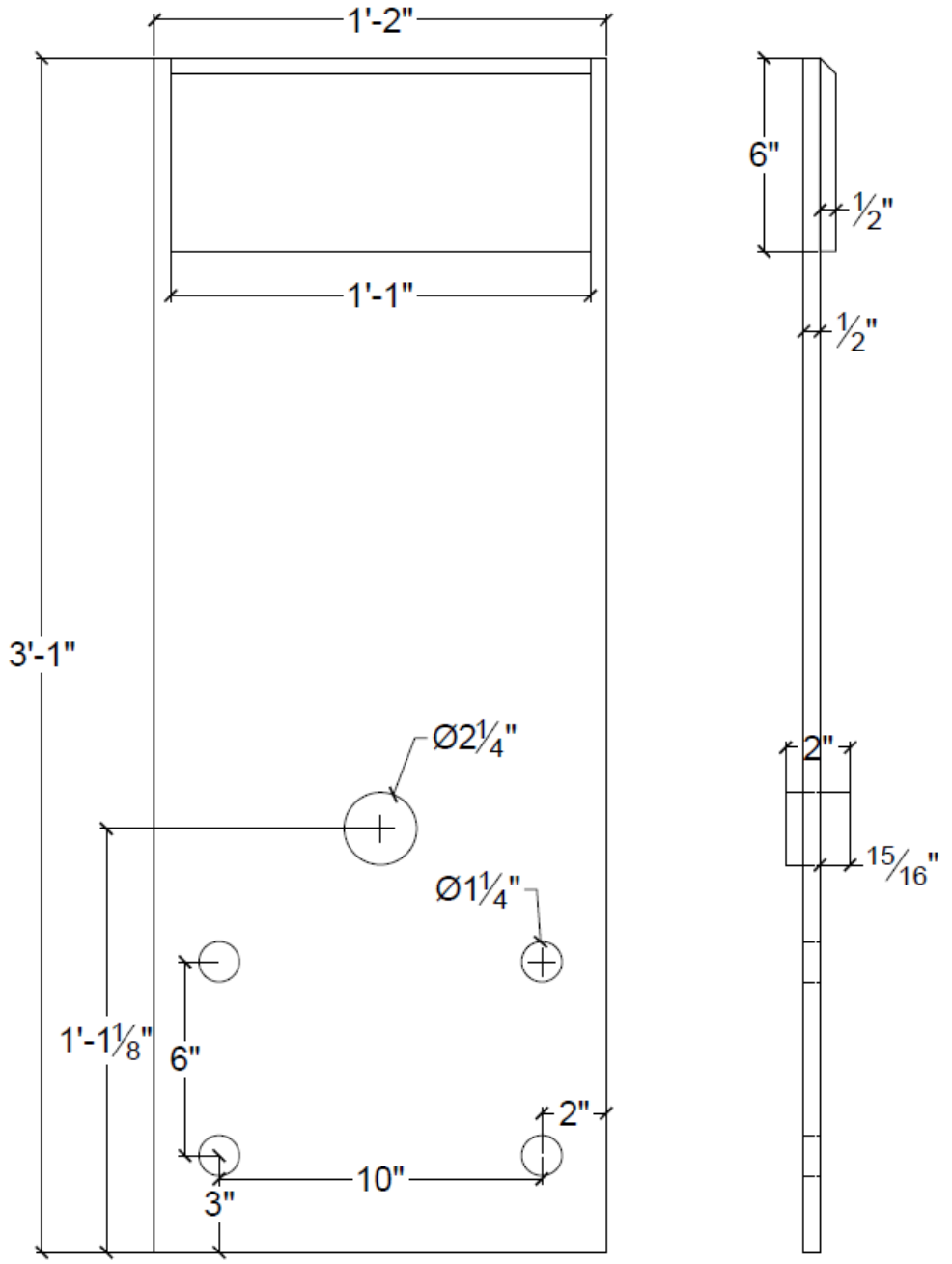

PLATE A

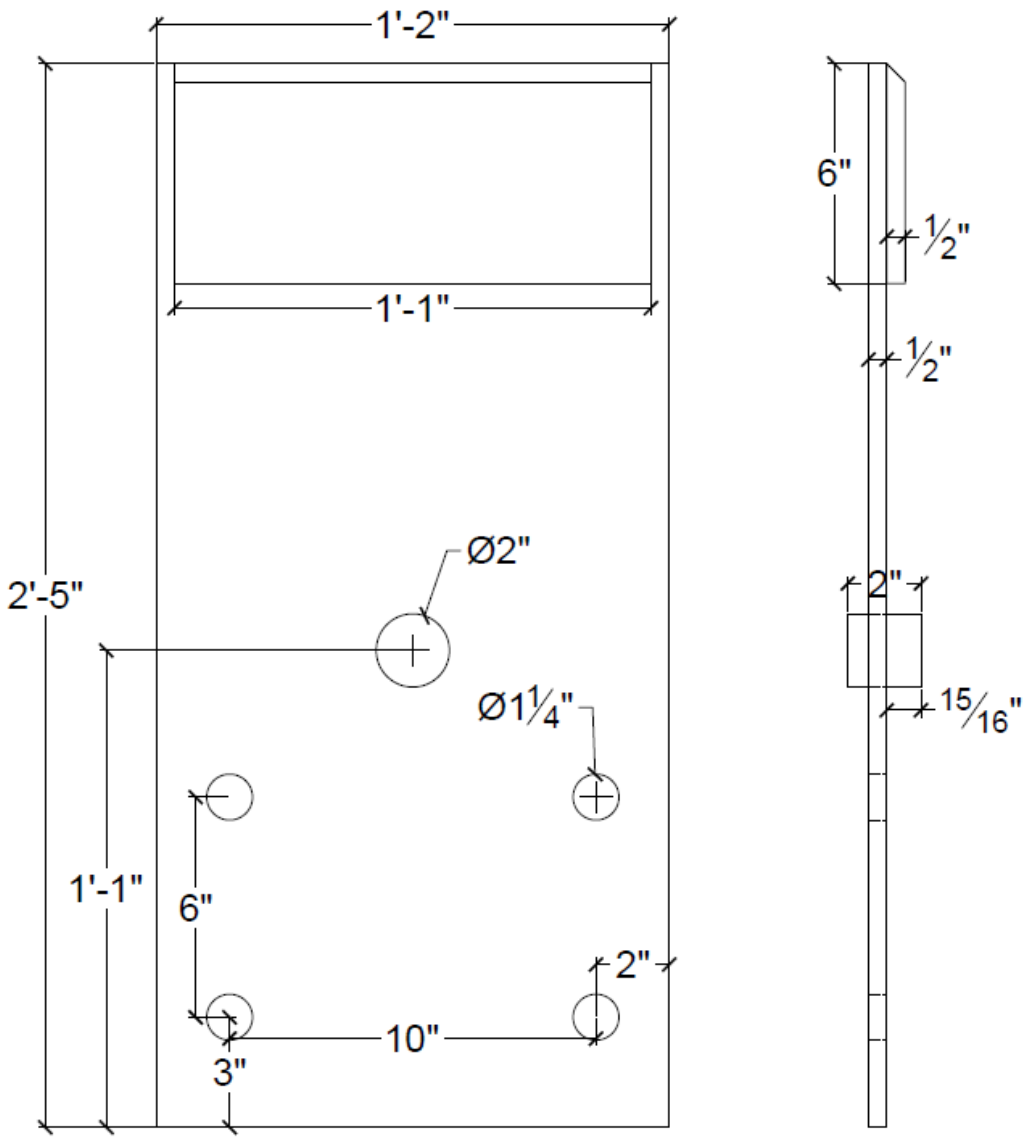

PLATE B

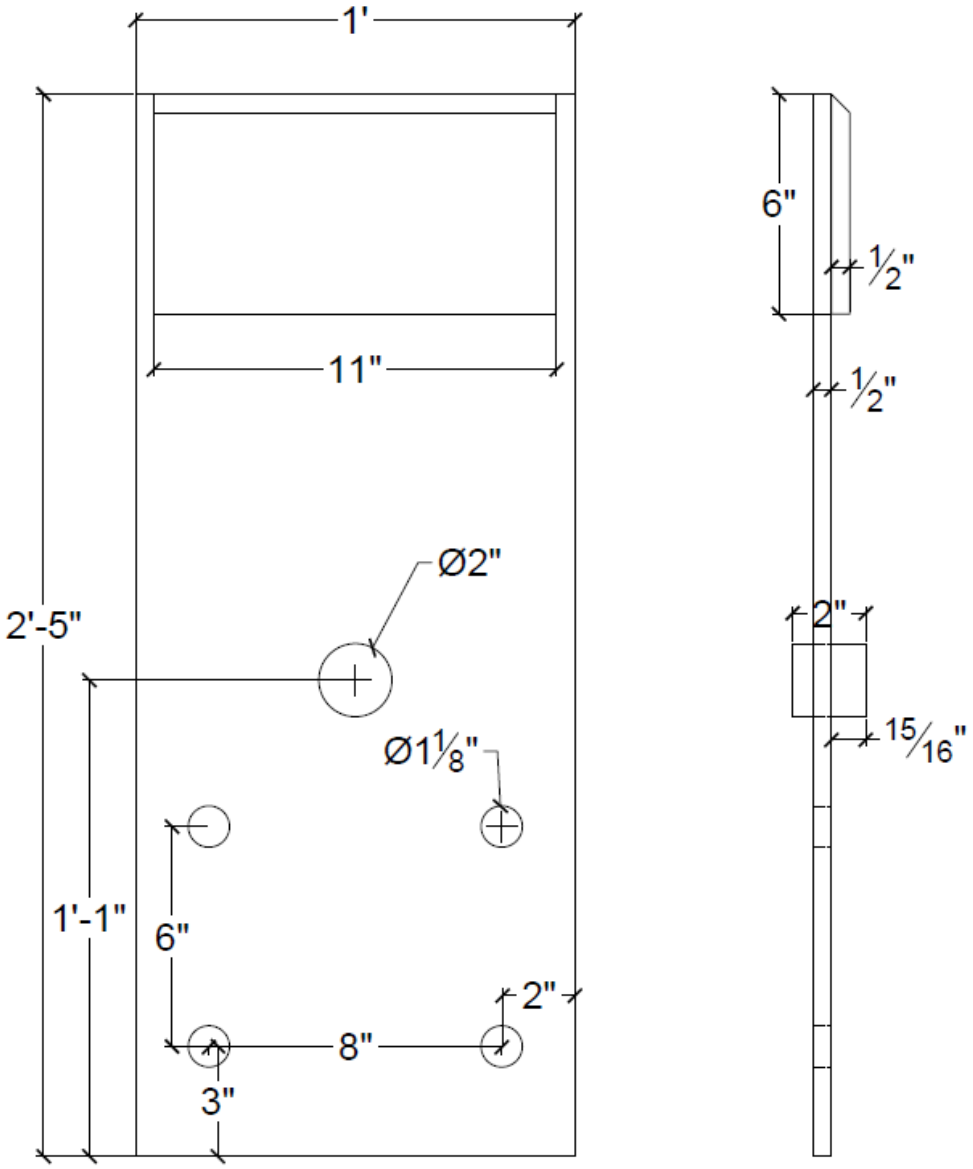

PLATE C

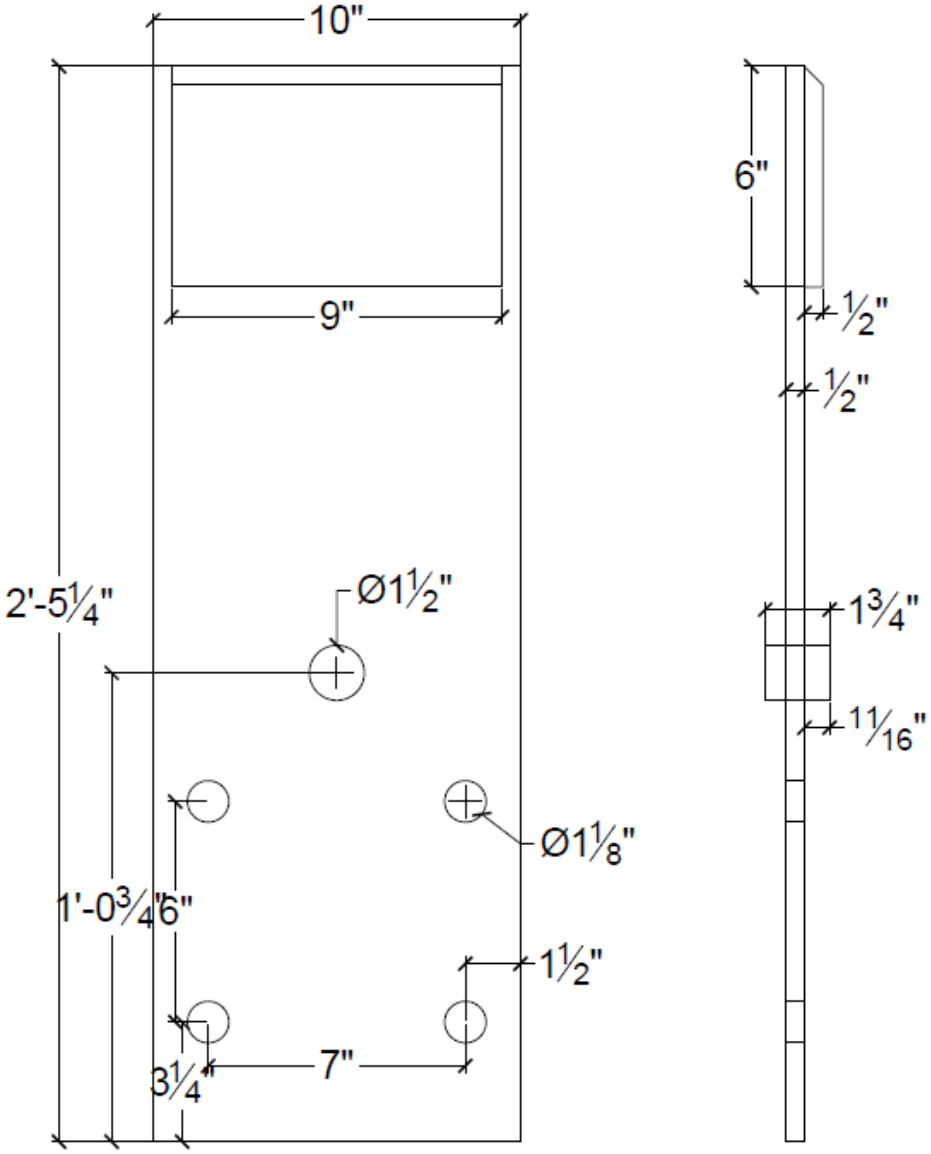

PLATE D

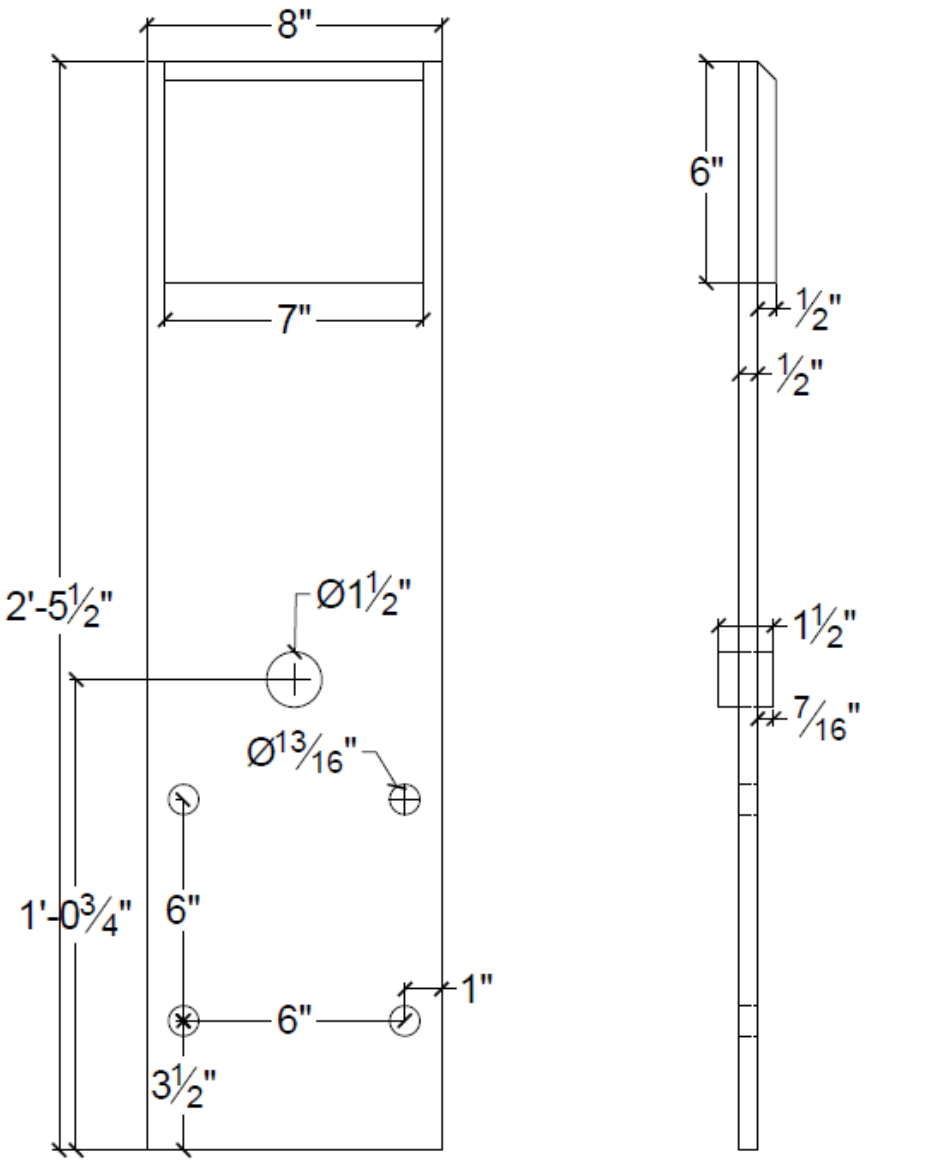

PLATE E

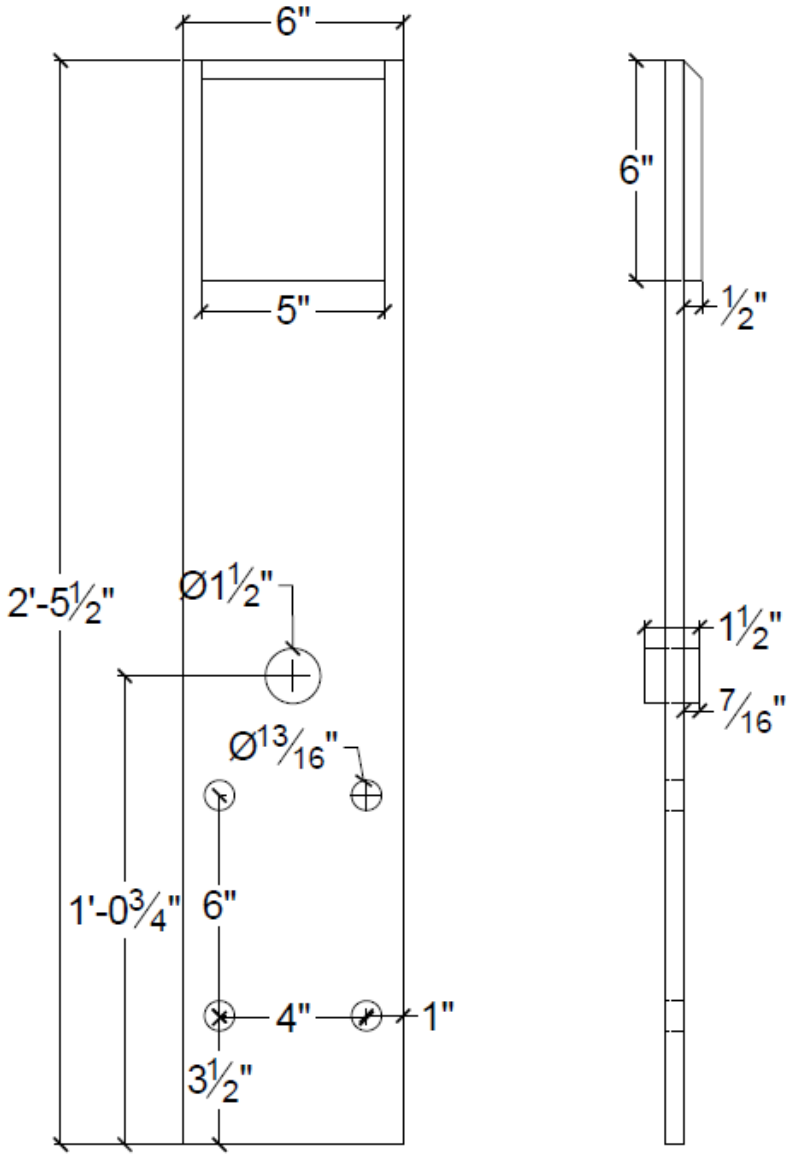

PLATE F

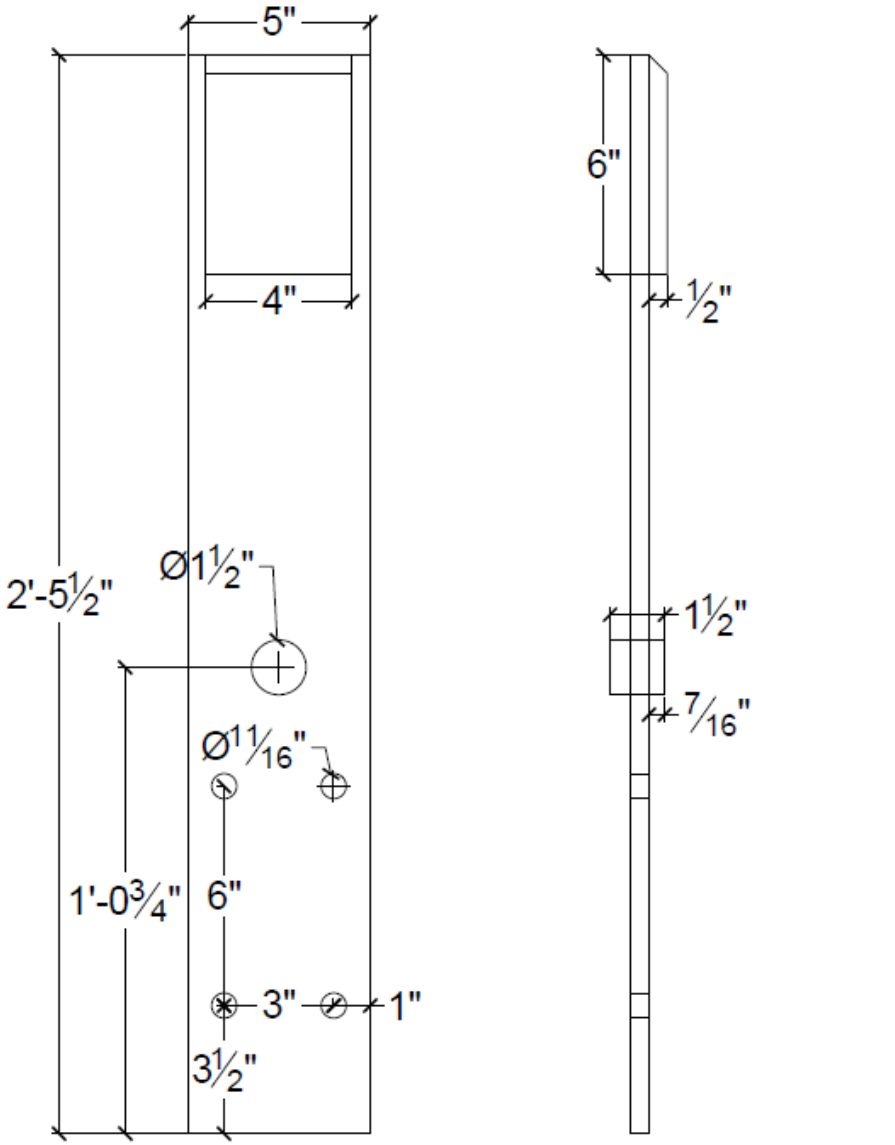

PLATE G